

FORMATION OF DISINFECTION BY-PRODUCTS
IN DRINKING WATERS: A COMBINATION OF
ADVANCED ANALYTICAL TECHNIQUES AND
MODELIZATION

Meritxell Valentí Quiroga



<http://creativecommons.org/licenses/by-nc/4.0/deed.ca>

Aquesta obra està subjecta a una llicència Creative Commons Reconeixement-NoComercial

Esta obra está bajo una licencia Creative Commons Reconocimiento-NoComercial

This work is licensed under a Creative Commons Attribution-NonCommercial licence



DOCTORAL THESIS

Formation of disinfection by-products in drinking waters: a combination
of advanced analytical techniques and modelization

Meritxell Valentí Quiroga

2024



DOCTORAL THESIS

Formation of disinfection by-products in drinking waters: a combination
of advanced analytical techniques and modelization

Meritxell Valentí Quiroga

2024

Supervised by:

Dr. Maria J. Martin

Dr. Pepus Daunis i
Estadella

Dr. Maria José Farré

Doctoral Programme in Water Science and Technology

Thesis submitted in fulfilment of the requirements for the degree of
Doctor from the Universitat of Girona



Dr. Maria J. Martin Sánchez, professor of the Department of Chemical, Agricultural, and Agri-food Technology Engineering and principal researcher of the LEQUIA Research Group at Universitat of Girona.

Dr. Pepus Danis i Estadella, professor of the Department of Computer Science, Applied Mathematics, and Statistics, and researcher of the Compositional Data Analysis and Statistics Research Group (GR-EADC) at University of Girona.

Dr. Maria José Farré, research scientist at Institut Català de Recerca de l'Aigua (ICRA)

WE DECLARE:

That the thesis entitled *Formation of disinfection by-products in drinking waters: a combination of advanced analytical techniques and modelization*", presented by Meritxell Valentí Quiroga to obtain a doctoral degree, has been completed under our supervision and meets the requirements to opt for Doctoral Degree with International Mention.

For all intents and purposes, we hereby sign this document.

ACKNOWLEDGEMENTS

Durant els anys que ha durat aquesta tesi he tingut algunes nits d'insomni que m'han fet revisar mentalment els motius que em feien seguir en aquest camí. De tots, sens dubte, els que sempre m'han acabat pesant més han estat aquells que m'han permès establir vincles nous que li han donat un sentit a tota la feina i esforç. Justament son aquestes els que m'agradaria agrair de tot cor ara que tanco aquest capítol. Revisant-ho amb una mica de calma han estat moltes les persones amb les que m'he creuat aquest temps i que, d'una forma o altra, han acabat tenint un petit impacte en el procés ja sigui a un o altre nivell. Penso que a totes us dec una part d'agraïment, i a algunes de forma més especial.

Em sembla que normalment la part més important es reserva pel final, però considero que sense fonaments no s'arriba enlloc i jo, a dia d'avui, si no fos per la meva mare no seria gaire lluny. He tardat uns anys en comprendre certes coses però tinc molt clar que si soc on soc, i com soc és gràcies a tu. De qui he après la importància de fer les coses ben fetes, que costa menys fer-ho bé que malament, a ser constant i tenir determinació, i sobretot, a posar el cor en les coses que faig, ha sigut de tu i el teu exemple. Gràcies per entregar-te a mi incondicionalment i donar-me ales per créixer. El papa i tu vau fer una gran feina, i sé que ell també n'estaria orgullós.

Pujant un esglaó més amunt, Maria, l'agraïment majúscul te'l dec a tu. Gràcies per obrir-me la porta del teu despatx i donar-me la oportunitat de treballar plegades (i també el llibre sobre NOM). Avui tinc clar que aquell dia quan marxava no sabia on m'estava posant, però vist en perspectiva diré que ho tornaria fer amb els ulls tancats. Per a mi ha estat una sort créixer de la teva mà. Gràcies per fer-me una mica més flexible: més enginyera i menys analítica. Gràcies als meus co-directors: Pepus, crec que al principi a tu també et van enganyar una mica com a mi, però gràcies per no pensar-t'ho gaire i acceptar. Hem tancat el cercle generacional i això per a mi te un valor incalculable. Amb el cor a la mà, moltes gràcies. Maria José, t'agraeixo a tu també acceptar a cegues i fer un forat per formar-me. Gràcies a tots tres per fer-me de mentors. De vosaltres he après moltíssim a nivell tècnic però sobretot he après ètica i bones pràctiques, i penso que això és el que de debò transforma una feina en professió. Gràcies per ensenyar-m'ho.

Gràcies a tot l'equip del LEQUIA, en especial al grup de potables: gràcies per sumar esforços i alleugerir els mals tràngols. Per suposat un gràcies especial als àngels de la guarda del laboratori: tot l'equip de tècniques que m'ha donat un cop de mà, sovint quan han estat els moments més crítics. Gràcies Fernando i Pere per apostar i creure en el mètode de HPSEC: veure que els esforços destinats en fer créixer un petit projecte poden ser d'utilitat, és el que per a mi li dona més sentit a la feina d'aquests anys. Un gràcies molt sentit al Paolo i tot el grup de la Universitat di Catania, qui van obrir les portes de casa seva a una completa desconeguda durant tres mesos per fer-me sentir una més de la *famiglia*.

I per últim, però sense restar-li intensitat, també em sento enormement agraïda per la paciència i suport dels meus amics i família, que sense entendre què he estat fent durant quatre anys, us heu preocupat, preguntat i interessat. Gràcies per fer-me sentir acompanyada en els moments feixucs i celebrar amb mi les petites victòries que he anat aconseguint. Que tant de bo seguim fent-nos grans de la mateixa manera.

This research was financially supported by the Spanish Ministry of Sciences, Innovation and Universities (CMT2017-83598-R & PID2020-112615RA-I00).

The author was awarded by AGAUR from the Generalitat de Catalunya, with a predoctoral grant (FI_SDUR 2020-00330).

LEQUIA has been recognized as a consolidated research group by the Catalan government (2017-SGR-1552).

INDEX

AKNOWLEDGEMENTS.....	4
INDEX.....	VI
LIST OF TABLES.....	XI
LIST OF FIGURES.....	XII
LIST OF ACRONYMS AND ABBREVIATIONS.....	XIV
DERIVED OUTREACH.....	XVI
SUMMARY.....	XVII
RESUM.....	XIX
RESUMEN.....	XXI
Chapter I: Introduction.....	1
1. THE CONCERN: DISINFECTION BY-PRODUCTS.....	2
1.1 Classification of main concern disinfection by-products.....	3
1.1.1 Organic and inorganic regulated DBPs.....	3
1.1.2 Unregulated emerging DBPs (N-DBPs, I-DBPs, and HMW-DBPs).....	4
2. THE PRECURSOR: NATURAL ORGANIC MATTER.....	6
2.1 Attributes of Natural Organic Matter.....	6
2.2 Tracking NOM.....	7
2.2.1 Size Exclusion.....	8
2.3 Reactivity of NOM towards disinfection.....	14
2.4 DBP minimization in conventional water treatment trains.....	15
2.4.1 Separation mechanisms: filtration, coagulation, and adsorption.....	16
2.4.2 Disinfection.....	17
Chapter II: Objectives.....	18
Chapter III: Materials & Methods.....	20
1. GENERAL WATER QUALITY PARAMETERS.....	21
2. DOM FINGERPRINTING.....	21
2.1 Size Exclusion.....	22

2.2	Fluorescence Excitation – Emission Matrix	23
2.3	High Resolution Mass Spectrometry	23
3.	DISINFECTION BY-PRODUCTS	24
3.1	Formation potential tests	24
3.2	DBP analysis.....	25
3.2.1	Head Space – Gas Chromatography – Mass Spectrometry (HS-GC-MS) analysis.....	25
3.2.2	Liquid-Liquid extraction and GC-MS analysis.....	25
3.3	Adsorbable organic halides.....	26
4.	STATISTICAL METHODS.....	27
4.1	Multiple Linear Regression (MLR)	27
4.2	Multiple correlation analysis and hierarchical clustering	27
4.3	K-fold Cross validation method.....	28
4.4	Pearsons’ correlation analysis	28
5.	CASE STUDIES.....	29
Chapter IV: Prediction of THMs-FP from DOC fractionation by HPSEC-DAD-OCD.....		32
1.	BACKGROUND AND OBJECTIVES	33
2.	METHODOLOGY	33
3.	RESULTS AND DISCUSSION.....	35
3.1	Evaluation of SEC methodology and DOM fractions	37
3.2	THMs- FP modelling & assessment.....	39
4.	FINAL REMARKS	45
Chapter V: In-deep analysis of humic substances process performance in drinking water treatments using size exclusion chromatography.....		46
1.	BACKGROUND AND OBJECTIVES	47
2.	METHODOLOGY	47
3.	RESULTS AND DISCUSSION.....	48
3.1	DOM characterization of source and treated waters	48
3.1.1	Treatment plants from river sources: PTL.....	48
3.1.2	Treatment plants from reservoir sources: PTT and PTC.....	50
3.2	Sequential Removal of DOM Fractions	51

3.2.1	Full Scale DWTPs.....	52
3.2.2	Ion Exchange Bench-Scale	53
3.3	Humic Substances Sub-Fractions.....	53
3.3.1	UV-Multiwavelength Analysis of Humic Substances Sub-Fractions	54
3.3.2	Evaluating the Removal of Humic Substances	56
3.4	Assessment of THM-FP through Conventional and IEX Treatments.....	58
3.4.1	THM-FP in Treatment plants from River Sources: PTL.....	58
3.4.2	THM-FP in Treatment plants from Reservoir Sources	59
3.5	Assessment of Humic Substances and THM-FP Correlation.....	59
4.	FINAL REMARKS.....	61

Chapter VI: Development of experimental data-based predictive models for regulated organic DBPs using a novel approach to select DOM spectroscopical variables..... 62

1.	BACKGROUND AND OBJETIVES.....	63
2.	METHODOLOGY.....	63
3.	RESULTS AND DISCUSSION.....	63
3.1	Water characterization (bulk & fractionated parameters pre/post chlorination).....	63
3.1.1	Bulk parameters.....	64
3.1.2	Fraction distribution.....	65
3.2	DBPs distribution.....	68
3.3	Evaluation of differential absorbance (DAS) of HPSEC-DAD-OCD humic substances after chlorination	69
3.3.1	Study of wavelength correlations and hierarchical clustering	70
3.4	Spectroscopic prediction models of DBPs.....	71
3.4.1	Predictive models based on DAS of HPSEC-DAD-OCD analysis on humic substances	71
3.4.2	Predictive models based on bulk measurements.....	73
4.	FINAL REMARKS.....	75

Chapter VII: Analysis of chlorination-driven changes in DOM fingerprints and their implications on DBPs formation. A comparison of advanced characterization techniques 76

1.	BACKGROUND AND OBJECTIVES.....	77
2.	METHODOLOGY.....	77
3.	RESULTS AND DISCUSSION.....	77
3.1	The direct effects of chlorination. DBPs distribution.....	77

3.2	Unravelling DOM Fingerprints.....	79
3.2.1	Starting from the bottom: Bulk surrogated parameters.....	79
3.2.2	The 1 st tier of DOM: Spectral signature	81
3.2.3	The 2 nd tier of DOM: Chemical behaviour.....	85
3.2.4	The 3 rd tier of DOM: Chemical identities of individual species	89
4.	FINAL REMARKS.....	95
Chapter VIII: Strategies for the mitigation and minimization of DBPs on drinking water treatment plants. An applied guideline to meet new legislation requirements		99
1.	BACKGROUND AND OBJECTIVES.....	100
2.	METHODOLOGY.....	100
3.	RESULTS AND DISCUSSION.....	100
3.1	Strategies to minimize DBPs formation	100
3.1.1	Source water control strategies.....	101
3.1.2	Removal of DBPs precursors.....	101
3.1.2.1	Separation.....	101
3.1.2.2	Biofiltration.....	103
3.1.2.3	Oxidation.....	103
3.1.3	Disinfection strategy selection	103
3.1.3.1	Pre-oxidation.....	104
3.1.3.2	Secondary disinfection	106
3.1.4	Removal of DBPs.....	106
3.2	Alternative treatment trains for controlling DBPs in drinking water.....	108
3.3	Guidelines.....	109
4.	FINAL REMARKS.....	111
Chapter IX: Final Discussion.....		112
Chapter X: General Conclusions		115
BIBLIOGRAPHY		118
APPENDIX.....		i
APPENDIX A. INTRODUCTION		i
APPENDIX B. MATERIALS & METHODS.....		iv
APPENDIX C. CHAPTER IV: RESULTS I.....		xii

APPENDIX D. CHAPTER V: RESULTS II..... xv
APPENDIX E. CHAPTER VI: RESULTS III..... xix

LIST OF TABLES

Table 1: Summary of unregulated DBPs main species.....	5
Table 2: Summary of most relevant methodological parameters of SEC methods for NOM characterization.	11
Table 3: Summary of predictive variables for THMs and HAAs-FP models based on SEC of NOM.	13
Table 4: Main reactions of chlorine and bromine involved in DBPs formation.....	14
Table 5: Standard protocols for water samples quality measurements.	21
Table 6: HPSEC-DAD-OCD methodological parameters.	22
Table 7: Summary of DOM fractions analyzed by HPSEC-DAD-OCD.	22
Table 8: EMM methodological parameters.....	23
Table 9: Fluorescence peak-pairs correlated to DOM features.	23
Table 10: Quenching reagents summary.....	24
Table 11: HS-GC-MS methodological parameters.	25
Table 12: GC-MS methodological parameters for DBP analysis.	26
Table 13: Summary of sampling campaigns.....	31
Table 14: Summary of the analytical workflow and methodologies used in Chapter IV.	33
Table 15: Summary of main HPSEC-DAD-OCD fractions with corresponding retention times (min). ...	34
Table 16: Summary of the analytical workflow and methodologies used in Chapter VI.....	48
Table 17: Bulk water parameters of the samples across treatment operations in the three DWTP evaluated.	48
Table 18: Distribution of DOC in DOM fractions by HPSEC-DAD-DOC.....	50
Table 19: Absorbance ratios of humic substances fraction of catchment samples.	55
Table 20: Summary of the analytical workflow and methodologies used in Chapter VII.....	63
Table 21: Individual cluster's centroids and representative values (mean values).....	71
Table 22: Summary of the analytical workflow and methodologies used in Chapter VII.....	77
Table 23: Summary of HRMS indexes and count of features of raw and treated samples characterization and their decrease (%) derived from corresponding treatments in each DWTP.	91
Table 24: Decrease (%) on DOM features from induced changes after chlorination of waters.	95
Table 25: Summary of pre-oxidation methodologies regarding effects on DBPs precursors, DBPs formation, main applicability advantages and disadvantages.	105
Table 26: Strategies for removal of regulated DBPs.	106
Table 27: Guidelines to select mitigation solutions for controlling DBPs regulated by the EU Directive 2020/2184 at WTPs.	109
Table 28: Rate of discussed approaches for prediction of DBPs.....	113

LIST OF FIGURES

Figure 1: DBP distribution according to TOX (%).	3
Figure 2: The four tiers of NOM characterization	7
Figure 3: Methods for NOM characterization based on its chemical behaviour.	8
Figure 4: State-of-the-art links between SEC methods for NOM characterization.	9
Figure 5: General timeline of SEC publications and their application in drinking water.	12
Figure 6: Detailed evaluation of SEC method applications in drinking water related to NOM and disinfection by-products.	13
Figure 7: Summary of strategies for DBP minimization in drinking water treatment procedures and most effective treatments	16
Figure 8: Case study situational map.	29
Figure 9: Scheme of the full-scale treatment trains of the case study DWTPs.	30
Figure 10: Example of DOM and A_{254} chromatogram deconvolution and quantification by HPSEC-DAD-OCD.	34
Figure 11: THMs-FP and yields of analysed samples from Llobregat DWTP (PTL), Ter DWTP (PTT), and Cardener DWTP (PTC), as a function of reaction time.	36
Figure 12: Comparison of overlapped chromatograms of the DOC and A_{254} spectroscopic responses of the catchment samples obtained by HPSEC-DAD-OCD and LC-OCD.	37
Figure 13: Chromatograms of the HPSEC-DAD-OCD spectroscopic slopes between absorbance wavelengths of 206–240 nm and 350–380 nm, and overlapped DOC profiles for the river catchment sample (PTLL) and reservoirs (PTT and PTC).	38
Figure 14: R^2_{adj} coefficients heatmap of the MLR simplified models fitting bulk measurements and DOM fractions obtained by LC-OCD and HPSEC-DAD-OCD.	39
Figure 15: Standardised coefficients (SC) and R^2_{adj} values as a function of reaction time (24 and 72 h) for modelling the total (tTHMs) and individual THMs-FPs from DOC fractionation (A) and spectroscopic hybrid signals A_{254} – $S_{206-240}$ (B). Note that FX_{254} refers to $F4_{254}$ for PTLL samples and $F5_{A_{254}}$ for PTT-PTC	41
Figure 16: Measured vs. predicted tTHMs-FP estimated with the HPSEC-OCD model and the spectroscopic hybrid model A_{254} – $S_{206-240}$ including the representation of 95% prediction bands and validation samples.	42
Figure 17: Measured vs. predicted FP for the distinct THMs congeners estimated with the HPSEC-OCD model and the spectroscopic hybrid model A_{254} – $S_{206-240}$ including the representation of 95% prediction bands and validation samples.	44
Figure 18: Overlapped DOC and UV-multiwavelength absorbance profiles from HPSEC chromatograms of catchments and treated waters after conventional treatment train (Rt 10.8 – 16 min: Biopolymers; Rt 16 – 22.5 min: HS; Rt 22.5 – 29 min: BB; Rt 29 – 33 min: low MW acids; Rt 33 – 60 min: low MW neutrals.	49
Figure 19: Differences in the concentration of DOC ($\mu\text{g/L}$) for each DOM fraction after treatments, calculated by subtraction of subsequent concentrations.	52
Figure 20: Overlap of absorbance spectra from Humic Substances peaks (HS1, HS2, HS3) of (A) PTL, (B) PTT and (C) PTC full scale treatment train.	54
Figure 21: Distribution of (A) DOC, (B) A_{254} , and (C) $SUVA_{254}$ amounts for each HS1, HS2, HS3, relative to all HS fraction according to conventional and advanced treatments in PTL, PTT, and PTC.	56

Figure 22: THMs-FP reduction in $\mu\text{g/L}$, expressed as differences in between unitary operations from the full-scale treatment and bench scale IEX tests (BS-1, BS-2) for each DWTP.....	58
Figure 23: Pearson's' correlation matrices of HS surrogate parameters and THMs-FP.....	60
Figure 24: Reduction of bulk parameters of samples from three different DWTPs with treatment operations.....	64
Figure 25: Overlapped DOC and absorbance chromatograms of raw waters from the (A) Montfullà, (B) Cardedeu, (C) Abrera DWTPs before (left) and after (right) their chlorination.....	66
Figure 26: NOM fraction distribution of pre- and post- chlorinated process samples from three different DWTP.....	67
Figure 27: Amounts of organic regulated DBPs after chlorination on FP tests of process samples from DWTPs.....	68
Figure 28: DAS chromatograms of humic substances fraction resulting from the subtraction of pre- and post- chlorinated raw water samples from Montfullà, Cardedeu, Abrera DWTPs.....	69
Figure 29: Hierarchical clustering of raw waters from Montfullà DWTP, Cardedeu DWTP, and Abrera DWTP.....	70
Figure 30: Heatmap of the R^2_{adj} values for MLR models based on DAS of HS using a single wavelength at 272 nm (A), multiwavelength approach (B), or multiwavelength approach based on raw measurements (C).....	72
Figure 31: Heatmap of the R^2_{adj} values for MLR models based on raw bulk absorbance of samples at 220 nm, 252 nm, 290nm, and 362 nm.....	73
Figure 32: Measured vs. predicted THMs-FP estimated with bulk raw absorbance MLR models including the representation of 95% prediction bands.....	74
Figure 33: Concentrations of DBPs and for raw and treated waters of Montfullà (A), Cardedeu (B), and Abrera (C) drinking water treatment plants, expressed as total concentration in $\mu\text{g/L}$ (1) and relative to unit mass (2).....	78
Figure 34: Bulk surrogated parameters of raw and treated waters in (A) Montfullà, (B) Cardedeu, and (C) Abrera DWTPs, along with their removal rate (%) with the treatment process.....	80
Figure 35: Integration of the main fluorescence peaks on raw and treated waters pre- and post-chlorination (1) and related to unit of mass (2).....	82
Figure 36: Absorbance profiles of raw and treated waters from (A) Montfullà, (B) Cardedeu, and (C) Abrera before (left) and after (middle) chlorination, and the difference (right).....	84
Figure 37: Overlapped DOC and absorbance chromatograms of raw and treated samples pre-(left), post- chlorination (middle), and induced difference (right) in (A) Montfullà, (B) Cardedeu, and (C) Abrera raw and treated waters.....	86
Figure 38: Quantification of DOC fractions of raw and treated waters prior and after their chlorination.....	87
Figure 39: Humic substances' absorbance (A_{254}) and SUVA_{254} trends on raw and treated waters before and after their chlorination, and removal (%) achieved with treatment in each drinking water treatment plant.....	88
Figure 40: Van Krevelen diagram with category assignation overlap.....	90
Figure 41: Van Krevelen diagrams before and after chlorination of raw and treated waters.....	94
Figure 42: Correlation matrix between indexes.....	97
Figure 43: Alternative treatment trains (advanced units (blue) are embedded into a conventional configuration (black)).....	108

LIST OF ACRONYMS AND ABBREVIATIONS

A ₂₅₄ : Absorbance at 254 nm	EfOM: Effluent Organic Matter
AC: Activated Carbon	
AMW: Apparent Molecular Weight	FP: Formation Potential
AOM: Algal Organic Matter	
AOX: Adsorbable Organic Halides	GAC: Granular Activated Carbon
	GC-MS: Gas Chromatography coupled to Mass Spectrometry
BAC: Biological Activated Carbon	
BB: Building Blocks	
BDCM: Bromodichloromethane	HAA: Haloacetic acid
BioP: Biopolymers	HAcAms: Haloacetoamides
	HANs: Haloacetonitiles
	HKs: Haloketones
CV: Coefficient of Variation	HMW: High Molecular Weight
	HNMs: Halonitromethanes
DAD: Diode Array Detector	HPSEC: High Performance Size Exclusion Chromatography
DAS: Differential Absorption Spectra	
DBCM: Dibromochloromethane	HRMS: High Resolution Mass Spectrometry
DBP: Disinfection by-product	
DOC: Dissolved Organic Carbon	HS: Humic Substances
DOM: Dissolved Organic Matter	
DON: Dissolved Organic Nitrogen	LC: Liquid Chromatography
DWTP: Drinking Water Treatment Plant	LMW: Low Molecular Weight
EDR: Electrodialysis Reversal	MLR: Multiple Linear Regression

NOM: Natural Organic Matter

PTT: Planta Tractament Ter (Ter Drinking Water Treatment Plant)

OCD: Organic Carbon Detector

SUVA₂₅₄: Specific UV Absorbance at 254 nm

PAC: Powdered Activated Carbon

TBM: Tribromomethane

PTC: Planta Tractament Cardener (Cardener Drinking Water Treatment Plant)

TCM: Trichloromethane

PTL: Planta Tractament Llobregat (Llobregat Drinking Water Treatment Plant)

THM: Trihalomethane

PTM: Planta Tractament Montfullà (Montfullà Drinking Water Treatment Plant)

TOC: Total Organic Carbon

tTHMs: Total Trihalomethanes (expressed as the sum of regulated THMs)

DERIVED OUTREACH

Journal publications derived from this thesis:

- NOM fractionation by HPSEC-DAD-OCD for predicting trihalomethane disinfection by-product formation potential in full-scale drinking water treatment plants. Valenti-Quiroga, M., Daunis-i-Estadella, P., Emiliano, P., Valero, F., & Martin, M. J. (2022). *Water Research*, 227. <https://doi.org/10.1016/j.watres.2022.119314>
- Upgrading water treatment trains to comply with the DBPs standards introduced by the Directive (EU) 2020/2184. Valenti-Quiroga, M., Farré, M. J., & Roccaro, P. (2024). *Current Opinion in Environmental Science & Health*, 100547. <https://doi.org/10.1016/j.coesh.2024.100547>
- In-deep multiwavelength size-exclusion chromatography analysis of Natural Organic Matter fractions in drinking water treatment trains: fate and role in trihalomethanes formation potential. Valenti-Quiroga, M., Cabrera-Codony., A., Emiliano, P., Valero, F., & Martin, M. J. *Prepared for submission*
- Development of experimental data-based predictive models for regulated organic disinfection by-products using a novel approach to select NOM spectroscopical variables. Valenti-Quiroga, M., Daunis-i-Estadella, P., Monclús, H., & Martin, M. J. *Prepared for submission*

Other milestones:

- Two-year collaboration agreement funded by Ens d'Abastament d'Aigües Ter Llobregat (ATL) (58.250 €) for the study of the characteristics of organic matter in water resources, treatment processes, and drinking water through size exclusion chromatography (HPSEC-DAD-OCD) and its relationship with the efficiency of potabilization processes and the formation of regulated disinfection by-products.

SUMMARY

Water treatment plants are responsible for producing and supplying quality drinking water to residents. To achieve this, various treatments are combined to eliminate contaminants, dissolved organic matter, and deactivate pathogens that may compromise consumers' health. A critical operation in the water treatment process is the final disinfection, as it must ensure that water is free from microbiological hazards from the moment it leaves the plant's reservoirs until it reaches the taps. This is typically done using chlorine-derived oxidants (hypochlorite, chloramines, or chlorine dioxide). However, the addition of these disinfectants can lead to unintended consequences. Despite their contribution to controlling microbiological risks, excessive dosing will react with any remaining dissolved organic matter (DOM) and form disinfection by-products (DBPs), an extensive family of contaminants with varying degrees of toxicity.

To this day, the main challenge for plant managers and operators is to strike a balance between ensuring microbiological safety and the toxicity derived from disinfection by-products. To effectively monitor water quality throughout the treatment process, it is necessary to have markers to track the removal of organic matter, one of the main precursors of DBPs. However, the high complexity of this matrix (heterogeneous composition, subject to seasonal changes, and site-specificity of the water source) means that it acts as a black box, typically monitored using surrogate parameters reflecting some of its general physicochemical characteristics such as total organic carbon (TOC) content or absorbance.

In order to optimize organic matter removal processes in water treatment and thus minimize DBP generation, it is crucial to establish specific markers for the reactivity of organic matter towards DBP formation. This requires a detailed study of the characteristics of the organic matter present in the waters to be treated.

This work proposes, as a first step, the development of an advanced characterization method based on high-performance size exclusion chromatography (HPSEC) that allows the separation of the main compounds in a complex mixture such as DOM based on their apparent molecular weight. This separation is combined with a diode array detector (DAD) and a dissolved organic carbon detector (OCD) to determine the spectroscopic absorbance signature of the compounds across the UV-VIS range, relative to their organic carbon content.

Based on various sampling campaigns at four water treatment plants located in northeastern Catalonia, a small database has been established to analyze in depth the characteristics of the main DOM fractions. Various specific markers of organic matter attributes are proposed, including DOC content and various spectroscopic parameters (wavelengths, spectroscopic slopes, and differential absorbance), to study their relationship with the formation of regulated organic disinfection by-products: trihalomethanes and haloacetic acids. Various statistical techniques are applied, from Pearson correlation analysis to multiple linear regression models

(MLR). Based on the results obtained, this work advocates for the development of spectroscopic methodologies, as they can serve to close the gap between advanced knowledge generated from exhaustive offline analysis and simple and economical online monitoring.

In addition, the information obtained from characterization using the HPSEC-DAD-OCD method is contrasted with other advanced characterization methodologies such as fluorescence and high-resolution mass spectrometry (HRMS).

Finally, the efficiency of the main conventional treatment processes and advanced treatments is evaluated through a literature review and by integrating knowledge derived from case studies. Application guidelines are proposed for implementation in water treatment plants to help mitigate and minimize DBP formation in accordance with current legislation.

The knowledge derived from this work contributes to United Nations Sustainable Development Goal (SDG) 6, which aims to ensure the availability and sustainable management of water and sanitation for all. Specifically, it contributes to targets 6.3 and 6.4 related to improving water quality and efficient management.

Les plantes potabilitzadores d'aigua són les responsables de produir i subministrar aigua potable de qualitat als habitants. Per fer-ho, es combinen diferents tractaments per eliminar contaminants, matèria orgànica dissolta, i inactivar patògens que puguin comprometre la salut dels consumidors. Una operació crítica del procés de potabilització és la desinfecció final, ja que ha d'assegurar que l'aigua es troba lliure de perill microbiològic des que surt dels dipòsits de la potabilitzadora fins que arriba a les aixetes de les cases. Aquesta desinfecció es sol fer típicament amb oxidants derivats del clor (hipoclorit, cloramines o diòxid de clor). No obstant això, l'addició d'aquests desinfectants pot derivar en una praxi amb contrapartida. Malgrat que la seva addició contribuirà a controlar el risc microbiològic, una dosificació excessiva reaccionarà amb la matèria orgànica que romangui dissolta (DOM) i formarà subproductes de desinfecció (DBPs) una família extensa de contaminants amb diferents graus de toxicitat.

Encara avui dia, el principal repte per als gestors i operadors de planta està en establir l'equilibri entre assegurar la seguretat microbiològica i la toxicitat derivada pels subproductes de desinfecció. Per tal de poder fer un bon control de la qualitat de l'aigua al llarg dels tractaments en planta, és necessari disposar de marcadors per dur a terme el seguiment de l'eliminació de la matèria orgànica, un dels principals precursors de DBPs. No obstant això, l'elevada complexitat d'aquesta matriu (composició heterogènia, subjecta a canvis estacionals i específica de l'origen de l'aigua), fa que aquesta actui com una caixa negra de la qual típicament es monitoritzen paràmetres substituïts que actuen com a reflex d'algunes de les seves característiques fisicoquímiques generals com poden ser el contingut en carboni orgànic total (TOC) o la seva absorbància.

Amb la finalitat d'arribar a optimitzar els processos d'eliminació de matèria orgànica en la potabilització d'aigües i aconseguir així minimitzar la generació de DBPs, és de vital importància establir marcadors específics de la reactivitat d'aquesta davant de la generació de subproductes. I per això és indispensable desenvolupar un estudi detallat de les característiques de la matèria orgànica que es troba en les aigües a tractar.

Aquest treball proposa en primer lloc la posada a punt d'un mètode de caracterització avançada basat en cromatografia d'exclusió molecular (HPSEC) que permet separar els principals compostos d'una barreja complexa com és la DOM basada en el seu pes molecular aparent. Aquesta separació es combina amb un detector de diode array (DAD) i un detector de carboni orgànic dissolt (OCD) per determinar la signatura espectroscòpica absorbància dels compostos en tot el rang de UV-VIS, respecte al seu contingut en carboni orgànic. A partir de diferents campanyes de mostreig en quatre potabilitzadores situades al Nord-est de Catalunya, s'ha establert una petita base de dades que ha servit per analitzar a fons les característiques de les principals fraccions de la DOM. Així es proposen diferents marcadors específics dels atributs de la matèria orgànica incloent el contingut de DOC i diferents paràmetres espectroscòpics (longituds d'ona, pendents espectroscòpics i absorbància

diferencial), per estudiar la seva relació amb la formació dels subproductes de desinfecció orgànics que estan sotmesos a regulació: trihalometans i àcids haloacètics. Per fer-ho s'apliquen diferents tècniques estadístiques, des de l'anàlisi de correlació de Pearson fins a Models de Regressió Lineal Múltiple (MLR). En base als resultats obtinguts, aquest treball aposta pel desenvolupament de metodologies espectroscòpiques ja que poden ser utilitzades com a pont entre el coneixement avançat generat d'anàlisis exhaustius off-line amb una monitorització en línia d'una forma senzilla i econòmica.

D'una forma complementària es contrasta la informació obtinguda mitjançant la caracterització amb el mètode de HPSEC-DAD-OCD amb altres metodologies de caracterització avançades com fluorescència i espectrometria de masses d'alta resolució (HRMS).

En última instància, s'avaluen mitjançant una revisió bibliogràfica i integrant el coneixement derivat dels casos d'estudi, l'eficiència dels principals processos de tractament convencional i tractaments avançats i es proposen unes guies d'aplicació per a la seva implementació en potabilitzadores i contribuir a mitigar i minimitzar la formació de DBPs en concordança amb la legislació vigent.

El coneixement derivat d'aquest treball contribueix a l'Objectiu de Desenvolupament Sostenible (ODS) 6 de les Nacions Unides (UN), que vetlla per garantir la disponibilitat d'aigua i la seva gestió de manera sostenible, així com sanejament per a tothom. Especialment, s'aporta a les metes 6.3 i 6.4 relacionades amb la millora de la qualitat de l'aigua i una gestió eficient.

Las plantas potabilizadoras de agua son las responsables de producir y suministrar agua potable de calidad a los habitantes. Para ello, se combinan distintos tratamientos para eliminar contaminantes, materia orgánica disuelta, e inactivar patógenos que puedan comprometer a la salud de los consumidores. Una operación crítica del proceso de potabilización es la desinfección final, puesto que debe asegurar que el agua se encuentra libre de peligro microbiológico desde que sale de los depósitos de la potabilizadora hasta que llega a las casas. Esta se suele hacer típicamente con oxidantes derivados del cloro (hipoclorito, cloraminas o dióxido de cloro). Sin embargo, la adición de estos desinfectantes puede devenir una praxis con contrapartida. A pesar de que su adición contribuirá a controlar el riesgo microbiológico, una dosificación en exceso reaccionará con la materia orgánica que permanezca disuelta (DOM) y formará subproductos de desinfección (DBPs) una familia extensa de contaminantes con distintos grados de toxicidad.

Todavía hoy en día, el principal reto para los gestores y operadores de planta está en establecer el equilibrio entre asegurar la seguridad microbiológica y la toxicidad derivada por los subproductos de desinfección. Con tal de poder hacer un buen control de la calidad del agua a lo largo de los tratamientos en planta, es necesario disponer de marcadores para realizar el seguimiento de la eliminación de la materia orgánica, uno de los principales precursores de DBPs. Sin embargo, la elevada complejidad de dicha matriz (composición heterogénea, sujeta a cambios estacionales y específica del origen del agua), hace que esta actúe como una caja negra de la cual típicamente se monitorean parámetros sustitutos que actúan de reflejo de algunas de sus características fisicoquímicas generales como el contenido en carbono orgánico total (TOC) o su absorbancia.

Con el fin de llegar a optimizar los procesos de eliminación de materia orgánica en la potabilización de aguas y lograr así minimizar la generación de DBPs, es de vital importancia establecer marcadores específicos de la reactividad de dicha materia orgánica frente a la generación de subproductos. Y para ello es indispensable desarrollar un estudio detallado de las características de la materia orgánica que se halla en las aguas a tratar.

Este trabajo propone en primera instancia la puesta a punto de un método de caracterización avanzada basado en cromatografía de exclusión molecular (HPSEC) que permite separar los principales compuestos de una mezcla compleja como es la DOM en base a su peso molecular aparente. Dicha separación se combina con un detector de diodo array (DAD) y un detector de carbono orgánico disuelto (OCD) para determinar la signatura espectroscópica absorbancia de los compuestos en todo el rango de UV-VIS, respecto a su contenido en carbono orgánico.

A partir distintas campañas de muestreo en cuatro potabilizadoras situadas en el noroeste de Cataluña, se ha establecido una pequeña base de datos que ha servido para analizar en

profundidad las características de las principales fracciones de la DOM. Así se proponen distintos marcadores específicos de los atributos de la materia orgánica incluyendo el contenido de DOC y distintos parámetros espectroscópicos (longitudes de onda, pendientes espectroscópicos y absorbancia diferencial), para estudiar su relación con la formación de los subproductos de desinfección orgánicos que están sometidos a regulación: trihalometanos y ácidos haloacéticos. Para ello se aplican distintas técnicas estadísticas, desde análisis de correlación de Pearson hasta Modelos de Regresión Lineal Múltiple (MLR). En base a los resultados obtenidos, este trabajo apuesta por el desarrollo de metodologías espectroscópicas puesto que pueden ser utilizadas como puente entre el conocimiento avanzado generado de análisis exhaustivos off-line con una monitorización en línea de una forma sencilla y económica.

De forma complementaria se contrasta la información obtenida mediante la caracterización con el método de HPSEC-DAD-OCD con otras metodologías de caracterización avanzadas como fluorescencia y espectrometría de masas de alta resolución (HRMS).

En última instancia, se evalúan mediante una revisión bibliográfica e integrando el conocimiento derivado de los casos de estudio, la eficiencia de los principales procesos de tratamiento convencional y tratamientos avanzados y se proponen unas guías de aplicación para su implementación en potabilizadoras y contribuir a mitigar y minimizar la formación de DBPs en acorde a la legislación vigente.

El conocimiento derivado de este trabajo contribuye al Objetivo de Desarrollo Sostenible (ODS) número 6 de las Naciones Unidas (UN) que vela para garantizar la disponibilidad de agua y su gestión de forma sostenible, así como saneamiento para todos. En especial, se aporta para las metas 6.3 y 6.4 relacionadas con la mejora de la calidad de agua y una gestión eficiente.

Chapter I

INTRODUCTION

Water has historically been at the centre of civilisations, starting from the ancient basins of Tigris and Euphrates, the Nile, or the Huang, up to the current nations. Not only essential for ecosystems and living beings, but water also rules social development in terms of economic growth and poverty reduction; hence, it is worldwide considered a wealth and power symbol. However, to achieve progress, it is crucial to ensure access to safe and available water.

Since 2010, the human right to water and sanitation has been recognized by the UN General Assembly, declaring everyone has the right to safe, sufficient, continuous, affordable, and physically accessible water for personal and domestic use (World Health Organization, 2010). Despite improvements, still nowadays one out of three people lacks access to safe drinking water, which represents 2.2 billion people, predominantly congregated in rural areas, that miss these fundamental rights (United Nations, 2023). To take specific actions and fight those inequalities, the UN established the Sustainable Development Goals (SDG), where goal 6 looks after water availability and sustainable management of sanitation worldwide, to be reached by 2030.

Moreover, the increasing demand for water caused by rapid population growth pushing towards greater urbanization, industrialization, and agricultural and energy production, makes the current outlook a labile scenario. This, coupled with poor management, misuse, overexploitation, and contamination of water reservoirs through decades of aggrieved water stress promoting deterioration of water-related ecosystems with a direct effect on human health and economics. Recently, the experience of Covid-19 pandemic illustrates the vital importance of sanitation and appropriate access to clean water for minimizing disease spreading.

In view of this current global situation where scenarios evolve quickly, with higher and higher demands, and limited resources, treatments are in need of an imminent rethinking and shifting into more water reuse technologies (SDG 6.3). Imperatively, the evaluation of water quality should also evolve into more robust and resolute tools capable of promptly responding to these extreme environmental situations.

1. THE CONCERN: DISINFECTION BY-PRODUCTS

It was at the beginning of the 1900s that ultimate water treatment goals were focused on removing disease-causing microbes to reduce water-borne illnesses and subsequently increase life expectancy (US EPA, 1999). In such a way, disinfection processes became a widespread practice in communities, usually based on chlorine as the main disinfectant. However, in the early 1970s, a new type of contaminants was reported as a result of those processes, named trihalomethanes (THMs), a specific group of disinfection by-products (DBPs). The water matrix is a mixture of natural organic matter (NOM), that, in some cases, depending on the source and activities, can also contain halogens (bromide, iodide) and other types of contaminants such as effluent organic matter (EfOM), ammonium, or anthropogenic trace contaminants (e.g., pesticides, pharmaceuticals, etc.). All of those components can act as precursors to the formation of the undesired DBPs during disinfection reactions. The release of these contaminants after water treatment is usually at very low ranges of concentrations (in the order of $\mu\text{g/L}$), and if it were for their potential health risks, they would probably not be concerning. However, after several toxicological studies, the US Environmental Protection Agency started regulating THMs for their mutagenic and carcinogenic properties (US EPA, 1979). Later on, haloacetic acids (HAAs), bromate, and chlorite also entered Stage 1 and Stage 2 Disinfectants/DBP Rules in the 1990s (US EPA, 2001, 2005). Simultaneously, the first European Directive on the quality of water intended for human consumption (Directive 98/83/EC) was published in the European Union, where THMs and bromate were listed as

concerning pollutants. At the latest revision, it included haloacetic acids (HAAs), chlorite and chlorate among other concerning pollutants (Directive (EU) 2020/2184). Hereto, member States from the European Union must implement national laws to not exceed the following levels:

- › trihalomethanes (100 mg/L) as the sum of chloroform, dichlorobromomethane, dibromochloromethane and bromoform;
- › bromate (10 mg/L);
- › chlorate (0.25 mg/L; up to 0.70 mg/L in case of disinfection with ClO_2);
- › chlorite (0.25 mg/L; up to 0.70 mg/L in case of disinfection with ClO_2);
- › haloacetic acids (60 mg/L) as the sum of the following five representative substances: monochloro-, dichloro-, and trichloro-acetic acid, and mono- and dibromo-acetic acid.

From the perspective of drinking water utilities, finding the balance between disinfection procedures to ensure microbial safety without exceeding DBPs' legislation requirements and maintaining feasible costs is yet an uphill battle, specially under the increasingly common and prompt-changing scenarios. However, DBPs formation and fate should not be put aside during the reassessment of water technologies, particularly when minimizing their formation becomes one of the main preventive actions to adopt while their regulations remain controversial.

1.1 Classification of main concern disinfection by-products

Several classifications of DBPs can be sorted depending on the structure, properties, or occurrence. Here, first partition is made according to the standing European regulation.

1.1.1 Organic and inorganic regulated DBPs

Regulated organic DBPs account for C_1 and C_2 compounds, representing only 30% of total halogen (TOX) in chlorine disinfected drinking waters (Mitch et al., 2023, Figure 1). As trihalomethanes (THMs) and haloacetic acids are the most occurrent organic DBPs in chlorinated drinking waters (up to hundreds of ppb), they are considered representative of organic DBPs in the eyes of legislation, accounting for the sum of several compounds. Above all, chloroform, dichloroacetic acid, and trichloroacetic acid are the most abundant THMs and HAAs respectively (Gilca et al., 2020; Richardson et al., 2007; Richardson & Plewa, 2020).

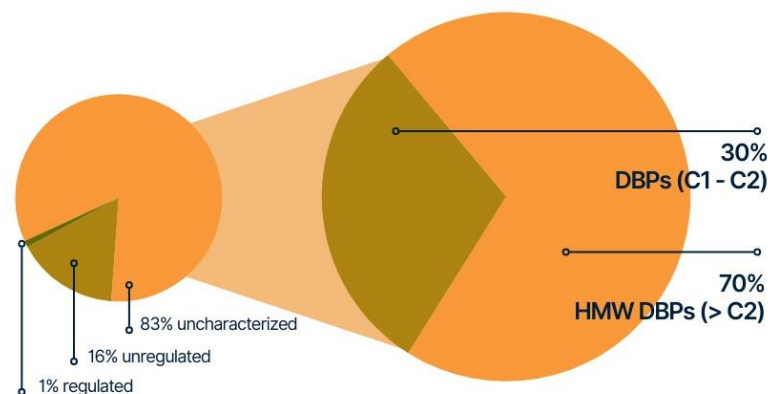


Figure 1: DBP distribution according to TOX (%), adapted from Mitch et al., 2023.

The formation of organic DBPs is a complex reaction between disinfectants and precursors, mainly including natural organic matter (NOM), as well as other species such as bromide or iodide, under given conditions of pH, temperature, and contact time. The contribution of this highly variable number of factors involved hinders establishing mechanistic approaches to a better understanding of their reactions. THMs structurally derive from a methane molecule where hydrogen atoms have been substituted with halogens (chlorine, bromine, or iodine). This rises to a total combination of 27 THMs, given the formation of the four following species the most relevant due to their occurrence: trichloromethane or chloroform (CHCl_3 , TCM), bromodichloromethane (CHBrCl_2 , BDCM), bromodichloromethane (CHBr_2Cl , DBCM), and tribromomethane or bromoform (CHBr_3 , TBM). In contrast to what might seem, the formation of THMs in chlorinated waters does not derive from reaction of chlorine with methane but it is a complex reaction between disinfectants and natural organic matter (Xie, 2004a).

Haloacetic acids (HAAs) are the second major group of DBPs formed in chlorinated drinking water. Structurally, this family of DBPs derive from a substituted acetic acid molecule that depending on the degree of substitution lead to the formation of three groups: monohaloacetic acids (CH_2XCOOH), dihaloacetic acids (CHX_2COOH) and trihaloacetic acids (CX_3COOH) which differ both in formation mechanisms and in chemical and biological properties. There are nine common HAAs: monochloroacetic acid (CH_2ClCOOH), monobromoacetic acid (CH_2BrCOOH), dichloroacetic acid (CHCl_2COOH), bromochloroacetic acid (CHBrClCOOH), dibromoacetic acid (CHBr_2COOH), trichloroacetic acid (CCl_3COOH), bromodichloroacetic acid ($\text{CBrCl}_2\text{COOH}$), chlorodibromoacetic acid ($\text{CBr}_2\text{ClCOOH}$) and tribromoacetic acid (CBr_3COOH). As with THMs, formation of HAAs derive from complex reactions between chlorine, bromine and NOM (Xie, 2004a).

Bromate (BrO_3^-), chlorite (ClO_2^-), and chlorate (ClO_3^-) are the most prevalent inorganic DBP. Hypochlorite is widely used as disinfectant but ageing of stock solutions may decompose simultaneously into chlorite and chlorate due to instability of hypochlorite ion (OCl^-). When chlorine dioxide is used as disinfectant, chlorate might be released after several conditions: i) from the generation of ClO_2 between sodium chlorite and free chlorine, ii) from the photodecomposition of ClO_2 at high pH ($\text{pH} > 9$), iii) from the reaction of the residual chlorite and free chlorine in secondary disinfection processes. Also, chlorite will be formed as an intermediate during the reaction between hypochlorite and chlorate (Gilca et al., 2020). Bromate is primarily generated from the oxidation of bromide during ozonation processes following different mechanisms that include the reaction with direct ozone, hydroxyl radicals, or pathways involving a combination of both (Xie, 2004b). Mainly, bromide is oxidized into hypobromous acid / hypobromite (HOBr/OBr^-) acting as an intermediate that leads to BrO_3^- through subsequent oxidations with O_3 or OH^\cdot . Another path goes through the final oxidation of bromine radicals (BrO^\cdot) after the generation of Br^\cdot previously released from the reaction between OH^\cdot and Br^- (Jahan et al., 2021).

1.1.2 Unregulated emerging DBPs (N-DBPs, I-DBPs, and HMW-DBPs)

With analytical improvements enabling lower detection limits, screening methodologies for DBPs strengthened, consequently increasing the number of reported by-products. Some of these new listed compounds, which are detected at very low concentrations in disinfected waters, can be named emerging DBPs (Gilca et al., 2020) and include nitrogenous-, iodinated-, and high molecular-weight DBPs. According to studies on their occurrence, formation, and toxicity; they appear to have the worst impacts on human health due to their cytotoxicity, genotoxicity, endocrine disruption, and carcinogenicity (MacKeown et al., 2022; Postigo & Zonja, 2019; Richardson et al., 2007; Wagner & Plewa,

2017). However, with limited information about their implications, they still remain unregulated in the EU and US.

When introducing nitrogenous DBPs (N-DBPs), there is a straight tendency to associate the generation of those pollutants with the direct use of chloramines as disinfectants. But the presence of nitrogen can also proceed from primary source waters, like in the case of wastewater effluent discharges (EfOM) that can contain considerable concentrations of ammonia or waters with high amounts of algal organic matter (AOM), where levels of organic dissolved nitrogen (DON) can also be significant to enhance the formation of those DBPs (Bond et al., 2011). Classification of most abundant N-DBPs is presented below Table 1.

Table 1: Summary of unregulated DBPs main species.

Main Family	Subclassification		Predominant Species	References
N-DBPs	Halogenated	Haloacetonitriles (HANs)	dichloroacetonitrile (DCAN)	(Bond et al., 2011; Gilca et al., 2020)
		Haloacetamides (HAcAms)	Dichloroacetamide (DCAcAm)	
		Halonitromethanes (HNMs)	Trichloronitromethane (chloropicrin)	
		Cyanogen halides	Cyanogen chloride (CNCl)	
	Non-halogenated	Nitrosamines	nitrosodimethylamine (NDMA)	
Inorganic	Nitrites, nitrates, and hydrazine			
I-DBPs	Iodomethanes (I-THMs):		dichloroiodomethane (CHCl ₂); bromochloroiodomethane (CHClI)	(Allard et al., 2015; H. Dong et al., 2019)
	Iodo-acetic acids (I-HAAs)		Iodoacetic acid (IAA)	
	Iodo-haloacetamides (I-HAMs)		Chloroiodoacetamide (CIIAM)	
	Iodo-aldehydes (I-HALs)		Iodoacetaldehyde (IAL)	
	Iodo-phenols (I-phenols)		2-iodophenol	
	Iodo-halocetonitriles (I-HANs)		Iodoacetonitrile (IAN)	
HMW-DBPs	> 1000 distinct elemental formulae detected in Chinese, Swedish and Spanish waters			(Mitch et al., 2023)

Chemical disinfection of waters containing iodide can result in another emerging family of DBPs known as I-DBPs (Table 1). Especially chloramination may lead to the formation of those compounds, but other oxidants such as permanganate, peracetic acid, ferrate, or ozonation can increase concentrations of I-DBPs (Bichsel & Von Gunten, 2000; MacKeown et al., 2022; Postigo & Zonja, 2019). In the first stage of the disinfection process, iodide is oxidized to hypiodous acid (HOI), which can subsequently react with NOM to form I-DBPs or be oxidized into iodate (IO₃⁻), a stable and safe end product.

Though I-DBPs usually range in low concentration levels (around ng/L to low µg/L), their occurrence has been reported worldwide (H. Dong et al., 2019; MacKeown et al., 2022). Both their cytotoxic and genotoxic effects are supposed to be worse than their brominated and chlorinated analogues (Krasner et al., 2006; Y. Yang et al., 2014). However, nowadays, I-DBPs are the only known group of DBPs that are not regulated in any country. One of the major concerns of those DBPs could be gaining ground when moving into upcycling water technologies, particularly those involving blending waters from

conventional treatments and waters from desalination processes, where concentrations of iodide could be relevant to the formation of those species when reacting with incoming NOM at the time of mixing.

Finally, there is a huge fraction (70% of TOX) that accounts for high-molecular-weight, non-volatile DBPs (HMW-DBPs, Table 1). Due to their physicochemical properties, HMW-DBPs are not amenable to being analysed by liquid chromatography coupled to mass spectrometry (LC-MS), so high-resolution mass spectrometry is required (Mitch et al., 2023). Recent studies report that this fraction of HMW-DBPs acts as an intermediate in early-stage reactions ending as C₁ and C₂ DBPs.

Unfortunately, there is still little information about all these emerging contaminants. Partly because of a lack of systematic measurements, mostly driven by the absence of quantification, as well as the need to develop analytical methods capable of reaching lower detection limits (MacKeown et al., 2022; Postigo & Zonja, 2019). Moreover, despite the knowledge about their potential toxicological activity, it is a must to obtain more conclusive studies about their human-health effects in order to push them into legislation. Overall, there is still plenty of room to cover when it comes to understanding the fate and effects of these DBPs, which call for new and advanced analytical techniques and collaborative research to face all the challenges associated.

2. THE PRECURSOR: NATURAL ORGANIC MATTER

2.1 Attributes of Natural Organic Matter

Water sources of drinking water ubiquitously contain natural organic matter (NOM) that derives from interactions with the environment (allochthonous NOM), the hydrologic cycle (autochthonous NOM), and though the name suggests the uniqueness of natural origins, organic compounds deriving from human activities are also included in the label. Thus, the characteristics, properties, and amounts of NOM are highly dependent on seasonality (Sillanpää, 2014). This heterogeneous and site-specific complex matrix of organic materials encompasses a wide range of compounds varying in chemical composition, molecular weight, and charge. The unique combination of functional groups (i.e., phenolic, carboxylic, hydroxyl, amino, nitroso, esteric, and quinone) constitutes a diversity of hydrophobic and hydrophilic compounds, ranging from 2 to 10 mg/L of dissolved organic carbon (DOC) in potable water sources, of which approximately 50% up to more than 90% correspond to hydrophobic acids, named humic substances (Crouè et al., 2000; Finkbeiner et al., 2020a; Matilainen et al., 2011). In turn, based on solubility criteria, humic substances can be sorted into (a) humic acids, which are soluble in alkali and insoluble in acid, (b) fulvic acids, which are both soluble in alkali and acid, and (c) humins, which are insoluble in both alkali and acid. Those hydrophobic NOM compounds contain a higher percentage of aromatic carbons, phenolic structures, and conjugated double bonds, whereas hydrophilic NOM is characterized by more aliphatic carbon structures and nitrogenous compounds like amino acids, carbohydrates, carboxylic acids, amino-sugars, or proteins.

NOM or DOM (dissolved organic matter) impacts significantly on water treatment, both affecting water quality (organoleptically causing odour, colour, or taste issues), acting as a carrier and complexation site for heavy metals and other hydrophobic organic chemicals, impacting performance of unit processes (responsible for biofilm growth, filter clogging and saturation, or corrosion). Moreover, NOM is considered as one of the major contributors to formation of DBPs. However, not all constituents account for the same reactivity: though hydrophobic and high molecular weight (HMW) NOM is reported to be responsible for major reactivity towards DBPs (Crouè et al., 2000; G. Hua & Reckhow, 2007), also

hydrophilic fractions and low molecular weight (LMW) compounds might impact the formation of DBPs during disinfection processes (Bond et al., 2009; G. Hua & Reckhow, 2007; Kitis et al., 2007).

That given, understanding the role and fate of the principal components conforming to this complex matrix seems to be of paramount importance to optimize their removal during treatment processes and consequently minimizing the formation of DBPs. In this sense, mastering the analytical techniques of advanced NOM characterization is essential to enabling an in-depth knowledge of fraction behaviour towards operational treatments.

2.2 Tracking NOM

Because of the high heterogeneity of NOM composition, the possibility of establishing a single and unique analytical methodology for its characterization is almost non-existent. No two compositions of NOM are alike in water sources, though they might have similar properties. At this point, the aim to evaluate each and every individual compound in the matrix makes no sense, whereas a more accurate approach is to group NOM molecules into categories (fractions) presenting similar characteristics: an operational classification based on the properties (e.g., hydrophobicity), structure (e.g., functional groups and moieties), or reactivity (e.g., DBP formation).

As far as each method targets a selective portion of NOM compounds (e.g., chromophores, fluorophores, hydrophobic vs. hydrophilic, etc) with sole measurements, only a single percentage of the overall composition can be outlined. Thus, the combination of several measurements has been adopted as the most feasible strategy to easily determine structural and/or compositional global transformations.

As a starting point, preliminary analyses to determine which combination of isolation, concentration and fractionation techniques is most suitable should be conducted. Usually, the amount of NOM present in a water sample is quantified as the amount of containing organic carbon (total and/or dissolved), and overall compositional information is determined from turbidity or suspended solids, and conductivity (as a surrogate for salt concentration).

Hereon, according to the multi-dimensional chemical entity of NOM, characterization can be assessed on four different tiers (Figure2, Crouè et al., 2000):

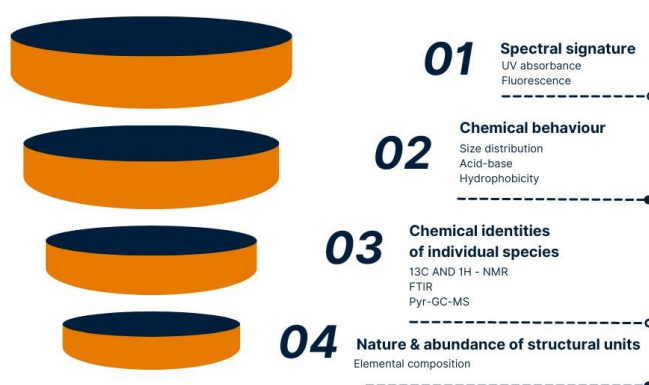


Figure 2: The four tiers of NOM characterization according to Crouè et al. (2000).

On a broader basis, the determination of the spectral signature of NOM in total is set, involving UV absorbance and fluorescence measurements. Both techniques present the advantage of experimental

simplicity (minimum to null pretreatment) paired with exceptional sensitivity, which makes them suitable for in-situ measurements while, also enabling easy tracking and quick data collection, making them ideal for generating historical databases. On a second level comes the study of the chemical behaviour of NOM, examining molecular size distribution, acid-base, and hydrophobic-hydrophilic properties. According to this, NOM compounds can be grouped into different classifications, as summarized in Figure 3. A further discussion on size exclusion will be provided afterward.

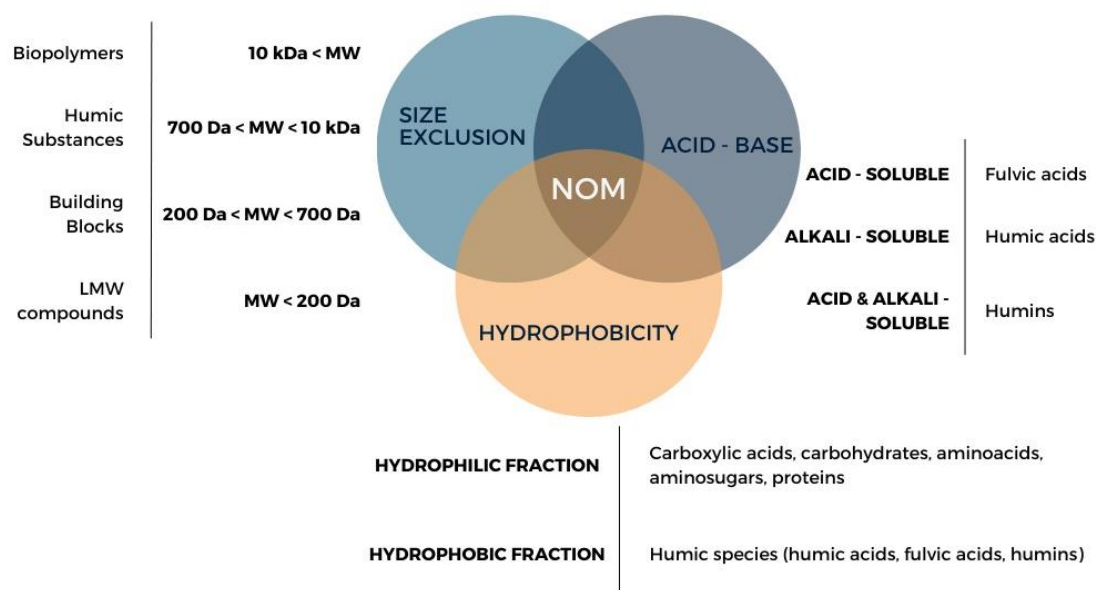


Figure 3: Methods for NOM characterization based on its chemical behaviour.

Narrowing down, steps three and four (Figure 2) account for specific chemical information, which requires substantial sample preparation compared to previous analyses and is consequently not suitable for point-of-use devices. Those methods comprise elemental composition analysis, ^{13}C - and ^1H - nuclear magnetic resonance (NMR) spectroscopy, Fourier-transformed infrared spectroscopy (FTIR), pyrolysis-gas chromatography-mass spectrometry (Pyr-GC-MS), and High-Resolution Mass Spectrometry (HRMS).

At one level or another, the importance of tracking changes in all of those NOM attributes is that they will indirectly reflect structural variations as a result of specific reactions, that is, their reactivity, which can be later correlated with the formation of DBPs or other emerging contaminants.

2.2.1 Size Exclusion

Particular emphasis is placed on size distribution separation, as it is one of the core methodologies of the present work. Here, size exclusion is achieved using the hyphenation of high-performance liquid chromatography (HPSEC) on a diode array detector (DAD) and an organic carbon detector (OCD). The methodological basis relies on the capacity of interaction of the analytes with the stationary phase of the chromatographic column. Thus, the smaller the molecule, the higher the ability to penetrate into the porous of the column, and consequently, the higher the retention time. Advantages of HPSEC include particularly minimal sample pretreatment and ease of operation. Moreover, compared to other separation technologies such as membranes, it is a more robust approach as it not only enables

apparent molecular weight (AMW) profiling but also quantification of fractions. What is achieved when HPSEC is coupled to multiple detectors such as organic carbon analysers or UV-VIS, resulting in a useful tool to tighten the gap between high compound identification potential techniques (e.g., MS detection-based) and high mass balancing potential ones (e.g., bulk DOC) (Cai et al., 2020; Her et al., 2003; Kawasaki et al., 2011). According to their molecular size, NOM compounds are typically divided into five main fractions named as biopolymers (MW > 10 kDa), humic substances (700 Da < MW < 10 kDa), building blocks (200 Da < MW < 700 Da), and low molecular-weight acids and neutrals (MW < 200 Da) (Crouè et al., 2000; Huber et al., 2011; Matilainen et al., 2011). Unveiling the molecular size distribution of NOM can help to understand its reactivity and provide insight on how to efficiently address water treatment works to reduce DBP formation (Krzeminski et al., 2019; Yan et al., 2012).

2.2.1.1 Methodology development

The selection of methodological parameters such as eluents, ionic strength, or pH will highly impact separation outcomes, promoting or suppressing nonideal interactions between the column stationary phase and analytes (Allpike et al., 2005), misrepresenting separation in terms of “real” molecular weight. This is important because in NOM complexity hydrophobicity, acid-base nature, and molecular weight, are all intimately related (Figure 3). A further discussion on the influence of the methodological setup is here assessed.

After years of research, several methods based on size exclusion chromatography for characterizing DOM attributes have been reported in the literature. Mostly, they derive from two principal approaches: tailor-made equipment (the Gräntzel thin-film reactor) designed and described by Huber & Frimmel (1991) or the hyphenation of available laboratory instrumentation following the set-up of Chin et al. (1994). A graphical contextualization of the most relevant state-of-the-art methods up to present and their relationships is presented in Figure 4.

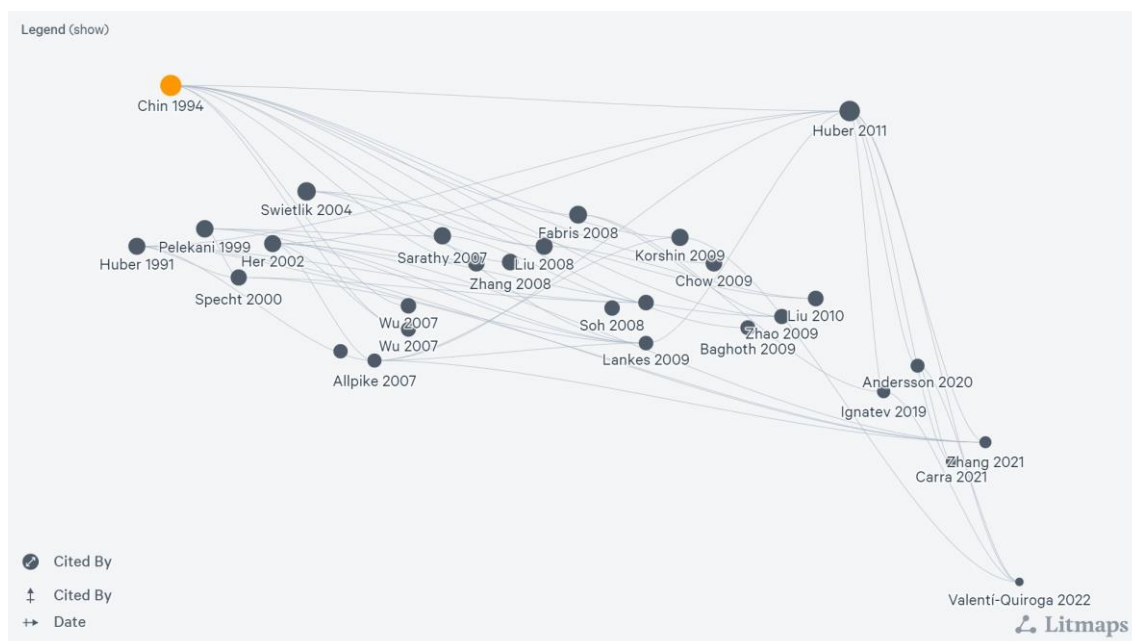


Figure 4: State-of-the-art links between SEC methods for NOM characterization.

A summary of the parameters of the most meaningful abovementioned methods related to UV-vis and DOC detection is listed in Table 2. A full table of the literature review is provided in the appendix (Appendix A, Table A 1)

Table 2: Summary of most relevant methodological parameters of SEC methods for NOM characterization.

LC -INSTRUMENT	INJ. VOL.	COLUMN (L x ID x particle size)	OVEN	RESIN TYPE	ELUENT (+IONIC STRENGTH)	FLOW	UV-VIS DETECTION	OCD	REF.
HPLC pump Solvent Delivery Module 112 (Beckman Instruments, USA) with sample injection pump P-500 (Pharmacia Biotech, Sweden)	1.5 mL	TSK HW-40 (900 mm x 16 cm x 30 µm), 50 Å pore size (Merk)		Hydroxylated methacrylate	Phosphate buffer (1.5 g/L Na ₂ HPO ₄ ·2H ₂ O +2.5g/L KH ₂ PO ₄), pH 6.37	1 mL/min	254 nm, UV-vis detector Model 200 Linear Instruments (USA)	OCD Gräntzel thin-film reactor	Huber & Frimmel, 1991
Waters 510 solvent pump (Waters Corporation, USA)	20 µL	Waters Protein-Pak 125 (300 mm x 19 mm x 10 µm), 125 Å pore size (Waters Corp., USA)		Glycol functionalised silica gel column	Phosphate buffer, pH 6.8 (+0.1 M NaCl)		224 nm, Waters 486 variable wavelength detector (Waters Corp., USA)		Chin & George Alken, 1994
LC-600 (Shimadzu Corporation, Japan)	150 µL 500 µL	Waters Protein-Pak 125 (Waters Corp., USA) Polyacrylamide Bio-Gel P-6 (Bio-Rad, USA) Toyopearl HW-50S (Tosoh Corp., Japan) Toyopearl HW-50S (250 mm x 22 mm x 30 µm), 125 Å pore size vs.		Glycol functionalised silica gel column Polyacrylamide Hydroxylated methacrylate	Phosphate buffer with NaCl Na ₂ SO ₄ (+0 to 0.15 M NaCl)		254nm, SPD-6A (Shimadzu Corp., Japan)	Modified Sievers Turbo Total Organic Carbon (TOC) analyser (Veolia, France)	Her et al., 2002
HP 1090 Series II (Hewlett Packard, USA)	100 µL 500 µL 2000 µL	semipreparative: Toyopearl HW-50S (250 mm x 10 mm x 30 um), 125 Å pore size (Tosoh Corp., Japan)		Hydroxylated methacrylate	10mM phosphate buffer (1.36 g/L KH ₂ PO ₄ + 3.58 g/L Na ₂ HPO ₄), pH 6.8	1 mL/min	254 nm, Photometric Detector (FPD)	OCD Sievers (Veolia, France)	Allpike et al., 2007
Waters Alliance 2690 (Waters Corp., USA)	1 mL	Protein KW-802.5 (300 mm x 8.0 mm x 5 µm), 400 Å pore size (Shodex, USA)	30 °C	Diol functionalised silica gel column	Phosphate buffer (1.5 g/L Na ₂ HPO ₄ ·2H ₂ O +2.5g/L KH ₂ PO ₄), pH 6.8	1.1 mL/min	MW: 205 nm to 285 nm (1.2 nm resolution), Waters 966 PDA, (Waters Corp., USA)	OCD Gräntzel thin-film reactor	Liu et al., 2010
S-100 HPLC pump (Knauer, Germany)	1 mL	Toyopearl HW-50S (250 mm x 20 mm x 30 µm), 125 Å pore size (Tosoh Corp., Japan)		Hydroxylated methacrylate	Phosphate buffer (1.5 g/L Na ₂ HPO ₄ ·2H ₂ O +2.5g/L KH ₂ PO ₄), pH 6.8	1.1 mL/min	254 nm, UVD S-200 (Knauer, Germany)	OCD Gräntzel thin-film reactor	Huber et al., 2011
LC-30AD (Shimadzu Corp., Japan)	50 µL	Yarra SEC-3000 (300 mm x 7.6 mm x 3 µm), 290 Å pore size, (Phenomenex, USA)	25 °C	Silica-based	5 mM phosphate buffer (0.45 g/L Na ₂ HPO ₄ ·2H ₂ O + 0.39 g/L NaH ₂ PO ₄ ·2H ₂ O), pH 6.8 (+0.1 mM)	1 mL/min	MW: 200 nm to 400 nm (1.2 nm resolution, 4.17 Hz), SPD-M20A PDA, (Shimadzu Corp., Japan)	TOC-L (Shimadzu Corp., Japan)	Ignatev & Tuhkanen, 2019
ACQ-QSM pump (Waters Corp., USA)	1 mL	Toyopearl HW-50S (250 mm x 25 mm x 30 µm), 125 Å pore size (Tosoh Corp., Japan)		Hydroxylated methacrylate	Phosphate buffer (1.6 mM Na ₂ HPO ₄ +2.4 mM NaH ₂ PO ₄), pH 6.8 (+ 0.1M Na ₂ SO ₄)	0.8 mL/min	254 nm, TUV Waters (Waters Corp., USA)	OCD Gräntzel thin-film reactor	Zhang et al., 2022

2.2.1.2 Application of the methodology

Since the first methodological development in the early 90s, the application of SEC methods has been employed in drinking water analysis for various purposes. This section provides a summary of principal applications based on results found in a Scopus search under the "Article Title, Abstract, and Key Words" (TITLE-ABS-KEY) filter. From a general overview, as summarized in

Figure 5, the first SEC method described and applied in drinking water analysis was based on the LC-OCD separation. Over 25 years, up to 69 publications have been released employing this method, of which only 15 are limited to disinfection/disinfection-by-product/chlorination topics. In comparison, HPSEC methods for drinking water analysis reached 70 publications in less than 10 years, with 11 exclusively focused on disinfection.



Figure 5: General timeline of SEC publications and their application in drinking water.

From a more detailed perspective (Figure 6), following the selection of disinfection-related publications employing SEC methods, LC-OCD has been predominantly employed for NOM characterization, particularly for evaluating fraction removal within treatments and their implications on DBPs formation potential (DBPs-FP). Only a few studies (3) specifically quantified correlations between LC-OCD fractions and FPs. Although fewer applications of HPSEC-hyphenated methodologies are reported, it has been preferred for developing predictive models for the formation of DBPs.

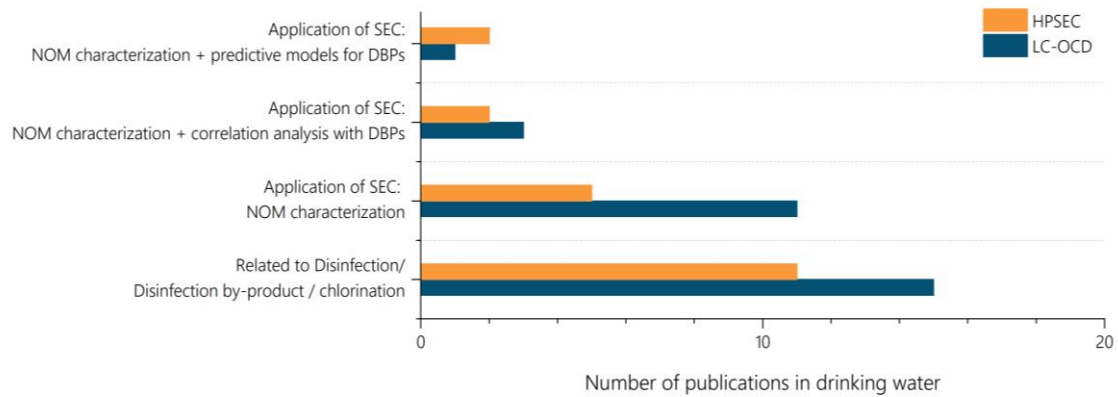


Figure 6: Detailed evaluation of SEC method applications in drinking water related to NOM and disinfection by-products.

As depicted in Figure 6, the number of publications of predictive models based on the SEC properties of NOM is still very limited. Usually, most models are based on surrogate NOM parameters (e.g., bulk TOC, A_{254} , differential absorbance, ΔA_{272} ...) and other water quality parameters (e.g., pH, bromide concentration, etc.) (Beauchamp et al., 2018; Chowdhury et al., 2009). Table 3 summarizes the details of predictive models for THMs and HAAs-FP based on SEC parameters.

Table 3: Summary of predictive variables for THMs and HAAs-FP models based on SEC of NOM.

SEC Method	Water type	Predictors (SEC variables)	DBP-FP	R^2_{adj}	Reference
HPSEC-OCD	Surface (China)	Humic Substances (~ 1650 Da) Building Blocks (~1300 Da)	THM-FP	0.92	Hidayah et al., 2017
HPSEC-OCD	Surface (China)	Humic Substances (~ 1650 Da) LMW (~630 Da)	HAA-FP	0.89	Hidayah et al., 2017
LC-OCD	Surface (UK)	Biopolymers (~10 KDa) Humic Substances (~ 1000 Da) LMW (~300-500 Da)	THMs-FP	0.925	Carra et al., 2021
LC-OCD	Surface (UK)	Biopolymers (~10 KDa) Humic Substances (~ 1000 Da) LMW (~300-500 Da)	HAAs-FP	0.897	Carra et al., 2021
HPSEC-DAD-OCD	Surface (Spain)	Biopolymers (~10 KDa) Humic Substances (10KDa – 700 Da) Building Blocks (700 – 200 Da)	THMs-FP (low Br)	0.994	Valenti-Quiroga et al., 2022
HPSEC-DAD-OCD	Surface (Spain)	Biopolymers (~10 KDa) Humic Substances (10KDa – 700 Da) LMW (< 200 Da)	THMs-FP (high Br)	0.980	Valenti-Quiroga et al., 2022

Findings from this literature review outline that SEC is a mature methodology with nearly 30 years of development. Its application still has room for further exploration, particularly in more qualitative approaches evaluating parameters derived from NOM characterization and its specific links with disinfection by-products.

2.3 Reactivity of NOM towards disinfection

Understanding the underlying mechanisms of NOM with disinfectants is hindered by the compositional variability of NOM. Overall reactivity will depend on NOM functionalities against disinfectants to form DBPs, though other parameters such as pH or temperature might also play a considerable role in DBP formation and speciation.

Disinfection by-products are mainly originated by the hydrolyzation of NOM moieties during the disinfection process, entailing several step-forward reactions and the formation of many intermediates. This process can be greatly affected by the presence of other inorganic halogens, like bromide. Although bromide does not directly react with NOM, when in the presence of oxidants (e.g., hypochlorite) it will rapidly form hypobromous acid and hypobromite, which are highly reactive towards organic moieties (up to 3 orders of magnitude higher than chloride) such as phenolic groups and ketones ($k_{app} = 10^3\text{-}10^5 \text{ M}^{-1} \text{ s}^{-1}$ at pH 7, Xie et al., 2004). The basic reactions of bromine and chlorine are presented in the following table (Table 4), including kinetic constants and rates that contribute to explain the speciation of DBPs during disinfection processes.

Table 4: Main reactions of chlorine and bromine involved in DBPs formation (Heeb et al., 2014).

Reaction	Equilibrium constant	Rate constants
$\text{HOCl} \leftrightarrow \text{OCl}^- + \text{H}^+$	$\text{pK}_a = 7.47$	
$\text{HOCl} + \text{Br}^- \leftrightarrow \text{HOBr} + \text{Cl}^-$	$1.5 \times 10^5 \text{ M}$	$k_1 = (1.55\text{-}6.84) \times 10^3 \text{ M}^{-1} \text{ s}^{-1}$
$\text{HOBr} \leftrightarrow \text{OBr}^- + \text{H}^+$	$\text{pK}_a = 8.8$	
$\text{Cl}_2 + \text{H}_2\text{O} \leftrightarrow \text{HOCl} + \text{Cl}^- + \text{H}^+$	$1.04 \times 10^{-3} \text{ M}^2$	$k_{13} = 2.23 \times 10 \text{ s}^{-1}$

Operational parameters such as doses, pH, temperature, and reaction times are crucial for reaction yields during disinfection reactions. In general, higher doses result in higher amounts of DBPs. For instance, at a fixed Cl_2 concentration, DBPs increase with increasing DOC only if Cl_2 free residual is present, favouring the formation of chlorinated species of organic DBPs (THMs and HAAs) (Chellam & Krasner, 2001). Moreover, the ratio of oxidant to DOC (Fabbricino & Korshin, 2004) is key to the speciation of DBPs. Besides, it's not only a matter of concentration but also reaction time. End products of NOM chlorination (THMs and HAAs) are generally increased after higher contact times, while some intermediates (e.g., dichloroacetonitrile and dichloropropanone) usually decrease after time, and some other DBPs, such as trichloropropanone, can be hydrolysed, also resulting in a diminution in their final concentration (Xie et al., 2004).

Both temperature and pH also interfere with the kinetics of DBPs formation. Since pH directly impacts hydrolysis reactions in aqueous media, DBP yields and speciation will also be influenced by the specific conditions. In chlorination, mostly higher pH results in higher THMs, and lower HAAs and TOX (Xie et al., 2004) due to the speciation of chlorine ruled by the equilibrium between HClO and ClO^- . In the case of ClO_2 , a low acidic pH should be preserved to minimize its decomposition and avoid the formation

of chlorate and chlorite. Also, in ozonation processes, increasing pH might increase ozone decay, diminishing the oxidation of DOM. Similar to the pH effect, increasing temperature tends to increase end by-product formation because of the faster kinetics, unless further degradation/volatilization takes place (Singer, 1992). In many cases, considerable intra-seasonal (short-term) and seasonal (long-term) variations in water temperature lead to pronounced variability in DBPs concentrations in drinking water (Abd El-Shafy et al., 2000.; Sérodes et al., 2003; Toroz & Uyak, 2005).

Moreover, the use of different reagents as disinfectants might lead to the speciation of one or another by-product. Free chlorine produces several DBPs, driven by higher amounts of total organic carbon and bromide concentrations. But fewer amounts of halogenated DBPs such as THMs or HAAs, will be formed with chloramines or chlorine dioxide. However, chloramination can enhance the formation of N-DBPs such as N-nitrosamines (Vikesland Y, Kenan Ozekin & Valentine, 2001), whereas ClO₂ might be the precursor of inorganic DBPs such as chlorite and chlorate. On the other side, disinfection via ozonation can produce biodegradable DBPs such as aldehydes, ketones, and carboxylic acids (Jahan et al., 2021), and the main related concern in this case is the formation of bromate and Br-DBPs (bromoform, brominated acetic acids, acetonitriles, or bromopicrin) that might form in bromide-containing waters resulting from the hypobromite anion (OBr⁻) and hypobromous acid (HOBr) equilibrium.

2.4 DBP minimization in conventional water treatment trains

To successfully minimize occurrence of DBPs in drinking water treatment plants (DWTPs), it is of paramount importance to understand the role of the different factors affecting their formation, as already discussed. Thus, depending on the focus, several strategies for minimizing DBP can be adopted, starting with the removal of (pre)formed DBPs, switching and/or combining disinfectants, or removing precursors (including both DOM and inorganic compounds) (Figure 7).

From an operational standpoint, selecting the most suitable strategy will depend on the specific circumstances of each plant. Otherwise, a single course of action could, in many cases, lead to a loss of resources. For example, techniques for removing already-formed DBPs (e.g., adsorption, biodegradation, membrane filtration technologies) prior to the final disinfection are an ideal approach when dealing with waters that already contain specific levels of those pollutants or when considerable amounts are attained during the treatment process itself.



Figure 7: Summary of strategies for DBP minimization in drinking water treatment procedures and most effective treatments (in brackets non-conventional processes).

The removal of precursors acts as a preventive measure. However, the optimization of treatments will depend on the water quality of each case study. Here, a brief summary of the mechanisms involving the most common conventional configurations in DWTPs is presented. A further discussion regarding the state of the art of novel alternative methodologies to minimize DBPs will be given in the results section.

2.4.1 Separation mechanisms: filtration, coagulation, and adsorption

Filtration processes, such as sand filtration (rapid and slow) or microfiltration themselves, are incapable of removing DOM at preventive levels for DBP formation. For that reason, a previous coagulation–flocculation step followed by clarification must be added to ensure effectiveness. Enhanced coagulation refers to the optimized process for the removal of DBP precursors, thus high molecular weight organic matter fractions are withdrawn, typically employing alum or ferric-based coagulants. Yet, other potential precursors of lower molecular weight, e.g., free amino acids, could remain in the effluent.

Porous adsorbents, such as activated carbon (AC), in powdered (PAC) or granular (GAC) form, are widely used in drinking water purification to retain colour, odour, taste, and organic contaminants, including DBP precursors (Ding et al., 2019). Effectiveness will depend on the filter design, configuration, concentration of precursors, and kinetic parameters. However, AC poorly removes DON or inorganic precursors (i.e. Br⁻) thus, increasing ratios of DON/DOC and/or Br/TOC and consequently enhancing the formation of N-DBPs / Br-DBPs. Also, filtration and adsorption mechanisms can affect the molar ratios of Br-DBPs to Cl-DBPs impacting overall toxicity.

Deriving from adsorption, biodegradation is a mature technology widely used to control the DBP levels in many DWTPs. Particularly, the biological activated carbon process can effectively decrease the formation potential of volatile and nitrogen- containing DBPs (Bond et al., 2011) as it can remove a fraction of the precursors of halogenated DBPs (THMs, HAAs, HKs, HAs, HANs, HAMs, and HNMs), while also demonstrating capability in removing bromate and halogenated DBPs, except for THMs (Ersan et al., 2019). Consisting of a conventional granular filter designed to remove particulates and dissolved organic matter through microbially mediated degradation, organic matter itself is utilized as substrate by the filter bacteria for cell maintenance, growth, and replication, so the overall process is cost-effective and does not require residual disposal. The filter media can be sand, anthracite or GAC

and the only prerequisite for maximizing bacteria in the absence of disinfectant in the filter influent or backwash water. Generally, biodegradation is employed after ozonation as a pre-oxidative procedure, which will be discussed later.

2.4.2 *Disinfection*

Even so, sometimes the effectiveness of those abovementioned measures is not enough to minimize formation of DBPs. As not all disinfectants have the same impact on NOM and precursors, they can enhance the formation of different DBPs. For that reason, considering alternative methods as complementary measures can help improve the final performance of DWTPs.

Switching conventional disinfectants to alternative reagents is one of the most conservative options in terms of implementation and plant configuration. Compared to chlorine (hypochlorite), chloramines, chlorine dioxide, or ozone produce less amounts of halogenated C-DBPs like THMs and HAAs; but the formation of N-DBPs (e.g. NDMA) or inorganic DBPs (ClO_2^- and ClO_3^-) could be enhanced. Additionally, ClO_2 or O_3 lack a stable residual, so a secondary disinfectant might be necessary to ensure oxidative effects throughout the distribution system, depending on specific regulations, as is the case in Spain.

Also, optimising the position of disinfection points along the treatment train can turn into a successful practice to control DBP formation without compromising disinfection against pathogens. If possible, combining a primary disinfection (pre-oxidation) to reduce both organic and inorganic precursors coupled with a final boost disinfection able to ensure a stable residual dosage to maintain microbial safety in the distribution system can lead to substantial DBP reductions of up to 50% of regulated THMs and HAAs, as reported by Rougé et al. (2020).

Amongst all these possibilities, characterizing and performing an in-depth analysis of the water matrix to identify which are the main DBP precursors is crucial for establishing the optimum disinfection configuration with the most suitable reagent so DBP formation is mitigated without compromising final water quality.

Chapter II

OBJECTIVES

The general aim of the present thesis is to study the relationship between natural organic matter, assessed as dissolved organic matter (DOM), and disinfection by-products using different advanced characterization techniques. The main questions that motivated this research are the following ones:

1. Is it possible to effectively assess DOM changes by size exclusion using a hyphenated chromatographic laboratory setup?
2. Do the detected DOM changes correlate with the formation potential of DBPs? How can they be quantitatively assessed? Do these variations in DOM distribution help us understand the efficiency of drinking water treatments?
3. What distinguishes size exclusion chromatography (SEC) from other analytical methods in terms of DOM characterization? Which benefits and drawbacks might the technique entail?

To tackle those research questions, the specific objectives to achieve are listed below:

- › Set up and optimize a methodology for assessing the apparent size distribution of DOM compounds dissolved in drinking water samples using SEC coupled to an online diode array detector (DAD) and a dissolved organic carbon detector (OCD): HPSEC-DAD-OCD. This section is mainly discussed on Chapter IV.
- › Investigate the changes in DOM SEC profiles following operational treatments in drinking water samples as well as specific changes driven by chlorination processes and determine possible correlations with the variations in the formation potential tests of DBPs employing different statistical approaches. Compare the effects of treatments on various drinking water sources and seasonal effects. Those objectives are addressed on Chapters V and VI.
- › Contrast various analytic approaches for characterizing DOM changes caused by disinfection reactions: from bulk analysis (TOC, absorbance, fluorescence) to advanced characterisation (HPSEC-DAD-OCD, HRMs). The comparison is extended on Chapter VII.

Chapter III

MATERIALS & METHODS

According to the objectives of the thesis, different analytical procedures have been employed to deal with NOM characterisation. Methodologies range from single measurements to determine bulk water quality parameters, up to the most sophisticated analysis such as high-resolution mass spectrometry (HRMS). Moreover, statistical methods for data treatment have also been applied according to each specific objective and results. All methodologies are detailed below.

1. GENERAL WATER QUALITY PARAMETERS

The summary of the methods for bulk water quality parameters is presented in Table 5. Those methods are usually performed to track water quality in drinking water treatment plants (DWTPs).

Table 5: Standard protocols for water samples quality measurements.

Parameter	Method / Conditions	Instrument
Conductivity	Standard Methods 2510 Conductivity	Multimeter MM 41, Crison
pH	Standard Methods 4500-H+ pH	pH 110, VWR
Ion chromatography	Eluent: sodium hydrogen carbonate and sodium carbonate: 0.168 g NaHCO ₃ , 0.678 g Na ₂ CO ₃ up to 2 L MilliQ. Chemical suppressor (cartridge with 3 resins) Run time: 41 min Injection volume: 40 µL Flow: 0.7 mL Oven temperature: 45 °C Injection loop: 250 µL Columns: precolumn (Metrosep A Supp 16 S-Guard/4.0) connected to Metrosep A Supp 7 - 150/4,0	Ionic chromatograph 882 Compact IC plus, Metrohm
Turbidity	Standard Methods 2130 Turbidity	TU5200, HACH
TOC	Sparging time: 7 min Acid ratio (HCl 2N): 1.5% Dilution rate: 1 Injection volume: 50 µL	TOC V-CSN analyser, Shimadzu
Absorbance	Detection wavelength: 200 nm to 600 nm Bandwidth: 1 nm Optical path: 5 cm	Cary UV-VIS compact, Agilent
Free Chlorine	DPD colorimetric method based on Standard Method 4500-Cl G	HI701 HANNA instruments (detection range 0 – 2.5 mg/L)
Free Chlorine	DPD colorimetric method based on Standard Method 4500-Cl G	LCK310 kits, HACH (detection range 0.05 – 2 mg/L)

2. DOM FINGERPRINTING

This subsection summarizes all the employed methods to perform DOM characterisation in terms of molecular weight distribution (HPSEC-DAD-OCD), spectroscopical properties (EEM), and molecular mass formula (HRMS).

2.1 Size Exclusion

The methodology for SEC characterization of DOM (HPSEC-DAD-OCD) was set up by hyphenating available instrumentation: Agilent 1260 Infinity II HPLC with a 1260 vial sampler and a diode array detector (DAD) coupled to Sievers M9 SEC organic carbon detector (OCD). Detailed parameters are listed in Table 6. Molecular weight separation was achieved using two analytical columns in series to increase column capacity and improve peak resolution, covering a MW cut-off from 100 Da to 500 kDa, with a baseline around 60 ppb DOC. System void volume was approximately 12.35 mL (elution time 16.60 min) determined with polystyrene sulfonate (PSS) 77 kDa (effective MW of 80,100 Da, PSS Polymer Standards Service GmbH), and the permeation volume was 27.27 mL (elution time 36.36 min), determined with acetone. Both size exclusion columns were calibrated with PSS standards, individual standards of humic and fulvic acid from the Suwannee River (3S101H and 3S101F, International Humic Substance Society), amino acids, and organic acids covering MW values from 204 Da to 77 kDa (Appendix B, Table A 2).

Table 6: HPSEC-DAD-OCD methodological parameters (Valenti-Quiroga et al., 2022a).

HPSEC	Autosampler temperature	4 °C
	Injection volume	400 µL
	Eluent	6.8 pH phosphate buffer with 0.1 M of ionic strength (0.2880 g/L NaH ₂ PO ₄ + 0.2864 g/L Na ₂ HPO ₄ · 2 H ₂ O + 3.5 g/L Na ₂ SO ₄ , from Sigma Aldrich)
	Flow rate	0.75 mL/min (0-45 min), 1 mL/min (45-60 min)
DAD	Columns	PL Aquagel-OH (7.5 × 300, 5 µm) × PL Aquagel-OH MIXED-M (7.5 × 300 mm, 8 µm), Agilent
	Column oven	25°C
	Sweep range	190 nm to 640 nm (2 nm step)
OCD	Acquisition rate	4s response time (1.25 Hz)
	Optical slit	1 cm
	Acquisition rate	4 s
	Oxidiser rate	2 µL s ⁻¹ (15% (NH ₄) ₂ S ₂ O ₈)

After HPSEC-DAD-OCD analysis, DOM fractions are mainly classified according to DOC signal as follows (Table 7):

Table 7: Summary of DOM fractions analyzed by HPSEC-DAD-OCD.

Signal	Fractions					
		Biopolymers	Humic substances	Building blocks	LMW acids	LMW neutrals
DOC	AMW	AMW > 10 kDa	10 kDa > AMW > 700 Da	700 Da > AMW > 200 Da	< 200 Da	
	Rt	10.8 – 17 min	17 – 24 min	24 – 30 min	30 – 60 min	

2.2 Fluorescence Excitation – Emission Matrix

Fluorescence excitation-emission matrices (EEM) measurements were performed following the detailed parameters in Table 8, using a Cary Eclipse Fluorescence Spectrophotometer, Agilent with Scan Application v.1.2 (147).

Table 8: EEM methodological parameters.

Cuvette	Quartz, 10 mm
Excitation	200 nm – 450 nm
Excitation slit	5 nm
Emission	250 nm – 580 nm
Emission slit	5 nm
λ increment	5 nm
Scan rate	2400 nm/min
PMT voltage	700 V

EEM and UV-abs (200 nm to 400 nm, 1 nm intervals) scans of organic-free water (AG00062500 Water, LC-MS, Sharlau) were used as a control to remove Raman scatter and inner filter effects in posterior data treatment. The data processing was performed following a peak-picking method that identifies DOM components based on their maximum intensity at given excitation/emission pairs (Table 9, Sgroi et al., 2017). Though it is a suitable technique for on-point sensors due to its ease, it might be limited to overlapping, shifts, or interferences between peaks (Carstea et al., 2016).

Table 9: Fluorescence peak-pairs correlated to DOM features adapted extracted from Sgroi et al., (2017).

Peak	Ex / Em (nm)	DOM attribute
I 1	225/290	Aromatic proteins, tyrosine-like
I 2	225/340	Aromatic proteins tryptophan -like
I 3	245/440	Fulvic-like, humic-like
I 4	275/345	Biopolymers, proteins, microbial byproducts, and tryptophan-like
I 5	345/440	Fulvic-like, humic-like

2.3 High Resolution Mass Spectrometry

For the High Resolution Mass Spectrometry (HRMS) analysis, first a DOM solid phase extraction (SPE) through cartridges was performed according to the described procedure by Sanchís et al. (2020b). Prior to the extraction, the SPE cartridges were washed with 1 mL of methanol three times the day before and left soaked overnight in 1 mL of methanol. Right before starting the extraction, cartridges were conditioned with 3 mL of formic acid 0.1% (v/v), and then a 2.5 L sample was loaded under vacuum (~2 mL/min). After the elution, cartridges were washed with 3 mL of formic acid 0.1% (v/v) and dried under vacuum for 15 min. Finally, extracts were eluted with 2 mL of methanol, applying pressure to maximize the recovery of the solvent. Extracts were collected in previously weighted liquid chromatography vials and stored at -20°C until their instrumental analysis with the HRMS spectrometer.

Extracts were injected in a LC-HRMS (Orbitrap Exploris 120) using a C18 Hypersil Gold (50 x 2.1) column from Thermo Scientific. Water 0.1 FA and acetonitrile 0.1% FA were used as the mobile phase. Acquisition was achieved using negative-mode electrospray ionization (ESI). A full scan mode (m/z 100 to 1000) with a 120,000 full width at half maximum resolution was set for data acquisition. The acquired HRMS spectra were exported in ".xlsx" format from the software (Xcalibur), and data was processed with a

custom script in R (v 4.1.1) to first remove noise signals from the spectra using the MFAAssignR package. Ultra Mass Explorer (Leefmann et al., 2019) was used to assign to each feature (signal) an empirical formula (Merder et al., 2020).

3. DISINFECTION BY-PRODUCTS

Here, methods used for the formation, identification, and quantification of DBPs that have been used through the development of the project are described.

3.1 Formation potential tests

The procedure for the formation potential (FP) test was adapted from Standard Methods 5710 A. Chlorination of samples (60 mL) was performed at standard conditions at pH ~7 adjusted with 1.24 mL of phosphate buffer (0.1 M), with an excess of free chlorine (from a NaOCl stock solution). The incubation periods ranged from 24 h to 48 h at 21 - 25 °C. At the end, a residual of at least 1 mg/L of free chlorine is required and must be quenched prior to posterior analysis.

In order to adjust the desired free chlorine residual, it is important to test the chlorine demand of each sample. For that reason, it is suggested to test three different doses of disinfectant during incubation. Based on previous experiences, samples with amounts of ~3 mg/L TOC doses ranging from 2 to 6 ppm of chlorine aim to lead to a residual chlorine level of around 0.5 to 1 ppm after 48 h of reaction. Once the incubation period was over, one of the duplicates was used to determine free and total chlorine, selected the doses that provided the desired concentrations and performed the quenching. Quenching agents depend on the subsequent analysis; a summary is provided in Table 10. After the quenching, samples were stored at 4°C until the extraction, but should not exceed 5 days.

Table 10: Quenching reagents summary.

Following Analysis	Quenching Agent	Dosage	Reference
DBP analysis	Ascorbic acid	2.5 mg/L per 1 ppm free chlorine	Sylvia Barrret
HPSEC-DAD-OCD / AOX	Sodium sulphite	3.5 mg/L per 1 mg/L of free chlorine	Farré et al., 2013
EEM	Ascorbic acid	2.5 mg/L per 1 ppm free chlorine	Sgroi et al., 2020
HAAs (CSIC)	Ascorbic acid	2mL of a 0.018mg/L solution in 1L of sample to quench 1 ppm free chlorine	Planas et al., 2019

3.2 DBP analysis

Two different methods had been tested to conduct analysis of DBPs. While both methods used gas chromatography to perform separation and mass spectrometry for detection (GC-MS), the main difference relied on the extraction process.

3.2.1 Head Space – Gas Chromatography – Mass Spectrometry (HS-GC-MS) analysis

A first method using headspace gas chromatography was optimized for the extraction of volatile DBPs, targeting the analysis of the four regulated THMs (TCM, BDCM, DBCM, and TBM). As an advantage, this method required little sample preparation, however it was limited to the analysis of THMs. Full analysis was performed with PAL RSI 85 tool for the headspace incubation and extraction coupled to a 7890B GC System and 5977B MSD from Agilent. Detailed parameters are summarized in Table 11.

Table 11: HS-GC-MS methodological parameters.

HEAD SPACE	Sample volume	12 mL	
	Incubation period	15 min	
	Incubation temperature	60 °C	
	Injection volume	1.5 mL	
	Injector temperature	200 °C	
	Split	6:1 (split ratio; split flow: 6 mL/min)	
	GC	Septum purge flow	3 mL/min
		Carrier gas	He
		GC - Column	HP-5MS UI 30 m x 250 µm x 0.25 µm
		Oven programme	40°C (2 min), 20°C/min up to 60°C (2 min), 20 °C/min up to 100 °C, 50°C/min up to 250°C (2 min)
Solvent Delay		0.50 min	
MS	Transfer line temperature	250 °C	
	Ionization voltage	Applied EM Voltage 1282	
	Acquisition type	SIM	
	R _t & m/z ions	0.50 min CHCl ₃ (m/z: 47, 83, 85)	
		2.00 min CHBrCl ₂ (m/z: 47, 48, 83)	
2.80 min CHBr ₂ Cl (m/z: 127, 129, 131)			
	4.00 min CHBr ₃ (m/z: 171, 173, 175)		

Qualitative and quantitative analysis was performed with Mass Hunter Workstation Software (version B.07.00).

The calibration curve for each THMs was performed preparing a dilution bank from the calibration mix (EPA 501/601 Trihalomethanes Calibration Mix 2000 µg/mL each in methanol, Supelco, 4M8140-U) at concentrations of 0.5, 5, 10, 25, 50, 75, and 100 µg/L. Each standard was analysed in triplicate; retention times, LODs, and equations are presented on the Appendix. (Appendix B, Table A 3).

3.2.2 Liquid-Liquid extraction and GC-MS analysis

This second method enabled the identification and quantification of THMs (TCM, BDCM, DBCM, TBM) and other nitrogenated DBPs: dichloroacetonitrile (DCAN), trichloroacetonitrile (TCAN), bromochloroacetonitrile (BCAN), dibromoacetonitrile (DBAN), 1,1-dichloropropanone (1,1-DCP), 1,1,1-trichloropropanone (1,1,1-TCP), and trichloronitromethane (TCNM).

The liquid-liquid extraction was performed following an adapted procedure from Standard Methods 5710 A. Prior, the extraction solution was prepared with Methyl-t-Butyl Ether (MtBe, 443808, Sigma Aldrich) containing 100 µL of the Internal Standard (IS) 1,2-dibromopropane (99+%, 140961, Sigma Aldrich). Then, 30 mL of sample were placed on vials, and pH was adjusted to approximately 3.5 with a 0.2 N H₂SO₄ (ACS grade) solution (note that not each sample might require the same amount of acid, so it is recommended to test before batch-adding). After, 3 mL of the extracting solvent MtBe were added to each sample containing the IS. Approximately 10 g of sodium sulphate were then added into samples and immediately vortexed for 1 min to avoid clumping of the salt. After settling for 5 min, ~1.5 - 2 mL of the organic layer (MtBe layer) were separated with a disposable glass Pasteur pipette and transferred to a GC autosampler vial, ensuring no crystals of sodium salts nor water were grabbed. Two vials per sample were filled: one for the analysis and one backup. Vials were stored at the freezer (-15°C) avoiding light exposure prior to analysis.

The calibration curve for the DBP quantification must be extracted for each batch analysis. Following the same procedure, extracts of 0.1, 1, 5, 10, 20, 50, and 100 µg/L concentrations were prepared from stock solutions containing EPA 551B Halogenated Volatiles Mix 2000 µg/mL each in methanol (Supelco, US010990), and EPA 501/601 Trihalomethanes Calibration Mix THM mix 2000 µg/mL each in methanol (Supelco, 4M8140-U).

The method for DBP separation and quantification was adapted from the Standard Operating Procedure for DBP Analysis (SOP No.: AWMC-60-624-0009.01) using TSQ Quantum 9000 triple quadrupole mass spectrometer system from Thermo Fisher Scientific (Waltham, MA, USA). The detailed parameters are summarized on Table 12.

Table 12: GC-MS methodological parameters for DBP analysis.

GC	Injection volume	2 µL
	Injector temperature	200 °C
	Split mode	Splitless
	Carrier gas	He (UHP), 1.5 mL/min
	Makeup gas	N ₂ (UHP)
	GC - Column	DB-5 Agilent (30 m length x 0.25 mm inner diameter x 1.0 µm film thickness)
MS	Oven programme	35 °C (5 min), 10°C /min up to 100 °C, 20°C /min up to 200 °C (1 min)
	Transfer line temperature	280 °C
	Source temperature	250 °C
	Ionization voltage	70 eV
	m/z ions	See list on Appendix B, Table A 4

For the analysis of HAAs, an online solid phase extraction (SPE) with liquid chromatography and mass spectrometry (LC-ESI-MS/MS) with TSQ Quantum triple quadrupole mass spectrometer from Thermo Fisher Scientific was followed (Planas et al., 2019). Analysed HAAs included: monochloroacetic acid (MCAA), monobromoacetic acid (MBAA), dichloroacetic acid (DCAA), dibromoacetic acid (DBAA), trichloroacetic acid (TCAA), and the sum of the five (HAA₅).

3.3 Adsorbable organic halides

Adsorbable organic halides (AOX) and their speciation as AOCl, AOBr, and AOI were analysed to report the halogen concentration in the samples after the chlorination. After homogenizing and filtering the

sample through 0.45 μm pore size filter, an aliquot of 100 mL was acidified with 5 mL of nitric nitrate stock solution (17 g NaNO_3 + 25 mL HNO_3 (65%) in 1 L H_2O). The acidified sample was adsorbed onto 50 mg of activated carbon AOX cartridges from Envirosience (Düsseldorf, Germany) at a flow rate of 3 ± 0.1 mL/min using the AOX TXA04 module. After, rinsing of the cartridge is performed by adding 25 ml of nitric nitrate wash solution to desorb all inorganic halide impurities. Next, the activated carbon cartridge is transferred to ceramic boats for pyrolysis at 1000°C at the Mitsubishi AQF-2100H Combustion Unit connected to the Ion Chromatograph (IC) system (Dionex Integrion HPIC from Thermo Scientific to quantify the resulting ions based on the concentration of Cl^- , Br^- and I^- .

4. STATISTICAL METHODS

Finally, this subsection summarised the most meaningful statistical methods used for data treatment.

4.1 Multiple Linear Regression (MLR)

In order to explore possible associations between the outputs coming from the different experimental analyses, MLR models were tested to evaluate the correlation between parameters through adjusting linear regressions, as follows (Eq. 1):

$$Y = \beta_1 x_1 + \beta_2 x_2 + \dots + \beta_n x_n \quad (\text{Eq. 1})$$

where β_i are coefficients corresponding to the different predictors (x_i). To rate the models, adjusted determination coefficients R^2_{adj} , were calculated as following (Eq. 2):

$$R^2_{\text{adj}} = 1 - \left[\frac{(1 - R^2)(n - 1)}{n - k - 1} \right] \quad (\text{Eq. 2})$$

Where R^2 represents the coefficient of determination, n is the number of sample points, and k corresponds to the number of variables used in the model. The ANOVA test's Probability F should also be analysed, with less than 0.05 being statistically significant for rejecting the null hypothesis, which stated the variables' significance. Compared to R^2 , R^2_{adj} penalizes independent variables that do not contribute to the dependent variable, preventing over-parameterization and resulting in high R^2 from unnecessarily well fitted data.

After, models were simplified using a stepwise multiple regression algorithm and independent variables that do not contribute significantly were removed. The β coefficients of the simplified linear models can be standardized (SC) using the standard deviation (Sd) as shown in (Eq. 3), to allow a better understanding of their contribution to the model.

$$SC_i = \beta_i \frac{\text{Sd}(x_i)}{\text{Sd}(Y)} \quad (\text{Eq. 3})$$

To ensure the validity of the predicted models, both normality and homoscedasticity assumptions of the residuals were tested using Shaphiro-Wilk and Brausch-Pagan tests, respectively. MLR adjustments, model simplifications and statistical tests were performed using R 4.1.1 (2021-08-10).

4.2 Multiple correlation analysis and hierarchical clustering

To evaluate the association between the DAD variables (wavelengths comprised between 200 – 400 nm in 2 nm steps) multiple correlation was tested using *cor* function available in R, package *stats* (version 3.6.2).

Then, hierarchical clustering was performed with the function *hclust* also from package *stats*, using the Ward method. As far as there were no precedents, the optimum number of clusters (*k*) was established according to the Calinski-Harabasz index (CHI), an unsupervised rule solely based on the data set and the clustering results. The CHI evaluates the ratio of in between-cluster sum of squares (BCSS) and within-cluster sum of squares (WCSS) dispersions normalized by the degrees of freedom (Eq. 4).

$$CHI = \frac{BCSS/(k-1)}{WCSS/(n-k)} \quad (\text{Eq. 4})$$

The BCSS (Eq. 5) determines the separation between the different clusters. It is calculated as the weighted sum of Euclidean distances between each cluster mean centroid (*c_i*) and the overall centroid (*c*) of the data points (*n_i*).

$$BCSS = \sum_{i=1}^k n_i \|c_i - c\|^2 \quad (\text{Eq. 5})$$

On the contrary, WCSS gauges the cohesion of the cluster (Eq. 6):

$$WCSS = \sum_{i=1}^k \sum_{x \in C_i} \|x - c_i\|^2 \quad (\text{Eq. 6})$$

Thus, the optimum number of clusters according to the CHI will depend on the value providing a minimum WCSS and maximum BCSS. In other words, it looks for the closest similarity in the same group and a higher difference amongst the other clusters.

4.3 K-fold Cross validation method

To further evaluate the selected variables through the proposed methodology of hierarchical clustering and test the robustness of the models, a k-fold cross-validation was applied. This is a common practice for machine learning systems to test their accuracy and predictability. Given the limited volume of data (*N*<50) coming from experimental analysis, it was decided to perform k-fold cross-validation to reduce possible biases from random partitions of the dataset. This procedure consists of executing *k* times (folds) the split of a data set into a training subset and a test subset. The first is used for the modelling, and the second is used to evaluate the goodness. In this work 5- and 10-time folds were applied for the validation of models. Finally, the mean values of the statistics from each fold are calculated and taken as representative (Jung & Hu, 2015).

4.4 Pearsons' correlation analysis

The calculation of Pearson linear correlation provides information about the association between two given variables *X* and *Y* (Eq. 7)

$$r = \frac{\text{Cov}(x_1, x_2)}{S_{x1} * S_{x2}} = \frac{\sum_{i=1}^N (x_i - \bar{x})(y_i - \bar{y})}{\sqrt{\sum_{i=1}^N (x_i - \bar{x})^2 \sum_{i=1}^N (y_i - \bar{y})^2}} \quad (\text{Eq. 7})$$

$$t = \frac{r}{\sqrt{\frac{1-r^2}{n-2}}} \sim t_{n-2} \quad (\text{Eq. 8})$$

Pearson coefficient values can range from -1 to 1, where 0 means no linear correlation, -1 a perfect negative correlation, and 1 a perfect positive correlation. To evaluate the signification of the coefficients, p-value of the statistic *t* (Eq. 8) based on a t-Student distribution with *N*-2 freedom degrees must be

assessed. Whether p-value is less than 0.05 the null hypothesis can be rejected, thus stating there is a significant linear correlation between variables.

5. CASE STUDIES

The aim of this section is to contextualize the emplacements where major samplings involved in the results and discussion of the present dissertation took place.



Figure 8: Case study situational map (Boundaries source: DIVA-GIS).

Overall, four drinking water treatment plants (DWTP) were involved in the study, all of them allocated in Catalonia (NE Spain, Figure 8).

Plants of Abrera, Cardedeu, and Cardener are operated by Ens d'Abastament d'Aigua Ter-Llobregat (ATL) and serve 4.5 million inhabitants in the metropolitan area of Barcelona, while Montfullà is operated by Cicle de l'Aigua del Ter (CATSA) serving the urban areas of Girona, Salt, and Sarrià de Ter. Only Abrera DWTP treats water which intake comes that is directly from the river, the other DWTPs influents come from reservoirs. Particularly, Cardedeu and Montfullà treat water coming from the same reservoir system, but each plant differs in processes and configuration. Treatments for each DWTPs are schematically presented in Figure 9.

Abrera DWTP (PTL, for shortness) has a treatment capacity of $3.2 \text{ m}^3/\text{s}$ and catches raw water from the Llobregat River by direct diversion of the flow. Immediately, peroxidation with potassium permanganate is applied, and then flocculation process takes place previous to filtration through sand and activated carbon (AC) filters. As a particularity, the upper part of the river basin is close to salt deposits where mining activities discharge high salinity effluents, giving the water a distinctive profile that calls for a peculiar treatment. The remedy ATL implemented was incorporating an electro dialysis reversal (EDR) desalination unit in the treatment train, with a total treatment capacity of $2.2 \text{ m}^3/\text{s}$ that operates at a variable rate depending on the raw water quality (Valero & Arbós, 2010). EDR is a variation of electro dialysis process that uses electrode polarity reversal to clean membrane surfaces, with the

particularity that polarity of the DC power is reversed two to four times per hour. In such way, source water compartments (dilute and concentrate) are also reversed, providing a self-cleaning capability enabling purification and recovery of up to 94% of source water and minimises the volume of waste requiring disposal. Thus, the flow right after AC filtration is split into EDR, finally converging for final disinfection with sodium hypochlorite before entering the storage tanks.

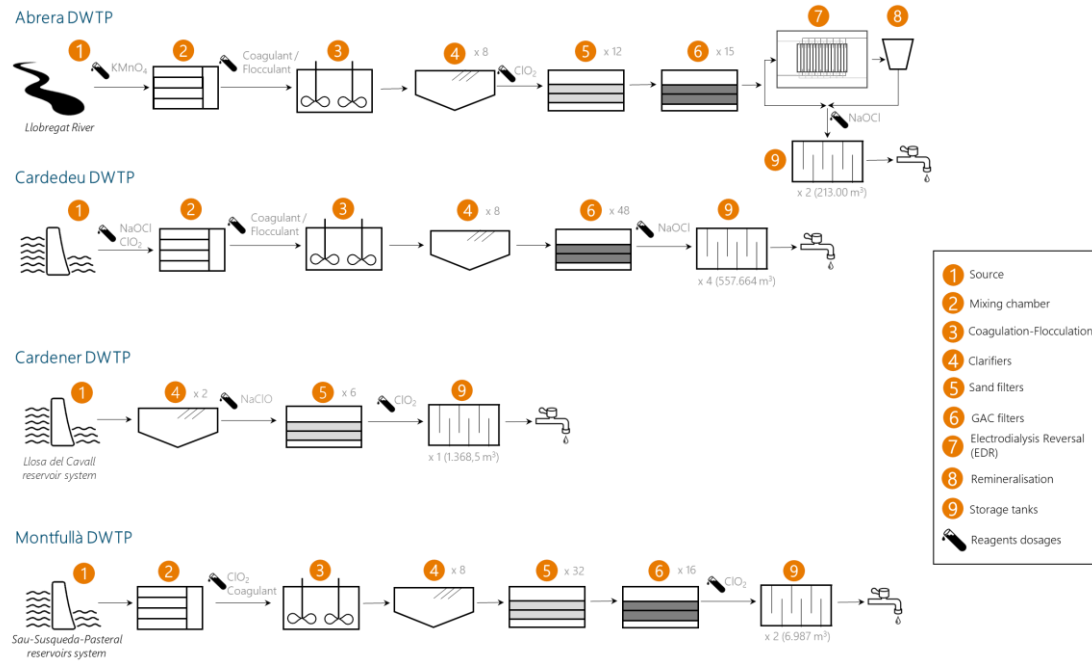


Figure 9: Scheme of the full-scale treatment trains of the case study DWTPs.

Cardedeu DWTP (PTT) receives water through a 56 km pipeline from the Sau-Susqueda-Pasteral system of connected in series water reservoirs along the Ter River. The plant has a maximum treatment capacity of 8 m³/s, and its configuration follows a conventional scheme, including a pre-oxidation dosing a combination of sodium hypochlorite and chloride dioxide, prior to coagulation-flocculation. After settling in the clarifiers, water is filtered through AC filters and chlorinated with sodium hypochlorite before storage.

Cardener DWTP (PTC) is the smallest of the facilities located in the municipality of Navès, Lleida, and has a total treatment capacity of 0.35 m³/s of water from Cardener River, an affluent of Llobregat, coming from the Llosa del Cavall reservoir. Its treatment configuration encompasses coagulation-flocculation and subsequent sand filtration.

Montfullà (PTM) also treats water from the Ter River coming from the Sau-Susqueda-Pasteral system of reservoirs. Once the flow enters the plant, coagulation is performed, and after clarification, it goes to a system of sand and AC filters prior to final disinfection with ClO₂.

Three sample campaigns were engaged to obtain the principal results reported in this dissertation. A brief summary with the most relevant scenario contextualization is given in the following Table 13, and the full characterization of samples is presented in Appendix B (Table A 5 and Table A 6) including the formation potentials of DBPs (Table A 7, Table A 8, Table A 9).

Table 13: Summary of sampling campaigns.

Sampling Campaign	Date	DWTP	Num. samples	Reservoir level (% capacity) / River flow	% EDR	Involved Chapter(s)
1	May 2021	Abrera	11	2.25 m ³ /s	40%	V, VI
1	May 2021	Cardedeu	7	149.63 hm ³ (90.5%, Sau); 221.13 hm ³ (94.9%, Susqueda)		V, VI
1	May 2021	Cardener	3	65 hm ³ (86.9%)		V, VI
2	April 2022	Abrera	2	1.50 m ³ /s	40%	V
2	April 2022	Cardener	1	35 hm ³ (47.1%)		V
3	January 2023	Montfullà	7	28.62 hm ³ (17.30% Sau); 83.50 hm ³ (35.8% Susqueda)		VII, VIII
3	Februy 2023	Abrera	5	1.75 m ³ /s	50%	VII, VIII
3	Februy 2023	Cardedeu	5	28.62 hm ³ (17.30% Sau); 83.50 hm ³ (35.8% Susqueda)		VII, VIII

Chapter IV

RESULTS I

Prediction of THMs-FP from DOM fractionation by HPSEC-DAD-OCD

Redrafted from:

NOM fractionation by HPSEC-DAD-OCD for predicting trihalomethane disinfection by-product formation potential in full-scale drinking water treatment plants.

Valenti-Quiroga, M., Daunis-i-Estadella, P., Emiliano, P., Valero, F., & Martin, M. J. (2022). *Water Research*, 227. <https://doi.org/10.1016/j.watres.2022.119314>

This chapter is centred on applying the optimized methodology (see section 3.2.1) for size exclusion (HPSEC-DAD-OCD) analysis to study and establish links between THMs-FP and DOM fractions. The work covered a diverse pool of samples from drinking water facilities taken alongside conventional full-scale, pilot-scale, and bench-scale set-ups.

1. BACKGROUND AND OBJECTIVES

Understanding DOM reactivity is crucial to predict formation of DBPs. Typically, specially from an operational point of view, DOM reactivity is tracked through the evaluation of surrogate parameters like dissolved organic carbon (DOC), ultraviolet absorbance at 254 nm (UV₂₅₄), or specific UV (SUVA). However, due to the year-round seasonal changes, these measures tend to be ineffective. To improve a deeper understanding of their behaviour, more extensive characterisation techniques such as size exclusion chromatography seem promising resources.

A limited number of publications referring to DOM fractions and their specific relationship with THMs are available to date (Carra et al., 2021a; Hidayah et al., 2017). Yet, none of them consider fractionated spectroscopic properties nor the predictability of specific THM compounds.

The main objectives of this study were the following:

- › Test the optimized HPSEC-DAD-OCD methodology on water samples collected on drinking water treatment plants and contrast obtained results with widespread methodologies (LC-OCD) implemented on laboratories established in the market.
- › Determine which of the measured signals enable the best prediction for the regulated THMs (TCM, BDCM, DBCM, TBM, and their sum).
- › Establish which DOM fractions are most correlated with regulated THMs-FP.

2. METHODOLOGY

The methodological summary employed in this chapter is presented on Table 14.

Table 14: Summary of the analytical workflow and methodologies used in Chapter IV.

SAMPLING	METHODOLOGICAL WORKFLOW			
DWTPs: - Abrera - Cardedeu - Cardener Nº Sampling campaign: 1 & 2 (Validation) Nº Samples: 21+ (3)				
	General Water Quality Parameters <i>(Chapt. III - 1)</i>	DOM fingerprinting SEC <i>(Chapt. III - 2.1)</i>	DBPs analysis Formation Potential Tests 24h-48h-72h <i>(Chapt. III - 3.1)</i> + LLE + GC-MS <i>(Chapt. III - 2.2.2)</i>	Statistical Analysis MLR Models <i>(Chapt. III - 4.1)</i>

General characterization parameters and THMs-FP are presented on Appendix B, Table A 5, and Table A 6.

Specific to this chapter, to test the SEC methodology, samples also were analysed via LC-OCD procedure (Huber et al., 2011) by the HET Waterlaboratorium (Harlem, The Netherlands).

Also, after the HPSEC-DAD-OCD analysis, UV signals at 206, 240, 350 and 380 nm were extracted for spectroscopic slopes calculations $S_{206-240}$ and $S_{350-380}$ calculated as following (Eq. 9), as well as signal at 254 nm, for further evaluation.

$$S_{\lambda_1-\lambda_2} = \frac{(A_{\lambda_1} - A_{\lambda_2})}{|(\lambda_1 - \lambda_2)|} \quad (\text{Eq. 9})$$

Also, deconvolution and integration of DOC and spectroscopic chromatograms obtained by HPSEC-DAD-OCD (Figure 10) were performed according to retention times summarized on Table 15.

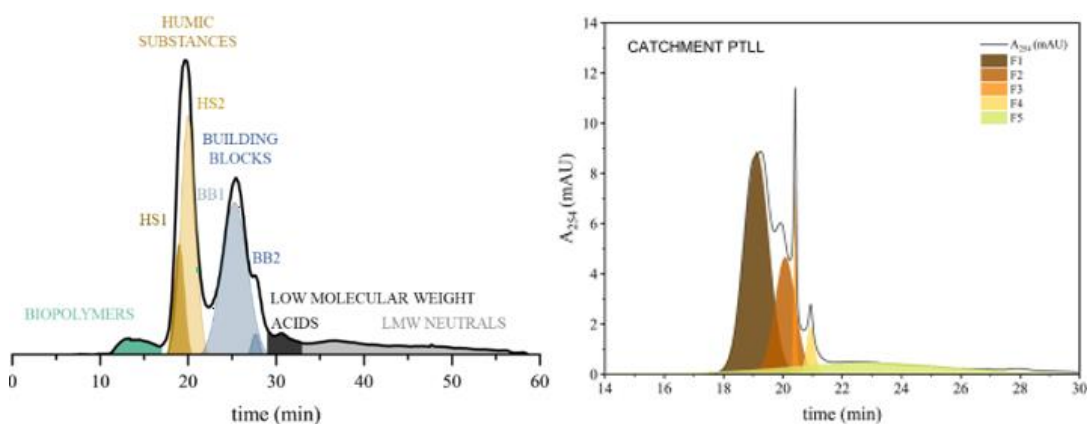


Figure 10: Example of DOM and A_{254} chromatogram deconvolution and quantification by HPSEC-DAD-OCD.

Table 15: Summary of main HPSEC-DAD-OCD fractions with corresponding retention times (min).

Signal	Fractions							
	Biopolymers	Humic substances				Building blocks	LMW acids	LMW neutrals
DOC	10.8 – 17	HS I 19 HS II 20				BB I 25.3 BB II 27.7	29 – 33	33 – 58.5
SPECTROSCOPIC		F1	F2	F3	F4	(F4) ₂₀₆₋₂₄₀	F5	F6
A_{254}		19.2	20.1	20.4	20.9		22.8	
$S_{206-240}$		19.3	20.1	21.0		23.2	24.9	33.5
$S_{350-380}$		19.2	20.1	20.4	20.9		22.7	

Full quantification of all DOC and spectroscopical fractions is presented on Appendix C (Table A 10 and Table A 11)

3. RESULTS AND DISCUSSION

Diversity of source waters nature led to different speciation profiles of THMs (Figure 11). With the highest DOC (3.17 mg/L) and salinity (554 µg/L of bromide and 189.3 mg/L chloride) concentrations, PTL presented the higher THMs-FP compared to the other plants, being brominated THMs the most prevalent species ($\text{CHBr}_2\text{Cl} > \text{CHBrCl}_2 > \text{CHBr}_3 > \text{CHCl}_3$) while high chlorinated THMs prevailed on PTT and PTC ($\text{CHCl}_3 > \text{CHBrCl}_2 > \text{CHBr}_2\text{Cl}$).

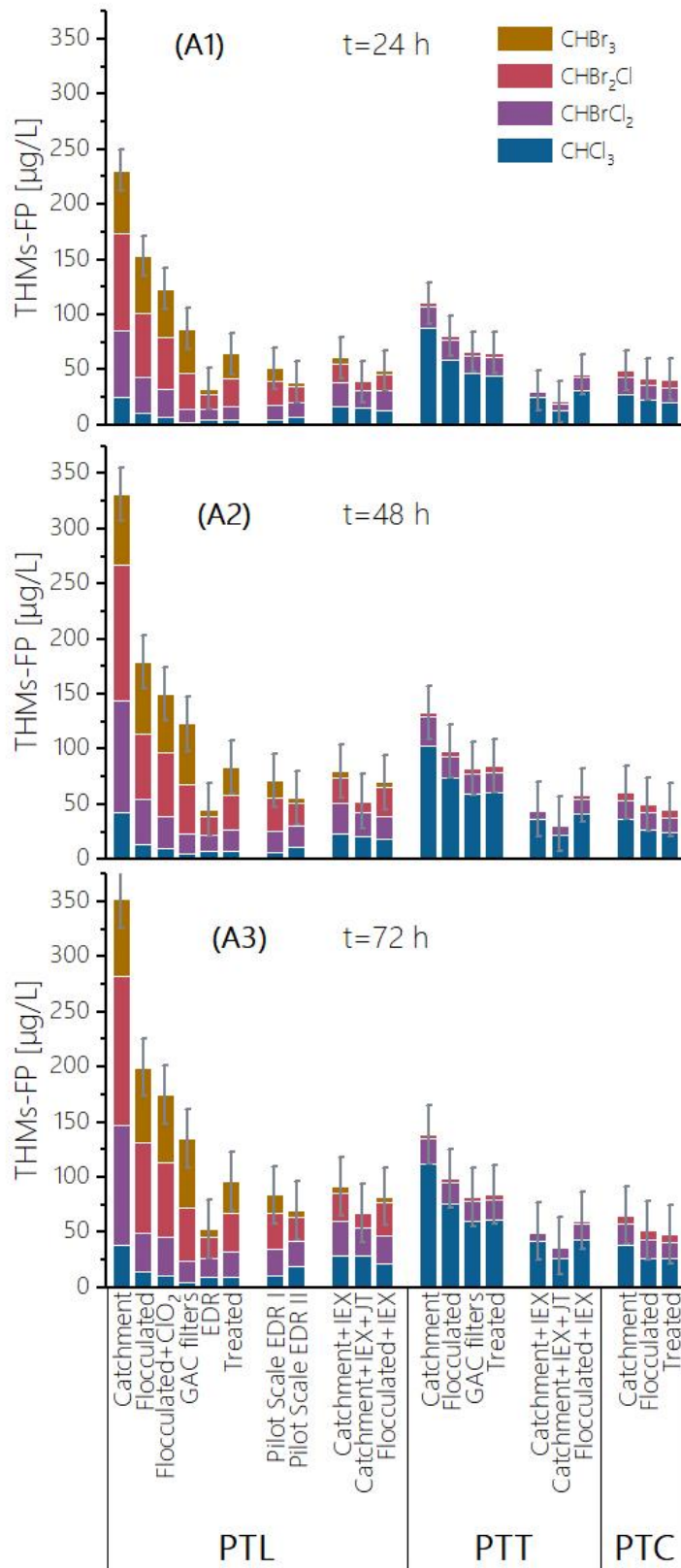


Figure 11: THMs-FP (A1–3) and yields (B1–3) of analysed samples from Llobregat DWTP (PTL), Ter DWTP (PTT), and Cardener DWTP (PTC), as a function of reaction time.

As expected, larger reaction times led to increasing concentrations of FPs, being PTL the most reactive water. At its turn, the decrease in DOC concentration caused by DOM removal through conventional treatment or either with alternative processes, led to a diminution of FPs. Samples subjected to IEX experienced highest DOC and Br⁻ reductions consequently resulting in lower THMs-FP. Comparable results were reached with the EDR treatments.

3.1 Evaluation of SEC methodology and DOM fractions

Comparison of overlapped SEC chromatograms applying two methods (LC-OCD vs. HPSEC-DAD-OCD) evidenced the addition of a second analytical column provided higher peak resolution, improving separation of humic substances, and building blocks (Figure 12). Thus, the proposed method enables a more precise profile interpretation.

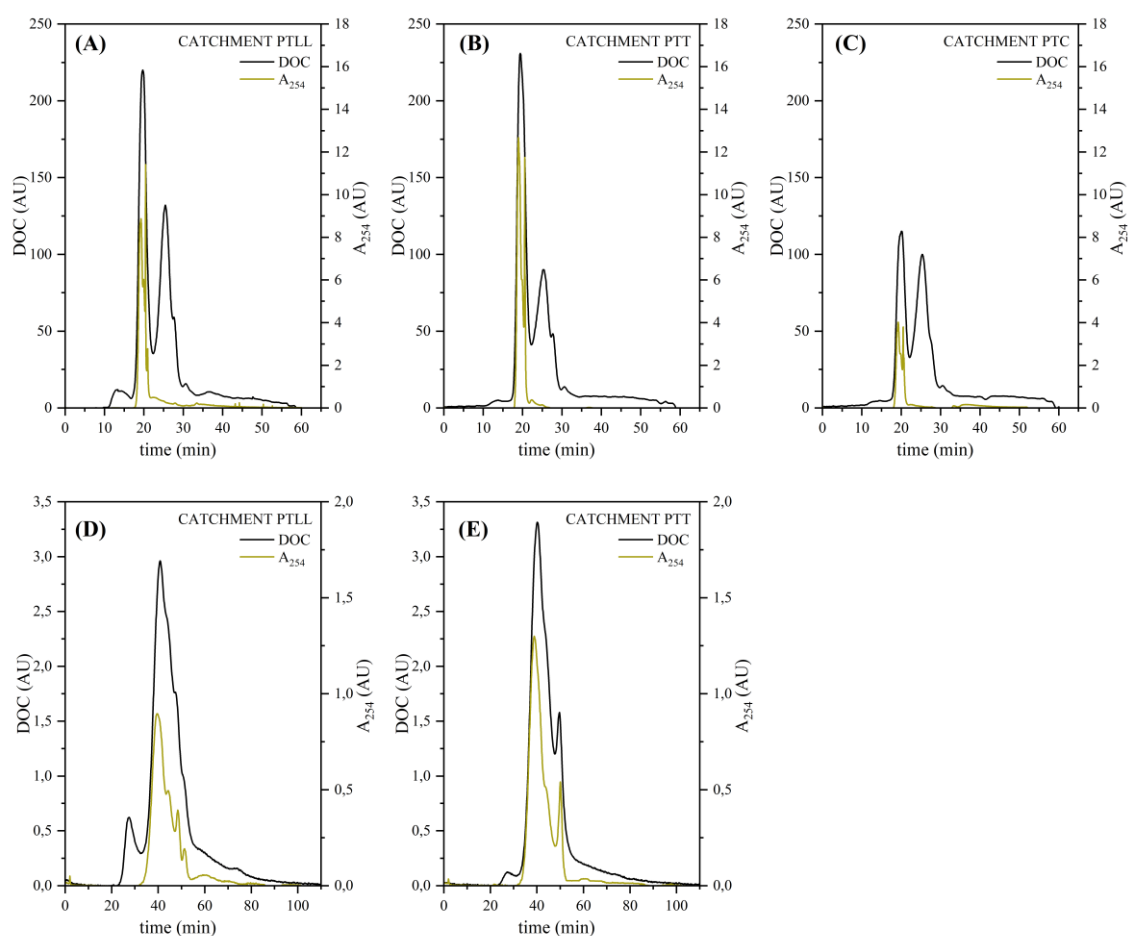


Figure 12: Comparison of overlapped chromatograms of the DOC and A_{254} spectroscopic responses of the catchment samples obtained by HPSEC-DAD-OCD (A, B, C) and LC-OCD (D, E). Samples from the Cardener DWTP (PTC) were not analysed by LC-OCD.

DOM profiles were assessed regarding DOC and UV detection (via spectroscopical slopes). An in-depth analysis of DOM fractions removal within the treatment processes was out of the scope of this chapter but impacts from operations were clearly evicted. Most removal in conventional processes was mainly achieved with coagulation, getting rid of high molecular weight compounds (humic substances and building blocks) diminishing their reactivity a 29% (PTL) and 17% (PTT) towards tTHMs-FP. The great

performance of EDR in removal of bromide (82%) and contribution to humic substances (3%) led to the major reductions in tTHMs-FP (54%).

Differences on raw water DOC fraction distribution were found between riverine sample (PTL) that presented higher concentrations of biopolymers and building blocks, compared to those from reservoirs (PTT-PTC). Also, these site-specific DOM differences were seen in spectroscopic chromatograms which interpretation was a bit more complex (Figure 13).

Chromophores from the analysed samples mostly absorbed at 254 nm and coeluted between 18 – 22 min, thus attributed to aromatic structures from humic substances. This represented 85, 92, and 88% of the total A_{254} area in PTL, PTT, and PTC respectively. The slope signal between 350 and 380 nm ($S_{350-380}$) encompassed a similar range to that of A_{254} , matching the chromophoric zone of humic substances. The major difference between riverine and reservoir samples was found around 20.9 min where a peak appeared in PTL but was undetectable in PTT-PTC.

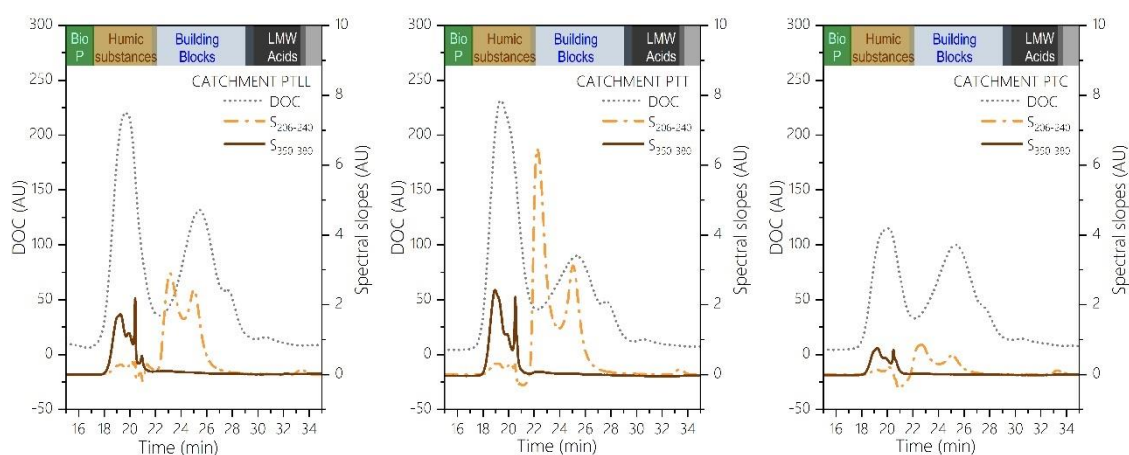


Figure 13: Chromatograms of the HPSEC-DAD-OCD spectroscopic slopes between absorbance wavelengths of 206–240 nm and 350–380 nm, and overlapped DOC profiles for the river catchment sample (PTLL) and reservoirs (PTT and PTC).

A complete distinct absorption profile was depicted in the lower wavelength slope ($S_{206-240}$), where strongest signal overlapped the region of medium and low molecular weight fractions (from 23 to 33.2 min). The influence of inorganic compounds might be carefully assessed at those wavelengths. On an ideal SEC separation where no secondary interactions between the solute and the stationary phase take place, retention is governed by molecular size; however, in the present HPSEC-DAD-OCD methodology, anions eluted within 23.2 min and 25.0 min. The neutral pH and low ionic strength conditions adjusted to maximize DOM resolution enhance electrostatic repulsion forces driving anions to elute sooner than expected according to their MW. After a cross-check analysis of spectroscopic properties between 206 nm and 240 nm of principal inorganic species (Birkmann et al., 2018) (see also Table A 2 in Appendix B for retention times of inorganic compounds), possible interferences were narrowed to nitrate and bromide whose effect was tested with standards. Finally, it was determined that feasible contributions could be expected to affect fractions $F4_{S_{206-240}}$ and $F5_{S_{206-240}}$.

3.2 THMs- FP modelling & assessment

Given all the analytical results, a total of 270 models were tested including bulk surrogated parameters (DOC, A_{254} , SUVA), and the different DOM fractionation methods (LC-OCD and HPSEC-DAD-OCD) considering DOC and spectroscopic signals. All SEC models were simplified, statistical assumptions were tested, and the fitting quality was evaluated through adjusted determination coefficients (R^2_{adj}) to avoid over-parametrization. Only few models did not pass the statistical tests for the assumptions (i.e., normality and homoscedasticity; Figure 14), and most failures were due to non-normality, which could be overcome by increasing the number of samples in the training set or testing alternative other non-linear models.

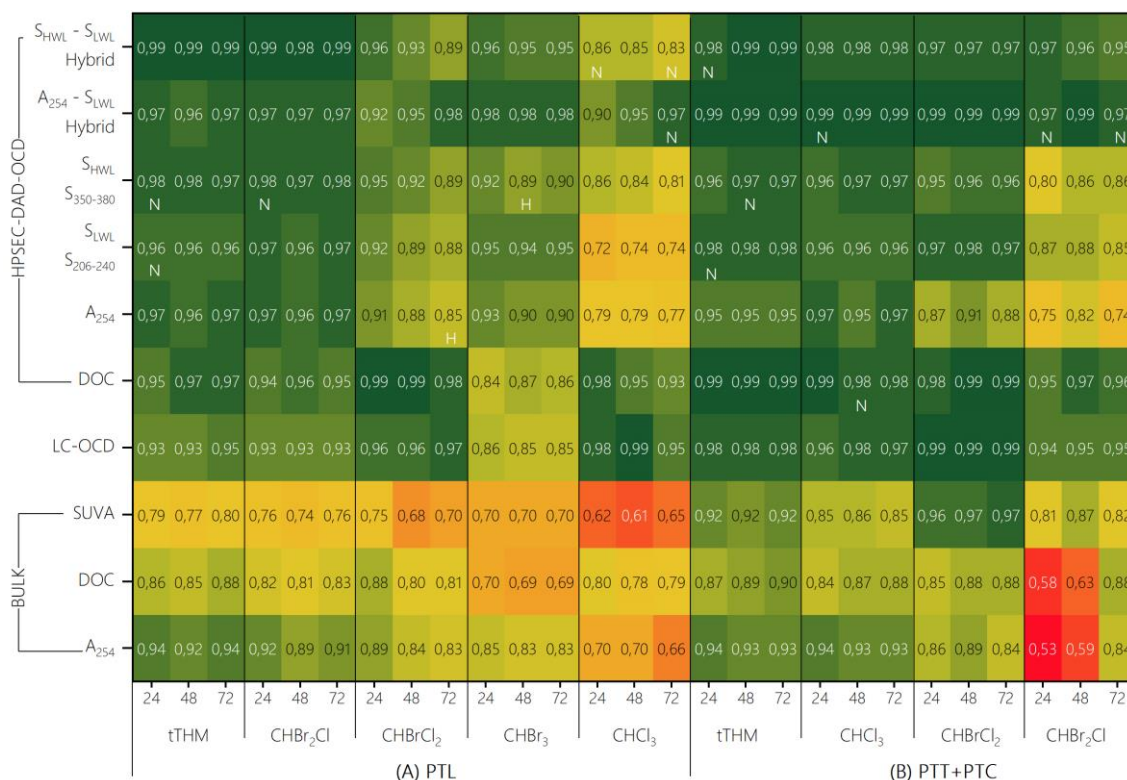


Figure 14: R^2_{adj} coefficients heatmap of the MLR simplified models fitting bulk measurements and DOM fractions obtained by LC-OCD and HPSEC-DAD-OCD. Results are shown for Llobregat (PTLL, A) and Ter-Cardener (PTT+PTC, B) DWTPs. Species are depicted on the x-axis in order of abundance. The tags H (homoscedasticity) and N (normality) refer to the failure of statistical assumptions. LC-OCD models did not include samples from PTC.

From the comparison between reaction times (i.e., 24, 48, and 72 h), non-relevant correlations between a specific parameter and kinetic effects of FPs were extracted. The R^2_{adj} values of the models with bulk parameters were comparable to those previously documented ($0.68 < R^2 < 0.89$, see Appendix C, Table A 12). Bulk models based on A_{254} exhibited the strongest association with FPs, specially for tTHMs. The correlations with DOC measurements were slightly weaker, while lowest links were reported in SUVA models. In general, the best adjustments were obtained for tTHMs regardless of speciation, reflecting the contribution of the most prevalent THM in each DWTP.

With the introduction of parameters from DOM fractionation analysis in the modelling, values of R^2_{adj} increased. This trend was lately stated by Carra and co-workers (2021), who assessed MLR models for tTHMs including MW fractions from LC-OCD analysis. They already reported better correlations when

considering SEC results compared to single bulk DOC models. The present work replicated the modelling contrasting results obtained with the LC-OCD separation to those of HPSEC-DAD-OCD, presenting the latest enhanced regression values (Figure 14).

Analyses of the distinct THMs-FPs were performed, demonstrating the unique contribution of each species. Although the tTHMs models presented better adjustments overall than those of individual species, the SEC technique accounted for a more refined speciation compared to bulk predictions. Except for the less prevalent species, spectroscopic models showed stronger links than DOC fractionated models. Fractionated A_{254} , $S_{206-240}$, and $S_{350-380}$, represented an improvement compared to bulk A_{254} predictions, slightly improving correlations of individual species and minor with A_{254} . Although A_{254} and $S_{350-380}$ overlap in retention times and are both related to aromatic moieties, they account for different information as higher wavelengths could reflect engagement of slow chromophores. This species had been reported to be involved in the formation of tautomeric ketones, a type of reaction adducts implied in DBP generation (Chen et al., 2020a). On the contrary, $S_{206-240}$ enclosed both organic and inorganic contributions. Therefore, the divergence in correlations could be due to the distinct mechanistic implications that the different signals reflect.

That given, two hybrid models were proposed from the combination of major intensity peaks from the spectroscopic signals to provide a more sensitive prediction. The first model merged main absorbance signals from A_{254} and $S_{206-240}$ ($A_{254} - S_{206-240}$), including $F1_{A_{254}}$ to $F4_{A_{254}}$ and $F3_{S_{206-240}}$ to $F6_{S_{206-240}}$ (See Table 15). The second hybrid model ($S_{350-380} - S_{206-240}$) replaced signals from A_{254} with the homologous at $S_{350-380}$ ($F1 - F3_{S_{350-380}}$, $F5_{S_{350-380}}$ and $F6_{S_{206-240}}$). While the first A_{254} peaks were representative of humic substances and building blocks chromophores (10 kDa to 700 Da), $S_{206-240}$ peaks covered the non-aromatic chromophores from the LMW range (< 200 Da) and accounted for the contribution of inorganic compounds (eluting during 21 – 33.5 min). The hybrid models were the best stated models explaining all the outlooks, presenting the $A_{254} - S_{206-240}$ models the strongest coefficients for both tTHMs and individuals ($R^2_{adj} > 0.90$).

After selecting the best fitting models (DOC and hybrid $A_{254}-S_{206-240}$ from HPSEC-DAD-OCD), though being far from a mechanistic approach, the analysis of standardised coefficients (SC) can provide further information about the most available reactive DOM fractions that could be enhancing FP of THMs (Figure 15). According to the SC, the most significant precursors of the studied halogenated THMs were DOM compounds eluding within humic substances and biopolymers. Strong contributions from the A_{254} fractions supported the role of aromatic moieties in THM formation, especially for $CHBr_2Cl$.

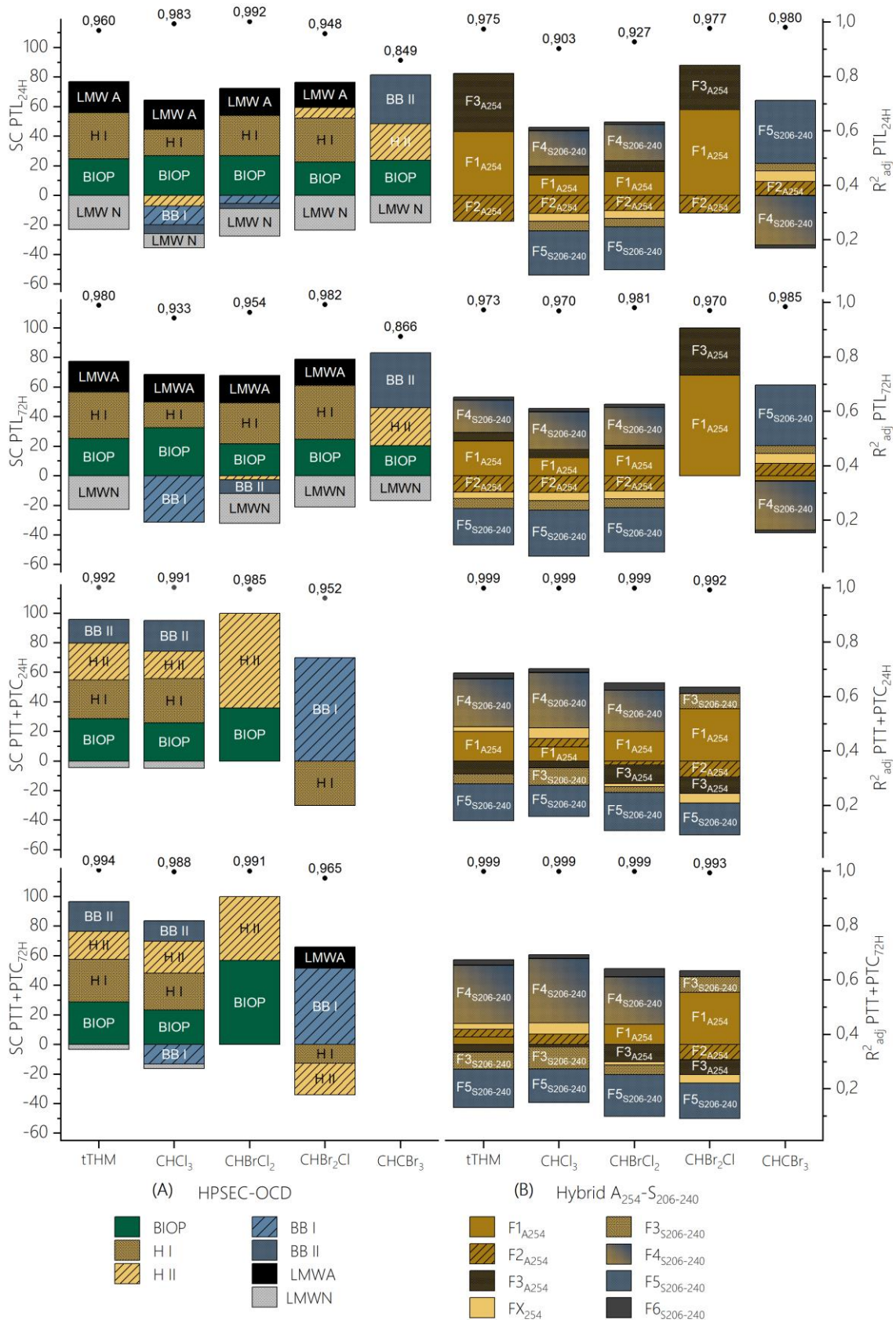


Figure 15: Standardised coefficients (SC) and R^2_{adj} values as a function of reaction time (24 and 72 h) for modelling the total (tTHMs) and individual THMs-FPs from DOC fractionation (A) and spectroscopic hybrid signals A₂₅₄-S₂₀₆₋₂₄₀ (B). Note that FX₂₅₄ refers to F4₂₅₄ for PTL samples and F5 A₂₅₄ for PTT-PTC (see Table 15).

A critical factor linked to speciation is the halogen-specific contribution of DOM moieties to FPs. From the results, SC revealed a different trend in the most abundant high-brominated THMs-FP (CHBr_2Cl in the PTT-PTC cluster, vs. CHBr_3 in PTL), compared to the others. Coefficients contributions were flipped for brominated species, see for example the building blocks fractions from the DOC models in PTT-PTC that exhibited a negative contribution to tTHMs and CHCl_3 , but positive for CHBrCl_2 and CHBr_2Cl . A similar trend was observed in PTL with the spectroscopic model for CHBr_3 where contributions of F3, F4, and F5 ($S_{206-240}$) were opposite. Considering previous knowledge about formation patterns of high-brominated THMs (Brezinski & Gorczyca, 2019a), these flipped fractions' behaviour could illustrate the effect of bromide substitution on DOM moieties where at a first stage disinfectants boost activation of reactive sites and after progressive bromide substitutions occur.

As a final stage for model evaluation, goodness of the predicting capacity was studied comparing the measured with the predicted values obtained through the proposed models. A 95% of probability was given to prediction bands, where differences in prediction accuracy of each model can be seen through bandwidth. The hybrid ($A_{254}-S_{206-240}$) model presented narrower bands turning to be more accurate than the DOC one (Figure 16). Mathematically the bandwidth might be partly biased by the limitations of the analytic process itself: accuracy and sensitivity of measurements and deconvolutions; as well as because of the samples conforming the dataset (number, deviation, etc.). Heterogeneity of samples, also impacts the band *amplitude*, the higher the variability, the broader the band; comparison of PTL and PTT-PTC adjustments exemplified this phenomenon in both models.

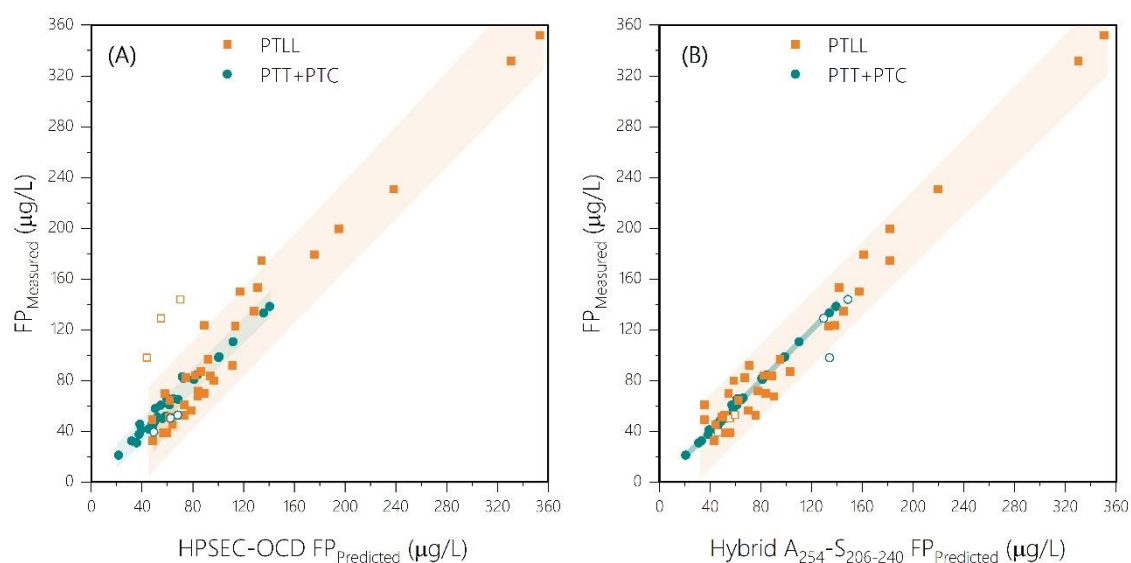


Figure 16: Measured vs. predicted tTHMs-FP estimated with the HPSEC–OCD model (A) and the spectroscopic hybrid model $A_{254}-S_{206-240}$ (B) including the representation of 95% prediction bands and validation samples (void symbols).

A cross-validation of the obtained results was performed adding two new samples collected a year after the initial set, coming from PTL (storage tanks), and PTC (treated water), (see Appendix B, Table A 5 and Table A 7 for the samples characterization). Hydrological conditions changed from one scenario to the other, though mean values of the water quality parameters did not significantly vary the end of a drought pre-warning scenario was experienced during the sampling of the validation test. This event specially impacted production of water in both DWTPs. In PTL water generated in situ was mixed with a partial supply from an external desalination plant in the storage tanks in order to meet distribution

network demands, and the EDR module was completely shut down, being GAC filtration the latest operation prior to final disinfection. In the case of PTC, a reduction of half of the reservoir level was reached at the end-of-drought pre-warning compared to the first sampling period lowering the flow rates.

As a result of this seasonal variations, distribution of DOM fractions fluctuated. In PTL, DOC concentrations of biopolymers, humic substances and neutrals increased a 19, 46, and 95 % respectively which also spanned absorbance intensities of $F1_{A254}$ and $F3_{A254} - F5_{A254}$, related to the higher contents of aromaticity in humic substances. Bromide and nitrate levels increased 2 to 3 times affecting areas of $F4_{S206-240}$ and $F5_{S206-240}$. On the contrary, building blocks and LMW acids minimally changed (< 10% variation). Similar effects were reported in PTC, with rising concentrations of biopolymers, humic substances and LMW neutrals, and a decrease in building blocks and acids of LMW. Those DOM fingerprint changes impacted the profiling of THMs-FP although tTHMs-FP concentrations were in the order of the training dataset (see Appendix B, Table A 7).

When predictive models are assessed for individual THMs (Figure 17), the effect of some confounding variables not included in the model could affect the explicative variable, such as the case resulting from inorganic contributions. This is seen in the hybrid model A254-S206-240 that indirectly considers the absorbing effects of inorganic compounds at lower wavelengths, which could explain better predictions in tTHMs, particularly in PTL where high bromide levels are a primary concern affecting speciation of DBPs. This effect becomes even clearer when contrasting predictions of $CHBr_3$ between the DOC and the spectroscopic model.

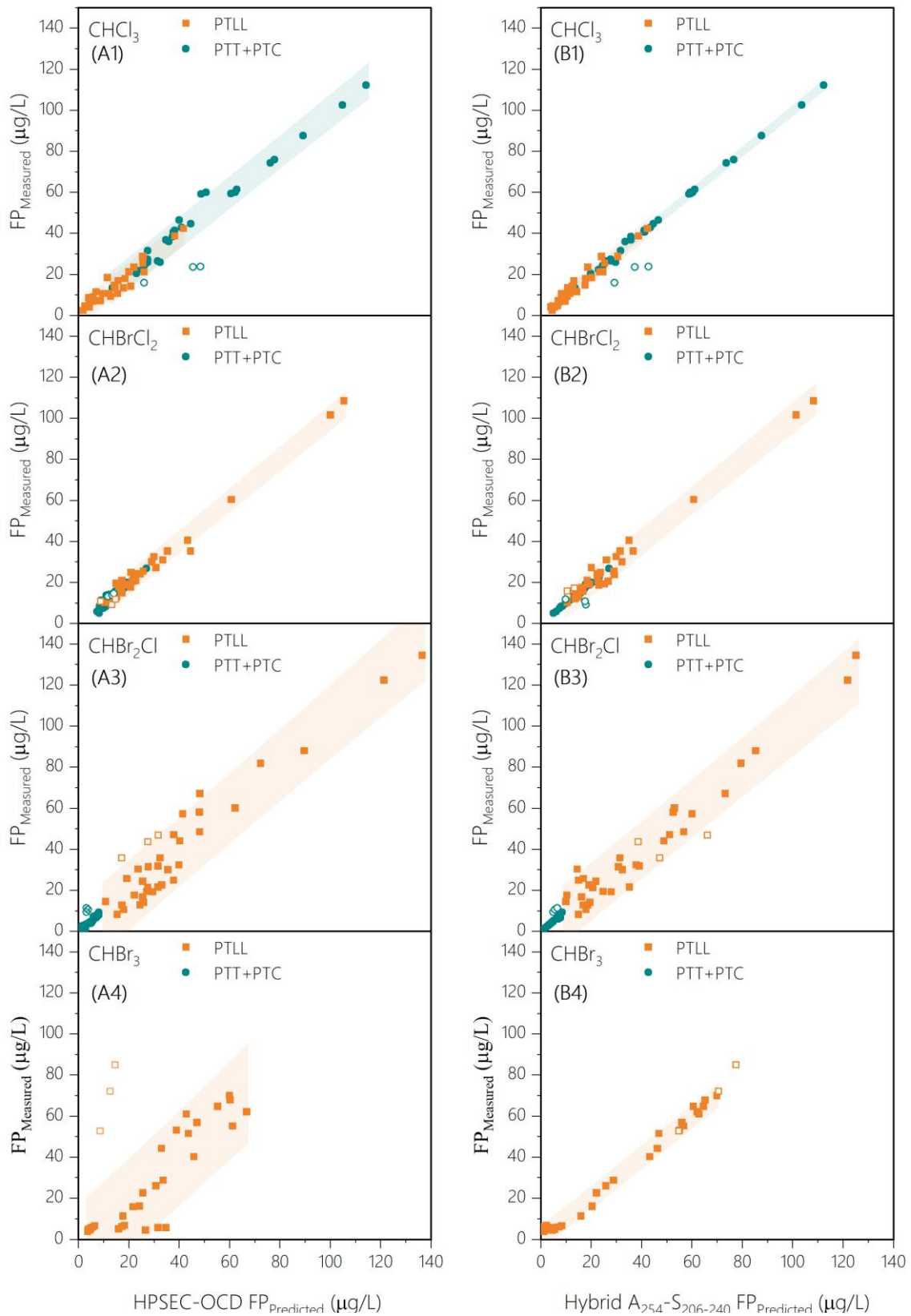


Figure 17: Measured vs. predicted FP for the distinct THMs congeners estimated with the HPSEC–OCD model (A1–4) and the spectroscopic hybrid model $A_{254}-S_{206-240}$ (B1–4) including the representation of 95% prediction bands and validation samples (void symbols).

The proposed models also suggest predictive advantages, accounting for operational simplifications, specially the based on fractionated spectroscopic signals: the use of a HPLC-DAD seems to be more efficient and accessible than an HPLC-OCD which is a highly specialized instrument. Though this modest validation of models proved their prediction ability, including a larger dataset accounting for more variable fluctuation and composition could upgrade a more robust model. Also, possible methodological modifications such as adjusting non-linear models or refining data treatment (involving deconvolution) could help to uplift predictability.

4. FINAL REMARKS

Site-specificity of DOM challenges the utterance of robust predictive models, what was observed during initial steps in the inability to encompass all samples. However, grouping samples based on overall water quality parameters lead to satisfactory results.

The in-depth analysis for modelling THMs-FP performing DOM characterization using HPSEC-DAD-OCD method turned out to be a novel approach to track FPs. The proposed SEC separation allowed to cover the full DOM fraction distribution including differences on molecular weight profiles and inorganic content. Compared to bulk-based, fractionated models improved correlations with THMs-FP, elucidating contribution and significance of most involved fractions, which differed in between river and reservoir waters, not only in terms of DOC detection but also spectroscopically.

This relevance enables to propose a link between precursors and products opening the door to further assessment of DOM removal, a benefit for targeted optimization of processes.

Chapter V

RESULTS II

In-deep analysis of humic substances
process performance in drinking water
treatments using size exclusion
chromatography

Prepared for submission

This chapter follows the previous discussed results and deepens in the evaluation of DOM fractions removal through the operations of the studied DWTPs using a novel multiwavelength approach.

1. BACKGROUND AND OBJECTIVES

Building upon the results obtained in the previous chapter, this section aims to conduct a detailed analysis of one of the primary contributors to THMs-FP: humic substances. While humic substances are commonly understood to be predominantly composed of humic and fulvic acids, here, we present an in-depth evaluation of their surrogate parameters and detailed absorbance profiles to elucidate the contribution of other compounds within the fraction.

To date, there is no preceding information about a detailed assessment of the spectroscopic profiles of humic substances from fractionated drinking water samples, considering subfractions of different AMW. Nor has a detailed correlation with UV absorbance and DBPs of those fractions been previously established.

Combining a diode array detector (DAD) for multiwavelength analysis with an organic carbon detector (OCD) right after chromatographic separation enables depicting the absorbance related to the carbon content of each MW fraction, two given datasets. After, possible relationship of those variations with THMs-FP were statistically studied through Pearson's correlation.

The main objectives of this chapter were the following:

- › Evaluate changes of DOM fractions within conventional full-scale and advanced bench scale treatments in DWTPs through HPSEC-DAD-OCD methodology to identify fractions most prone to removal.
- › Provide an in-deep analysis of the most abundant DOM fraction present in analysed waters (humic substances)
- › Evaluate the impact of operational treatments on specific THMs-FP reduction, and determine possible links between abovementioned HS characteristics and the changes on THMs-FP.

2. METHODOLOGY

Table 16 presents the references of the employed methodology involved in this chapter. General characterization parameters and THMs-FP are found on Appendix B, Table A 5 and Table A 6.

Table 16: Summary of the analytical workflow and methodologies used in Chapter VI.

SAMPLING	METHODOLOGICAL WORKFLOW			
DWTPs: - Montfullà - Cardedeu - Abrera Nº Sampling campaign: 3 Nº Samples: 21				
	General Water Quality Parameters <i>(Chapt. III - 1)</i>	DOM fingerprinting SEC <i>(Chapt. III - 2.1)</i>	DBPs analysis Formation Potential Tests – 72h <i>(Chapt. III - 3.1)</i> + LLE + GC-MS <i>(Chapt. III - 3.2.2)</i>	Statistical Analysis Pearson's Correlation <i>(Chapt. III - 4.4)</i>

3. RESULTS AND DISCUSSION

3.1 DOM characterization of source and treated waters

HPSEC-DAD-OCD constitutes an advanced tool for probing the compositional changes within DOM fractions, offering useful insights for treatment optimization (Huber et al., 2011b). Differences in UV absorbance profiles and DOC concentration among DOM fractions across the diverse water sources and DWTP treatment highlight the heterogeneous nature of DOM composition. Overall, the differences water quality parameters reflect the variations between river and reservoir sources, with implications for subsequent treatment processes and water quality management. To comparatively assess the efficiency of the treatment trains, an initial analysis of source and final treated water was performed.

3.1.1 Treatment plants from river sources: PTL

Starting with the bulk water quality parameters (Table 17), PTL, which sources water from the Llobregat River, the TOC concentration is 3.17 mg·L⁻¹, indicating a moderate level of organic carbon content. The UV absorbance at 254 nm (A_{254}) was 5.98 UA, suggesting a significant presence of organic matter with absorbance properties and a high turbidity at 23.00 NTU. This water has a high concentration of ions, particularly Br⁻, NO₃⁻ and SO₄²⁻, which concentrations were 0.55 mg·L⁻¹, 4.10 mg·L⁻¹ and 123.78 mg·L⁻¹, respectively.

Table 17: Bulk water parameters of the samples across treatment operations in the three DWTP evaluated.

DWTP	Sample	TOC [mg·L ⁻¹]	A ₂₅₄ [ua]	SUVA [ua·L·mg ⁻¹]	Conductivity [μS·cm ⁻¹]	Turbidity [NTU]	pH	Br ⁻ [mg·L ⁻¹]	NO ₃ ⁻ [mg·L ⁻¹]	SO ₄ ²⁻ [mg·L ⁻¹]
	Catchment	3.17	5.98	1.89	1186	23.00	8.07	0.55	4.10	123.78
PTL	Coagulation	2.57	4.65	1.81	1204	0.33	7.72	0.56	3.71	123.59
Full	Adsorption	1.74	2.73	1.57	1212	0.48	7.64	0.56	4.68	123.58
Scale	EDR	1.22	1.37	1.12	345	0.28	6.91	0.10	0.98	27.30
	Chlorination	1.49	2.43	1.64	647	0.28	7.91	0.18	2.17	49.48
	IEX (BS-1)	1.83	1.52	0.83	1295	14.1	8.04	0.09	0.85	3.65
PTL	Coagulation	1.99	2.91	1.46	1293	2.3	7.68	0.00	0.92	20.06
BS	(BS-1)									
	IEX (BS-2)	1.64	1.15	0.70	1298	0.37	7.71	0.09	0.76	3.93

PTT Full Scale	Catchment	2.92	6.61	2.26	392	0.85	8.08	<LOQ	1.91	10.87
	Coagulation	2.51	4.21	1.68	382	0.27	7.72	0.15	5.30	29.03
	Adsorption	2.00	2.74	1.37	376	0.35	7.77	0.12	4.03	21.89
	Chlorination	1.86	2.82	1.51	396	0.21	7.84	<LOQ	3.92	18.88
PTT BS	IEX (BS-1)	1.32	1.04	0.79	460	0.70	8.02	<LOQ	0.60	1.64
	Coagulation (BS-1)	2.53	1.39	0.55	458	0.64	7.69	0.02	0.67	20.16
	IEX (BS-2)	1.02	0.79	0.77	461	0.37	7.75	<LOQ	0.47	1.67
PTC	Catchment	1.38	2.51	1.82	568	0.60	8.09	0.01	0.98	79.99
	Coagulation	1.30	2.42	1.86	568	0.33	8.11	0.01	0.99	80.52
	Chlorination	1.27	1.49	1.17	572	0.15	8.11	<LOQ	0.82	62.26

Differences in distributions and intrinsic characteristics of DOM fractions were qualitatively evaluated using HPSEC-DAD-OCD analysis through the overlap of the SEC chromatograms, encompassing both DOC and UV-absorption spectra (Figure 18).

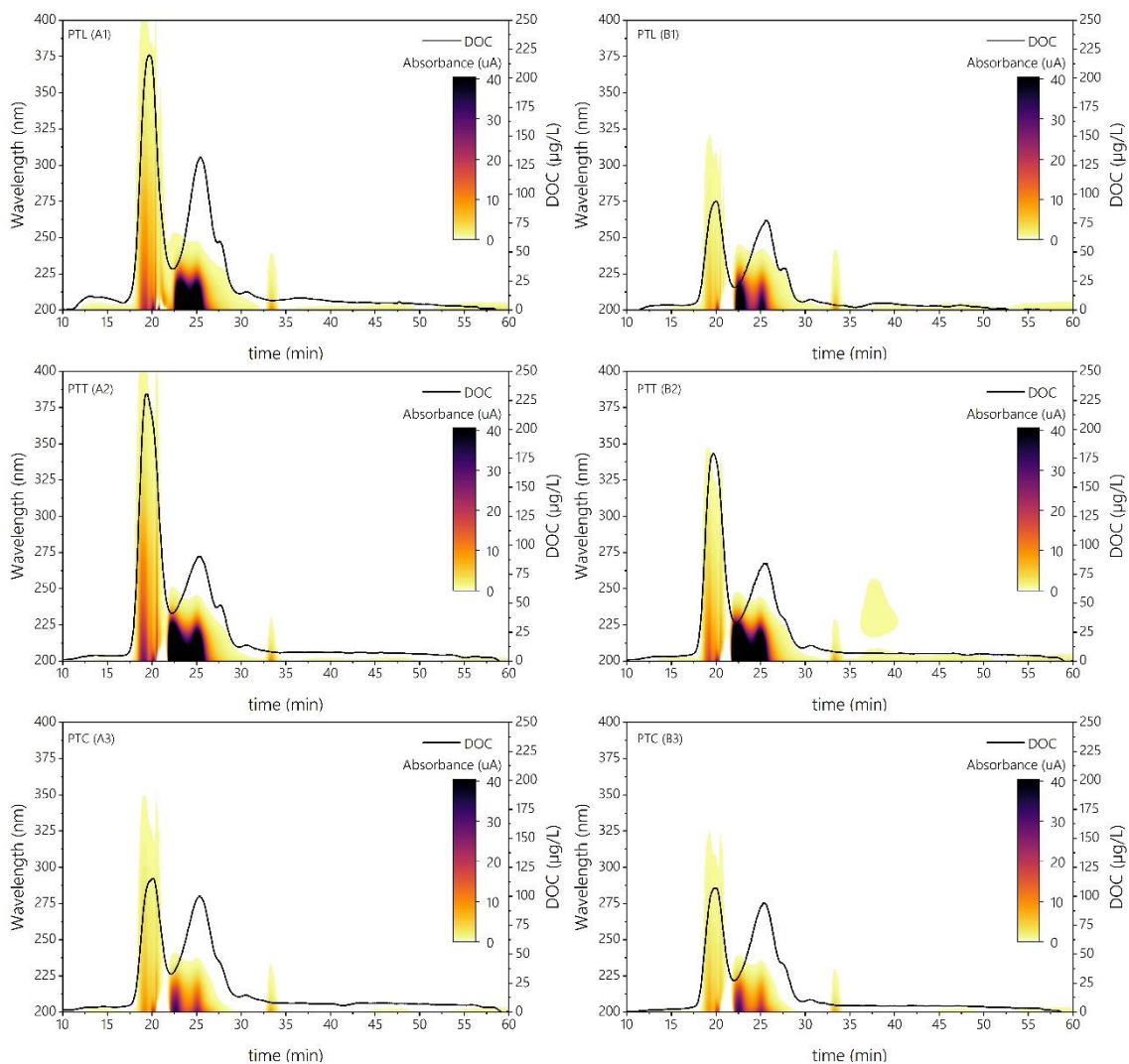


Figure 18: Overlapped DOC and UV-multiwavelength absorbance profiles from HPSEC chromatograms of catchments (A1-3) and treated waters (B1-3) after conventional treatment train (Rt 10.8 – 16 min: Biopolymers; Rt 16 – 22.5 min: HS; Rt 22.5 – 29 min: BB; Rt 29 – 33 min: low MW acids; Rt 33 – 60 min: low MW neutrals).

PTL water catchment presented the greatest prevalence of DOM fractions in the range of 10 kDa to 200 Da. This corresponds to humic substances (HS, 16 min – 24 min) and building blocks (BB, 24 min – 29

min), accounting for 40.9% and 39.2% of DOC respectively (Table 18). Additionally, 4.1% of the DOC corresponded to biopolymers (R_t 10.8 min – 16 min), a notably higher value compared to the other studied plants, which treat waters from reservoirs.

Table 18: Distribution of DOC in DOM fractions by HPSEC-DAD-DOC.

DWTP	Sample	BioP [%]	HS [%]	BB [%]	LMW acids [%]	LMW neutrals [%]
PTL Full Scale	Catchment	4.1	40.9	39.2	3.4	12.3
	Coagulation	3.0	34.7	44.3	4.3	13.7
	Adsorption	1.6	31.2	50.5	4.1	12.6
	EDR	2.5	31.2	47.8	3.4	15.2
	Chlorination	2.8	37.8	44.8	3.6	11.0
PTL BS	IEX (BS-1)	7.0	22.1	46.3	4.9	19.7
	Coagulation (BS-1)	3.4	32.8	26.6	11.6	25.6
	IEX (BS-2)	5.5	21.7	43.7	6.0	23.1
PTT Full Scale	Catchment	1.9	48.9	33.7	3.3	12.2
	Coagulation	1.5	47.6	35.8	3.3	11.7
	Adsorption	1.6	41.6	42.1	2.7	12.0
	Chlorination	2.2	43.9	36.4	3.6	13.9
PTT BS	IEX (BS-1)	3.1	30.9	31.9	9.5	24.6
	Coagulation (BS-1)	2.4	36.7	18.3	11.3	31.4
	IEX (BS-2)	3.8	29.2	29.9	10.6	26.5
PTC	Catchment	2.3	30.5	46.4	4.3	16.5
	Coagulation	2.3	29.7	48.5	4.2	15.4
	Chlorination	1.8	32.2	49.5	3.4	13.1

The absorbance of HS spanned nearly the entire UV range (200 nm – 400 nm) with moderate intensity. However, the BB fraction exhibited the strongest signal intensity from 200 nm to 230 nm (R_t 22.5 min to 27 min). However, it must be noted that the ions contained in PTL samples are removed through HPSEC separation from all DOM fractions except those within the BB region, where inorganic ions co-elute (R_t 23.2 min and 25 min) (Valenti-Quiroga et al., 2022b). Thus, in this specific region, the UV profiles at lower wavelengths (< 220 nm) may not solely reflect the properties of DOM but also residual ions (Ignatev & Tuhkanen, 2019b; Korshin et al., 1997).

After the full treatment, as shown in Figure 18 B, the absorbance decreased due to the removal of chromophoric compounds, combined with a reduction in DOC of the predominant HS fraction. This resulted in a decrease in the signal intensity and in the narrowing of the absorption wavelength ranges up to 325 nm. Also, bromide, nitrate, and sulphate were reduced up to 0.18 mg·L⁻¹, 2.17 mg·L⁻¹, and 49.48 mg·L⁻¹ respectively in the effluent sample.

3.1.2 Treatment plants from reservoir sources: PTT and PTC

For PTT catchment, the TOC bulk concentration was 2.92 mg·L⁻¹, and the A_{254} value was 6.61 ua, indicating a comparable level of organic carbon content and absorbance properties to PTL. Turbidity was lower at 0.85 NTU, suggesting less suspended particles compared to PTL.

According to the DOM fraction analysis, HS supposed the 48.9% of the DOM fractions, with BB representing the 33.7% of the DOC (Table 18). The source of PTT had lower levels of nitrate (1.91 mg·L⁻¹), sulphate (10.87 mg·L⁻¹), and undetectable levels of bromide. However, it presented the highest intensities among all samples, both in the influent and effluent (Figure 18, A2 – B2).

Regarding the PTT effluent (Figure 18, B2), the final concentrations of main absorbing fractions, especially BB, still accounted for high intensity, suggesting minimal removal of those most highly absorbing chromophores. However, the spectral range narrowed, shifting towards lower wavelengths.

Similarly, for PTC, the catchment water quality parameters were in a similar range. The bulk TOC concentration was $1.38 \text{ mg}\cdot\text{L}^{-1}$, indicating a lower level of organic carbon compared to PTL and PTT. A_{254} was 2.51 UA and turbidity was 0.60 NTU, suggesting a moderate presence of organic matter compared to PTL. PTC had the lowest amounts of inorganic ions ($0.98 \text{ mg}\cdot\text{L}^{-1} \text{ NO}_3^-$, $79.99 \text{ mg}\cdot\text{L}^{-1} \text{ SO}_4^{2-}$, and undetectable concentrations of Br^-).

However, the DOM presented a completely distinct distribution profile, characterized by lower amount of HS corresponding to 30.5% of DOC, and higher percentage of BB corresponding to the 46.4%. Similarly, compared to the other catchment samples, lower quantities of chromophoric compounds were detected in these samples (Figure 18, A3). Also, PTC showed the least DOC removal (7%) within the treatment train (Figure 18, B3), with scarce variations in the maximum wavelength absorption (from 325 nm to 350 nm) of the chromophores associated with the HS.

When comparing HPSEC elution times, which are indicative of the molecular weight of the DOM fractions, peak maximums of HS and BB in PTT exhibited higher values compared to those in PTL and PTC. Specifically, in PTT, the R_t for HS and BB were 19.3 min and 25.6 min, respectively, while in PTL, they were 19.8 min for HS and 25.2 min for BB. Similarly, in PTC, the elution times were 20.1 min for HS and 25.3 min for BB.

3.2 Sequential Removal of DOM Fractions

Upon analysing samples from the operational works, each DOM fraction exhibited different responses after undergoing the water treatment operations. All HPSEC chromatograms can be seen in Appendix D (Figure A 2 to Figure A 5). To facilitate the visualization of precise changes, Figure 19 presents the reduction in each DOC fraction concentration ($\mu\text{g}/\text{L}$) after each successive treatment operation calculated by subtracting the concentration measured before and after the operation.

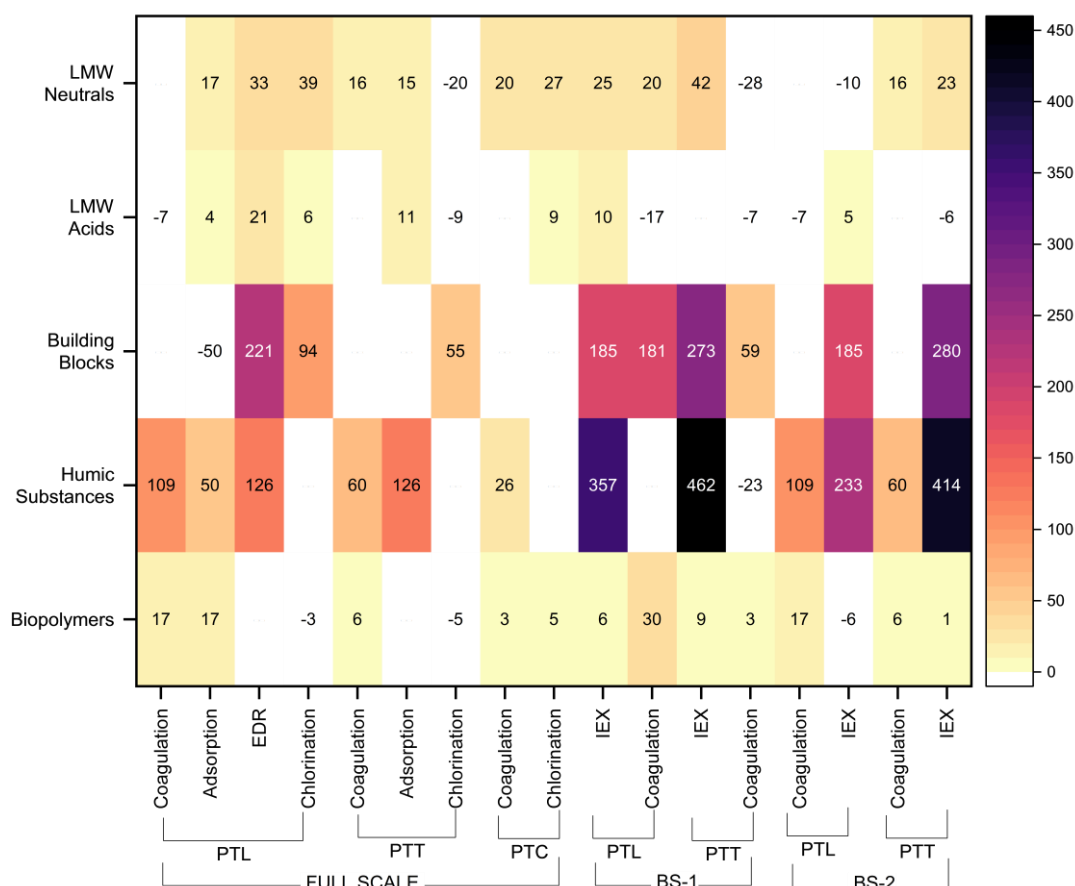


Figure 19: Differences in the concentration of DOC ($\mu\text{g/L}$) for each DOM fraction after treatments, calculated by subtraction of subsequent concentrations. The intensity of colours represents the magnitude of differences, with more intense colours indicating higher decrease of DOC.

3.2.1 Full Scale DWTPs

Coagulation, as a physicochemical process performed in the three DWTPs studied, affects the repulsive potential of the electrical charge and hydrophobicity of DOM constituents, facilitating their aggregation into microparticles and turbidity removal. The variation in DOM nature and the operational conditions among DWTPs lead to variations in the efficiency of the process. Coagulation accounted for a significant removal of HS fraction in the full-scale treatment configuration, being comparatively lower in the reservoir waters PTT ($60 \mu\text{g/L}$) and PTC ($26 \mu\text{g/L}$) than in PTL ($109 \mu\text{g/L}$) as presented in Figure 19. Notably, there was no reduction in the BB fraction DOC concentration after coagulation in any of the DWTPs, while biopolymers experienced a slight decrease, which was expected given their high molecular weight. This results in changes in the DOC distribution across the different DOM fractions after coagulation in the three DWTPs evaluated, reducing proportion of HS and increasing BB (Table 18).

PTL and PTT account with GAC adsorption after coagulation operation unit. Unlike coagulation, GAC targets the HS of lower molecular weight and lower aromaticity, and the BB fractions. In PTL, a HS reduction of $50 \mu\text{g/L}$ was achieved, while in PTT the reduction reached $126 \mu\text{g/L}$. In PTL, a DOC increase was detected in the BB fraction ($-50 \mu\text{g/L}$), suggesting the possibility of organic material release from the activity of the filters.

The EDR, as part of the full-scale treatment in PTL, reported significant DOC reductions in the BB fraction of 221 µg/L. While the inorganic ions elude at the same R_t than BB in the HPSEC separation, they do not contribute to the DOC signal. Consequently, the observed differences in DOC are attributed to DOM removal.

The final disinfection stage entailed variations primarily in BB for both PTL and PTT DWTPs, as measured by the DOC detector. However, no significant effect was produced over PTC. Chlorination reactions might consume that specific DOM fraction, leading to the formation of DBPs, including THMs.

3.2.2 Ion Exchange Bench-Scale

Ion exchange (IEX) performance was evaluated in bench scale in both PTL and PTT. Two configurations were considered in each case: IEX applied to the catchment water followed by a coagulation process (BS-1), and the reverse order, IEX applied after the full-scale coagulation operation (BS-2). The order and combination of processes involving IEX may play a significant role in the performance, since the treatment decreases the charge density of the water, thereby facilitating the removal of higher hydrophilic compounds during the subsequent coagulation processes (Andersson et al., 2020; Finkbeiner et al., 2020b; Tan & Kilduff, 2007).

In PTL the removal of HS achieved in a single IEX process (357 µg/L) surpassed the combined removal achieved by coagulation, adsorption and EDR in full scale. This increase was even more pronounced in PTT, where IEX achieved a HS removal of 462 µg/L. Using the configuration BS-2, the efficiency of HS removal was decreased, since a significant part of this fraction was previously removed by coagulation in the full-scale, leading to the same overall HS reduction in both configurations for both DWTPs.

On the contrary, there was a significant difference in the removal efficiency of the BB fraction depending on the BS configuration for both DWTPs. In PTL, IEX achieves a removal of 185 µg/L of BB regardless of the configuration. However, post-IEX coagulation achieved an additional 181 µg/L that was not removed before IEX. Similarly, in PTT, coagulation before IEX did not result in any BB removal, while IEX removed approximately 280 µg/L in both configurations, with an additional 59 µg/L removal after coagulation.

Throughout all treatments, including full and bench-scale processes, it was observed that LMW compounds, including both acids and neutrals, exhibited high recalcitrance. In particular, acids showed minimal alterations, and the most noticeable changes were observed in the removal of neutrals after processes involving ion removal such and IEX. Therefore, following BS treatments there is a noticeable shift in the distribution of DOC across DOM fractions (Table 18).

3.3 Humic Substances Sub-Fractions

In light of water characterization, HS are identified as the most abundant fraction constituting DOM, displaying diverse removal efficiencies across treatment operations. This section focuses on assessing the performance of both full-scale treatment processes and bench-scale IEX technologies, with particular attention to the predominant HS sub-fractions. The alterations in BB sub-fractions were lesser compared to those of the HS, yet slight significant variations were observed, suggesting that lower MW DOM fractions, with certain aromaticity, may play a role as THMs precursor.

3.3.1 UV-Multiwavelength Analysis of Humic Substances Sub-Fractions

A more profound analysis of divergences between HS sub-fractions was performed by evaluating their full absorbance profile. Figure 20 shows the spectroscopic profile in UV absorbance spectra (200 nm to 400 nm) within the humic substances HS1, HS2, and HS3 after each treatment unit. By considering the full absorbance spectra rather than single-wavelength monitoring, the sensitivity of the analysis is enhanced, allowing for a more accurate determination of the relationships between DOM fractions and DBPs formation (Helms et al., 2008).

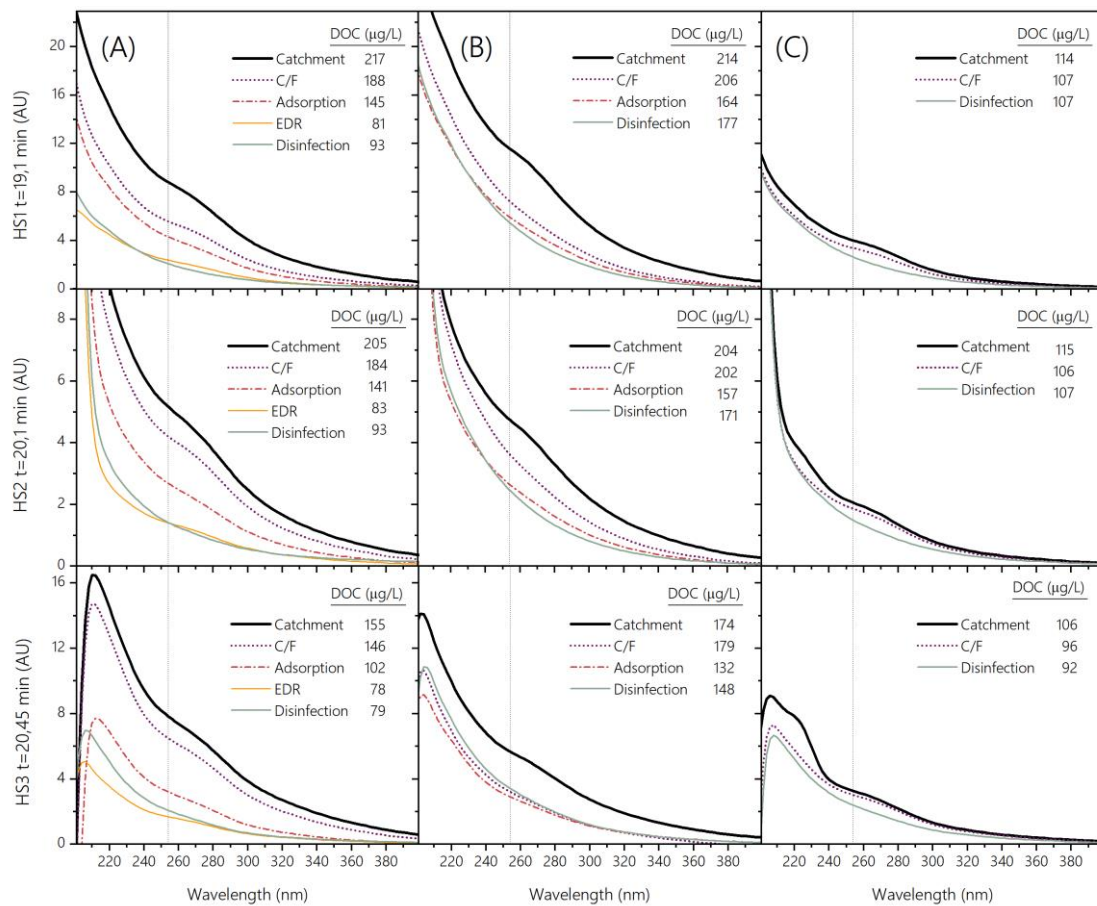


Figure 20: Overlap of absorbance spectra from Humic Substances peaks (HS1, HS2, HS3) of (A) PTL, (B) PTT and (C) PTC full scale treatment train. Vertical lines mark 254 nm.

The absorbance profiles of both HS1 and HS2 were similar in PTL and PTT, despite the different source of these DWTPs. PTC presented a lower profile, particularly in HS1 and HS3 than the other plants, which was consistent with the bulk values previously observed (Table 18). Across the three waters evaluated, there was a maximum in the absorbance of each HS sub-fractions around 270 nm, with higher intensity in PTT compared to PTL and PTC. This wavelength has been widely associated to aromatic groups related to DBP formation (Korshin et al., 2009). Compared to the distinct spectra of humic and fulvic acid standards from the Suwanee River (3S101H and 3S101F both from IHSS; see Appendix D, Figure A 6) where virtually two main maximums are noticed around 240 nm and 270 nm, Figure 20 evidences the heterogeneity of humic substances constitution by creating an absorbance profile with multiple overlaps.

Further differences were observed in adsorption features, with additional absorbance peaks around 200 nm, 250 nm, and 270 nm, revealing the presence of benzene adsorption bands (Brezinski & Gorczyca, 2019b). Moreover, a shoulder near 280 nm is observed in both PTL and PTT, while electronic transitions $\pi \rightarrow \pi^*$ from benzene rings bound to double C = O are denoted with an absorbance maximum at 310 nm (Chen et al., 2020b). These transitions are typical of oxidation products acting as DBP precursors. Regarding HS3, an adsorption peak around 230 nm suggests the presence of carboxylic and aromatic chromophores (Korshin et al., 2009).

Throughout the treatment processes, spectroscopic changes are observed particularly in the range between 240nm and 310 nm. The variations noted in HS2 sub-fraction in PTT were minor than in HS1, where the intensity of the signal dropped significantly, particularly at lower wavelengths (200 - 240 nm).

The relationship between the differential absorbance at 272 nm and its correlation with THMs has been extensively studied (Roccaro et al., 2009). In PTT, after coagulation, this absorbance maximum was smoothed out for all three subfractions, indicating the early depletion of these chromophores during the initial stages of treatment. However, a distinct behavior was observed in PTL, where this maximum disappeared only after the late treatments of EDR and disinfection. The phenolic compounds present in the HS undergo electrophilic aromatic substitution reactions with chlorine (Criquet et al., 2015a). These reactions affect fast chromophores such as carboxylic and aromatic groups, which absorb at wavelengths below 250 nm. Subsequently, the formation of cyclic and tautomeric ketones, hydroquinones, and catechols may occur, with adsorption peaks above 250 nm, encompassing the reactivity of slower chromophores like activated aromatic groups (Chen et al., 2020b). This mechanism is associated with the reactivity of the low MW phenols via two-electron oxidation reaction and is considered the main pathway for DBP formation (Wenk et al., 2013). Finally, it is worth noting that the effect of halogenation at higher wavelength ($\lambda > 350$ nm) is spectroscopically negligible (Byrne et al., 2011). Although the absorbance variation in that range after chlorination processes should be genuinely characteristic of DOM constituents, it was not observed in our findings.

The absorbance ratios at specific wavelengths have been linked with DOM properties such as aromaticity (A_{210}/A_{254}), polarity (A_{220}/A_{254}) or proportion between autochthonous and terrestrial DOM (A_{254}/A_{436}) (Cascone et al., 2022a; Ignatev & Tuhkanen, 2019b). The calculation of these ratios for the different HS sub-fractions provides deeper insights into the composition of these substances (Table 19).

Table 19: Absorbance ratios of humic substances fraction of catchment samples.

DWTP	Ratio	HS1 (19.1 min)	HS2 (20.1 min)	HS3 (20.45 min)
ABRERA		2.1	2.6	2.1
CARDEDEU	210/254	1.9	2.3	2.2
CARDENER		2.1	2.9	2.7
ABRERA		1.7	1.8	1.8
CARDEDEU	220/254	1.6	1.7	1.8
CARDENER		1.7	1.9	2.4
ABRERA		15.8	14.9	14.1
CARDEDEU	254/436	18.8	18.3	14.5
CARDENER		24.6	21.5	18.9

In terms of aromaticity and polarity, PTT accounted for the highest features, reflected in the lowest A_{210}/A_{254} and A_{220}/A_{254} ratio, followed by PTL and PTC. Specifically, HS1 was the most aromatic polar fraction, while HS2 presented the lowest aromaticity, and HS3 exhibited the least polar properties. The highest A_{254}/A_{436} ratios were observed for PTC and PTT, suggesting more terrestrial characteristics, as expected for reservoir waters in comparison with PTL. Across all samples, higher molecular weight HS sub-fractions showed the highest A_{254}/A_{436} ratios (HS1 > HS2 > HS3). The variability was more pronounced in PTC, where both HS1 and HS2 were similar as PTT. In contrast, PTL exhibited similarities between HS2 and HS3, the lowest MW humics.

3.3.2 Evaluating the Removal of Humic Substances

To assess a comprehensive evaluation of the diverse humic substances composition, Figure 21 depicts the distributions of DOC, and $SUVA_{254}$ within the HS sub-fraction at the three given retention times (HS1, 19.1 min; HS2, 20.1 min; and HS3, 20.45 min). The excluded portion of the fraction mainly gathers the lower weight tail of the peak, referred to as HS_{LMW} .

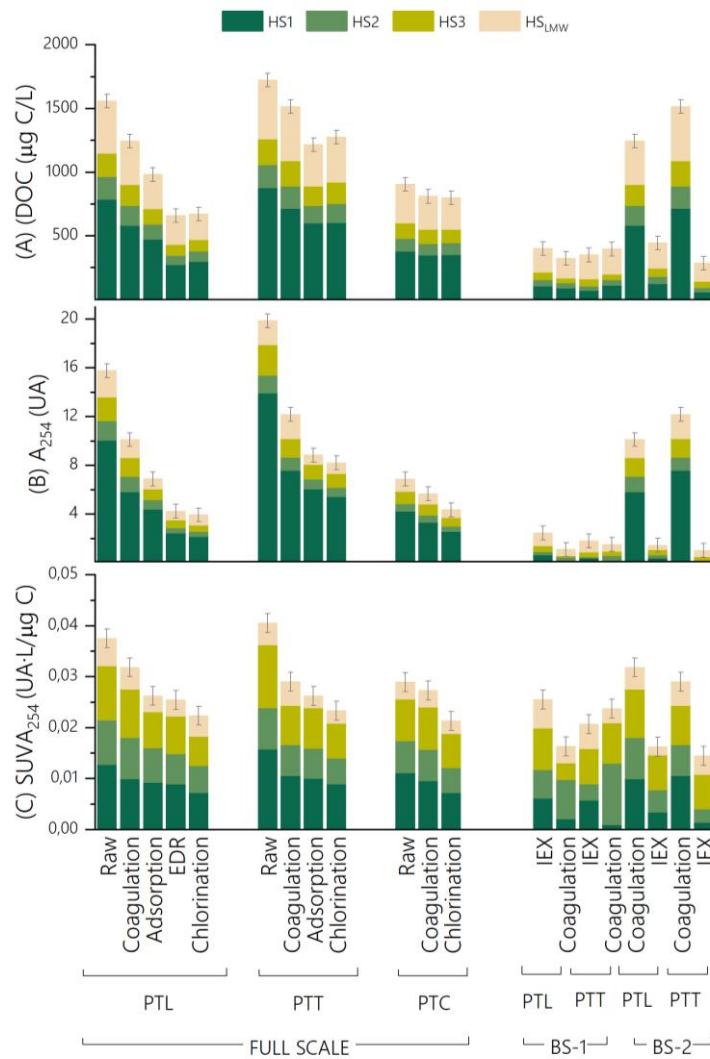


Figure 21: Distribution of (A) DOC, (B) A_{254} , and (C) $SUVA_{254}$ amounts for each HS1, HS2, HS3, relative to all HS fraction according to conventional and advanced treatments in PTL, PTT, and PTC.

The DOC quantification of HS sub-fractions revealed that HS1, the sub-fraction of higher apparent MW, was the most abundant across all water samples, a proportion that was maintained during both conventional and advanced treatments. Regarding aromaticity, HS1 also exhibited the highest absorbance at 254 nm compared to HS2 and HS3 in general terms. The evaluation of the treatment operations across the DWTPs revealed varied responses to HS sub-fractions removal, emphasizing the complex dynamics of DOM removal.

Coagulation mainly reduced chromophores in the HS fractions of higher molecular weight and aromaticity: HS1. The A_{254} was reduced by 42%, 45%, and 21% and the DOC concentration in 26%, 19% and 8% for PTL, PTT, and PTC respectively. These findings sustain the selectivity of coagulation-flocculation processes on removing compounds of HMW and hydrophobicity. Overall, the impact of coagulation-flocculation on HS removal suggests that DOM chromophores were predominantly of a higher nucleophilic nature. Notably, absorbance differences in HS were most pronounced between 200 nm and 240 nm, with steeper slopes compared to higher wavelength regions (i.e., 360 nm to 400 nm), where absorbances remained relatively consistent across treatments (Figure 20).

Moreover, the comparison of the A_{210}/A_{254} ratio highlights differences in the composition after coagulation, with PTT showed a higher proportion of aliphatic HS fractions compared to PTL. This contributes to the sustained reduction of performance in the subsequent adsorption processes. Contrasting observations in PTC, where differences in $SUVA_{254}$ were evident but DOC removals of HS fractions were nearly equal, suggest that short wavelength chromophores removal may arise predominantly from coagulation.

GAC filtration targeted fractions of lower apparent MW, i.e., HS2, HS3, and HS_{LMW} , resulting in DOC removal efficiencies ranging from 21 to 26% in both TPs. However, the corresponding decrease in A_{254} was much more pronounced in PTL compared to PTT, as evidenced in Figure 21. Adsorption removal is enhanced by electrostatic forces, thus the diverse susceptibilities of the DOM fractions to the treatment. Low MW HS are richer in saturated moieties of less hydrophobicity, yet they are polar enough to be prone to adsorption removal. However, except from adsorption, low MW fractions remained recalcitrant in other conventional treatments, turning them into precursors for DBPs formation.

Although EDR mainly targets the removal of anions, it still led to a significant decrease in aromatic compounds, especially those of higher molecular weight in HS1 and HS2, with DOC removal of 24% and 19% respectively.

Ion-exchange accounted for the highest removals both in terms of concentration and absorbance over the conventional treatments (>80%). Specially targeting fractions of higher molecular weight (HS1), yet HS2, HS3, and HS_{LMW} were largely removed (>50%) compared to other treatments. Those findings suggest that ion exchange could be a suitable technology for compounds containing ionized groups such as carboxylic and phenolic groups, electron-rich structures of high molecular weight which abundant in HS.

The detailed analysis of $SUVA_{254}$ revealed the metric's utility as a surrogate parameter, although the complexities arising from interactions between fractions and treatment processes affect the theoretical mechanisms reflecting DOM reactivity. Despite that in terms of $SUVA_{254}$ the reactivity of HS1 and HS3 was mostly equal on conventional treatments, HS2 showed an increase with the coagulation after IEX treatment (BS-1).

3.4 Assessment of THM-FP through Conventional and IEX Treatments

3.4.1 THM-FP in Treatment plants from River Sources: PTL

In PTL, the initial THM-FP (72h) of the catchment water before treatment showed concentrations of 38.8 µg/L of TCM, 108.55 µg/L of BDCM, 134.54 µg/L of DBCM and 70.1 µg/L of TBM. This distribution reflects the bromide concentration of the catchment water (Table 18). Figure 22 illustrates the reduction on the THM-FP (µg/L) achieved after each operation during the water treatment processes, for each specie and for the total, referred as THM₄.

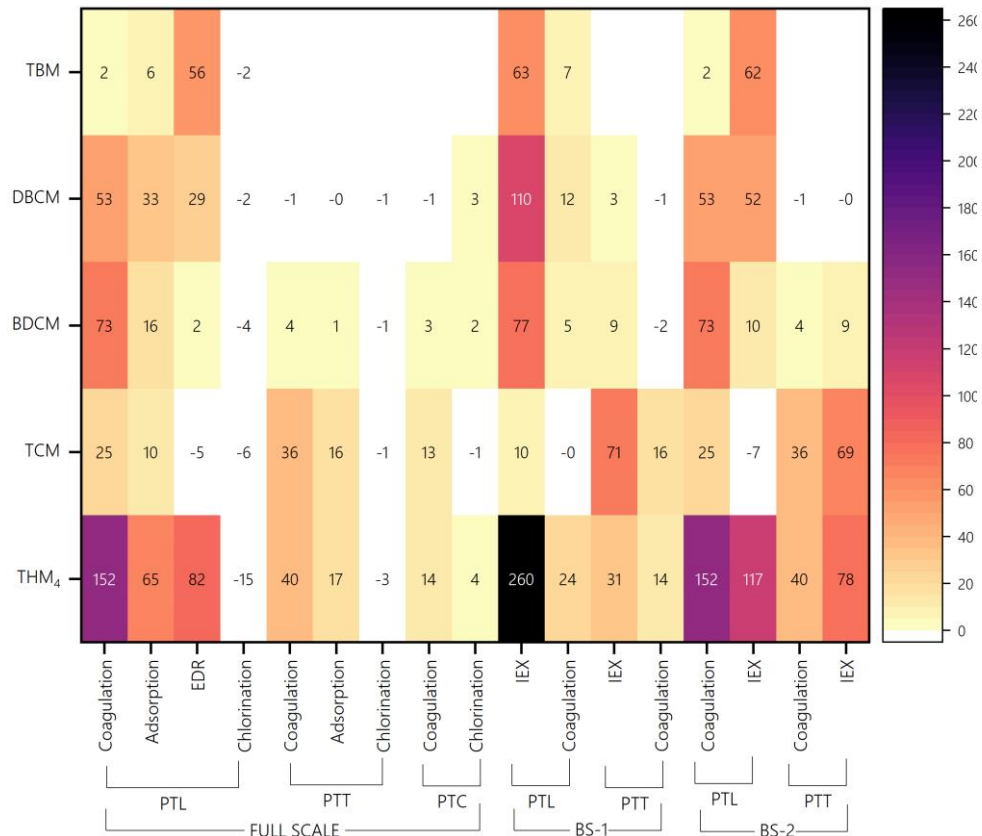


Figure 22: THMs-FP reduction in µg/L, expressed as differences in between unitary operations from the full-scale treatment and bench scale IEX tests (BS-1, BS-2) for each DWTP.

Coagulation was found to be the most effective operation for reducing THM₄-FP in PTL, primarily targeting the reduction of BDCM and DBCM. Additionally, after adsorption, further reductions in THM₄-FP were observed, influenced by the alterations on the DOM fractions distribution (Figure 19) that affected particularly HS of lower MW (Figure 21), causing a decrease of DBCM. The application of EDR resulted in a significant alteration in their reactivity, enhancing the removal of bromide, and consequently the FP of brominated THMs (TBM and DBCM).

The reduction in THM₄-FP indicated the effectiveness of the treatment processes in reducing the THM-FP. Specifically, after completing the whole treatment train process, there was a reduction of 73% in THM₄-FP, and the final FP showed concentrations between 4.2 µg/L for TCM, and 24.5 for DBCM.

In the bench-scale IEX testing, combining IEX and coagulation led to more pronounced reductions in THM₄-FP. The order and combination of processes played a significant role in the speciation of THMs,

with IEX treatment decreasing the charge density of the water and facilitating the removal of higher hydrophilic compounds during subsequent coagulation processes (Andersson et al., 2020; Finkbeiner et al., 2018). The overall decrease in the FP of brominated THMs achieved in bench scale was higher than in conventional full scale.

3.4.2 THM-FP in Treatment plants from Reservoir Sources

In contrast to PTL, PTT had undetectable levels of bromide (Table 18), leading to a different profile of brominated DBPs. In catchment water the most abundant species were TCM (112.2 µg/L), followed by BDCM (23.1 µg/L) and DBCM (3.1 µg/L), with undetectable levels of TBM. Consequently, the total initial THM₄-FP was half of PTL.

Coagulation was effective in reducing THM₄-FP in PTT, primarily targeting the reduction of TCM. Additionally, after adsorption processes, there were slight reductions in THM₄-FP in PTT. However, the effects were less pronounced compared to PTL. After completing the entire treatment process, there was a reduction of 40% in THM₄-FP. Likewise, in bench-scale IEX testing, the reductions in THM₄-FP were less significant in PTT compared to PTL.

Similar to PTT, PTC also had undetectable levels of bromide. The initial THM₄-FP was 65.5 µg/L, distributed as 38.5 µg/L of TCM, 19.2 µg/L of BDCM and 7.8 µg/L of DBCM. Coagulation was effective in reducing THM₄-FP, primarily targeting the reduction of the dominant specie, TCM, achieving a reduction of 14% in THM₄-FP.

3.5 Assessment of Humic Substances and THM-FP Correlation

As previously discussed, most treatment processes targeted HS, whose changes can be tracked through DOC quantification and absorbance measurement. Also, previous studies have highlighted the key role of HS in the formation of THMs given their singular structural composition of high MW, aromatic, and hydrophobic moieties. These attributes make HS reactive towards chlorine via electron capture reactions (Chowdhury et al., 2010; Westerhoff et al., 2004). This section aims for gathering the observed changes on HS measured by means of surrogate parameters (DOC, A_{254} , and $SUVA_{254}$) fractions and discussing their impact on measured THMs-FP. To quantitatively evaluate the relationships between the HS sub-fractions with THMs-FP, Pearson's' correlation analysis was performed and the results are presented in Figure 23. Due to the different speciation of THM compounds resulting from the presence of bromide in the river water of PTL catchment, the results are analysed separately.

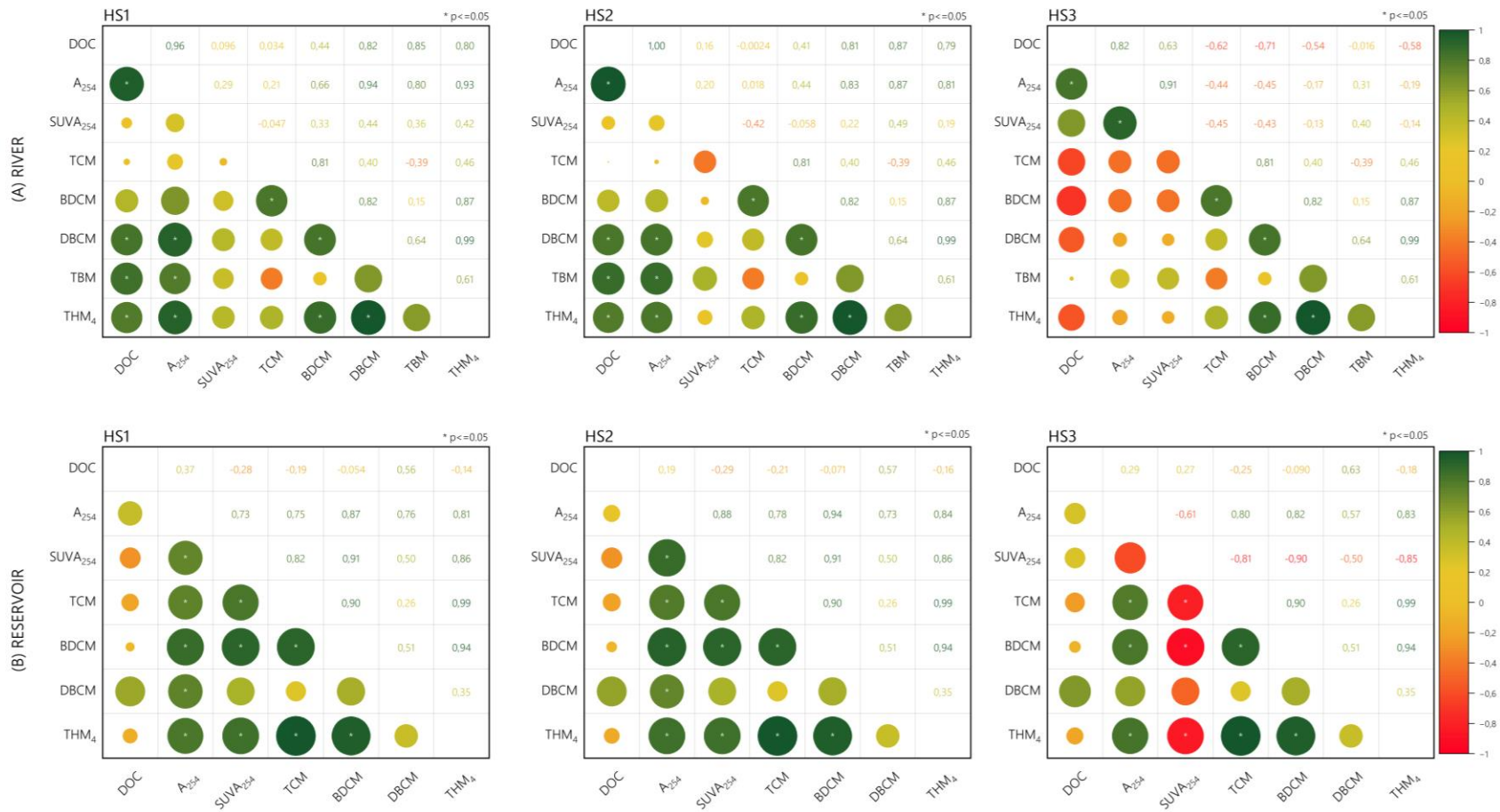


Figure 23: Pearson's correlation matrices of HS surrogate parameters and THMs-FP. Significant correlations (p-value ≤ 0.05) are marked with * symbol inside the circle.

Significant correlations (p -value ≤ 0.05) were identified between both DOC and A_{254} and the THM₄-FP for HS1 and HS2 in PTL. These correlations were notably influenced by the high regression coefficients observed for the brominated THM species BDCM and TBM, indicating a clear correlation between their formation potential and the DOC and A_{254} of sub-fractions HS1 and HS2. However, no significant relation was obtained with the HS3 sub-fraction in any case in PTL. Also, the FP of TCM and BDCM did not correlate significantly with the surrogate parameters of none of the HS fractions in PTL.

In contrast, reservoir water demonstrated a different pattern. In this case, the TCM-PF showed a clear correlation with the A_{254} of the three HS sub-fractions, that was also observed for BDCM-FP. However, this spectroscopic correlation did not extend in terms of DOC. Overall, the A_{254} of the major sub-fraction HS1 exhibited a strong correlation with the THM₄-FP.

The findings indicate that spectroscopic changes reflect the behaviour of specific DOM fractions after undergoing treatments, correlating with THMs-FP. This suggests that multiple chromophores are involved in reactions that lead to the formation of THMs, in agreement with (Awad et al., 2016), who reported that sole monitoring of general parameters such as DOC proxies in presence of bromide might be insufficient to understand the reactivity of DOM towards DBPs formation. By contrast, a detailed spectroscopical analysis can provide further information about DOM functionalities.

4. FINAL REMARKS

The application of HPSEC-DAD-OCD enabled a detailed analysis of the absorbance profiles of DOM fractions and HS sub-fractions, shedding light on their role as DBPs precursors. The analysis revealed differences in DOM composition, highlighting the heterogeneity within the samples and providing insights into their reactivity as THM precursors.

Conventional water treatment processes, such as coagulation and GAC adsorption, mainly targeted higher MW DOM fractions, while EDR and IEX were more effective for the removal of lower MW fractions, including building blocks and LMW compounds, which often remained recalcitrant to standard treatments.

Spectroscopic analysis provided valuable insights into DOM functionalities, supporting the differentiation of reactivity between samples, compared to unspecific measurements like DOC. This approach not only reinforced the importance of characterizing waters but also emphasised the site-specificity of treatment requirements, enabling more efficient treatment tailoring. The evaluation of absorbance ratios A_{210}/A_{254} and A_{220}/A_{254} provided further understanding of the behaviour of DOM fractions based on their physicochemical properties.

River-sourced water exhibited distinct THM speciation compared to reservoir-sourced water, influenced by the presence of bromide. Significant correlations between surrogate parameters and THM₄-FP for specific HS sub-fractions elucidate the link between DOM characteristics and THM formation potentials. In river-sourced water, brominated THM species showed clear correlations with both DOC and A_{254} of HS1 and HS2, while in reservoir-sourced water, A_{254} of major HS sub-fractions exhibited strong correlations with THM₄-FP. These findings underscore the importance of spectroscopic analysis in predicting DBPs formation and optimizing treatment strategies.

Chapter VI

RESULTS III

Development of experimental data-based predictive models for regulated organic disinfection by-products using a novel approach to select DOM spectroscopical variables

1. BACKGROUND AND OBJETIVES

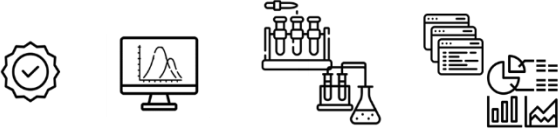
Striking the balance between disinfectants to ensure the microbiological safety of drinking water and the formation of disinfection by-products (DBPs) is a challenge the operators of drinking water facilities daily deal with. To optimize disinfection and minimize generation of DBPs is crucial to find suitable proxies to track the reactivity of major precursors, such as dissolved organic matter (DOM), during disinfection processes. Given the optical properties of DOM, developing spectroscopic-based tools to monitor changes of these precursors seems a promising technology, considering its ease of implementation and data processing. However, selecting the most appropriate signals can be a difficult and confusing task.

Commonly, absorbance at 254 nm is used as a surrogate parameter of water quality, reflecting aromaticity, molecular weight, or reactivity (Korshin et al., 2007; Peacock et al., 2014). Also, finding a proxy between NOM reactivity towards chlorination processes and the formation of DBPs has been widely investigated through differential absorbance (DAS), mostly at 272 nm (Cascone et al., 2022b; Korshin et al., 2002; Roccaro & Vagliasindi, 2009). Here, a novel method for variable selection based on spectroscopical changes derived from chlorination and their role in predicting THMs and HAAs-FPs is presented.

2. METHODOLOGY

Table 20 presents the references to the employed methodology in this chapter. Parameters of the full general characterization and DBPs-FP are presented in Appendix B (Table A 6 and Table A 8).

Table 20: Summary of the analytical workflow and methodologies used in Chapter VII.

SAMPLING	METHODOLOGICAL WORKFLOW			
<p>DWTs:</p> <ul style="list-style-type: none"> - Montfullà - Cardedeu - Abrera <p>N° Sampling campaign: 3 (1 included for validation)</p> <p>N° Samples: 17 + (26)</p>				
	<p>General Water Quality Parameters <i>(Chapt. III - 1)</i></p>	<p>DOM fingerprinting SEC <i>(Chapt. III - 2.1)</i></p>	<p>DBPs analysis Formation Potential Tests – 48 h <i>(Chapt. III - 3.1)</i> + HS-GC-MS <i>(Chapt. III - 3.2.1)</i></p>	<p>Statistical Analysis Multiple Correlation & Hierarchical Clustering <i>(Chapt. III - 4.2)</i> + K-fold Cross Validation <i>(Chapt. III - 4.3)</i></p>

3. RESULTS AND DISCUSSION

3.1 Water characterization (bulk & fractionated parameters pre/post chlorination)

This section summarizes water characterization regarding bulk and advanced HPSEC-DAD-OCD analysis of samples before and after their chlorination.

3.1.1 Bulk parameters

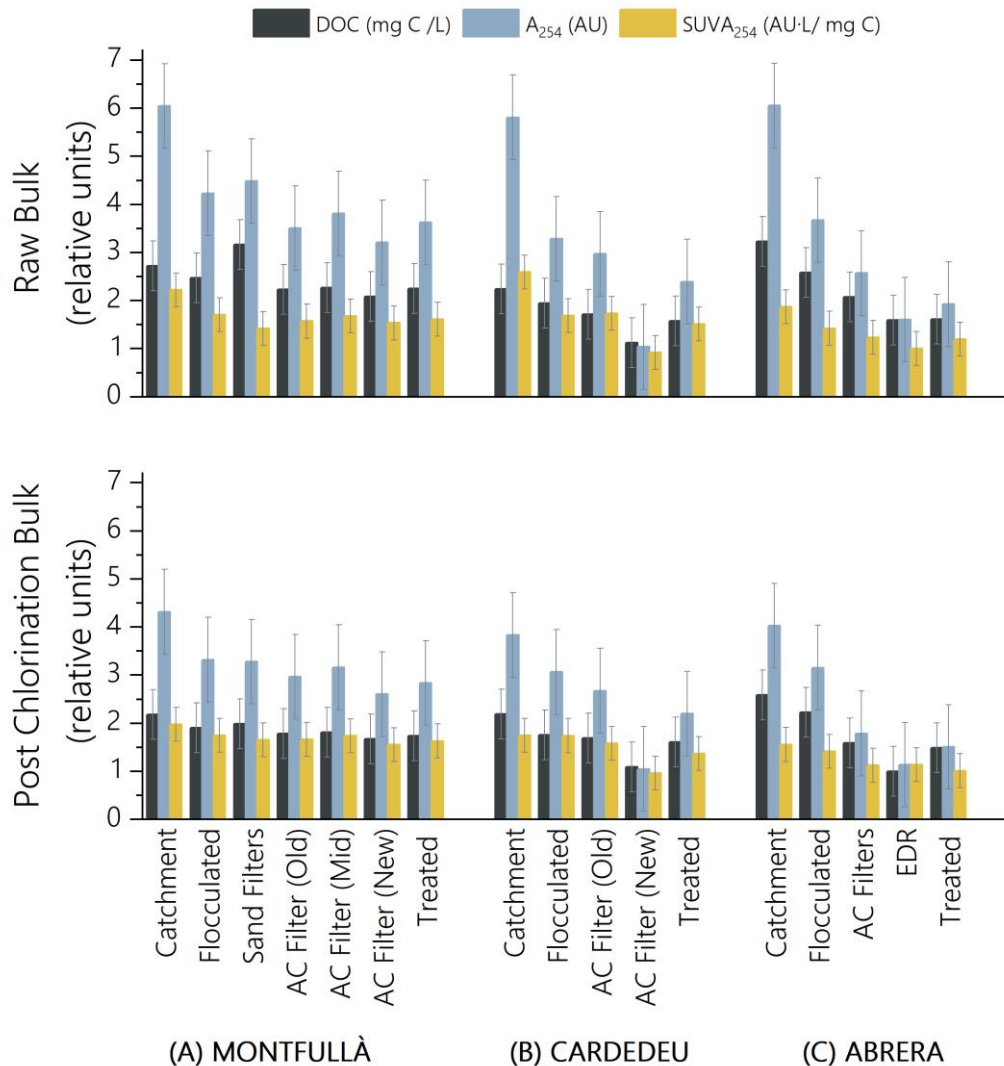


Figure 24: Reduction of bulk parameters of samples from three different DWTPs with treatment operations.

Overall, as illustrated in Figure 24, the sequence of treatments aids in reducing the general water quality parameters, especially TOC, but also absorbance at 254 nm (A_{254}). All three raw source waters exhibited similar levels of TOC (~ 3 ppm) and A_{254} (~ 6 AU). The main differences between treated waters resulted from applying different operations or specific operational conditions to each DWTP. Overall, variations between pre- and post-chlorination (raw vs. after formation potential) were higher in source waters and during the first treatments (coagulation/flocculation), which might indicate higher DOM reactivity compared to final processes. Along with treatments, DOM fractions potentially acting as DBPs precursors are removed, thereby decreasing their capability to react (Korshin et al., 2007; Moyo et al., 2020).

The Montfullà DWTP (PTM) achieved the main TOC and A_{254} reductions through initial flocculation (Figure 24A), although levels slightly increased following sand filtration, which can be attributed to biological activity on filters (Peacock et al., 2014). Subsequent adsorption on AC filters reduced TOC

and A_{254} to 2.2 ppm C and 3.6 AU. A comparison of filter ageing did not reveal significant differences between the oldest and middle time-of-use. However, the newest filters achieved greater adsorption capacities. After chlorination, changes in DOM structural configuration resulting from the formation of DBPs were reflected in the decrease of bulk parameters. In terms of $SUVA_{254}$, post-chlorination values increased compared to raw waters, which depicts its reactivity: the breakdown of higher structures led to smaller fractions of DOM presenting a higher degree of conjugation (high A_{254}) per unit of TOC.

In the Cardedeu DWTP (PTT), flocculation was also responsible for the highest reduction of TOC and here, mostly A_{254} (Figure 24, B). This situation suggests fractions of DOM being targeted through flocculation exhibited higher chromophoric units. Here, the most glaring disparity is the effect of the new regenerated AC filters, which exhibited the sharpest reductions on TOC and A_{254} (42% and 68%, respectively). In terms of $SUVA_{254}$, a similar trend to PTM was observed. This suggests that, despite treatments and operational conditions, the reactivity of treated waters coming from the same reservoir is similar between plants.

A peculiarity of the Llobregat DWTP (PTL) are the EDR modules, which play a remarkable role in reducing chromophores: EDR achieves a 38% reduction in A_{254} compared to a 20% reduction in coagulation (Figure 24, C). When compared to the reservoir waters, $SUVA_{254}$ values were lower, and post-chlorination values did not exceed the raw levels, indicating a distinct reactivity.

3.1.2 *Fraction distribution*

Advanced characterization of DOM was performed using HPSEC-DAD-OCD to depict the molecular weight distribution of their compounds. Overlapped DOC and absorbance chromatograms of raw waters are presented in Figure 25. Chromatograms of the full AMW distribution of fractions from the whole sampling campaign are presented in Appendix E (Figure A 7, Figure A 8, and Figure A 9)

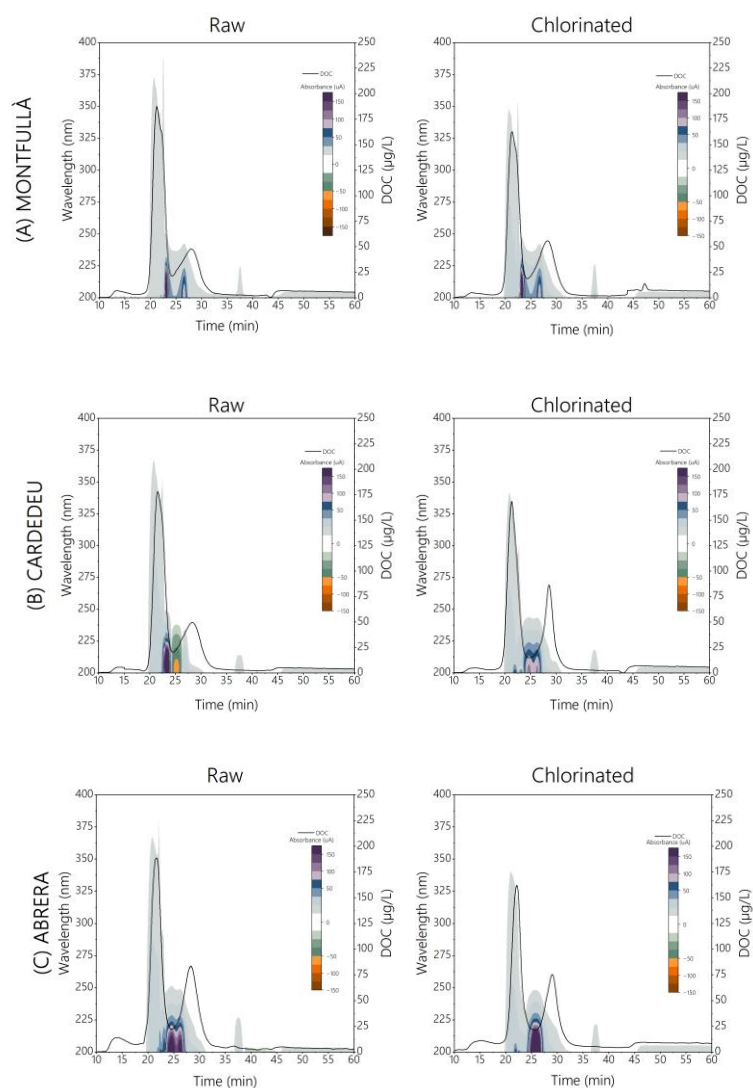


Figure 25: Overlapped DOC and absorbance chromatograms of raw waters from the (A) Montfullà, (B) Cardedeu, (C) Abrera DWTPs before (left) and after (right) their chlorination.

Overall, chlorination led to subtle changes in DOM profiles. Mostly, absorbing ranges as well as intensities were reduced after the chlorination reactions in the regions of humic substances and building blocks.

Results from the quantitative analysis are presented in Figure 26, which depicts the differences in DOM fraction distribution observed depending on the source. Raw water from the Llobregat River presented higher concentrations of biopolymers compared to raw water from the Ter reservoir. Usually, this fraction is naturally removed from the reservoir through the natural filtration of the strata. The most abundant fractions in both sources were attributed to humic substances. The riverine water also presented higher amounts of building blocks and low molecular weight compounds that considerably increased after chlorination, in contrast to the behaviour of the reservoir samples (Figure 26, B).

The initial distribution of fractions in reservoir samples was similar, but differences in treatments resulted in divergences in terms of final concentrations, particularly concerning humic substance fractions. Based on measured levels, PTT demonstrated better efficiency than PTM in removing humic

substances. However, chlorination effects varied slightly between plants, suggesting that treatments did not affect reactivity but rather concentration (Figure 26).

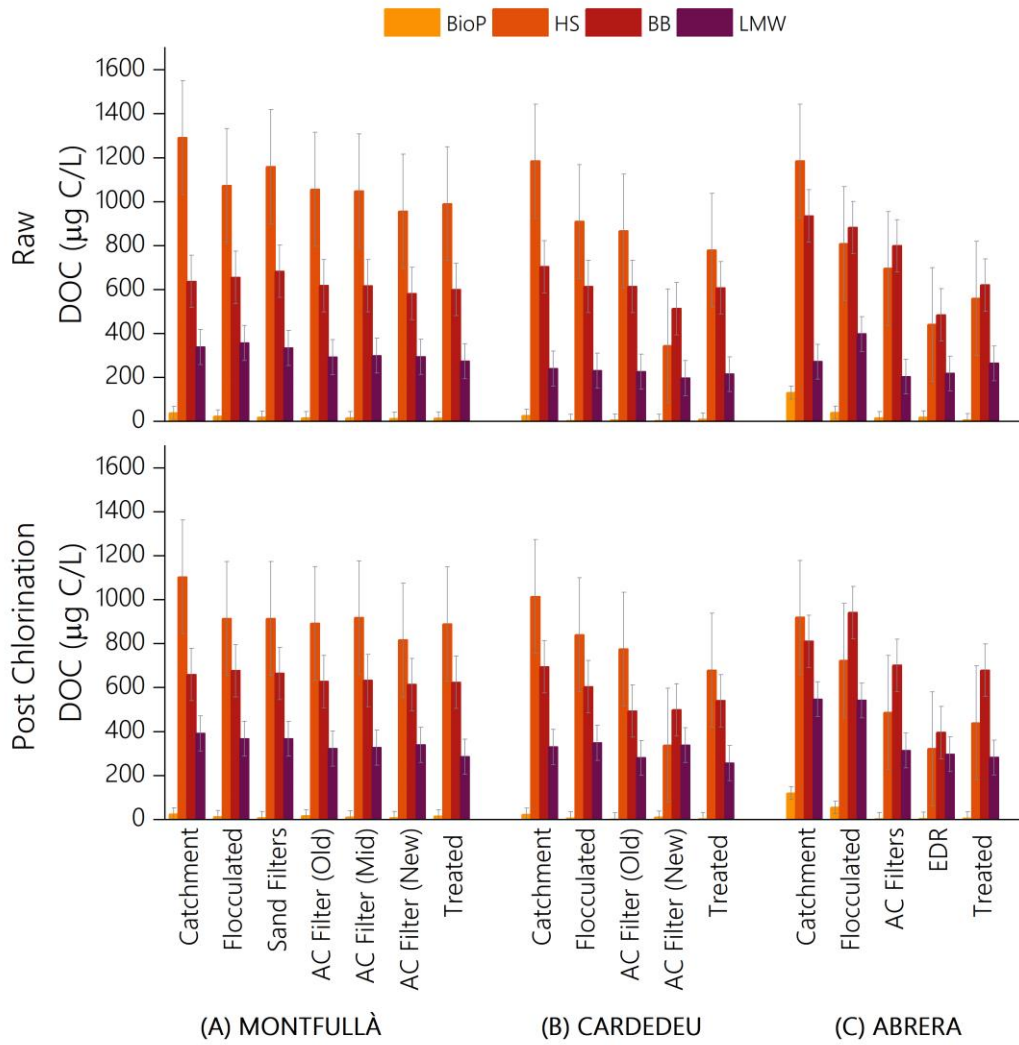


Figure 26: NOM fraction distribution of pre- and post-chlorinated process samples from three different DWTP.

3.2 DBPs distribution

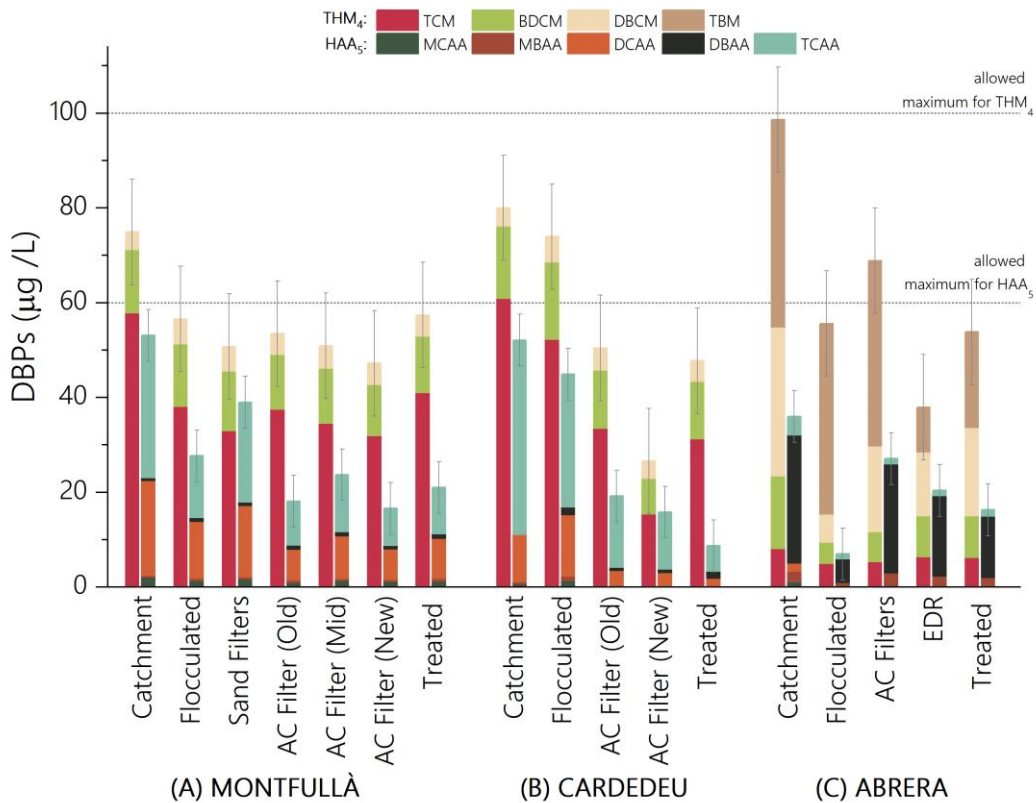


Figure 27: Amounts of organic regulated DBPs after chlorination on FP tests of process samples from DWTPs. Regulation limits are represented with horizontal lines.

The site specificity of water sources highly impacts DBPs speciation during chlorination reactions, as shown in Figure 27. While catchment waters in PTM and PTT exhibited similar trends in the formation of THMs and HAAs formation at very similar levels, PTL presented a completely different speciation profile.

In reservoir waters (Figure 27 A and B), higher chlorinated THMs (TCM and BDCM), and HAAs (DCAA and TCAA, more than MCAA) were predominantly formed. Additionally, few brominated DBPs were detected, including BDCM and DBCM, while brominated HAAs (DBAA and MBAA) were scarcely found, and TBM was undetected in either of the DWTPs.

A very different distribution was observed in the riverine samples (Figure 27), where brominated DBPs were the most abundant species. Concentrations of TBM and DBCM were higher than those of BDCM and TCM. Regarding HAAs, the concentration of DBAA exceeded that of TCAA, MBAA, DCAA, and MCAA. This tendency in speciation can be attributed to bromide naturally present in the Llobregat River at relatively high concentrations (0.6 mg/L), acting as a precursor for the formation of Br-DBPs.

Compared to the reservoir waters, the riverine samples were more prone to the formation of THMs but less prone to HAAs generation. On no account, the total amounts of THMs (THM₄, expressed as the sum of TCM, DBCM, BDCM, and TBM), as well as the total amounts of HAAs (HAA₅, as the sum of

MCAA, MBAA, DCAA, DBAA, and TCAA) did not exceed the established levels on the European Directive (EU) 2020/2184 on drinking water of 100 µg/L and 60 µg/L respectively.

3.3 Evaluation of differential absorbance (DAS) of HPSEC-DAD-OCD humic substances after chlorination

Given that humic substances were the most abundant NOM fraction in the studied waters and also contributed significantly to absorbance, a detailed study on the differential absorbance spectra (DAS) profile was specifically performed over their spanning region (17 – 24 min). An example of the resulting DAS chromatograms of the humic substances fraction of each raw water is presented in Figure 28.

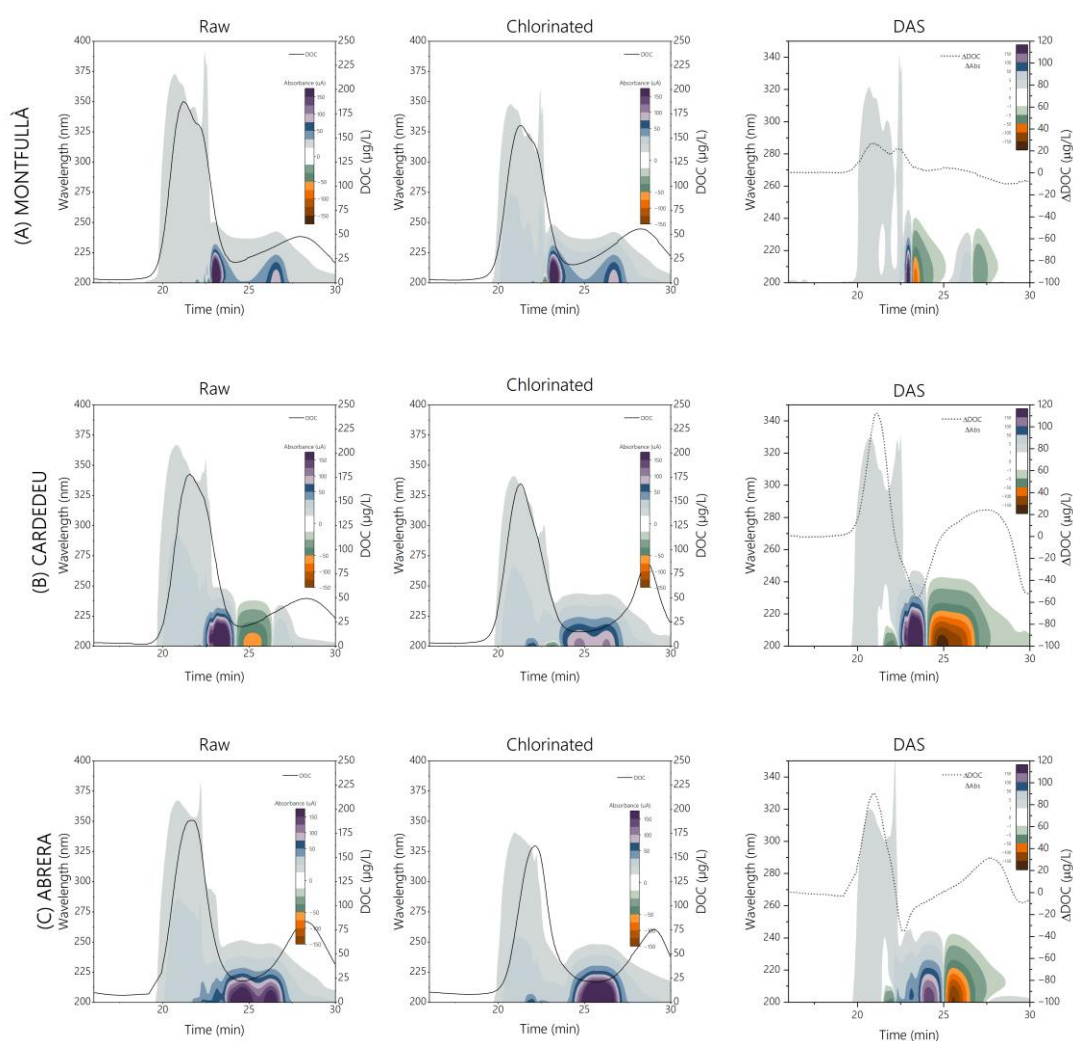


Figure 28: DAS chromatograms of humic substances fraction resulting from the subtraction of pre- and post-chlorinated raw water samples from (A) Montfullà, (B) Cardedeu, (C) Abrera DWTPs.

In all cases, a decrease in absorbance was experienced after the chlorination as a result from active moieties reaction. As discussed in the introduction, the absorption capacity of a molecule will depend on the chromophoric groups, meaning those functionalities are able to exchange electrons. Historically, absorbance at 254 nm has been widely studied as a surrogate of those properties, as it corresponds to the maximum of one characteristic absorption band of benzene, providing at its time information about structure and reactivity. Related to the reactivity of drinking water towards disinfection, a maximum near

272 nm is described to selectively reflect changes after chlorination processes. Thus, their relationship with DBPs formation has been previously studied (See Appendix E Table A 13).

Often, selection of wavelengths for monitoring can remain unclear or inaccurate. High variability in DOM composition, substitution, and conformation might affect the sensitivity of methods based on a single wavelength measurement. Multiple substituents from molecules conforming DOM can exhibit similar frequencies (vibrational energy of their electrons), resulting in a mathematical correlation between wavelengths. This work aimed to study those possible wavelength associations between 200 nm and 400 nm, on the spectra resulting from the effects of chlorination. After, through applying a hierarchical cluster analysis over the correlation matrices, four wavelengths were extracted and selected as representative of the spectroscopic changes induced by reactivity with choline on the humic substance fractions.

3.3.1 Study of wavelength correlations and hierarchical clustering

To specifically evaluate the effects of chlorination over the spectroscopical properties of DOM, the DAD spectra of pre-chlorinated samples were subtracted to their respective after chlorination. From the resulting DAS, data corresponding to the humic substances fraction (17 min - 24 min) was extracted to assess changes driven by the formation of DBPs of the most abundant and, theoretically, precursor fraction (see Figure 28). This procedure constitutes a complete novel approach to assess correlation within disinfection by-products and specific DOM fractions based on their multiwavelength DAS.

First, correlation analysis between variables (wavelengths ranging from 200 to 400 nm, 2 nm step) was conducted. This analysis was performed individually for each sample, as slight differences were found between source waters and treated waters at different stages. Overall, closely located wavelengths showed higher correlations with each other ($0.75 \leq r \leq 1$), while lower wavelengths (below 242 nm) tended to be inversely correlated ($-1 \leq r \leq -0.25$) with wavelengths above 280 nm.

Subsequently, hierarchical clustering was applied to the correlation matrices to determine the most representative wavelengths. The optimum number of clusters (4) was determined evaluating the Canlinski-Harabaz index (CHI) (See Appendix E, Table A 14). Centroids of each cluster were extracted for each sample, (See Figure 29 for an example), and the mean values of the specific centroids of each sample were calculated (See Table 21).

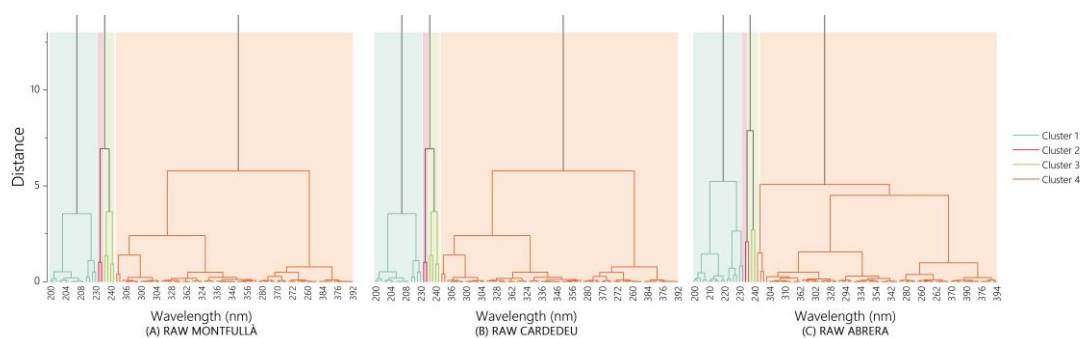


Figure 29: Hierarchical clustering of raw waters from (A) Montfullà DWTP, (B) Cardedeu DWTP, and (C) Abrera DWTP.

While minor variations were observed between samples and sources, the highest dispersion (10% of coefficient variation, CV) was found between the values of the third centroid. Nonetheless, single values were selected regardless of the source water to ensure a robust approach.

Table 21: Individual cluster's centroids and representative values (mean values).

DWTP	Sample	Centroid 1 (nm)	Centroid 2 (nm)	Centroid 3 (nm)	Centroid 4 (nm)
PTM	Catchment	216	236	241	322
	Flocculated	219	243	282	359
	Sand Filters	216	238	275	354
	AC Filter (Old)	219	243	302	379
	AC Filter (Mid)	219	243	274	351
	AC Filter (New)	217	239	285	364
	Treated	216	237	281	361
PTT	Catchment	216	236	241	322
	Flocculated	221	272	327	386
	AC Filter (Old)	221	272	323	385
	AC Filter (New)	221	265	317	386
	Treated	221	268	319	384
PTL	Catchment	216	237	244	324
	Flocculated	218	239	286	354
	AC Filters	221	270	306	373
	EDR	222	271	328	386
	Treated	221	270	306	373
	MEAN	219	252	290	362
	CV%	1	6	10	6

These results are consistent with those reported by Chen and co-workers (Chen et al., 2020a), who observed similar characteristics and changes in the DAS after chlorination of humic substances standards. They described chlorination-induced changes on the absorbance maximum around 272 nm, while also noting weak features at wavelengths near 220 nm, 240 nm, 320 nm, and 380 nm, which match the values of the centroids (Table 21). Likewise, Yan (Yan et al., 2014), described strong correlations between chlorine consumption and FP of THM₄ and HAA₉ with the log transformation of DAS at 350 nm.

3.4 Spectroscopic prediction models of DBPs

3.4.1 Predictive models based on DAS of HPSEC-DAD-OCD analysis on humic substances

Once the cluster centroids were determined, the integration of the DAS spectra within the region of elution of humic substances was performed at the four selected wavelengths: 220 nm (instead of 219 nm, due to the available acquisition frequency), 252 nm, 290 nm, and 362 nm. Additionally, DAS at 272 nm was considered as an extended reference for DOM reactivity towards DBP-FPs based on bibliographic findings.

Subsequently, MLR models were adjusted to predict the FP of regulated THMs and HAAs under two scenarios: (a) considering samples from both sources, or (b) splitting the database between riverine

samples and those from reservoirs. The goodness of the modelling is summarized by the significant R^2_{adj} values presented in Figure 30, and full details of model parameters are included in Appendix E (Table A 15, Table A 16, Table A 17).

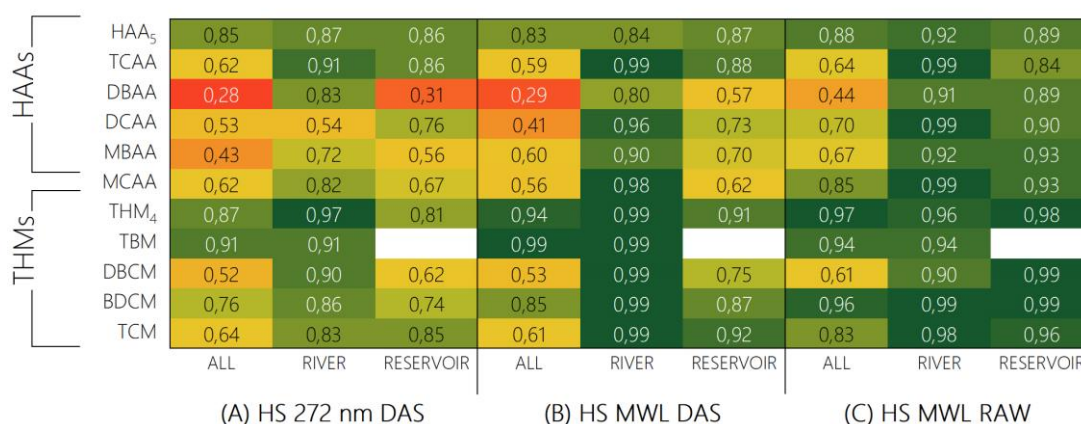


Figure 30: Heatmap of the R^2_{adj} values for MLR models based on DAS of HS using a single wavelength at 272 nm (A), multiwavelength approach (B), or multiwavelength approach based on raw measurements (C).

Overall, predictions improved when splitting the data set depending on the water source, this effect was already observed and discussed previously in Chapter IV. However, strong correlations were also observed when aggregating the entire dataset for THM₄ (R^2_{adj} 0.94 and 0.87, on both DAS approaches respectively) and HAA₅ (R^2_{adj} 0.83 and 0.88). The multiwavelength approach based on the clustering from DAS on HS provided better predictions compared to models based on single DAS at 272 nm as observed in Figure 30, especially for riverine samples.

This finding supports the hypothesis that a multiwavelength method can contribute to minimizing random errors associated with single signal monitoring, that can be caused by a strong dependence on a major functionality or fraction (G.-S. Wang & Hsieh, 2001).

After evaluating the multiwavelength approach on the DAS of HS, a new outlook involving the raw absorbance of the humic substances fraction before chlorination was examined (Figure 30, C). This perspective aims at simplifying the experimental procedures for predicting the FP of DBPs and to determining whether a single absorbance measurement could avoid the differential calculation after chlorine dosing.

In general, using the multiwavelength raw absorbance of HS improved adjustments compared to the multiwavelength approach based on the DAS. Indeed, higher sensitivity is needed to quantify the subtle changes derived from chlorination compared to the values of a single measurement. Thus, models based on a raw multiwavelength signal enhanced the predictability. The improvements were particularly noticeable in reservoir samples, where DAS calculations were smaller than in the riverine case.

Models for specific DBPs presented stronger correlations in the separate scenarios, ranging from $0.96 < R^2_{adj} < 0.99$ and $0.84 < R^2_{adj} < 0.93$ for individual THMs and HAAs in reservoir waters, to $0.90 < R^2_{adj} < 0.99$ and $0.91 < R^2_{adj} < 0.99$ respectively in the river source. When considering both sources to account for maximum variability in terms of DOM specificity, only a few cases improved, such as TCM,

TBM, and MCAA, but predictions of totals notably increased for THM₄ ($R^2_{adj}=0.97$) and HAA₅ ($R^2_{adj}=0.88$).

3.4.2 Predictive models based on bulk measurements

To further explore the potential of the applied methodology, assess the validity of the selected predictors, and determine the scope of the proposed models, a new approach was evaluated under two different assumptions aimed at assessing the feasibility of developing an online implementable method.

In this case, absorbance values at the representative wavelengths came from two sources: (a) bulk measurements of samples instead of the integration of humics substances from fractionation, and (b) raw absorbance instead of the calculated differential induced by the chlorination. Consequently, measurements from single probe positioned on the treatment train could predict FP without the need of a previous MW separation nor specific reactions.

The dataset used for computing these bulk-based models was expanded by incorporating measurements from a previous sampling campaign (Sample Campaign 1, Table 13). This expansion aimed to cover a broader range of DOM profiles resulting from seasonal changes, although analysis of HAAs-FP was not available for this dataset.

Moreover, the k-fold cross-validation was performed to evaluate the models. For the full dataset, 10-k folds were applied whereas, a 5-k fold was made for the split datasets due to the smaller sample size (N=26). A summary of fitting's goodness is presented in Figure 31, full models' parameters are detailed in Appendix E, Table A 18

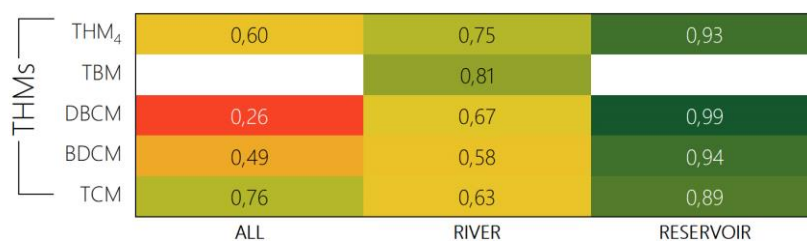


Figure 31: Heatmap of the R^2_{adj} values for MLR models based on raw bulk absorbance of samples at 220 nm, 252 nm, 290nm, and 362 nm.

Compared to the previous fittings on HS raw absorbance (Figure 30 C), the bulk-based models were less capable of predicting THMs-FP, especially for the full combo dataset and the riverine samples. However, for the reservoir water, predictions were close enough to measurements, with R^2_{adj} between 0.89 to 0.99. Yet, models for THM₄ and TBM, the most abundant THM, for river samples, were also significant. From the totality of the models, all source-dependant adjustments fulfilled normality and homoscedasticity assumptions, whereas only TCM of the full dataset met both requirements.

Differences on correlations suggest chromophores engaged on THMs-FP in the reservoir waters mainly corresponded to those gathered on the humic substances' fraction. Therefore, the contribution of other chromophoric compounds to the bulk absorbance in the case of the river samples not solely related to the THMs-FP, but to other DBPs such as HAAs or acetonitriles. Predictability is represented in Figure 32 through 95% confidence bands.

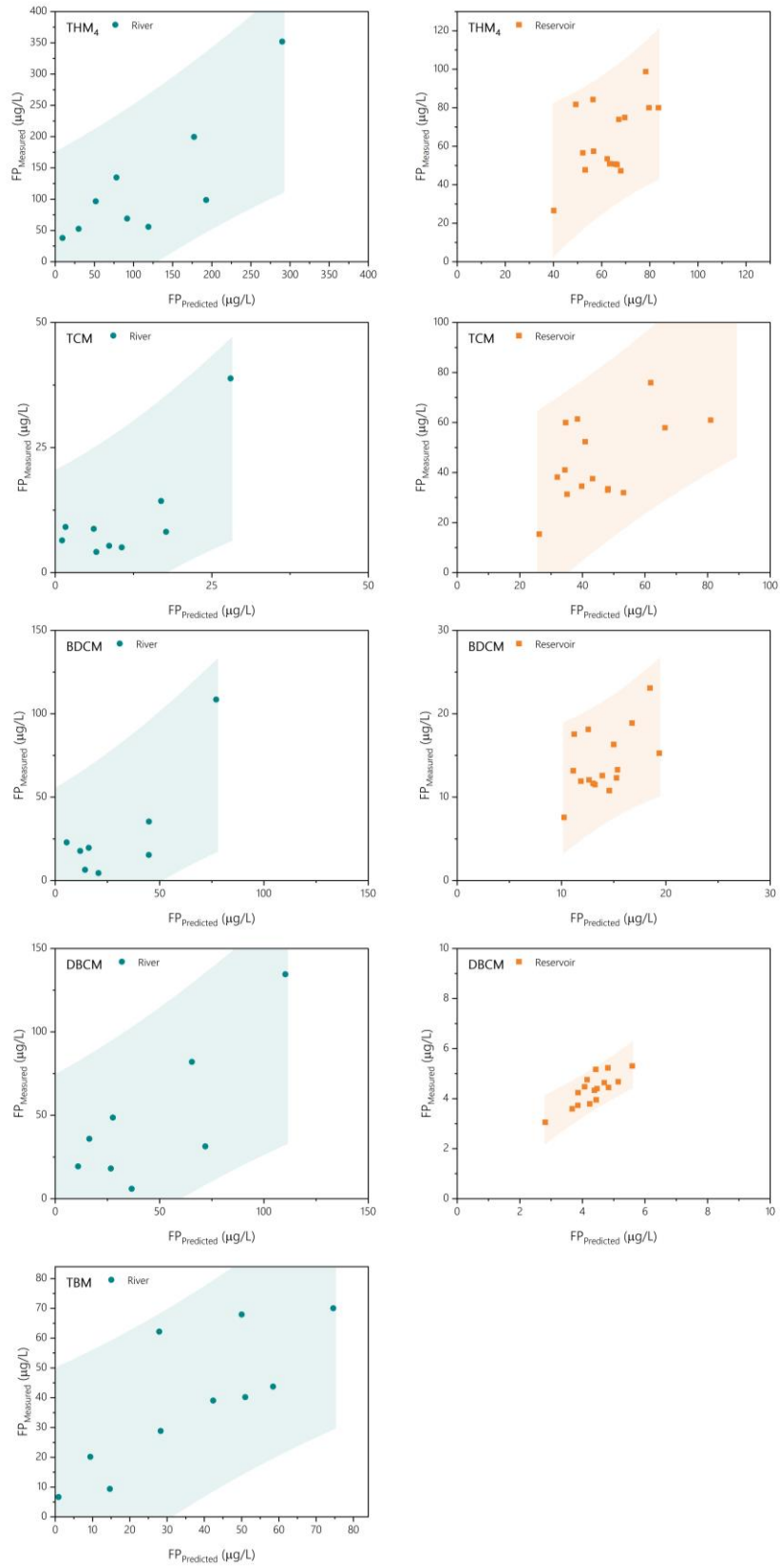


Figure 32: Measured vs. predicted THMs-FP estimated with bulk raw absorbance MLR models including the representation of 95% prediction bands.

Band widths in Figure 32 reflect both data dispersion and capacity of prediction. Despite the high R^2_{adj} values of models, the self-variability from a limited data set ($N=26$, split into $N_{river}=10$, $N_{reservoir}=16$) contributed to broadening the final prediction bands. Also, the variability effect could either be a reflection of the site-specificity heterogeneity of DOM or the given influence of other absorbing precursors, such as bromide in the case of riverine water.

However, the results imply that this ultimate method, relying on raw bulk absorbance measurements, might be appropriate for devising an on-site technique to forecast FPs, particularly in water bodies with minimal input from inorganic precursors, albeit requiring calibration tailored to the specifics of each water sample.

4. FINAL REMARKS

This work presents a novel approach for selecting NOM proxies to provide information about its role as an active precursor in the formation potentials of THMs and HAAs. By far, reactivity of DOM has been studied using parameters based on mechanistic theory, i.e., absorbance at 254 nm. Usually, monitoring variables come from simplified models such as maximum absorbance bands of benzene, yet they are far from the complex and heterogeneity reality of DOM. Here, selection of variables is done based on experimental measurements, thus considering actual interactions between reactive moieties and structural composition that might alter the theoretical absorbance spectra. Hence, is thought to be an approach that comes closer to the casuistries DWTPs constantly deal with.

The strong correlations found on models based on differential absorbance on humic substances' fractions point that those wavelengths at 220 nm, 252 nm, 290 nm, and 362 nm act as good proxies for the prediction of THMs- and HAAs- FP, compared to wider studied parameters like ΔA_{272} nm even on raw water measurements, which would simplify monitoring processes related to chlorination/disinfection procedures. Moreover, the final approach based on bulk measurements indicate, such variables can strongly predict FP of abovementioned DBPs.

Spectroscopic measurements present several advantages thanks to their simple preparative, fast analysis, easiness in data interpretation, and deployed probe monitoring that can be key in moving towards developing a useful technology to assess decision-making of operators and managers of DWTPs given the constantly changing scenarios. Even though, further research must be performed following this work to enlarge the data set and determine whether selected variables reflect mechanistic implications that can be consolidated as general proxies, or if this methodology should be developed towards a tailor-made technology considering on site-specificity.

Chapter VII

RESULTS IV

Analysis of chlorination-driven changes in DOM fingerprints and their implications on disinfection by-products formation. A comparison of advanced characterization techniques

Prepared for submission

1. BACKGROUND AND OBJECTIVES

Understanding the significance and fate of dissolved organic matter (DOM) is crucial for optimizing treatments to enhance their efficiency and minimize the formation of undesired contaminants such as disinfection by-products (DBPs). However, unravelling DOM composition poses a challenge given that numerous factors, such as seasonality, climate events, or anthropogenic activities, can contribute to increasing the heterogeneity of its composition. Moreover, site-specificity characteristics play a significant role, underscoring the importance of comparing and establishing reference standards.

From a molecular level perspective, this multifaceted variability manifests a myriad of compounds with diverse moieties, reactive groups, and heteroatoms, leading to intricate intra- and inter-interactions and exhibiting diverse behaviors and properties. Given this labile scenario, establishing a single methodology for characterizing DOM is virtually impossible. Therefore, this chapter aims to compare various techniques ranging (from simple to advanced) to evaluate DOM from different perspectives and endeavour to understand its role in the formation of certain DBPs.

2. METHODOLOGY

Table 22 presents the references of the employed methodology involved in this chapter.

Table 22: Summary of the analytical workflow and methodologies used in Chapter VII

SAMPLING	METHODOLOGICAL WORKFLOW			
<p>DWTPs:</p> <ul style="list-style-type: none"> - Montfullà - Cardedeu - Abrera <p>N° Sampling campaign: 3</p> <p>N° Samples: 6</p>				
	<p>General Water Quality Parameters (Chapt. III - 1)</p>	<p>DOM fingerprinting</p> <p>SEC (Chapt. III - 2.1) + EEM UV (Chapt. III - 2.2) + HRMS (Orbitrap) (Chapt. III - 2.3)</p>	<p>DBPs analysis</p> <p>Formation Potential Tests - 48h (Chapt. III - 3.1) + AOX (Chapt. III - 3.3) + LLE-GC-MS (Chapt. III - 3.2.2)</p>	<p>Statistical Analysis</p> <p>Pearsons' Correlation (Chapt. III - 4.4)</p>

3. RESULTS AND DISCUSSION

3.1 The direct effects of chlorination. DBPs distribution

Formation potential analysis of regulated trihalomethanes (THMs), haloacetic acids (HAAs), and some unregulated DBPs, including nitrogenated compounds and ketones, was conducted on raw and treated waters prior to the final disinfection from the three DWTPs. Distribution and amounts of each compound are presented in Figure 33.

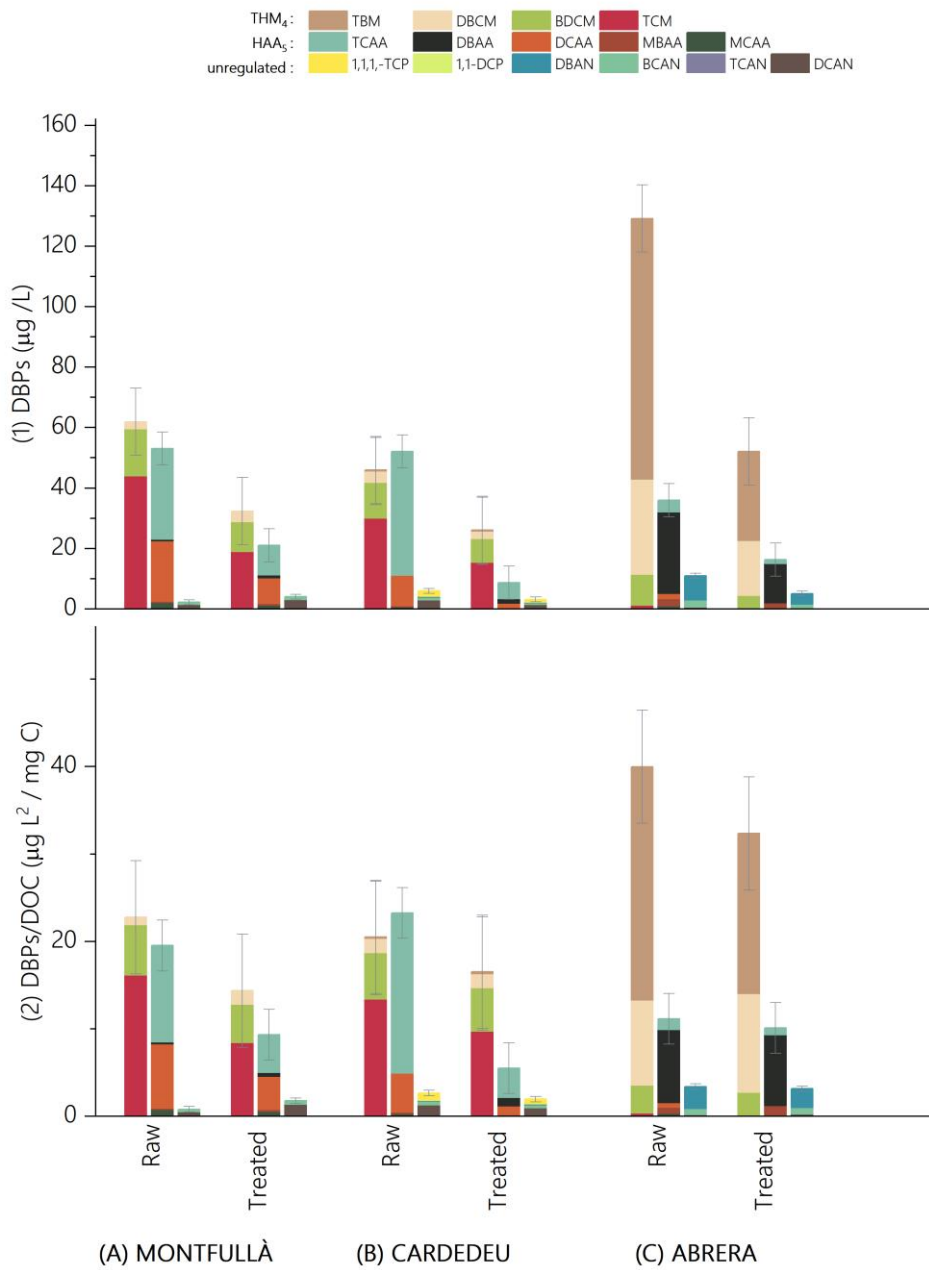


Figure 33: Concentrations of DBPs and for raw and treated waters of Montfullà (A), Cardedeu (B), and Abrera (C) drinking water treatment plants, expressed as total concentration in $\mu\text{g/L}$ (1) and relative to unit mass (2).

Differences in formation trends of DBPs seen in Figure 33 already suggest the role that specific characteristics of raw water may play in the speciation and formation of contaminants. The highest concentrations of THM₄ were formed over raw water from the Llobregat River reaching $129 \mu\text{g/L}$, which decreased to $52 \mu\text{g/L}$ after the whole treatment train. Raw waters from Montfullà and Cardedeu DWTPs, both coming from the same Ter River reservoir system, led to $62 \mu\text{g/L}$ and $46 \mu\text{g/L}$ of THM₄ respectively, that were reduced to $32 \mu\text{g/L}$ and $26 \mu\text{g/L}$ after treatment. Also, different speciation profiles were observed between sources. As a particularity, the Llobregat River contains a high concentration of

bromide due to the mining activities near the upper basin; therefore, during chlorination processes considerable amounts of hypobromous acid (HOBr) are formed rapidly ($k=1.5 \cdot 10^3 \text{ M}^{-1}\text{s}^{-1}$) by the reaction of Br^- and HOCl (Kumar & Margerum, 1987). Compared to HOCl, the reactivity of HOBr in halogenation reactions involving phenolic compounds is much higher, reported to be up to 3000 times superior on average (Criquet et al., 2015b; Heeb et al., 2014) favouring the formation of brominated DBPs.

For HAAs, maximum concentrations were observed in the reservoir waters, with an average of 52.5 $\mu\text{g/L}$ HAA₅, compared to 36 $\mu\text{g/L}$ in raw water from the Llobregat River. Treatment works at the Cardedeu DWTP effectively removed those DBPs precursors, resulting in final concentrations of 8.7 $\mu\text{g/L}$ HAA₅, while levels in Montfullà remained at 21 $\mu\text{g/L}$, and in Abrera at 16 $\mu\text{g/L}$. In all cases, levels of regulated organic DBPs after the formation potentials in treated waters remained far below the legislation requirements of 100 $\mu\text{g/L}$ per THM₄ and 60 $\mu\text{g/L}$ for HAA₅.

When considering the analysed unregulated DBPs, raw water from Llobregat lead to higher DBPs concentrations (11 $\mu\text{g/L}$), compared to raw waters from Cardedeu (6 $\mu\text{g/L}$), or Montfullà (4 $\mu\text{g/L}$). Overall, the highest concentrations of quantified DBPs came from riverine raw water (176 $\mu\text{g/L}$), while the lowest amounts were found in reservoir waters (117 $\mu\text{g/L}$ and 104 $\mu\text{g/L}$).

Regarding levels in treated waters, the most efficient treatment in terms of DBPs mitigation occurred at the Cardedeu plant, with a 64% reduction in total measured DBPs, followed by Abrera (58%) and Montfullà (51%). However, it is essential to remember that the ultimate water quality will be determined by the toxicity of the DBPs. Although unregulated DBPs were detected at lower concentrations, nitrogenated DBPs (i.e., HANs) are reported to be more cytotoxic and genotoxic than the currently regulated DBPs. Furthermore, even among regulated DBPs, there are differences in toxicity, with Br-DBPs being more toxic than Cl-DBPs (Richardson & Plewa, 2020; Wagner & Plewa, 2017).

The same trends in speciation of DBPs were observed between raw and treated waters, and they persisted when concentrations were normalized per unit of mass (DOC) as illustrated in Figure 33. This indicates that differences in DBPs formation and distribution result from variations in DOM composition and structure. The following sections will explore which attributes of DOM differ from one water to another regarding routine and advanced techniques of characterization to cover a wider spectrum of the DOM moieties according to their properties.

3.2 Unravelling DOM Fingerprints

3.2.1 Starting from the bottom: Bulk surrogated parameters

Traditionally, drinking water treatment plants rely on the measurements of surrogate parameters for DOM characterisations such as total or dissolved organic carbon (DOC), absorbance at 254 nm (A_{254}) or SUVA_{254} (A_{254}/DOC) for monitoring purposes. These parameters have historically served as general proxies for tracking DOM levels and reactivity. While DOC provides insight into the overall mass of DOM it might not adequately explain structural changes. In contrast, A_{254} indicates aromaticity, thus reflecting changes in active sites for reactions with disinfectants. Consequently, SUVA_{254} may serve as a surrogate for DOM reactivity. Figure 34 summarizes these parameters for raw and treated waters before and after chlorination.

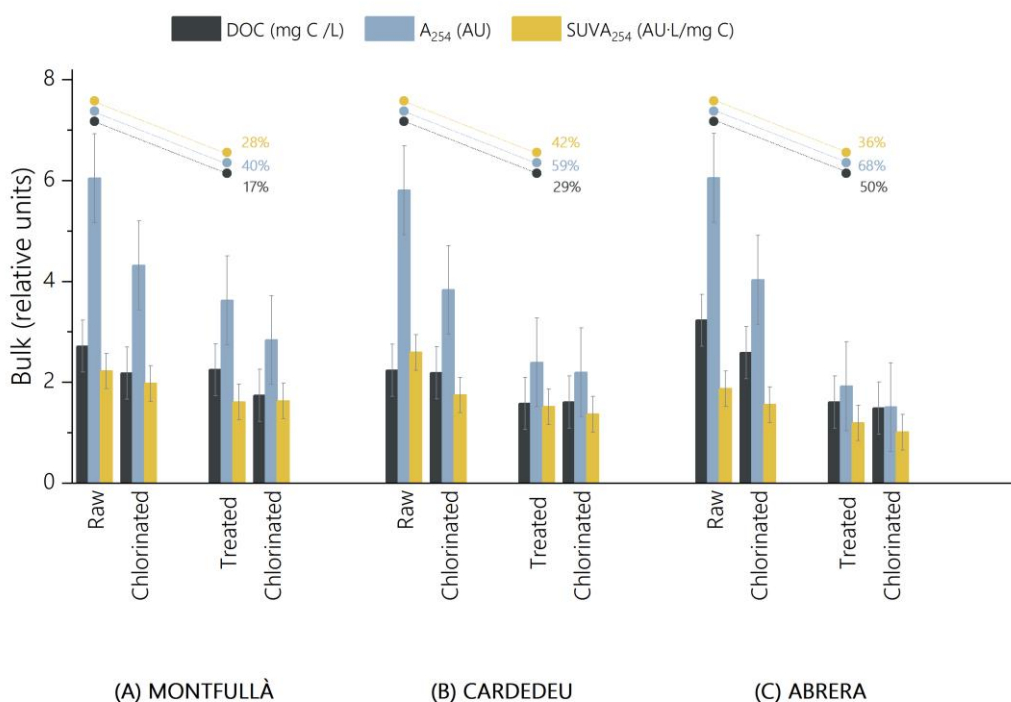


Figure 34: Bulk surrogated parameters of raw and treated waters in (A) Montfullà, (B) Cardedeu, and (C) Abrera DWTPs, along with their removal rate (%) with the treatment process

According to results presented in Figure 34, the raw water from Abrera exhibited the highest concentration of DOC (3.2 mg C/L) followed by Montfullà (2.7 mg C/L), and Cardedeu (2.2 mg C/L). Regarding A₂₅₄, similar intensities were observed at all DWTPs, close to 6 UA. However, concerning overall DOM concentrations, the highest reactivity (SUVA₂₅₄) was observed in Cardedeu (2.6 UA·L/mg C), followed by Montfullà (2.2 UA·L/mg C), and Abrera (1.9 UA·L/mg C). After chlorination, only a slight reduction in DOC was found in Cardedeu (2% DOC removal), while approximately a 25% decrease occurred in Montfullà and Abrera. However, A₂₅₄ diminished the most on Cardedeu (52%), followed by a 50% decrease in Abrera, and a 40% decrease in Montfullà. Overall, this represents a variation in reactivity of 48% in Cardedeu, ahead of a 20% variation in Abrera, and the least, 13% in Montfullà.

Based on these findings, it would be expected that raw water from Cardedeu is the most prone to the formation of DBPs due to the abundance of aromatic moieties per unit of mass. Yet, it is noteworthy that the highest concentrations of DBPs were found in the riverine water from Llobregat (Figure 33). This suggests two possibilities: first, that the raw water in Cardedeu serves as the primary precursor to other non-analysed DBPs, as evidenced by the low percentage of measured AOX (21%) compared to, for instance, Abrera (92%). Second, that other precursors beyond those measured by aromaticity might be responsible for the formation of DBPs in the Llobregat. Indeed, this second assumption is supported by the presence and role of bromide in the riverine water as previously stated.

The most significant reductions in DOM through treatment trains, as depicted in Figure 34, were achieved in Abrera, followed by Cardedeu, and Montfullà. According to these reactivity proxies and the previous comparison on the formation of DBPs in raw vs. treated waters (see prior section), the 36% SUVA₂₅₄ decrease in Abrera should account for its 58% reduction in DBPs formation, the 42% reduction of SUVA₂₅₄ described the 64% DBPs loss in Cardedeu, and the 28% SUVA₂₅₄ drop in Montfullà should

explain its 51% minimization. Based on the treatment configurations of each DWTP and the acquired knowledge discussed in previous chapters, following an in-depth analysis of DOM removal with specific operations, major reductions in DBPs precursors result from their coagulation processes. Differences in removal efficiency depend on operational conditions such as coagulant doses and pH. A distinctive feature is observed in the EDR modules in Abrera, originally designed to address high salinity issues, which also play a significant role in removing DOM, contributing to achieving the highest percentages of elimination.

3.2.2 *The 1st tier of DOM: Spectral signature*

Taking a deeper dive into DOM characterization, a thorough analysis of the spectral signature of DOM can unveil additional insights into the structural composition of the constituent compounds. This encompasses both UV absorbance and fluorescence measurements, which, based on optical properties, they provide complementary information.

The majority of chromophores and fluorophores originate from lignin structures. Chromophores typically consist of sp^3 isolated aromatic rings with varying degrees of oxidation, resulting in hydroxylated or alkoxyated aromatics, oxidized quinones, ketones, or aldehydes. In contrast, fluorophores tend to be moieties containing carbonyl groups ($C=O$), which readily undergo fast intersystem crossing, transitioning to an excited triplet state and emitting light as they return to their fundamental state (a phenomenon known as fluorescence). These structures typically include aromatic ketones, aldehydes, and ketones, exhibiting lower degree of fluorescence compared to hydroxy benzoic acids, hydroquinones, or phenol-derived, which display higher fluorescence signatures (Hanson et al., 2022).

Here, the evaluation of fluorescence excitation-emission matrices (EEM) and absorption profiles are presented to discuss their changes throughout chlorination and the overall treatment processes. Figure 35 depicts the variations in the integration of the main fluorescent peaks (Φ_i) as described by Sgroi and co-workers (2017).

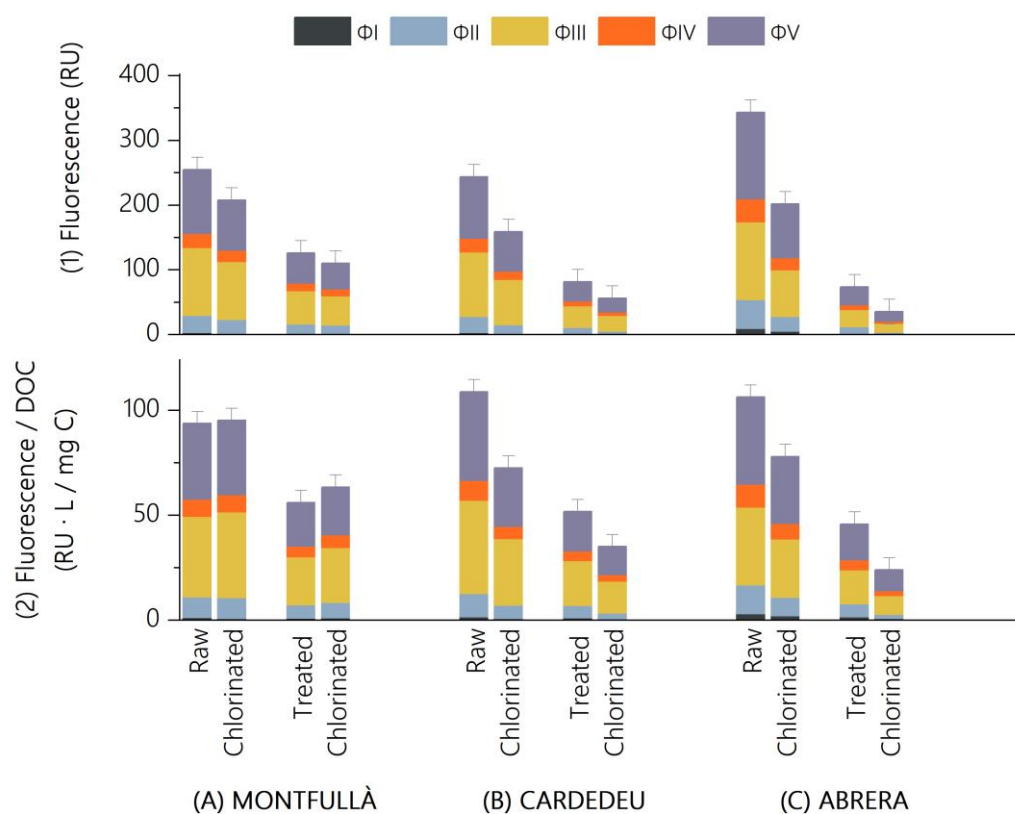


Figure 35: Integration of the main fluorescence peaks on raw and treated waters pre- and post-chlorination (1), and related to unit of mass (2).

Overall, the most abundant peaks were found within excitation/emission pairs of 245/440 nm (Φ III), and 345/440 nm (Φ V), both corresponding to fulvic and humic-like attributes of DOM. Additionally, peaks at 275/345 nm (Φ IV) and 225/340 nm (Φ II) were also notable, associated with protein-like compounds such as tryptophan-like molecules, biopolymers, and microbial by-products.

Total fluorescence was relatively higher in Llobregat raw water (Figure 35, 1C), compared to raw waters from the reservoir, suggesting either a higher number of fluorophores or moieties emitting stronger fluorescence intensities. However, as discussed earlier, a higher variation in intensity does not solely reflect a direct variation in concentration but may indicate less fluorescence signature per unit of mass. This phenomenon can be clearly observed in Figure 35, 2; where similar proportions were found in both waters from Abrera and Cardedeu, suggesting fluorophoric moieties are of similar characteristics.

After chlorination, significant reductions were observed in contributions from protein-like proxies (Φ II and Φ IV), with a 48% decrease in Abrera and a 42% decrease in Cardedeu. Fulvic and humic-like indicators (Φ III and Φ V) accounted for a 39% and a 33% diminution, respectively. Reactivity in Montfullà remained similar in both cases, with a 18% reduction, barely affecting its reactivity (Figure 35, 2A).

Although it is commonly thought that humic and fulvic-like substances are the primary precursors to THMs formation, these results suggest that fluorophoric active moieties originating from protein-like substances may also significantly contribute to the formation of other DBPs. Since these compounds are typically rich in nitrogen-containing elements, they could serve as precursors for N-DBPs. Indeed,

this is supported by the concentrations of DBAN and BDCAN found in Abrera, as well as its high levels of Φ_{IV} and Φ_{II} , compared to the other water sources.

Gathering this information with overall DOC reductions (Figure 35, 2), the variation on the sum of total fluorescence from the analysed peaks (Φ_{TOTAL}) caused by the reaction with chlorine explained the following decreases: a diminution of 18% on total fluorescence related to a 25% of DOC in Montfullà, a 35% on total fluorescence over a 2% on DOC in Cardedeu, and a 41% on fluorescence over a 25% of DOC in Abrera. According to this, reactivity tracked by the provided fluorescence markers, presented the best changes on raw water from Cardedeu (highest decrease in fluorescence per less amount of carbon), which comes in agreement with the above discussed bulk parameters.

Treatment works contributed to remove DOM with fluorescence character up to a 79% in Abrera, 67 % in Cardedeu, and 51% in Montfullà according to the sum of the five peaks (Φ_{TOTAL}). Despite this overall reduction, consumption driven by chlorine reaction mostly equalled those achieved with raw waters: 10%, 43% and 64% respectively in Montfullà, Cardedeu and Abrera for protein-like compounds; and 13%, 27% and 48% respectively related to fulvic and humic-like compounds. This suggests that treatment trains were effective in reducing whole concentrations of DOM but non-specifically so that remaining moieties exhibited same behaviour towards the oxidant.

Another spectral signature is the absorbance profiling of waters. Figure 36 depicts spectra from 200 nm to 400 nm of raw and treated waters prior to and after chlorination.

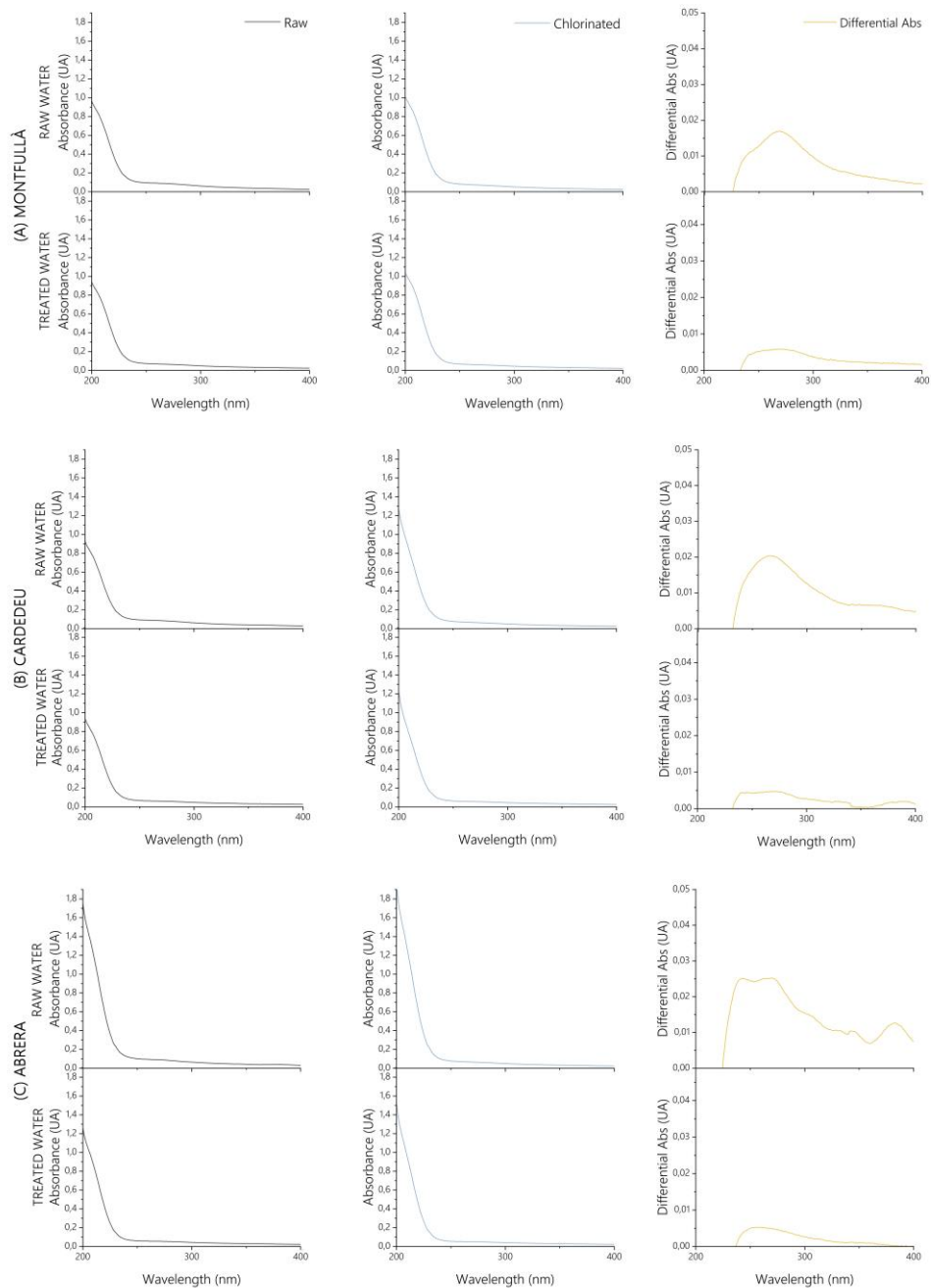


Figure 36: Absorbance profiles of raw and treated waters from (A) Montfullà, (B) Cardedeu, and (C) Abrera before (left) and after (middle) chlorination, and the difference (right).

Most chromophores are thought to be enrolled in reactions of DBPs formation. The structure of aromatic compounds presents many active moieties (hydroxyls, carboxyl, ketones, etc.) that can easily react towards oxidants such as chlorine and enhance production of DBPs. During these reactions, changes in structures are triggered by bond cleavage; thus, loss of aromaticity usually results in an absorbance decrease. Some characteristic wavelengths have been widely reported to entail a close correlation with DOM reactivity, and they mostly derive from benzene absorption bands (Korshin et al., 1997), with the most representative absorbance at 254 nm. When it comes to chlorination, changes

around a maximum at 272 nm (differential absorbance, DAS) has also been reported to be associated with this specific reactivity (Beauchamp et al., 2018; Korshin et al., 2002; Roccaro & Vagliasindi, 2009).

Figure 36 presents the swept from 200 nm to 400 nm, covering the full UV absorbance spectra of analysed waters. In all raw waters (Figure 36, left), the most noticeable change was gathered over the region of 250 nm to 300 nm where chlorination produced a signal decrease, encompassing the maximum at 272 nm (Figure 36, right). In contrast, chlorination of treated waters led to much more subtle variations, most clearly seen in Figure 36 (right graphs), which suggests that treatment processes enhanced the removal of such chromophores. This phenomenon comes in agreement with what has been previously discussed on the bulk section, where the reduction of absorbance at 254 nm caused by chlorination (9 to 28%) was much lower compared to obtained values driven by treatments (40% to 68%). Moreover, according to the measured DBPs, absorbance directly reflects the potential of DOM as a precursor: the higher the intensity, the higher the by-products levels.

Aside from this region, other two distinct areas can be identified on the spectra: the first section from 200 nm to 250 nm, with the steepest slopes; and the ending tail (300 nm to 400 nm) with the lowest intensities. Not all chromophores exhibit the same properties neither are involved in the same way in reaction mechanisms during the stepwise processes of chlorination, and that is reflected in these profiles' variations (Korshin & Chang, 2008). The first reactive type of chromophores known as "fast chromophores" are consumed during first chlorination stages, yet their degradation is not clearly related to a significant formation of end by-products such as THMs or HAAs. The second class, the "slow chromophores" absorb at higher wavelengths (> 300 nm) that is the region with lower spectroscopical variability. Evaluating the slopes through the log-transformed scale, can help improve sensitivity in those regions and depict their engagement (Korshin et al., 2007; Yan et al., 2014). Findings discussed in previous chapters of this dissertation also underpin the role some precursors absorbing at lower or higher wavelengths can play in explaining certain DBPs-FP. Certainly, raw water from Abrera exhibits a distinct maximum around 240 nm (Figure 36, right C) evidencing the presence of different components compared to the other source water.

3.2.3 *The 2nd tier of DOM: Chemical behaviour*

The next step in DOM characterization concerns deepening into its chemical behaviour. Here, size exclusion chromatography analysis using the developed method early described (HPSEC-DAD-OCD, see Chapter III) was performed to depict apparent molecular weight (AMW) distribution and classify each water into the main DOC fractions.

Figure 37 displays the profiles of DOM AMW fractions in raw and treated waters before and after their chlorination, and the difference induced by reaction. Each figure overlaps the OCD chromatogram with the DAD absorbance matrix. Thus, a characteristic absorbance signature can be attributed to each DOC fraction. Also, the difference between fingerprints is depicted to ease identify which fractions were mostly altered during the chlorination process.

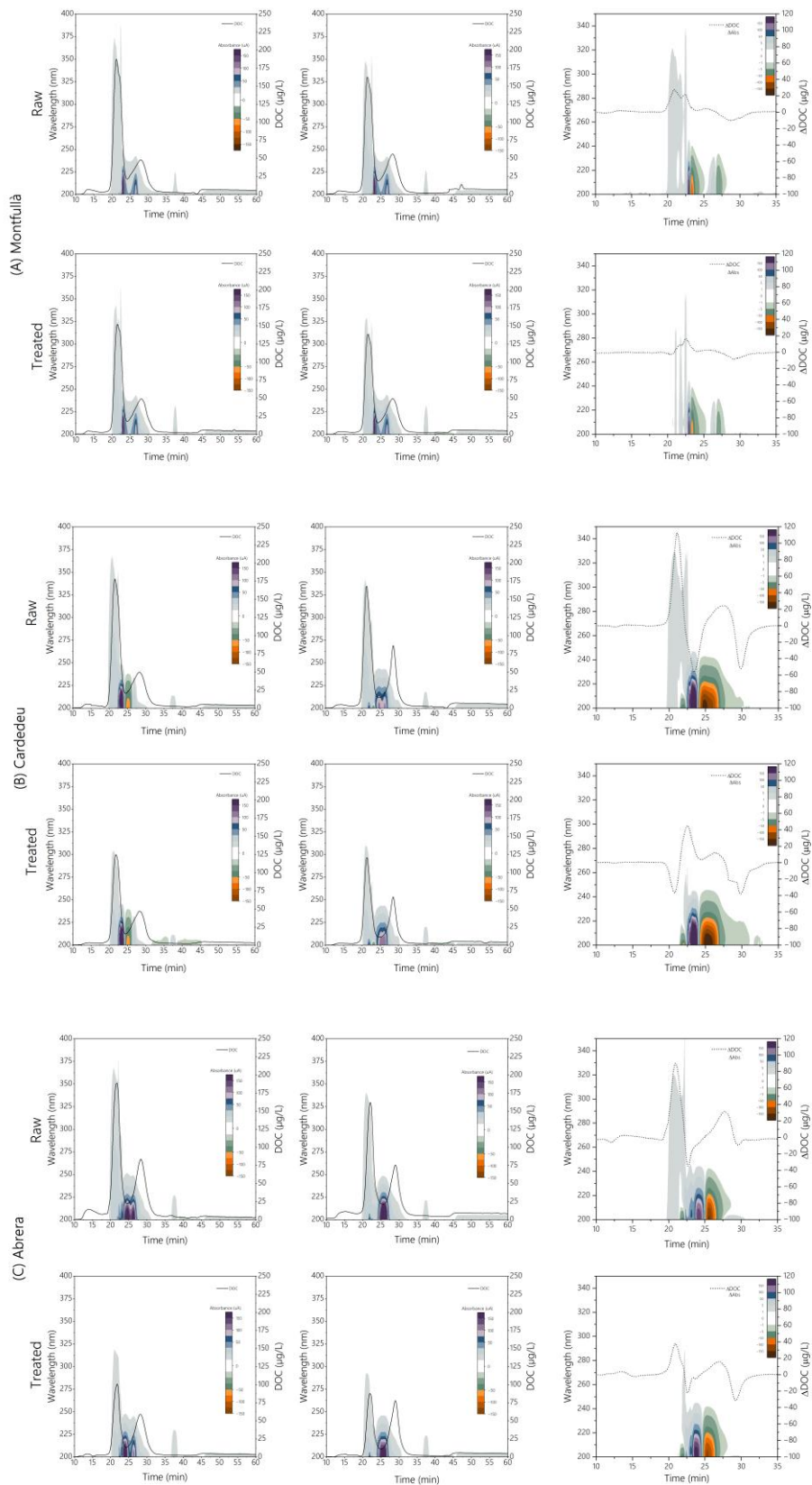


Figure 37: Overlapped DOC and absorbance chromatograms of raw and treated samples pre-(left), post-chlorination (middle), and induced difference (right) in (A) Montfullà, (B) Cardedeu, and (C) Abrera raw and treated waters

Compared to the previous absorbance discussion (see prior section), when coupled to SEC, an itemised evaluation of major chromophoric compounds can be assessed. According to the MW separation, as shown in Figure 37, most absorbance was gathered between humic substances (R_t : 20 – 25 min, 700 Da < AMW < 10 KDa) and building blocks (R_t : 25 – 30 min, 200 Da < AMW < 700 Da) fractions, that is high molecular weight with high to medium UV-absorbance compounds (i.e. humic and fulvic acids), and lower molecular weight with high UV-absorbance compounds (i.e. carbohydrates, amino acids). Moreover, the highest absorption intensities were focused on lower wavelengths (< 230 nm) at around 25 min, tallying with the elution range of inorganic compounds.

According to the chromatograms and the reduction in absorbance intensities, most chromophores were removed during treatment processes, especially those coming from humic substances. However, an increase in absorbance on lower molecular fractions was experienced, suggesting an increase in unsaturated structures. Also, when comparing the differences, the lesser changes after chlorination of treated samples compared to the raw waters also suggest the decrease in reactivity driven by the removal of those precursors.

A different AMW distribution was observed in each raw water, particularly between waters from distinct sources. The quantification of each DOM fraction according to its DOC concentration is presented in Figure 38 to ease visualization and comparison.

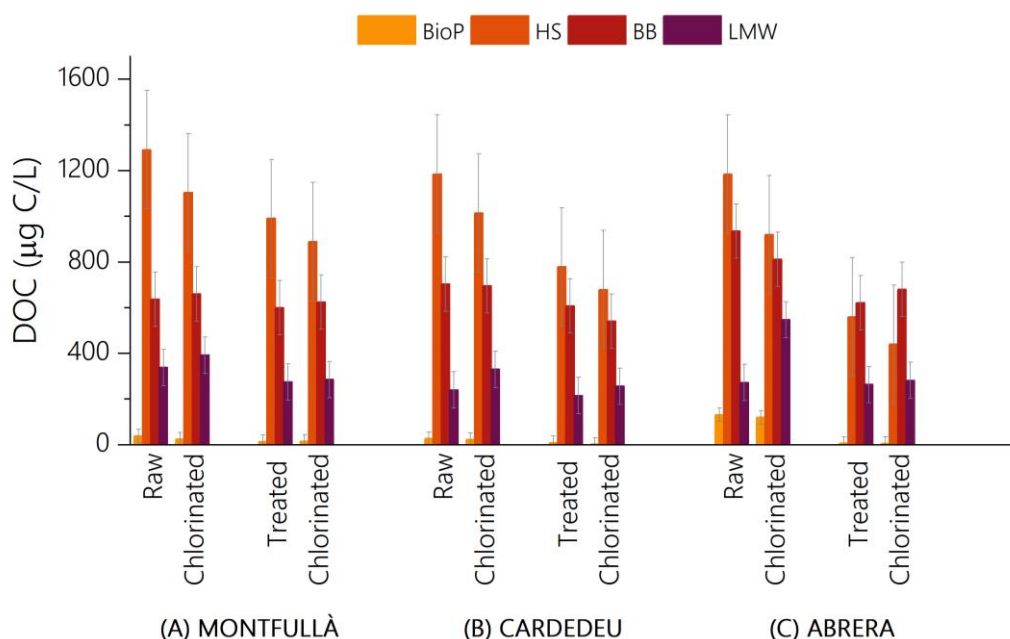


Figure 38: Quantification of DOC fractions of raw and treated waters prior and after their chlorination

Higher concentrations of biopolymers (5% of the total DOC) were found in the riverine raw water (Figure 38 C) compared to those from reservoir (~1.5%). Generally, this fraction is naturally removed through natural filtration on soil thus explaining their lower levels on Montfullà and Cardedeu. This sustains the higher intensities in fluorescence benchmarks of protein-like compounds found in Abrera discussed in the previous section. Philibert and co-workers (2022), recently reported the association between fluorescence indexes and DOC fractions. Though they employed different methodologies (PARAFAC and LC-OCD for SEC separation) they found fluorescence at 330/404 nm (ex/em) correlated with

oxidised humics and building blocks fractions (1000 – 300 Da), and 275/302 nm (ex/em) were related to low molecular weight amino acids (< 350 Da). In this case, those described fluorescent pairs account for intensities of Φ_{III} and Φ_{IV} peaks. Also, Wassink and co-authors (2011) reported a strong correlation ($r^2 = 0.99$) between 270/490 (ex/em) fluorescence index (corresponding to hereto discussed Φ_V) and humic substances LC-OCD fraction in waters from a Canadian river, and similar results were also reported by Nurul and co-workers (2017) correlating humic substances peak from HPSEC-OCD with C2 (250 – 360 /460 nm) PARAFAC component ($r^2= 0.83$) and both humic substances and building blocks fraction with C3 (250 – 340 /420 nm) with $r^2=0.82$ and 0.85 respectively.

Also, slightly higher concentrations of building blocks were exhibited in Abrera (37%) compared to ~30% in reservoir waters. Similar concentrations of lower molecular weight fractions (acids and neutrals) were found in all raw waters, approximately representing 12% of their total DOC. In all cases, the predominant amount of DOC corresponded to compounds gathered into the humic substances fraction by more than 50% of DOC.

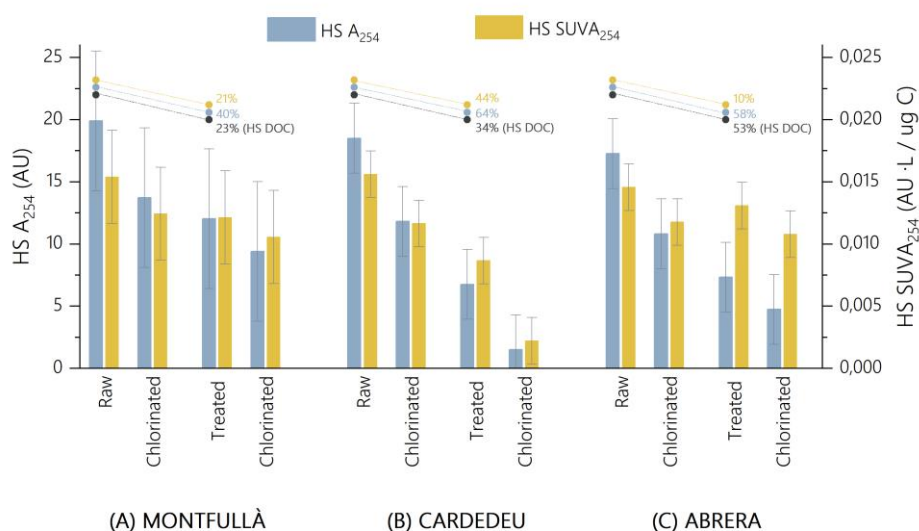


Figure 39: Humic substances' absorbance (A_{254}) and $SUVA_{254}$ trends on raw and treated waters before and after their chlorination, and removal (%) achieved with treatment in each drinking water treatment plant.

An in-depth analysis of the surrogate properties of humic substances fraction is presented in Figure 39. Compared to the bulk measurements discussed in previous sections, the overall absorbance reduction mostly resulted from the removal of humic substances, thus leading to general absorbance decrease in the three DWTPs. This underscores the strong aromatic behaviour of this DOM group of constituents.

The removal of DOM through treatment led to a redistribution of the AMW profiles, as seen in Figure 38, specially in Abrera, where high reductions of humic substances (>50%) left concentrations underneath building blocks. Yet, in all DWTPs, smaller molecular weight fractions were the most recalcitrant over treatments.

Related to disinfection reactions, increased amounts of building blocks and LMW fractions (<700 Da) were observed in all waters over the consumption of higher AMW compounds. This, related to the formation of DBPs, implies humic substances and biopolymers might act as main DOM precursors. Apart from their decrease determined through the measure of DOC concentration, consumption of

those constituents is also reflected in the decrease of protein-like targets from fluorescence (Φ_{II} and Φ_{IV}), as well as the decrease in differential absorbance profiles. In the case of Abrera and Montfullà, raw and treated waters, those DOM precursors will mostly lead to the formation of THM₄. However, Cardedeu raw water mostly generated HAA₅ (52 µg/L) compared to THM₄ (46 µg/L) and other analysed DBPs (6 µg/L), while final water led to higher concentrations of THM₄ (26 µg/L), followed by HAA₅ (9 µg/L), and only 3µg/L of other DBPs. These findings suggest several types of precursors with different reactivities towards chlorine were present in Cardedeu raw water, mostly gathered in the humic substances fraction, which were unequally removed in the treatment process.

3.2.4 *The 3rd tier of DOM: Chemical identities of individual species*

The next rank of DOM characterization ends with unravelling the chemical identities of individual species composing DOM matrices. Here, Orbitrap-MS analysis was applied to detect subtle changes in DOM profiles at the level of high mass resolution, enabling a non-targeted detection of some molecular structures present in the waters.

With the Orbitrap-MS analysis compounds of small structural units (i.e., CH₂, COOH, CH₂O, etc.) are identified as peaks with different intensities depending on their concentrations. To ease visualization and interpretation of this data, the Van Krevelen diagrams sort elemental compositions using molar ratios of hydrogen-to-carbon (H/C) and oxygen-to-carbon (O/C) on their axes. Thus, the aggregation of possible formulas containing a given type of elements (known as features, e.g., CHO, CHON or CHOS) are located creating a map of structural relationships between families of components depending on their degree of condensation (aromatics, aliphatics, condensed aromatics, etc.), which can likewise refer to their biological precursors as lipids, proteins, cellulose, lignin or condensed polyaromatic-carbon like compounds (Kim et al., 2003) (Figure 40). Therefore, each DOM matrix will exhibit a singular fingerprint reflecting its source and seasonal nature. Apart from the elemental ratios per carbon and classification, some indexes, such as the double bond equivalent (DBE) and the modified aromatic index (AI_{mod}) are usually assessed to evaluate the degree of unsaturation and aromaticity respectively (Koch & Dittmar, 2006; Leefmann et al., 2019; H. Zhang, Zhang, Shi, Hu, et al., 2012; H. Zhang, Zhang, Shi, Ren, et al., 2012).

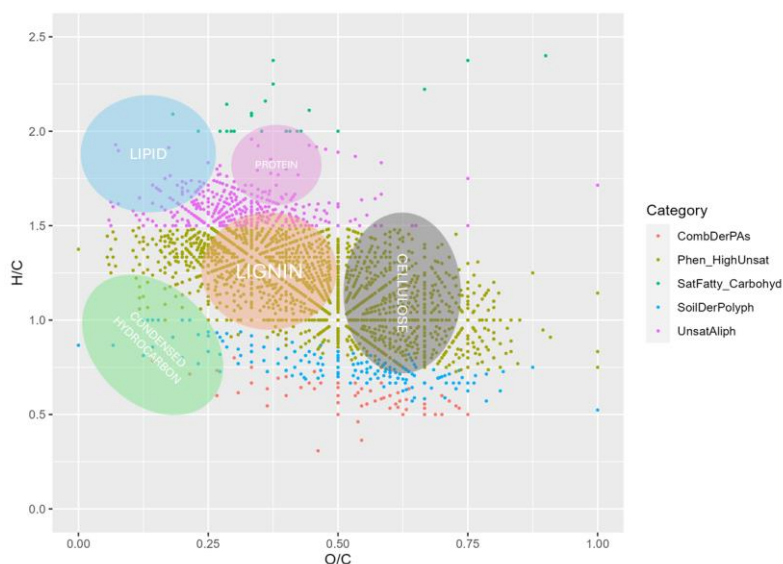


Figure 40: Van Krevelen diagram with category assignment overlap according to Kim et al., (2003) (the circles), and Merder et al., (2020), (background features).

The Van Krevelen diagrams of raw waters are presented in Figure 41 with classified features according to categories described by Merder and co-authors (2020). Waters from the Ter reservoir system exhibited a close fingerprint with abundant features spanning over the regions of unsaturated (low and high) O/C compounds, and below 1.5 H/C ratio, which can be attributed to soot and lignin-like compounds. Also, quite significant features were found related to aromatics and condensed aromatics, which could be structural subunits of protein-like compounds (e.g., amino acids). Comparatively, raw water from the Llobregat River presented more features within 1 to 1.5 H/C and 0.25 to 0.5 O/C ratios, and a denser region over the 1.5 H/C ratio, associated with aliphatic compounds also related to lipidic structures, fitting the results from SEC, presenting the highest concentrations of biopolymers. Lesser features were detected at lower H/C (< 1) and higher O/C (>0.5) ratios. Yet, scattered features related to aromatics and condensed aromatics were identified on a lower basis compared to the reservoirs. Those findings are in agreement with previous characterization of the same raw waters discussed by Sanchís and co-workers (Sanchís et al., 2020, 2021).

Both waters from the reservoirs presented the same degree of unsaturation and aromaticity according to the calculated indexes (Table 23). Comparatively, raw water from the Llobregat River presented a less aromatic behaviour, with a higher degree of unsaturation (lower DBE, AI_{mod} and O/C ratio with greater H/C). Those results sustain the previous observations discussed from bulk measurements and SEC, where Cardedeu accounted for the highest $SUVA_{254}$, as well as presented the broader absorbance spectra. Variations below 0.3 % were considered insignificant according to the estimated mean coefficient variation between duplicates (CV = 0.31%). The little variations (<5%) in the indexes after the full treatment works suggested that the removal of DOM during treatment barely altered its elemental composition. Instead, it indicated the selective removal of certain groups of compounds (Table 23).

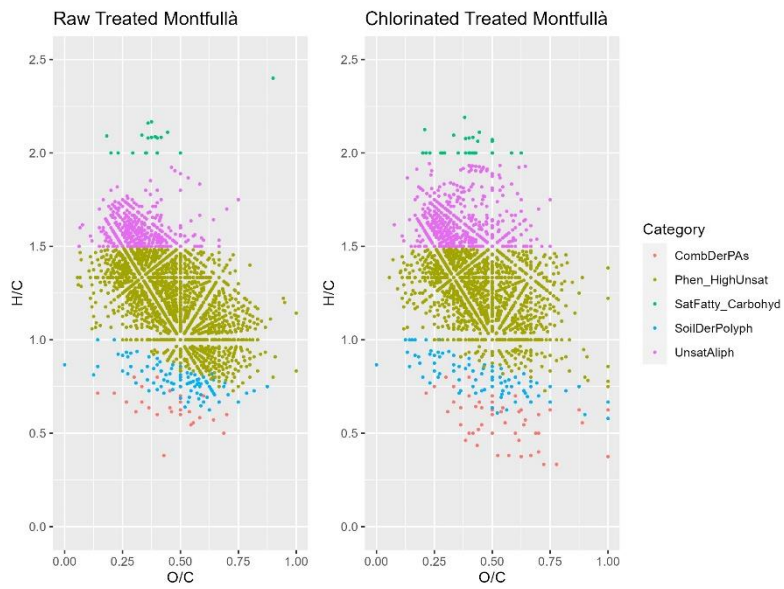
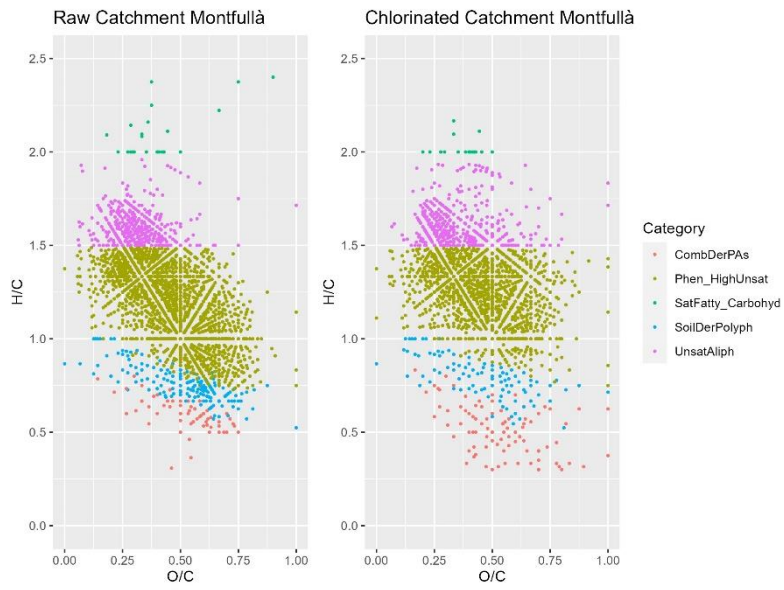
Table 23: Summary of HRMS indexes and count of features of raw and treated samples characterization and their decrease (%) derived from corresponding treatments in each DWTP.

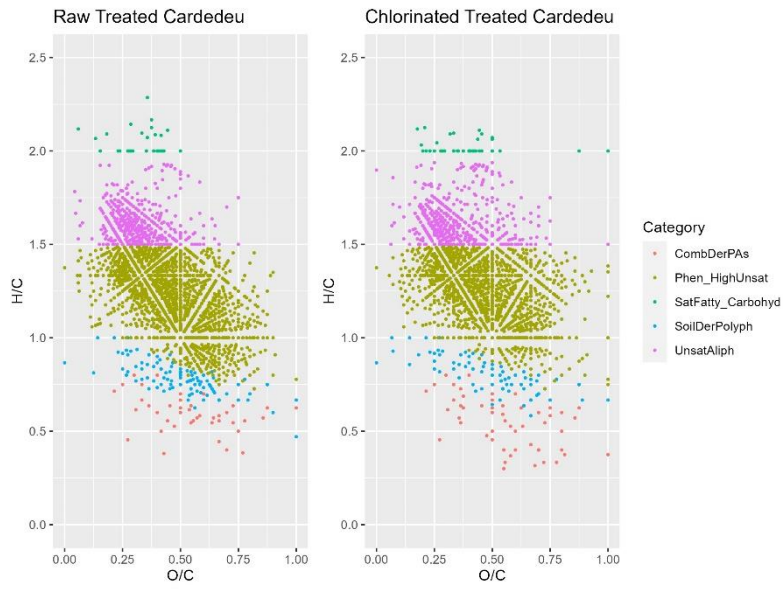
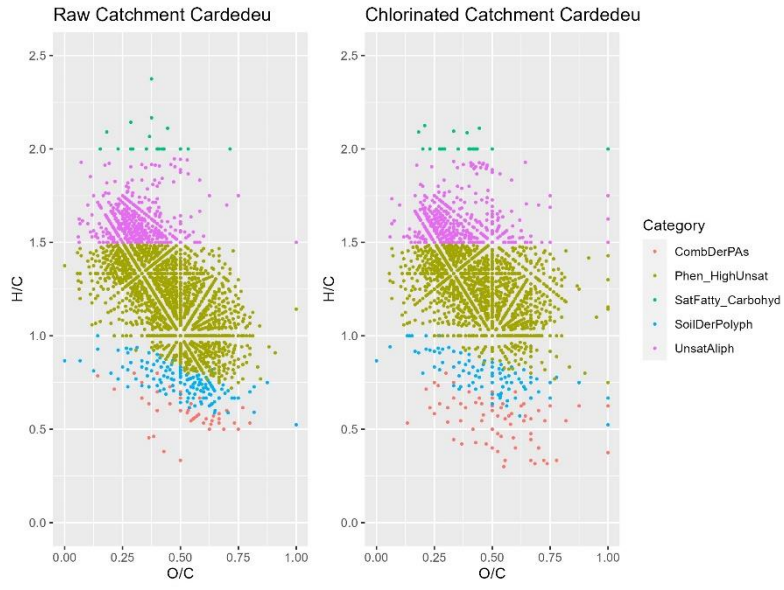
DWTP	Sample	DBE	Al _{mod}	O/C	H/C	Comb DerPAs	Phen HighUnsat	SatFatty Carbohyd	SoilDer Polyph	Unsat Aliph
Montfullà	Raw	8.5	0.24	0.448	1.273	247	2779	120	445	785
	Treated	8.3	0.23	0.452	1.288	119	2540	79	243	697
	% DECREASE	2.4	4.2	-0.9	-1.2	52	9	34	45	11
Cardedeu	Raw	8.6	0.24	0.444	1.277	194	2618	111	415	768
	Treated	8.2	0.23	0.467	1.281	176	2606	104	262	792
	% DECREASE	4.7	4.2	-5.2	-0.3	9	0.5	6	37	-3
Abrera	Raw	7.5	0.21	0.430	1.334	146	2447	157	254	845
	Treated	8.0	0.22	0.446	1.312	94	2473	127	172	776
	% DECREASE	-6	-4.8	-3.7	1.6	36	-1	19	32	8

Usually, coagulation-flocculation and filtration processes preferably remove oxygen-rich unsaturated moieties (high O/C ratios, with low H/C and low DBE) of moderate AMW (300 – 500 Da) (He et al., 2022; Phatthalung et al., 2021; Raeke et al., 2017; Shi et al., 2021) conforming tannin ($0.67 < O/C < 0.97$ and $0.53 < H/C < 1.5$) and lignin-like ($0.25 < O/C < 0.67$ and $0.75 < H/C < 1.5$) compounds as well as condensed aromatics ($0.7 < O/C < 1.1$ and $1.5 < H/C < 2.4$), which are considered as main precursors of THMs and HAAs. These observed results reinforce the effect of conventional treatments on removing high molecular weight hydrophobic fractions (humic fractions) rich in aromatic structures, as previously stated in SEC findings. With these considerations and regarding the raw water characteristics of each source, Abrera DWTP seemed to exhibit the most efficient treatment in removing DOM precursors.

Disinfection processes also impact DOM fingerprints. Preferably, it produces the oxidation of compounds with low O/C ratios and high unsaturation degree (high DBE), entailing the cleavage of unsaturated structures (i.e., double bonds), thus reducing aromaticity (Al_{mod}) and increasing H/C ratios, leading to the reduction of lignin and lipid-like structures and an increase of tannin-like compounds.

The Van Krevelen diagrams of raw and treated waters before and after chlorination are presented in Figure 41.





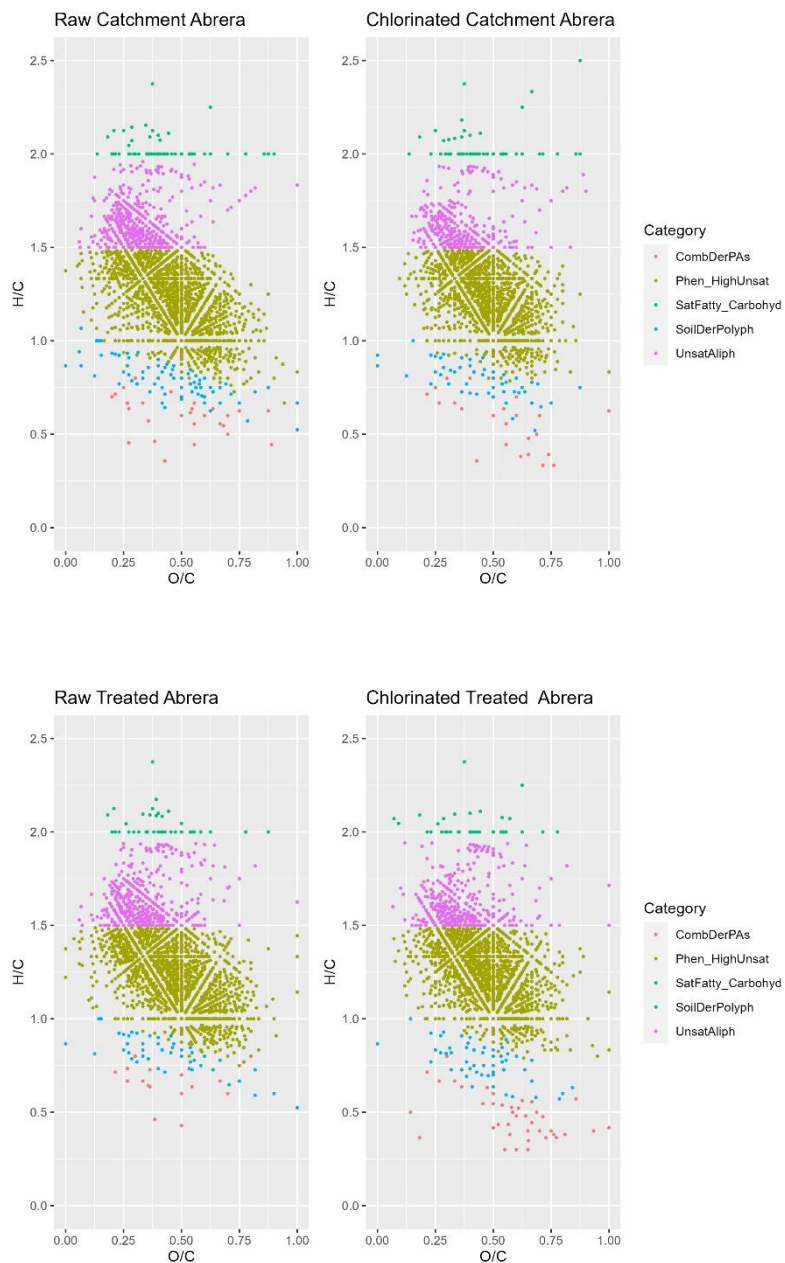


Figure 41: Van Krevelen diagrams before and after chlorination of raw and treated waters.

The following table (Table 24) summarizes the decrease (%) in the DBE and AI_{mod} indexes, O/C and H/C ratios, and categories according to Merder and co-workers (2020) classification, after the formation potential tests of each raw and treated waters to assess the changes on DOM features after the chlorination of samples.

Table 24: Decrease (%) on DOM features from induced changes after chlorination of waters.

DWTP	Sample	DBE	Al _{mod}	O/C	H/C	Comb DerPAs	Phen HighUnsat	SatFatty_Carbohyd	SoilDer Polyph	Unsaturated Aliphatic
Montfullà	Raw	9.4	4.7	-3.1	-1.2	-24	22	33	48	1
	Treated	6.6	5.5	-1.6	-1.0	-82	12	-70	9	-32
Cardedeu	Raw	8.8	4.9	-3.4	-0.9	-36	14	15	45	-4
	Treated	6.1	2.5	-2.3	-0.4	-22	16	-6	25	-2
Abrera	Raw	3.3	5.2	-1.7	-0.3	19	16	20	26	22
	Treated	4.4	1.2	-3.8	0.5	-99	13	<0.3	-47	-0.3

Similar to the comparison between raw and treated waters, little variations (<5%) were found on HRMS indexes after chlorination waters. However, the Van Krevelen diagrams (Figure 41) depicted that mostly lignin and soot features were consumed during chlorination, while oxidated structures overlapping the tannin-like compounds slightly increased in waters from reservoirs. In comparison, Abrera exhibited a less dense fingerprint on enriched structures after chlorination, and the most reactive features were those from the lignin-like region with low saturation and condensation, including the protein-like compounds. Those changes are mechanistically justified as chlorination processes oxidate primary and secondary alcohols to carbonyls, resulting in aldehydes and ketones, thus reducing the H/C ratio and increasing oxidation degree (higher O/C) (Sanchís et al., 2020) thus decreasing DBE and Al_{mod} due to the breakdown of unsaturated structures. The effects of the increase in saturated structures of lower molecular weight correlates with the increase in LMW fractions detected by SEC analysis.

Comparatively, the fingerprint of treated water from Abrera presented more products resulting from the chlorination, specially in high oxidation and saturated (O/C >0.6 and 1 < H/C < 1.5) features. Those differences suggest that treatment processes affected DOM reactivity by removing or structurally altering specific DBPs precursors. Changes were less evident in treated waters from Ter, where less high oxidated and low unsaturated features were identified.

On a more profound fingerprint analysis conducted by Sanchís and co-workers (2020b) on chlorination of Ter water from Cardedeu and their effects on DBPs-FP, they reported two regions corresponding to the lignin-like compounds that exhibited strong correlations with THMs- and HAN-FPs. However, in this exploratory work, the data from chlorination analysis was insufficient to assess a sound statistical analysis.

4. FINAL REMARKS

In this section, a summary gathering all findings related to the effects of chlorination on DOM is assessed with the aim of evaluating complementarity of techniques. On a starting basis, bulk measurements provide information on the overall DOM composition. The DOC analysis is a rough measure of the total organic concentration regardless of structure, thus providing little information about the physicochemical behavior of the compounds. Thus, a decrease in DOC concentration will be strictly related to the removal of organic matter but will not reflect structural changes nor fragmentations which could affect entire reactivity. For this reason, usually DOC pairs with absorbance measurements at 254 nm, which provides a little more insight into structural composition. A clear example from the results, is

the lowest variation in total C- concentration after chlorination experienced in raw water from Cardedeu by the time it attained the highest reduction in aromaticity. This suggests how chlorination reactions could enhance the fragmentation of high unsaturated structures to form DBPs. However, bulk measurements, will mostly portray the contributions of major compounds. To further understand the distribution of constituents or identify differences among moieties, advanced characterization techniques must be applied. SEC enlightens the DOC black-box by providing a deployment of the molecular weight distribution, which at the same time, with the hyphenation of an optic detector (DAD) their chromophoric behavior can also be depicted. As seen in the analysis, chlorination consumes the most abundant DOM fraction which, according to the measured attributes, can be tagged as a high molecular weight, highly aromatic, and hydrophobic portion (humic substances). Moreover, those compounds usually share similar O/C and H/C ratios as a consequence of their aromaticity and saturation degree, therefore exhibiting similar m/z features. Also, some of them might as well present fluorophobic behavior and can be detected at certain Ex/Em pairs. Thus, consumption of humic substances can be monitored using any of the discussed techniques. However, the challenge mostly comes from the tracking of less abundant fractions enrolled in disinfection reactions. SEC analysis and fluorescence revealed high molecular weight compounds with little absorption (biopolymers) were also consumed during chlorination, but their engagement was less evident through HRMS or absorbance analysis. Because of the consumption of high molecular weight compounds, an increase in lower molecular weight fractions with greater absorption at lower wavelengths, that is higher instauration degrees (building blocks) was released after disinfection reactions. At the latest, Orbitrap analysis figured all those changes by reflecting the depletion of lignin-like and soot kind of compounds, typically coming from humic and fulvic structures, and the enrichment of tannins, standing for the unsaturated low molecular weight compounds being released.

This chapter aimed for an exploratory analysis of the cross-linking between techniques. Though few data were available to conduct sound statistical analysis for evaluating and comparing their predictability capacity towards disinfection by-products, the correlation between the discussed indexes of the 12 analyzed samples was tested with Pearson analysis (Figure 42).

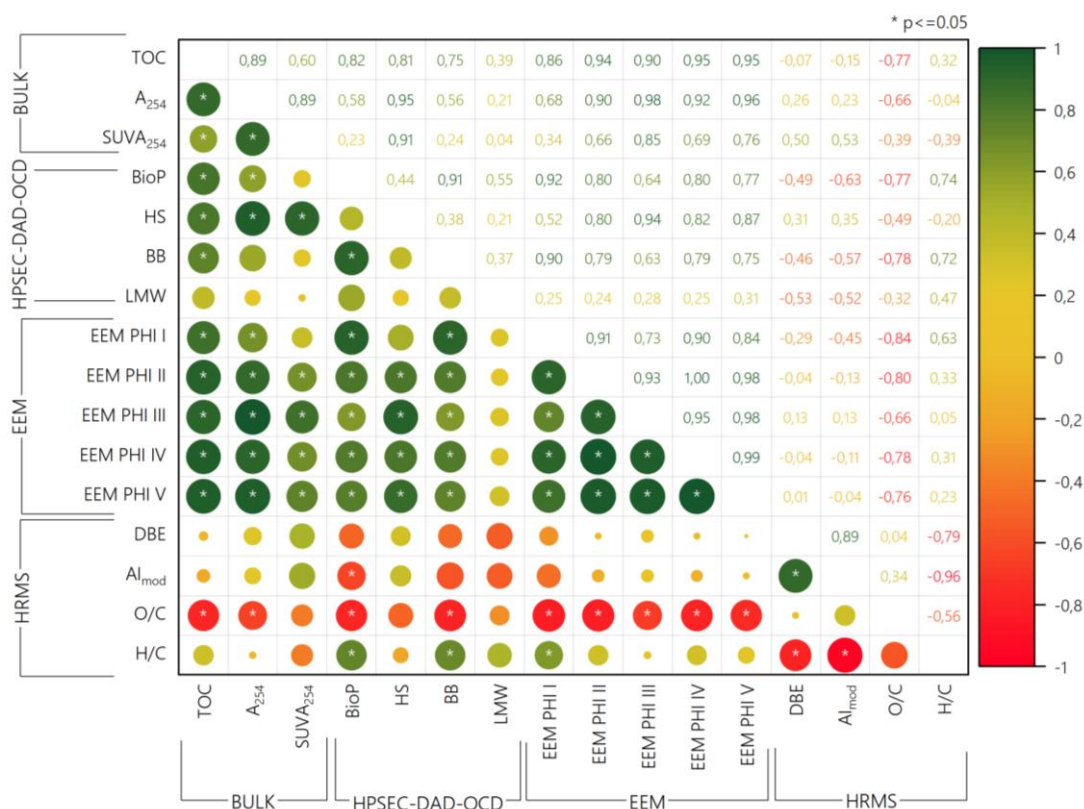


Figure 42: Correlation matrix between indexes. On the upper diagonal Pearson's coefficients, on the lower diagonal significance of correlations (p-values ≤ 0.05) are marked with a * symbol.

Results from Pearson's correlation analysis presented in Figure 42 support the discussed association between measurable DOM attributes and structural resemblance. Bulk surrogate properties, as they are global measurements of the most abundant compounds, exhibited strong correlations with indexes from other techniques such as SEC or fluorescence. However, their ability to provide information about physicochemical properties is limited. Fluorescence indexes showed strong correlations with most variables, including bulk absorbance at 254, indicating that spectroscopical properties may overlap due to similar functionalities in DOM moieties. Slightly stronger correlations were observed between ΦII, ΦIV and biopolymers and building blocks (which include unbundled chains of proteins and polyaromatic acids originated from the breakdown of humic substances and biopolymers), as well as ΦIII, ΦV, and humic acids. Low molecular weight compounds exhibited non-significant correlations with neither parameter. Similarly, HMRS indexes presented few significant correlations.

Given the preliminary discussion derived from this exploratory analysis, it is unfeasible to determine which of the evaluated methodologies is more accurate for studying the role of DOM in the formation of DBPs. However, some considerations can be extracted:

- Each characterization technique is focused on a specific property, thus targeting different moieties entailed in DOM. Thereof, results from each analysis will be subjected to the limitations of each technique which, from a general overview, will be in a certain way biased (MW cutoff, specific optical properties, etc.). In this sense, advanced characterization techniques are not substitutes for

each other, but complementary approaches that must be tight together to unveil the complexity of the DOM matrix.

- The identification and tagging of representative compounds fulfilling certain types of characteristics and their overlap between approaches facilitates comprehension of DOM conforming structures (e.g., humic- and fulvic-like, protein-like, etc.).
- Bulk measurements are basic assessments that provide little information about the physicochemical properties of DOM thus not contributing to a further comprehension of its reactivity. They can act as good surrogates for tracking overall reductions but will not excel at optimizing treatments neither minimize formation of DBPs unless a prior, in-depth characterization of waters had been done.
- Most of the developed techniques, specially the spectroscopic ones, are centred on the evaluation of more abundant fractions, which usually tend to be the most reactive. However, their sensitivity is lower against recalcitrant fractions (i.e., lower molecular weight, higher saturation, and less hydrophobicity) which might also play a role in the formation of DBPs (Carra et al., 2021a; Finkbeiner et al., 2020c). Exploring other properties, such as zeta potential or hydrophobicity fractionation, can also contribute to a further evaluation of those minority yet significant constituents (Sillanpää et al., 2018).

Chapter VIII

RESULTS V

Strategies for the mitigation and minimization of DBPs on drinking water treatment plants. An applied guideline to meet new legislation requirements

Redrafted from:

Upgrading water treatment trains to comply with the DBPs standards introduced by the Directive (EU) 2020/2184

Valenti-Quiroga, M., Farré, M. J., & Roccaro, P. (2024).
Current Opinion in Environmental Science & Health, 100547.
<https://doi.org/10.1016/j.coesh.2024.100547>

1. BACKGROUND AND OBJECTIVES

This chapter aims to assess different approaches for enhancing conventional drinking water treatment plants (DWTPs) to minimize the formation of the regulated DBPs. Recently, the revised European Directive (EU) 2020/2184 on drinking water adds standards for new DBPs such as haloacetic acids, chlorite, and chlorate, in addition to trihalomethanes and bromate. Therefore, Member States of the European Union must set specific national laws to meet standard requirements. New limits are included for chlorate and chlorite both at 0.25 mg/L, with an allowance of up to 0.70 mg/L in the case of disinfection with chlorine dioxide (ClO₂). Additionally, the EU 2020/2184 sets a limit for haloacetic acids at 60 µg/L, which includes the sum of five representative substances (monochloro-, dichloro-, and trichloro-acetic acid, and mono- and dibromo-acetic acid). Furthermore, the Directive maintains existing regulations for trihalomethanes (THMs) at 100 µg/L, which is calculated as the sum of chloroform, dichlorobromomethane, dibromochloromethane, and bromoform and a limit of 10 µg/L for bromate.

Those new DBPs standards will impact the treatment processes of conventional DWTPs, which might need upgrades to remove specific DBPs or DBPs precursors. Four key strategies are identified and discussed: (1) source water quality control, (2) enhanced precursor removal, (3) alternative disinfection/pre-oxidation, and (4) removal of already formed DBPs. However, though the focus is set on those regulated DBPs, formation of other organic and inorganic DBPs can be still generated (Chaukura et al., 2020; Gilca et al., 2020), and even when the drinking water quality standard is met, the question regarding the best treatment processes to minimize the risk to DBPs exposure remains open. The advantages and disadvantages of such strategies will be discussed considering also the formation of other emerging unregulated DBPs.

2. METHODOLOGY

A bibliographic review of latest studies on advanced methodologies for mitigation of DBPs and DBPs precursors at real plant scale application was made to elaborate a comparison of techniques considering their implementation feasibility. Finally, some treatment train configuration and guidelines are proposed to aid selection of more appropriate processes to reduce overall DBPs formation.

3. RESULTS AND DISCUSSION

3.1 Strategies to minimize DBPs formation

The following strategies can be employed to control formation of regulated DBPs in drinking water without compromising microbial protection (US EPA, 1999):

- › source water quality control;
- › removal of DBPs precursors;
- › disinfection strategy selection;
- › removal of already formed DBPs

3.1.1 *Source water control strategies*

Protecting source water is always a priority and an effective approach, preventing the need for numerous DWTPs upgrades. Measures involve managing the source water to reduce NOM and bromide concentration and reactivity. As well as avoiding contamination from point sources (e.g., industrial discharges) and non-point sources (e.g., agricultural runoff).

Source control strategies should be tailored to the specific characteristics and challenges of the water source and the local environment such as controlling nutrients and algae to help limit the formation of DBPs, avoid brine or saltwater intrusion to prevent bromide presence or implementing land-use planning and zoning to uphold the areas. It is crucial to continuously evaluate and adapt these strategies to address changing conditions and emerging threats to drinking water quality. Deployment of advanced monitoring tools and early warning systems integrated with artificial intelligence to track water quality should also be considered as preventive measures. Collaboration among various stakeholders, including water utilities, government agencies, and the public to raise awareness and establish policies about the importance of preserving water sources is key to the success of source water protection programs.

Furthermore, chlorate impurities may be present in stock solution of sodium hypochlorite, which should be checked before its use. Bromate can be present too but at much lower concentration, while chlorite occurrence is less reported (Asami et al., 2009).

3.1.2 *Removal of DBPs precursors*

Enhancing removal of DBPs precursors is the optimal strategy for mitigating its formation. Organic substances and bromide are considered as the main precursors, and can be effectively eliminated through several processes of separation (coagulation, adsorption, ion-exchange, and membrane filtration) (Q. Lin et al., 2020; P. Wang et al., 2021; Yin et al., 2020), biofiltration (slow sand filtration, biological activated carbon) (C. Liu et al., 2017), or pre-oxidation processes (using ozone, chloride dioxide, and advanced oxidation processes) (Chu et al., 2012; Y. Lin et al., 2022; Rougé et al., 2020).

3.1.2.1 *Separation*

Separation techniques encompass enhanced coagulation, adsorption on activated carbon (AC), filtration (including membrane processes), and ionic exchange resins (IEX).

Coagulation followed by flocculation, clarification (sedimentation or flotation) and/or filtration is the most common technique employed for the removal of solids, including colloids, from water. Coagulation removes about 10-30% of NOM from water, and though sand filtration contributes also on decreasing NOM levels, isolated filtration is unable to reduce precursors to prevent formation of DBPs below the limits. The U.S. EPA (US EPA, 1999) defined enhanced coagulation processes as a suggested method for improving the removal of DBPs precursors (NOM) in conventional water treatment plants. The principal mechanism during coagulation is the sorption of dissolved organic matter (DOM) onto precipitated metal hydroxides generated with the addition of alum or ferric-based coagulants, or a combination of them, to enhance removal of precursors. During the process, high molecular weight hydrophobic fractions of DOM are targeted, while considerable concentrations of lower molecular weight and hydrophilic DBPs precursors might remain in the effluent. An effective method to reduce this subsequent formation of DBPs could be the use ion-exchange. Coupling IEX processes after

coagulation might enhance removal of a broader distribution of molecular weight compounds, including those of lower molecular weight, reducing the formation of THMs and HAAs.

Adsorption is the most basic and commonly used method employed in water purification. AC is a highly porous, effective adsorbent widely used for drinking water treatment for the removal of colour, odour, taste, and organic contaminants, including DOM. Effectiveness of precursor removal depends on several filters design parameters, but overall AC removes efficiently aromatic DOM molecules, which are precursors for THMs and HAAs (Ding et al., 2019; Wu et al., 2022). However, through the adsorption of DOM, a key factor to consider for subsequent treatments is the increase of Br/TOC ratio in the effluent, which will be responsible for an enhanced brominated DBPs (Br-DBPs) versus carbonaceous DBPs (C-DBPs) formation and therefore rising overall toxicity (C. Zhang et al., 2020). On the other hand, chlorine coupled to granular activated carbon (GAC) combination was found effective to remove high molecular weight DBPs (HMW-DBPs), also lowering the toxicity (Jiang et al., 2018; Lau et al., 2023).

Results from the in-deep analysis performed on DWTPs depict the effects of NOM removal driven by enhanced coagulation and adsorption and their role in DBPs-FP. As presented on Chapters V, VI and VII, coagulation targeted mostly humic substances fractions of higher apparent molecular weight, leading to reductions ranging between 7% to 28% on DOC and between 22% to 36% in absorbance at 254 nm depending on the raw water quality and operational conditions. Alternatively, adsorption accounted for reductions between 19% to 29% of DOC and 36% to 43% of absorbance at 254 nm; mainly targeting humic substances of lower molecular weight and building blocks. Ultimately, such reductions entail lower DBP-FPs.

Membrane technologies such as reverse osmosis, nanofiltration, or electrodialysis reversal (EDR), are energetically demanding but offer the advantage to not only remove DOM but also inorganic ions such as bromide and iodide from water (Watson et al., 2012). The main mechanism is based on size rejection and the principal associated concern is the alteration of halogen/DOC ratio in permeates which as previously stated might affect final toxicity, and the major drawback of membranes is the fouling due to DOM itself, that can be controlled implementing backwashing. Another limitation of membrane filtration is the need for disposal of the concentrate, which is not easy in inland locations.

From the case studies, Abrera DWTP (See Chapter IV) implemented in 2009 an EDR unit to deal with high salinity issues, specially related to bromide with concentrations ranging between 0.5 and 1.2 mg/L. Though enhanced coagulation and GAC can efficiently remove NOM, bromide mostly remains unaltered. Therefore, the ratio bromide to NOM is higher, shifting formation of brominated DBPs. After the GAC filtration and by a derivation of water pipeline, the EDR step takes feedwater prior to final chlorination to remove part of those DBPs precursors and reduce levels of THMs. The plant has two hydraulic EDR stages including 576 EDR stacks, which make it the world's largest plant using this technology. After, remineralization dosing lime and CO₂ is applied prior to blending with product water from the conventional treatment to produce up to 3,2 m³/s. From 2009 to 2022, the EDR plant has produced more than 275 hm³ and the technology has showed to be very robust. After the NOM fractionation studies (See Chapters V and VI) his membrane technology has shown to significantly reduce amounts of DBPs precursors (~48% of DOC and 70% 254 nm absorbance reductions), specially bromide but also considerable amounts of humic substances and building blocks fractions, lowering the formation potentials of THMs. Removal mechanisms of such compounds might be driven by the electrostatic repulsions between charged sites of NOM and membrane polarity.

Finally, as DOM is partially ionized at neutral pH conditions due to the presence of acidic functional groups (i.e. carboxyl), its removal by anion exchange resins is also feasible. It has been reported that anion exchange has the potential to remove components resistant to other conventional treatment processes, like more charged and hydrophilic components, which can make significant contributions to DBPs formation during chlorination. Compared to the abovementioned techniques, DOM removal via ion exchange is thought to involve several mechanisms such as size exclusion and electrostatic interactions (Tan et al., 2005). However, there is a lack of consensus in literature as some studies indicate that resins are most efficient in removing more aromatic DOM with high molecular weight, while some researchers report the opposite, what suggests that more research is still needed. From the obtained results (Chapter VI), findings showed IEX was effective in reducing a 43%-54% of DOC when placed prior to coagulation, while DOC reductions of 29% and 59% were achieved when coupled afterwards the coagulation. Moreover, SEC analysis reported lesser removals of lower MW fractions on the latest compared to higher removals of HS when acting on raw waters. Nevertheless, the capability of performing on-site regeneration of resins makes this a cost-effective addition to conventional treatment facilities. Although overall efficiency might be determined by resin characteristics, enhanced coagulation with ion exchange resins (IEX) was found to be more effective for removing THMs and HAAs precursors than coagulation alone (Singer & Bilyk, 2002).

3.1.2.2 Biofiltration

Biological filtration is cost effective since the bacteria that are naturally present in the water supply can colonize existing filter media, does not produce a residual that needs disposal, and requires almost no modification of ambient conditions. The only prerequisite for maximizing bacterial substrate utilization in filters is the absence of disinfectant in the filter influent or in the backwash water. The filter media colonized by bacteria can be sand, anthracite, or GAC (referred as biological activated carbon, BAC). Due to the relatively low proportion of biodegradable fractions in NOM (biodegradable DOC/DOC = 0.1–0.3) (Escobar & Randall, 2001), ozone is dosed before filtration to increase the biodegradable DOC (O_3/BAC). Liu and co-authors (C. Liu et al., 2017) reported that biofiltration can remove a fraction of the precursors of halogenated DBPs including THMs, HAAs, and other emerging DBPs such as haloketones (HKs), haloacetonitriles (HANs), haloacetoamides (HAcAms) halonitromethanes (HNMs), or nitrosamines. Efficacy of biofiltration will depend on filter design and operational conditions (i.e. contact time).

3.1.2.3 Oxidation

The oxidative effect of selective agents such as O_3 , Fe(IV), Mn(VII), and ClO_2 on NOM towards DBPs formation have been recently investigated (J. Li et al., 2023; X. Yang et al., 2015). Such chemicals were found to selectively react with electron-rich moieties in DOM (e.g., phenols, amines, and olefines), affecting the precursors characteristics. Generally, such oxidants reduce the formation of regulated DBsP in post-chlorination, even though some emerging DBPs such as HNMs, CH, or HKs may increase (Hu et al., 2018; J. Li et al., 2023). The use of alternative oxidants as pre-oxidation step within the WTPs is also discussed in the following section.

3.1.3 Disinfection strategy selection

Disinfection strategy include several actions that can be implemented:

- › move downstream the disinfection point to avoid formation of DBPs where precursors are still present at high concentration;
- › avoid or minimize intermediate disinfection (i.e. adding chlorine before filtration): though it is a common praxis to avoid microbial growth in filters, the long contact time between disinfectants and precursors at relatively high concentrations might enhance formation of undesired DBPs;
- › combine different disinfectants or oxidants for primary and secondary disinfection to reduce formation of DBPs from a single disinfectant:
 - substitute chlorine as a pre-oxidant with alternative reagents such as ozone, chlorine dioxide, potassium permanganate, ferrate, chloramines, or AOPs;
 - use alternative or supplemental final disinfectants such as chloramines instead of chlorine.

Shifting to alternative disinfectants as well as optimizing the dosing positions can turn into a successful praxis to reduce DBPs formation. Delaying chlorination after operations prone to remove hydrophobic high molecular weight NOM fractions (main precursors) could lead to a substantial reduction of DBPs, specially THMs and HAAs, up to 50% (Rougé et al., 2020). As a result, chlorine can be used as secondary disinfection also to ensure a stable residual dosage able to maintain controlled levels of pathogenic microbes in the distribution system without exceeding permitted levels of DBPs.

3.1.3.1 Pre-oxidation

Pre-oxidation processes are applied to i) remove compounds that will further be transformed in particulate species removed by precipitation, like iron and manganese, ii) reduce taste and odor, iii) inactivate pathogens, iv) reduce NOM reactivity towards DBP formation, v) remove contaminants of concern, and vi) enhance subsequent coagulation efficiency. Replacing chlorine as a pre-oxidant with alternative reagents (i.e. chlorine dioxide, ferrate, ozone, or permanganate) can help minimize DBP precursors and the following formation of DBPs in final disinfections thanks to their selective reaction with electron-rich moieties of NOM. Selection of most appropriate pre-oxidant should be assessed carefully considering factors such as raw water characteristics (Gilca et al., 2020; J. Li et al., 2023). A summary of main advantages and disadvantages of the most reported pre-oxidation methods is presented in Table 25.

Table 25: Summary of pre-oxidation methodologies regarding effects on DBPs precursors, DBPs formation, main applicability advantages and disadvantages (adapted from Chaukura et al., 2020; Gilca et al., 2020; Li, Song, et al., 2023; Y. Lin et al., 2022).

Oxidant	Effects on DBPs precursor	Effects on DBPs	Applicability Disadvantages	Applicability Limitations
O ₃	Highly oxidant towards saturated moieties, and protein bound-compounds, more effectively than to humic-like substances	<ul style="list-style-type: none"> - Negligible formation of THMs and HAAs - Can promote the formation of BrO₃⁻ when significant concentrations of Br⁻ (> 50 µg/L) are present in the media - Can increase brominated THMs and HAAs if chlorination follows 	<ul style="list-style-type: none"> - Taste, odour and colour compound removal - Removal of trace organic compounds 	<ul style="list-style-type: none"> - Unstable residual - Not appropriate for high brominated waters - High costs for implementation, maintenance, and training of operators
ClO ₂	Oxidant towards saturated moieties, amines and amino-acids	<ul style="list-style-type: none"> - Much less formation of THMs and HAAs than chlorine - Generation of ClO₂⁻ and ClO₃⁻ (inorganic DBPs) 	<ul style="list-style-type: none"> - Taste and odour compound removal 	<ul style="list-style-type: none"> - Unstable residual - High costs for implementation, maintenance, and training of operators
Fe(VI)	Oxidizes aromatic phenols, higher efficiency on removing precursors than ClO ₂	<ul style="list-style-type: none"> - No formation of THMs and HAAs - Might generate halogenated DBPs if substantial concentrations of algal organic matter is present 	<ul style="list-style-type: none"> - Effectively removes THMs and HAAs precursors 	<ul style="list-style-type: none"> - High reactive dosing and high operating costs, economically unfeasible
Mn(VII)	Acts on electron donating moieties, specially N-containing	<ul style="list-style-type: none"> - No generation of THMs and HAAs 	<ul style="list-style-type: none"> - Minimizes THMs up to 45 % - It is reduced and forms MnO₂ enhancing effects of subsequent coagulation 	<ul style="list-style-type: none"> - High reactive dosing and high pH required - Dosing might be limited to avoid residual manganese affecting final water quality
AOPs	Non-selective methodology for oxidative pathways involving electron oxidations and H-abstractions	<ul style="list-style-type: none"> - No formation of THMs and HAAs (if chlorine is not used), otherwise it can promote formation of C-DBPs (including THMs & HAAs) 	<ul style="list-style-type: none"> - Acts towards trace organic compounds - O₃ /AOPs perform slightly better than UV based AOPs in DOM mineralization 	<ul style="list-style-type: none"> - High costs for implementation, maintenance, and training of operators

In general, pre-oxidizing NOM is effective in reducing the NOM reactivity in DBPs formation during the final disinfection. However, some oxidants might be avoided in specific cases. For example, in high bromine containing waters, ozonation might increase formation of bromate and brominated DBPs,

which are of greater toxicity than C-DBPs. ClO₂ is used to reduce the formation of many regulated organic DBPs (THMs or HAAs) as well as of some emerging DBPs, such as HANs and HAcAms (Chaukura et al., 2020) but generates chlorite and chlorate. AOPs are often based on ozonation or UV irradiation and are more expensive than conventional oxidation processes. Permanganate is often used to remove Mn, but it should be applied at pH>8.5 to be effective. Ferrate application in full-scale plant is limited to its high operating costs. In addition to the advantages and disadvantages reported in Table 1, it is noteworthy to report that pre-oxidation by using ClO₂, Fe (VI), O₃, or Mn (VII) usually reduce the formation of regulated DBPs upon final disinfection such as THMs, while might increase the formation of unregulated and more toxic DBPs (e.g. haloaldehydes, HNMs, HAcAms, and NDMA) in the following chlorination or chloramination (Hu et al., 2018; J. Li et al., 2023).

3.1.3.2 Secondary disinfection

In many countries, a secondary disinfection is required to reach and maintain microbiological stability through the distribution system and ensure safe water reaches household taps. Chlorine and chloramines are the most common disinfectants. Chlorine is preferred due to its cost-benefit balance, and it provides a strong and stable residual, however it can enhance the formation of C-DBPs such as THMs and HAAs (F. Dong et al., 2022, 2023). Alternatively, in cases where maintaining appropriate levels of regulated DBPs is challenging, chloramine can be a suitable option, though N-DBPs may be formed, and nitrification might occur (Bond et al., 2011). If the distribution system is small, chlorine dioxide will also minimize C-DBPs but residual stability might be limited (Gilca et al., 2020). To select the optimum disinfectant, it is crucial to characterize and perform tests on water matrix to discern which are the main DBPs precursors and accordingly choose the most suitable disinfectant and operational conditions to minimize formation of DBPs.

3.1.4 Removal of DBPs

Prior to the final disinfection, in some cases the removal of already formed DBPs could be feasible and needed to fulfill the water quality standards. This strategy has been lately reported to be a successful approach in removal of chlorite, chlorate, bromate, and some organic DBPs. A summary of proposed strategies is presented in Table 26.

Table 26: Strategies for removal of regulated DBPs.

DBPs	Technology / Procedure	Reference
Bromate	<ul style="list-style-type: none"> - Membranes (RO & NF): removals up to 79 % - 100% - Microbial reduction - Biological filtration (e.g. BAC) - IEX 	Jahan et al., 2021; Von Gunten, 2003
Chlorite and Chlorate	<ul style="list-style-type: none"> - Addition of reducing compounds (i.e ferrous iron) - Lowering pH - Adsorption on GAC or Powdered AC (PAC), (less efficient) - IEX/Membranes 	Cassol et al., 2022; Sorlini et al., 2014
THMs and HAAs	<ul style="list-style-type: none"> - Adsorption on AC/ PAC - Biological filtration (HAAs) 	Chaukura et al., 2020; Yin et al., 2020

As bromate can be particularly difficult to remove once it is formed (Von Gunten, 2003), it is more effective minimizing its formation on first oxidative reactions. Recently it was reported that bromate can be efficiently removed (up to undetectable levels) by biological filtration (Jahan et al., 2021; Von Gunten, 2003) thanks to its reductive surface activated through microbiological action. The other inorganic regulated DBPs, chlorite and chlorate, have been lately reported to be efficiently removed by means of GAC filtration on optimum conditions at acidic pH (~ 5). Indeed, ClO_2^- is reduced to ClO^- by GAC, especially at pH5, while ClO_3^- is not reduced by GAC and is mostly adsorbed on GAC (Gonce & Voudrias, 1994). Furthermore, mineral carbons offer higher removal efficiency for chlorite than vegetal carbons. Finally, an empty bed contact time (EBCT) of 15-20 minutes is required for efficient chlorite removal (Sorlini et al., 2014). Another process for chlorite removal is the addition of ferrous iron acting as a reducer during coagulation, leading to complete removal in short reaction times (3 to 5s), under $5 < \text{pH} < 7$ conditions (Cassol et al., 2022). In the case of organic regulated DBPs, most efficient proposed methods for already-formed compounds involve biological filtration (BAC) for removing biodegradable by-products like HAAs (C. Liu et al., 2017).

3.2 Alternative treatment trains for controlling DBPs in drinking water

Based on the knowledge discussed on prior sections, some alternative treatment train configurations including upgrading options of conventional trains are proposed in Figure 43 to achieve better control of DBPs in drinking water.

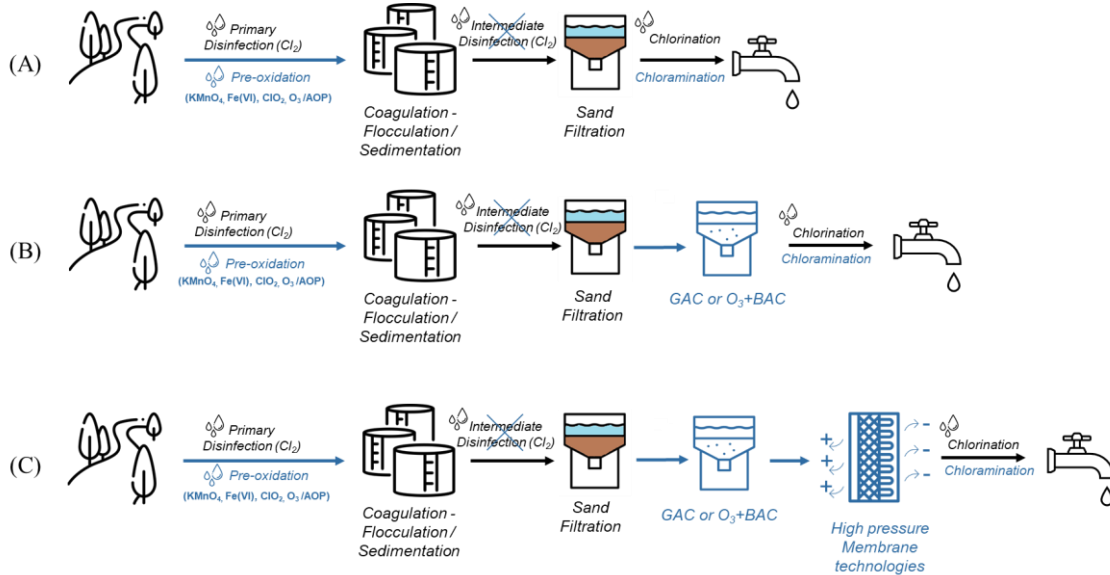


Figure 43: Alternative treatment trains (advanced units (blue) are embedded into a conventional configuration (black)).

Starting from the most conventional configuration, the first suggestion to minimize formation of regulated DBPs could be switching onto alternative disinfectants. For example, in waters with higher amounts of generated organic-DBPs avoiding chlorine as final disinfectant and moving onto chloramines could be beneficial for lowering levels of THMs and HAAs and fulfil the standards set by the European Directive (EU) 2020/2184. This is a solution that might reduce indistinctively all types of regulated DBPs. Also, monochloramine guarantees a stable residual and offers good stability and biofilm control in the network. However, generation of nitrogenous by-products (specially NDMA) and nitrification might then occur. As an alternative, chlorine dioxide can be used as final disinfectant but only in small distribution systems due to its low stability. In a complementary way, adding alternative pre-oxidants (see Table 25 for more detailed selection criteria) prior to coagulation (Scheme A in Figure 43) might be a feasible modification to reduce DBPs as they act on removal of precursors. As previously discussed, the use of alternative pre-oxidant might enhance and diminish formation of different DBPs, which can have a huge impact on final toxicity regardless of regulated species. Hu et al. (2018) examined the cytotoxicity and genotoxicity indexes (CTI/GTI respectively) of produced drinking water by conventional treatment trains (coagulation/sedimentation/filtration with and without final GAC filtration or O₃/GAC) with alternative pre-oxidants and final chlorination or chloramination. None of the studied pre-oxidants (KMnO₄, O₃, K₂FeO₄, ClO₂) resulted in relevant CTI decreases while they substantially increased GTI. Particularly, sole pre-ozonation implemented to conventional treatment configuration (i.e. Scheme A in Figure 43) reported the highest increases in genotoxicity, as it was found to considerably enhance formation of unregulated DBPs such as trichloronitromethane, chloral hydrate, dichloroacetamide, and trichloroacetamide. AOPs may be also used for pre-oxidation, even though the UV based AOPs are not very effective because of the high turbidity.

If feasible, the implementation of GAC filters can enhance the removal of already formed DBPs and will also remove efficiently DBPs precursors (Scheme B in Figure 43) reducing the subsequent formation of regulated organic DBPs such as THMs and HAAs. Particularly, adding a GAC filtration as the latest treatment prior to final disinfection in conventional trains including also pre-oxidation, was reported by Hu et al. (2018) to successfully decrease CTI and GTI. Moreover, coupling O₃ prior to GAC filtration (O₃/BAC), was found to lead highest decreases on toxicity indexes, especially when using ClO₂ as pre-oxidant. Although it is encouraged to minimize intermediate disinfection, if no pre-oxidation is applied prior to filtration, it can be used in conventional trains to avoid microbial growth in the filter media (Figure 43).

Finally, in specific cases the use of high-pressure membranes (NF, RO, EDR) can be needed to remove DBPs precursors that are recalcitrant to the above-mentioned processes, i.e., in high salinity scenarios where bromide and iodide can be a main concern (Scheme C in Figure 43).

3.3 Guidelines

To success in minimizing DBPs a variable number of factors such as selecting the most appropriate processes, operational conditions, economic and energetic factors might be carefully examined. Given the site-specificity of them, it is virtually impossible to establish a priory single optimal treatment configuration. Therefore, Table 27 is designed as a guideline to aid decision-makers selecting the most convenient configuration (Figure 43), that at first instance should be tested in laboratory to evaluate the specificity of DBPs precursors and other water constituents.

Table 27: Guidelines to select mitigation solutions for controlling DBPs regulated by the EU Directive 2020/2184 at WTPs.

DBPs	Causes of generation	Mitigation Solutions
All regulated	Disinfectant dose, type and point of addition	<ul style="list-style-type: none"> - Move the point of disinfection downstream - Lower disinfectants dose - Avoid/minimize intermediate disinfection - Use two or more different disinfectants/oxidants (e.g., substitute chlorine as a pre-oxidant with alternative oxidants; use an alternative disinfectant for final disinfection)
	High levels of precursors in water	<ul style="list-style-type: none"> - Advanced removal of organic precursors by selected pre-oxidation, enhanced coagulation, adsorption on PAC/GAC, O₃/BAC - Enhance removal of inorganic precursors (e.g. bromide) by high pressure membrane (EDR, RO, NF, etc.) or ion exchange if economically feasible - Use two or more different disinfectants/oxidants (e.g., substitute chlorine as a pre-oxidant with alternative oxidants; use an alternative disinfectant for final disinfection)
THMs	Chlorination and related operating conditions	<ul style="list-style-type: none"> - Move the point of disinfection downstream - Lower chlorine dose - Avoid/minimize intermediate chlorination - Use two or more different disinfectants/oxidants (e.g., substitute chlorine as a pre-oxidant with alternative oxidants; use an alternative disinfectant for final disinfection)
	High levels of precursors in water	<ul style="list-style-type: none"> - Add pre-oxidation process with ClO₂, O₃, Fe(VI) or Mn(VII) - Promote organic precursors removal via enhanced coagulation/flocculation processes, PAC/GAC adsorption, O₃/BAC - Enhance removal of inorganic precursors (e.g. bromide) by high pressure membrane (RO, NF, EDR, etc.) or ion exchange if economically feasible

	Others/general	<ul style="list-style-type: none"> - Lower pH to slow the THMs formation - Remove THMs by adsorption, even though low effective - Remove THMs by aeration, although non-volatile DBPs will remain in solution
HAAs	High dose of disinfectant	<ul style="list-style-type: none"> - Move the point of disinfection downstream - Lower chlorine dose - Avoid/minimize intermediate chlorination - Use two or more different disinfectants/oxidants (e.g., substitute chlorine as a pre-oxidant with alternative oxidants; use an alternative disinfectant for final disinfection)
	High levels of precursors in water	<ul style="list-style-type: none"> - Add pre-oxidation process with ClO_2, O_3, Fe(VI) or Mn(VII) - Promote organic precursors removal via enhanced coagulation/flocculation processes, PAC/GAC adsorption, O_3/BAC, biological filtration - Enhance removal of inorganic precursors (e.g. bromide) by high pressure membrane (EDR, RO, NF, etc.) or ion exchange if economically feasible
	Others/general	<ul style="list-style-type: none"> - Remove HAAs by biological filtration
Bromate	O_3 doses (in high brominated waters)	<ul style="list-style-type: none"> - Lowering O_3 dose by improvement of water quality (e.g., removal of NOM before adding O_3, even though O_3 is often used as pre-oxidant) - Optimize O_3 dosing and contact time - Add ammonia or H_2O_2 as inhibitors but pre-test is strongly advised - Lower pH may decrease bromate formation but pre-test is strongly advised
	High levels of precursor (Br-) in water	<ul style="list-style-type: none"> - Implementing membrane technologies (NF, RO, EDR, etc.) to remove Br^-, if economically feasible - Do not employ ozonation
	Others/general	<ul style="list-style-type: none"> - Remove BrO_3^- by biofiltration (e.g., BAC) - Implementing membrane technologies (NF, RO, EDR, etc.) to remove BrO_3^-, if economically feasible - Check bromate impurities in stock solution of sodium hypochlorite
Chlorite	ClO_2 dose	<ul style="list-style-type: none"> - Lowering ClO_2 dose by improvement of water quality (e.g., removal of NOM before adding ClO_2, even though ClO_2 is often used as pre-oxidant) - Optimize ClO_2 dosing
	Others/general	<ul style="list-style-type: none"> - Removal of ClO_2^- via reduction by: i) addition of reducing compounds, such as sulfur dioxide and sodium sulfite, ferrous chloride, and ferrous sulfate; ii) addition of powdered (PAC) - Combine the use of ClO_2 with O_3 or free Cl_2 but ClO_3^- will be formed - Removal of ClO_2^- via reduction by GAC filtration at low pH, high EBCT (>15 min.), and mesoporous mineral-based GAC - Check chlorite impurities in stock solution of sodium hypochlorite
Chlorate	ClO_2 dose	<ul style="list-style-type: none"> - Lowering ClO_2 dose by improvement of water quality (e.g., removal of NOM before adding ClO_2, even though ClO_2 is often used as pre-oxidant) - Optimize ClO_2 dosing
	Instability hypochlorite stock solution	<ul style="list-style-type: none"> - Use hypochlorite solutions that contain less than 1500 mg chlorate/L, have a pH greater than 12, and contain less than 0.08 mg/L of transition metals - Use hypochlorite solutions within 3 months from delivery - Store hypochlorite solutions in a cool dry location where the temperature does not exceed 30°C and away from sunlight
	Others/general	<ul style="list-style-type: none"> - Removal of ClO_3^- by GAC adsorption under optimal conditions to be determined - Check chlorate impurities in stock solution of sodium hypochlorite - Avoid the combination of ClO_2 with O_3 or free Cl_2

4. FINAL REMARKS

The accomplishment of the new DBPs standards, set by the Directive (EU) 2020/2184, might require upgrading current treatment trains operated at the DWTPs. Yet, it seems that a relevant research gap is related to the use and optimization of novel processes/technologies for pre-oxidation of water and/or for final disinfection that may minimize the level of DBPs. Based on the reviewed knowledge the following insights can be outlined:

- The preferred approach to control DBPs in WTPs is to optimize/reduce the dose and the contact time of disinfectants. Furthermore, controlling the quality of the used reagents is very important (e.g. chlorate can be formed due to the instability of the hypochlorite stock solution).
- Removal of DBPs precursors is the most effective strategy for DBPs control. For this purpose, enhanced coagulation and pre-oxidation are important, but final adsorption on GAC filter is often needed. Furthermore, in many cases the O₃/GAC can be employed instead of the GAC filter because could lower the overall toxicity of the produced water (Scheme B in Figure 42).
- The removal of already formed DBPs is often less effective, but in some cases could be necessary. Usually, reduction within GAC filtration or by dosing ferrous ion during coagulation can remove chlorine and to some extent chlorate. Bromate can be removed by biofiltration but more studies are needed to assess the process effectiveness. BAC can effectively remove HAAs and to some extent THMs.
- When no additional process can be implemented due to lack of area for new infrastructure, PAC can be added during coagulation and alternative pre-oxidation could be implemented based on the available area (Scheme A in Figure 43).
- When the removal of inorganic precursors (mainly bromide) is required, a desalination unit could be included in the treatment train before final disinfection to minimize the formation of brominated DBPs and overall DBPs level (e.g. THMs).
- The proposed guideline can be used for the selection of alternative water treatment trains to minimize DBPs in drinking water. Yet, it is mandatory to perform laboratory and pilot tests to select the final treatment train after the evaluation performed by using the proposed guidelines. Such tests should analyze not only the regulated DBPs but also the toxicity of the produced water.

Chapter IX

FINAL DISCUSSION

Disinfection by-products constitute the primary issue stemming from dissolved organic matter (DOM), presenting the most significant challenge in unlocking a successful solution, which hinges upon understanding DOM's role as a precursor. Given the matrix's complexity (heterogeneity, site-specificity, seasonality variations, etc.), most applied techniques in drinking water facilities still treat DOM as a black box, relying on bulk surrogate parameters to track reactivity. However, these approaches often result in inefficient treatments.

With the present work, the use of HPSEC-DAD-OCD methodology seems to be a powerful tool to deeply understand DOM behavior under specific treatments and disinfection reactions. This contributes to decision-making aimed at optimizing processes and minimizing DBPs formation.

Predictive models based on SEC-DOC signal strongly predicted THMs-FP in the studied waters, both from the Llobregat River (with high bromide concentrations) and reservoir waters. The integration of models of this type based on the distribution of DOM molecular weight help taking a step further and understand from which DOM fractions are more prone to DBPs formation and how to track treatment processes to improve their efficiencies.

A summary of all tested approaches evaluated through this dissertation is presented in Table 28 to underscore main divergences. To facilitate comparison, a ranking has been established (being 1 the lowest value and 5 the highest score) to give a global assessment of each of the approaches.

Table 28: Rate of discussed approaches for prediction of DBPs

FEATURES	BULK-BASED MODELS	HPSEC-DOC DECONVOLUTED MODELS	HPSEC SPECTROSCOPIC DECONVOLUTED MODELS	HPSEC BASED ON DAS OF HS	HPSEC BASED ON RAW ABS OF HS
DISCUSSED IN	Chapter IV & VI	Chapter IV	Chapter IV	Chapter VI	Chapter VI
DOM ATTRIBUTE-BASE	DOC & A254	DOC	Spectro MWL (literature variable selection)	Spectro MWL (experimental variable selection)	Spectro MWL (experimental variable selection)
DATA ACQUISITION COMPLEXITY (INCLUDING EXPERIMENTAL PROCEDURE)	★ ★ ★ ★ ★	★ ★ ★ ★ ★	★ ★ ★ ★ ★	★ ★ ★ ★ ★	★ ★ ★ ★ ★
DATA TREATMENT & CURATION	★ ★ ★ ★ ★	★ ★ ★ ★ ★	★ ★ ★ ★ ★	★ ★ ★ ★ ★	★ ★ ★ ★ ★
PREDICTABILITY	★ ★ ★ ★ ★	★ ★ ★ ★ ★	★ ★ ★ ★ ★	★ ★ ★ ★ ★	★ ★ ★ ★ ★
WATER SOURCE DEPENDENCE	★ ★ ★ ★ ★	★ ★ ★ ★ ★	★ ★ ★ ★ ★	★ ★ ★ ★ ★	★ ★ ★ ★ ★
TECH-TRANSFER POTENTIAL	★ ★ ★ ★ ★	★ ★ ★ ★ ★	★ ★ ★ ★ ★	★ ★ ★ ★ ★	★ ★ ★ ★ ★

Among all the tested approaches, models derived from dissolved organic matter (DOM) fractionation demonstrate higher prediction capabilities compared to bulk-based models. Deconvoluted models exhibit the highest predictability, particularly those employing spectroscopic methods, although they require tedious data treatment. In comparison, approaches based on the absorbance of humic substances streamline data processing while achieving excellent prediction capacities. Furthermore,

they show greater potential for transferring knowledge to sensor-based technologies compared to methods based solely on OCD.

Moreover, the use of spectroscopic measures has recently garnered significant interest. Spectroscopy offers the required sensitivity to detect subtle changes in DOM composition, with the added advantage of being economical, easy to handle (with little to no sample preparation), enabling quick data acquisition, and featuring straightforward data treatment techniques. Consequently, markets are developing sensors based on this methodology for tracking DOM in drinking water treatment plants.

However, the key to successfully implementing these sensors to enhance treatment efficiencies lies in selecting the most appropriate variables (wavelengths) that reflect DOM behaviour for monitoring purposes. Following this research, HPSEC-DAD-OCD is considered a powerful bridge between offline advanced characterization techniques, like SEC, and inline real-time measurements. The application of HPSEC-DAD-OCD allows for thorough DOM characterization by evaluating the full absorbance spectra based on the apparent molecular weight distribution of its compounds, thus enabling the identification of the most significant wavelengths of the most prone precursors. The results discussed previously represent a significant step forward in developing tailored sensor-based technology for predicting DBPs in drinking waters. These advancements stem from the expertise gained in advanced DOM characterization techniques. However, it is very necessary to build a broader data repository to establish more robust models.

One of the principal drawbacks of the hyphenated SEC technology, especially compared to the LC-OCD, is the lack of methodology standardization. Variations derived from instrumental differences will impact the final separation, hindering the comparison of final results. Other methodologies for DOM characterization can also provide valuable information to gain knowledge about the composition of its main constituents. Far from the bulk measurements that reflect the effects of major compounds, specific details can be obtained by settling the analytical window on a specific target, such as fluorescence, or by employing high resolution compound identification techniques (such as Orbitrap). Both approaches can offer compositional and structural information about DOM compounds, but the selection of the most appropriate methodology for characterization will depend on the specific objectives. From a mechanistic point of view, HRMs can aid in better understanding the transformation of DOM under specific treatments or conditions. However, it might not be the most practical from an applied standpoint given its difficult interpretation or pre-treatment steps (e.g., extraction, concentration). Similarly, fluorescence measurements, which rely on very limited DOM functionalities, also involve tedious data treatment and sample handling.

Chapter X

GENERAL CONCLUSIONS

This dissertation aimed to delve into the study of DOM. To this end, a refined SEC method (HPSEC-DAD-OCD) was developed, optimizing the separation of DOM fractions, specially in the regions of high molecular weight fractions, including biopolymers, humic substances, and building blocks. Characterization based on the apparent molecular weight distribution, measured in terms of dissolved organic carbon and absorbance, allows a detailed profile of structural properties closely associated with DOM reactivity.

The development of the HPSEC-DAD-OCD method has facilitated the depiction of the apparent molecular weight distribution of DOM fractions. This capability provides valuable insights into their behaviour under specific treatment conditions. Such specific knowledge is crucial for identifying recalcitrant fractions and optimizing process efficiencies in terms of overall removal and the formation of DBPs, both of which significantly impact final water quality. As expected from bulk reductions and reported studies, coagulation-flocculation processes aimed at major DOM removal in conventional treatments. However, HPSEC-DAD-OCD revealed differences in selective removal according to the AMW distribution of constituting compounds. As emphasized in Chapter V, variations in humic substances' removal were observed based on their physicochemical behavior. Only advanced treatments such as EDR or ion exchange resins were capable of removing recalcitrant fractions of lower AMW and hydrophobicity (i.e., building blocks). The capability of a methodology such as HPSEC-DAD-OCD analysis to assess full DOM removal plays a key role in evaluating the fate of remaining fractions as DBPs precursors.

Consequently, these insights have been leveraged to propose various predictive models for the formation potentials of the regulated organic DBPs, including trihalomethanes and haloacetic acids. Bulk models mostly described on literature are based on properties of the most abundant compounds, thus mostly efficient in predicting the formation of the most abundant DBPs but are not specific enough. However, predictive models, including the contribution of different DOM compounds, help understand the speciation of DBPs. The in-depth analysis resulting from the HPSEC-DAD-OCD characterization has enabled the selection of the most suitable variables based on specific DOM properties, ranging from the carbon content (DOC) of the different fractions to more precise spectroscopic variables, including slopes and differential absorbance spectra of the most abundant fraction (humic substances) after chlorination processes (discussed in Chapters IV and VI). The overall learning process concluded with the identification of four wavelengths (220 nm, 252 nm, 290 nm, 362 nm) to monitor specific DOM variations related to formation of abovementioned DBPs.

Compared to other advanced characterization methodologies, HPSEC-DAD-OCD falls in between the complexities of high-resolution compound identification (such as HRMS) and mass-balancing techniques (bulk measurements, fluorescence). However, understanding the points of convergence between characterization techniques and integrating information acquired through various methodologies is crucial for advancing expertise in dissolved organic matter analysis from a broader perspective.

To approach disinfection processes from a holistic perspective that ensures high water quality, it is necessary to delve into the use of advanced characterization techniques of this type. Acquiring the necessary understanding of the reactivity of precursors from easily measurable properties (e.g., absorbance) that correlate with the formation of emerging contaminants such as DBPs, is critical for developing tools that ease the application and transfer of this knowledge to real case-scenarios.

Without losing sight of the main challenge water treatment plants still deal with day-to-day, understanding the role of DOM as a precursor to DBPs is paramount. And this happens not to exhaustively identify its composition but to understand its behavior towards both conventional and advanced treatments. At the same time, it is essential to foster collaborations between institutions and develop historical data repositories to facilitate the understanding of seasonal variations and to report unusual episodes that could help act in future situations. By pursuing this approach, a dual victory for both citizens and plant managers becomes achievable: maximizing treatment efficiency while minimizing the generation of DBPs.

BIBLIOGRAPHY

- Abd El-Shafy, M., Gru, A., & Nwald, È. (2000). THM formation in water supply in South Bohemia, Czech Republic. www.elsevier.com/locate/watres
- Allard, S., Tan, J., Joll, C. A., & Von Gunten, U. (2015). Mechanistic Study on the Formation of Cl-/Br-/I-Trihalomethanes during Chlorination/Chloramination Combined with a Theoretical Cytotoxicity Evaluation. *Environmental Science and Technology*, 49(18), 11105–11114. <https://doi.org/10.1021/acs.est.5b02624>
- Allpike, B. P., Heitz, A., Joll, C. A., & Kagi, R. I. (2007). A new organic carbon detector for size exclusion chromatography. *Journal of Chromatography A*, 1157(1–2), 472–476. <https://doi.org/10.1016/j.chroma.2007.05.073>
- Allpike, B. P., Heitz, A., Joll, C. A., Kagi, R. I., Abbt-Braun, G., Frimmel, F. H., Brinkmann, T., Her, N., & Amy, G. (2005). Size exclusion chromatography to characterize DOC removal in drinking water treatment. *Environmental Science and Technology*, 39(7), 2334–2342. <https://doi.org/10.1021/es0496468>
- Andersson, A., Lavonen, E., Harir, M., Gonsior, M., Hertkorn, N., Schmitt-Kopplin, P., Kylin, H., & Bastviken, D. (2020). Selective removal of natural organic matter during drinking water production changes the composition of disinfection by-products. *Environmental Science: Water Research & Technology*, 6(3), 779–794. <https://doi.org/10.1039/C9EW00931K>
- Asami, M., Kosaka, K., & Kunikane, S. (2009). Bromate, chlorate, chlorite and perchlorate in sodium hypochlorite solution used in water supply. *Journal of Water Supply: Research and Technology - AQUA*, 58(2), 107–115. <https://doi.org/10.2166/aqua.2009.014>
- Awad, J., van Leeuwen, J., Chow, C., Drikas, M., Smernik, R. J., Chittleborough, D. J., & Bestland, E. (2016). Characterization of dissolved organic matter for prediction of trihalomethane formation potential in surface and sub-surface waters. *Journal of Hazardous Materials*, 308, 430–439. <https://doi.org/10.1016/j.jhazmat.2016.01.030>
- Beauchamp, N., Dorea, C., Bouchard, C., & Rodriguez, M. (2018). Use of differential absorbance to estimate concentrations of chlorinated disinfection by-product in drinking water: Critical review and research needs. *Critical Reviews in Environmental Science and Technology*, 48(2), 210–241. <https://doi.org/10.1080/10643389.2018.1443668>
- Beauchamp, N., Dorea, C., Bouchard, C., & Rodriguez, M. (2019). Multi-wavelength models expand the validity of DBP-differential absorbance relationships in drinking water. *Water Research*, 158, 61–71. <https://doi.org/10.1016/j.watres.2019.04.025>
- Bichsel, Y., & Von Gunten, U. (2000). Formation of iodo-trihalomethanes during disinfection and oxidation of iodide-containing waters. *Environmental Science and Technology*, 34(13), 2784–2791. <https://doi.org/10.1021/es9914590>

- Birkmann, J., Pasel, C., Luckas, M., & Bathen, D. (2018). Uv spectroscopic properties of principal inorganic ionic species in natural waters. *Water Practice and Technology*, 13(4), 879–892. <https://doi.org/10.2166/wpt.2018.097>
- Bond, T., Henriot, O., Goslan, E. H., Parsons, S. A., & Jefferson, B. (2009). Disinfection byproduct formation and fractionation behavior of natural organic matter surrogates. *Environmental Science and Technology*, 43(15), 5982–5989. <https://doi.org/10.1021/es900686p>
- Bond, T., Huang, J., Templeton, M. R., & Graham, N. (2011). Occurrence and control of nitrogenous disinfection by-products in drinking water - A review. In *Water Research* (Vol. 45, Issue 15, pp. 4341–4354). Elsevier Ltd. <https://doi.org/10.1016/j.watres.2011.05.034>
- Brezinski, K., & Gorczyca, B. (2019a). Multi-spectral characterization of natural organic matter (NOM) from Manitoba surface waters using high performance size exclusion chromatography (HPSEC). *Chemosphere*, 225, 53–64. <https://doi.org/10.1016/j.chemosphere.2019.02.176>
- Brezinski, K., & Gorczyca, B. (2019b). Multi-spectral characterization of natural organic matter (NOM) from Manitoba surface waters using high performance size exclusion chromatography (HPSEC). *Chemosphere*, 225, 53–64. <https://doi.org/10.1016/j.chemosphere.2019.02.176>
- Byrne, A. J., Chow, C., Trolio, R., Lethorn, A., Lucas, J., & Korshin, G. V. (2011). Development and validation of online surrogate parameters for water quality monitoring at a conventional water treatment plant using a UV absorbance spectrolyser. *Proceedings of the 2011 7th International Conference on Intelligent Sensors, Sensor Networks and Information Processing, ISSNIP 2011*, 200–204. <https://doi.org/10.1109/ISSNIP.2011.6146515>
- Cai, M. H., Wu, Y. P., Ji, W. X., Han, Y. Z., Li, Y., Wu, J. C., Shuang, C. D., Korshin, G. V., Li, A. M., & Li, W. T. (2020). Characterizing property and treatability of dissolved effluent organic matter using size exclusion chromatography with an array of absorbance, fluorescence, organic nitrogen and organic carbon detectors. *Chemosphere*, 243, 125321. <https://doi.org/10.1016/j.chemosphere.2019.125321>
- Carra, I., Fernandez Lozano, J., Johannesen, S., Godart-Brown, M., Goslan, E. H., Jarvis, P., & Judd, S. (2021). Sorptive removal of disinfection by-product precursors from UK lowland surface waters: Impact of molecular weight and bromide. *Science of the Total Environment*, 754, 142152. <https://doi.org/10.1016/j.scitotenv.2020.142152>
- Carstea, E. M., Bridgeman, J., Baker, A., & Reynolds, D. M. (2016). Fluorescence spectroscopy for wastewater monitoring: A review. In *Water Research* (Vol. 95, pp. 205–219). Elsevier Ltd. <https://doi.org/10.1016/j.watres.2016.03.021>
- Cascone, C., Murphy, K. R., Markensten, H., Kern, J. S., Schleich, C., Keucken, A., & Köhler, S. J. (2022). AbspectroscOPY, a Python toolbox for absorbance-based sensor data in water quality monitoring. *Environmental Science: Water Research & Technology*, 8(4), 836–848. <https://doi.org/10.1039/D1EW00416F>
- Cassol, G. S., Shang, C., Li, J., Ling, L., Yang, X., & Yin, R. (2022). Dosing low-level ferrous iron in coagulation enhances the removal of micropollutants, chlorite and chlorate during advanced

- water treatment. *Journal of Environmental Sciences (China)*, 117, 119–128. <https://doi.org/10.1016/j.jes.2022.03.022>
- Chaukura, N., Marais, S. S., Moyo, W., Mbali, N., Thakalekoala, L. C., Ingwani, T., Mamba, B. B., Jarvis, P., & Nkambule, T. T. I. (2020). Contemporary issues on the occurrence and removal of disinfection byproducts in drinking water - A review. In *Journal of Environmental Chemical Engineering* (Vol. 8, Issue 2). Elsevier Ltd. <https://doi.org/10.1016/j.jece.2020.103659>
- Chellam, S., & Krasner, S. W. (2001). Disinfection byproduct relationships and speciation in chlorinated nanofiltered waters. *Environmental Science and Technology*, 35(19), 3988–3999. <https://doi.org/10.1021/es010775n>
- Chen, B., Zhang, C., Zhao, Y., Wang, D., Korshin, G. V., Ni, J., & Yan, M. (2020a). Interpreting main features of the differential absorbance spectra of chlorinated natural organic matter: Comparison of the experimental and theoretical spectra of model compounds. *Water Research*, 185. <https://doi.org/10.1016/j.watres.2020.116206>
- Chen, B., Zhang, C., Zhao, Y., Wang, D., Korshin, G. V., Ni, J., & Yan, M. (2020b). Interpreting main features of the differential absorbance spectra of chlorinated natural organic matter: Comparison of the experimental and theoretical spectra of model compounds. *Water Research*, 185, 116206. <https://doi.org/10.1016/j.watres.2020.116206>
- Chin, Y.-P., & George Alken, It. (1994). *Molecular Weight, Polydispersity, and Spectroscopic Properties of Aquatic Humic Substances* (Vol. 28).
- Chowdhury, S., Champagne, P., & James McLellan, P. (2010). Investigating effects of bromide ions on trihalomethanes and developing model for predicting bromodichloromethane in drinking water. *Water Research*, 44(7), 2349–2359. <https://doi.org/10.1016/j.watres.2009.12.042>
- Chowdhury, S., Champagne, P., & McLellan, P. J. (2009). Models for predicting disinfection byproduct (DBP) formation in drinking waters: A chronological review. *Science of the Total Environment*, 407(14), 4189–4206. <https://doi.org/10.1016/j.scitotenv.2009.04.006>
- Chu, W., Gao, N., Yin, D., Deng, Y., & Templeton, M. R. (2012). Ozone-biological activated carbon integrated treatment for removal of precursors of halogenated nitrogenous disinfection by-products. *Chemosphere*, 86(11), 1087–1091. <https://doi.org/10.1016/j.chemosphere.2011.11.070>
- Criquet, J., Rodriguez, E. M., Allard, S., Wellauer, S., Salhi, E., Joll, C. A., & von Gunten, U. (2015a). Reaction of bromine and chlorine with phenolic compounds and natural organic matter extracts – Electrophilic aromatic substitution and oxidation. *Water Research*, 85, 476–486. <https://doi.org/10.1016/j.watres.2015.08.051>
- Criquet, J., Rodriguez, E. M., Allard, S., Wellauer, S., Salhi, E., Joll, C. A., & von Gunten, U. (2015b). Reaction of bromine and chlorine with phenolic compounds and natural organic matter extracts - Electrophilic aromatic substitution and oxidation. *Water Research*, 85, 476–486. <https://doi.org/10.1016/j.watres.2015.08.051>
- Crouè, J.-P., Korshin, G. V., Leenheer, J., & Benjamin, M. M. (2000). Characterisation of Natural Organic Matter in Drinking Water Disinfection by-products control in drinking water Influence of natural

- organic matter and mineral surfaces on the speciation of radionuclides in the environment. <https://www.researchgate.net/publication/238199485>
- Ding, S., Deng, Y., Bond, T., Fang, C., Cao, Z., & Chu, W. (2019). Disinfection byproduct formation during drinking water treatment and distribution: A review of unintended effects of engineering agents and materials. In *Water Research* (Vol. 160, pp. 313–329). Elsevier Ltd. <https://doi.org/10.1016/j.watres.2019.05.024>
- Directive 98/83/EC. (n.d.). <https://competition-cases.ec.europa.eu/>
- Directive (EU) 2020/2184. (n.d.). <https://competition-cases.ec.europa.eu/>
- Dong, F., Pang, Z., Yu, J., Deng, J., Li, X., Ma, X., Dietrich, A. M., & Deng, Y. (2022). Spatio-temporal variability of halogenated disinfection by-products in a large-scale two-source water distribution system with enhanced chlorination. *Journal of Hazardous Materials*, 423. <https://doi.org/10.1016/j.jhazmat.2021.127113>
- Dong, F., Zhu, J., Li, J., Fu, C., He, G., Lin, Q., Li, C., & Song, S. (2023). The occurrence, formation and transformation of disinfection byproducts in the water distribution system: A review. In *Science of the Total Environment* (Vol. 867). Elsevier B.V. <https://doi.org/10.1016/j.scitotenv.2023.161497>
- Dong, H., Qiang, Z., & Richardson, S. D. (2019). Formation of Iodinated Disinfection Byproducts (I-DBPs) in Drinking Water: Emerging Concerns and Current Issues. *Accounts of Chemical Research*, 52(4), 896–905. <https://doi.org/10.1021/acs.accounts.8b00641>
- Ersan, M. S., Liu, C., Amy, G., & Karanfil, T. (2019). The interplay between natural organic matter and bromide on bromine substitution. *Science of the Total Environment*, 646, 1172–1181. <https://doi.org/10.1016/j.scitotenv.2018.07.384>
- Escobar, I. C., & Randall, A. A. (2001). Assimilable organic carbon (AOC) and biodegradable dissolved organic carbon (BDOC). *Water Research* (Vol. 35, Issue 18).
- Fabbricino, M., & Korshin, G. V. (2004). *Probing the mechanisms of NOM chlorination using fluorescence: formation of disinfection by-products in Alento River water*. <https://iwaponline.com/ws/article-pdf/4/4/227/417399/227.pdf>
- Farré, M. J., Day, S., Neale, P. A., Stalter, D., Tang, J. Y. M., & Escher, B. I. (2013). Bioanalytical and chemical assessment of the disinfection by-product formation potential: Role of organic matter. *Water Research*, 47(14), 5409–5421. <https://doi.org/10.1016/j.watres.2013.06.017>
- Finkbeiner, P., Moore, G., Pereira, R., Jefferson, B., & Jarvis, P. (2020a). The combined influence of hydrophobicity, charge and molecular weight on natural organic matter removal by ion exchange and coagulation. *Chemosphere*, 238, 124633. <https://doi.org/10.1016/j.chemosphere.2019.124633>
- Finkbeiner, P., Moore, G., Pereira, R., Jefferson, B., & Jarvis, P. (2020b). The combined influence of hydrophobicity, charge and molecular weight on natural organic matter removal by ion exchange and coagulation. *Chemosphere*, 238, 124633. <https://doi.org/10.1016/j.chemosphere.2019.124633>

- Finkbeiner, P., Moore, G., Pereira, R., Jefferson, B., & Jarvis, P. (2020c). The combined influence of hydrophobicity, charge and molecular weight on natural organic matter removal by ion exchange and coagulation. *Chemosphere*, 238. <https://doi.org/10.1016/j.chemosphere.2019.124633>
- Finkbeiner, P., Redman, J., Patriarca, V., Moore, G., Jefferson, B., & Jarvis, P. (2018). Understanding the potential for selective natural organic matter removal by ion exchange. *Water Research*, 146, 256–263. <https://doi.org/10.1016/j.watres.2018.09.042>
- Gilca, A. F., Teodosiu, C., Fiore, S., & Musteret, C. P. (2020). Emerging disinfection byproducts: A review on their occurrence and control in drinking water treatment processes. In *Chemosphere* (Vol. 259). Elsevier Ltd. <https://doi.org/10.1016/j.chemosphere.2020.127476>
- Golea, D. M., Upton, A., Jarvis, P., Moore, G., Sutherland, S., Parsons, S. A., & Judd, S. J. (2017). THM and HAA formation from NOM in raw and treated surface waters. *Water Research*, 112, 226–235. <https://doi.org/10.1016/j.watres.2017.01.051>
- Hanson, B., Wünsch, U., Buckley, S., Fischer, S., Leresche, F., Murphy, K., D'Andrilli, J., & Rosario-Ortiz, F. L. (2022). DOM Molecular Weight Fractionation and Fluorescence Quantum Yield Assessment Using a Coupled In-Line SEC Optical Property System. *ACS ES and T Water*, 2(12), 2491–2501. <https://doi.org/10.1021/acsestwater.2c00318>
- He, H., Xu, H., Li, L., Yang, X., Fu, Q., Yang, X., Zhang, W., & Wang, D. (2022). Molecular transformation of dissolved organic matter and the formation of disinfection byproducts in full-scale surface water treatment processes. *Science of the Total Environment*, 838. <https://doi.org/10.1016/j.scitotenv.2022.156547>
- Heeb, M. B., Criquet, J., Zimmermann-Steffens, S. G., & Von Gunten, U. (2014). Oxidative treatment of bromide-containing waters: Formation of bromine and its reactions with inorganic and organic compounds - A critical review. *Water Research*, 48(1), 15–42. <https://doi.org/10.1016/j.watres.2013.08.030>
- Helms, J. R., Stubbins, A., Ritchie, J. D., Minor, E. C., Kieber, D. J., & Mopper, K. (2008). Absorption spectral slopes and slope ratios as indicators of molecular weight, source, and photobleaching of chromophoric dissolved organic matter. *Limnology and Oceanography*, 53(3), 955–969. <https://doi.org/10.4319/lo.2008.53.3.0955>
- Her, N., Amy, G., Foss, D., Cho, J., Yoon, Y., & Kosenka, P. (2002). Optimization of method for detecting and characterizing NOM by HPLC-size exclusion chromatography with UV and on-line DOC detection. *Environmental Science and Technology*, 36(5), 1069–1076. <https://doi.org/10.1021/es015505j>
- Her, N., Amy, G., McKnight, D., Sohn, J., & Yoon, Y. (2003). Characterization of DOM as a function of MW by fluorescence EEM and HPLC-SEC using UVA, DOC, and fluorescence detection. *Water Research*, 37(17), 4295–4303. [https://doi.org/10.1016/S0043-1354\(03\)00317-8](https://doi.org/10.1016/S0043-1354(03)00317-8)
- Hidayah, E. N., Chou, Y. C., & Yeh, H. H. (2017). Comparison between HPSEC-OCD and F-EEMs for assessing DBPs formation in water. *Journal of Environmental Science and Health - Part A Toxic/Hazardous Substances and Environmental Engineering*, 52(4), 391–402. <https://doi.org/10.1080/10934529.2016.1262607>

- Hu, J., Chu, W., Sui, M., Xu, B., Gao, N., & Ding, S. (2018). Comparison of drinking water treatment processes combinations for the minimization of subsequent disinfection by-products formation during chlorination and chloramination. *Chemical Engineering Journal*, 335, 352–361. <https://doi.org/10.1016/j.cej.2017.10.144>
- Hua, G., & Reckhow, D. A. (2007). Comparison of disinfection byproduct formation from chlorine and alternative disinfectants. *Water Research*, 41(8), 1667–1678. <https://doi.org/10.1016/j.watres.2007.01.032>
- Hua, L. C., Chao, S. J., Huang, K., & Huang, C. (2020). Characteristics of low and high SUVA precursors: Relationships among molecular weight, fluorescence, and chemical composition with DBP formation. *Science of the Total Environment*, 727, 138638. <https://doi.org/10.1016/j.scitotenv.2020.138638>
- Huber, S. A., Balz, A., Abert, M., & Pronk, W. (2011). Characterisation of aquatic humic and non-humic matter with size-exclusion chromatography - organic carbon detection - organic nitrogen detection (LC-OCD-OND). *Water Research*, 45(2), 879–885. <https://doi.org/10.1016/j.watres.2010.09.023>
- Huber, S. A., & Frimmel, F. H. (1991). Flow Injection Analysis of Organic and Inorganic Carbon in the Low-ppb Range. *Analytical Chemistry*, 63(19), 2122–2130. <https://doi.org/10.1021/ac00019a011>
- Ignatev, A., & Tuhkanen, T. (2019). Step-by-step analysis of drinking water treatment trains using size-exclusion chromatography to fingerprint and track protein-like and humic/fulvic-like fractions of dissolved organic matter. *Environmental Science: Water Research and Technology*, 5(9), 1568–1581. <https://doi.org/10.1039/c9ew00340a>
- Jahan, B. N., Li, L., & Pagilla, K. R. (2021). Fate and reduction of bromate formed in advanced water treatment ozonation systems: A critical review. In *Chemosphere* (Vol. 266). Elsevier Ltd. <https://doi.org/10.1016/j.chemosphere.2020.128964>
- Jiang, J., Li, W., Zhang, X., Liu, J., & Zhu, X. (2018). A new approach to controlling halogenated DBPs by GAC adsorption of aromatic intermediates from chlorine disinfection: Effects of bromide and contact time. *Separation and Purification Technology*, 203, 260–267. <https://doi.org/10.1016/j.seppur.2018.04.050>
- Jung, Y., & Hu, J. (2015). A K-fold averaging cross-validation procedure. *Journal of Nonparametric Statistics*, 27(2), 167–179. <https://doi.org/10.1080/10485252.2015.1010532>
- Kawasaki, N., Matsushige, K., Komatsu, K., Kohzu, A., Nara, F. W., Ogishi, F., Yahata, M., Mikami, H., Goto, T., & Imai, A. (2011). Fast and precise method for HPLC-size exclusion chromatography with UV and TOC (NDIR) detection: Importance of multiple detectors to evaluate the characteristics of dissolved organic matter. *Water Research*, 45(18), 6240–6248. <https://doi.org/10.1016/j.watres.2011.09.021>
- Kim, S., Kramer, R. W., & Hatcher, P. G. (2003). Graphical Method for Analysis of Ultrahigh-Resolution Broadband Mass Spectra of Natural Organic Matter, the Van Krevelen Diagram. *Analytical Chemistry*, 75(20), 5336–5344. <https://doi.org/10.1021/ac034415p>

- Kitis, M., Kaplan, S. S., Karakaya, E., Yigit, N. O., & Civelekoglu, G. (2007). Adsorption of natural organic matter from waters by iron coated pumice. *Chemosphere*, 66(1), 130–138. <https://doi.org/10.1016/j.chemosphere.2006.05.002>
- Koch, B. P., & Dittmar, T. (2006). From mass to structure: An aromaticity index for high-resolution mass data of natural organic matter. *Rapid Communications in Mass Spectrometry*, 20(5), 926–932. <https://doi.org/10.1002/rcm.2386>
- Korshin, G., Chow, C. W. K., Fabris, R., & Drikas, M. (2009). Absorbance spectroscopy-based examination of effects of coagulation on the reactivity of fractions of natural organic matter with varying apparent molecular weights. *Water Research*, 43(6), 1541–1548. <https://doi.org/10.1016/j.watres.2008.12.041>
- Korshin, G. V., Benjamin, M. M., Chang, H. S., & Gallard, H. (2007). Examination of NOM chlorination reactions by conventional and stop-flow differential absorbance spectroscopy. *Environmental Science and Technology*, 41(8), 2776–2781. <https://doi.org/10.1021/es062268h>
- Korshin, G. V., & Chang, H.-S. (2008). Spectroscopic Studies of the Roles of Distinct Chromophores in NOM Chlorination and DBP Formation. *ACS Symposium Series*, 995(Disinfection By-Products in Drinking Water, Chapter 11), 158–171.
- Korshin, G. V., Li, C.-W., & Benjamin, M. M. (1997). Monitoring the properties of natural organic matter through UV spectroscopy: a consistent theory. *Wat. Res*, 31(97), 1787–1795.
- Korshin, G. V., Wu, W. W., Benjamin, M. M., & Hemingway, O. (2002). Correlations between differential absorbance and the formation of individual DBPs. In *Water Research* (Vol. 36).
- Krasner, S., Weinberg, H., Richardson, S., Pastor, S., Chinn, R., Scilimenti, M., Onstad, G., & Thruston Jr., A. (2006). Occurrence of a new generation of disinfection by-products. *Environmental Science and Technology*, 40, 7175–7185.
- Krzeminski, P., Vogelsang, C., Meyn, T., Köhler, S. J., Poutanen, H., de Wit, H. A., & Uhl, W. (2019). Natural organic matter fractions and their removal in full-scale drinking water treatment under cold climate conditions in Nordic capitals. *Journal of Environmental Management*, 241(August 2018), 427–438. <https://doi.org/10.1016/j.jenvman.2019.02.024>
- Kumar, K., & Margerum, D. W. (1987). Kinetics and Mechanism of General-Acid-Assisted Oxidation of Bromide by Hypochlorite and Hypochlorous Acid. In *Inorg. Chem.*
- Lau, S. S., Feng, Y., Gu, A. Z., Russell, C., Pope, G., & Mitch, W. A. (2023). Cytotoxicity Comparison between Drinking Water Treated by Chlorination with Postchloramination versus Granular Activated Carbon (GAC) with Postchlorination. *Environmental Science and Technology*, 57(36), 13699–13709. <https://doi.org/10.1021/acs.est.3c03591>
- Leefmann, T., Frickenhaus, S., & Koch, B. P. (2019). UltraMassExplorer: a browser-based application for the evaluation of high-resolution mass spectrometric data. *Rapid Communications in Mass Spectrometry*, 33(2), 193–202. <https://doi.org/10.1002/rcm.8315>

- Li, J., Song, Y., Jiang, J., Yang, T., & Cao, Y. (2023). Oxidative treatment of NOM by selective oxidants in drinking water treatment and its impact on DBP formation in postchlorination. In *Science of the Total Environment* (Vol. 858). Elsevier B.V. <https://doi.org/10.1016/j.scitotenv.2022.159908>
- Li, W. T., Jin, J., Li, Q., Wu, C. F., Lu, H., Zhou, Q., & Li, A. M. (2016). Developing LED UV fluorescence sensors for online monitoring DOM and predicting DBPs formation potential during water treatment. *Water Research*, *93*, 1–9. <https://doi.org/10.1016/j.watres.2016.01.005>
- Lin, Q., Dong, F., Miao, Y., Li, C., & Fei, W. (2020). Removal of disinfection by-products and their precursors during drinking water treatment processes. *Water Environment Research*, *92*(5), 698–705. <https://doi.org/10.1002/wer.1263>
- Lin, Y., Lou, Y., Li, A., Wei, Y., Li, H., Zhou, M., & Li, Y. (2022). Effects of pre-oxidation by ozone, permanganate and ferrate on generation and toxicities of disinfection byproducts. *International Journal of Environmental Science and Technology*, *19*(7), 5969–5984. <https://doi.org/10.1007/s13762-021-03526-5>
- Liu, C., Olivares, C. I., Pinto, A. J., Lauderdale, C. V., Brown, J., Selbes, M., & Karanfil, T. (2017). The control of disinfection byproducts and their precursors in biologically active filtration processes. In *Water Research* (Vol. 124, pp. 630–653). Elsevier Ltd. <https://doi.org/10.1016/j.watres.2017.07.080>
- Liu, S., Lim, M., Fabris, R., Chow, C. W. K., Drikas, M., Korshin, G., & Amal, R. (2010). Multi-wavelength spectroscopic and chromatography study on the photocatalytic oxidation of natural organic matter. *Water Research*, *44*(8), 2525–2532. <https://doi.org/10.1016/j.watres.2010.01.036>
- Mackeown, H., von Gunten, U., & Criquet, J. (2022). Iodide sources in the aquatic environment and its fate during oxidative water treatment – A critical review. In *Water Research* (Vol. 217). Elsevier Ltd. <https://doi.org/10.1016/j.watres.2022.118417>
- Matilainen, A., Gjessing, E. T., Lahtinen, T., Hed, L., Bhatnagar, A., & Sillanpää, M. (2011). An overview of the methods used in the characterisation of natural organic matter (NOM) in relation to drinking water treatment. *Chemosphere*, *83*(11), 1431–1442. <https://doi.org/10.1016/j.chemosphere.2011.01.018>
- Merder, J., Freund, J. A., Feudel, U., Hansen, C. T., Hawkes, J. A., Jacob, B., Klapproth, K., Niggemann, J., Noriega-Ortega, B. E., Osterholz, H., Rossel, P. E., Seidel, M., Singer, G., Stubbins, A., Waska, H., & Dittmar, T. (2020). ICBM-OCEAN: Processing Ultrahigh-Resolution Mass Spectrometry Data of Complex Molecular Mixtures. *Analytical Chemistry*, *92*(10), 6832–6838. <https://doi.org/10.1021/acs.analchem.9b05659>
- Mitch, W. A., Richardson, S. D., Zhang, X., & Gonsior, M. (2023). High-molecular-weight by-products of chlorine disinfection. *Nature Water*, *1*(4), 336–347. <https://doi.org/10.1038/s44221-023-00064-x>
- Moyo, W., Chaukura, N., Motsa, M. M., Msagati, T. A. M., Mamba, B. B., Heijman, S. G. J., & Nkambule, T. T. I. (2020). Investigating the fate of natural organic matter at a drinking water treatment plant in south africa using optical spectroscopy and chemometric analysis. *Water SA*, *46*(1), 131–140. <https://doi.org/10.17159/wsa/2020.v46.i1.7893>

- Peacock, M., Evans, C. D., Fenner, N., Freeman, C., Gough, R., Jones, T. G., & Lebron, I. (2014). UV-visible absorbance spectroscopy as a proxy for peatland dissolved organic carbon (DOC) quantity and quality: Considerations on wavelength and absorbance degradation. *Environmental Sciences: Processes and Impacts*, 16(6), 1445–1461. <https://doi.org/10.1039/c4em00108g>
- Phatthalung, W. N., Suttinun, O., Phungsai, P., Kasuga, I., Kurisu, F., Furumai, H., & Musikavong, C. (2021). Non-target screening of dissolved organic matter in raw water, coagulated water, and chlorinated water by Orbitrap mass spectrometry. *Chemosphere*, 264. <https://doi.org/10.1016/j.chemosphere.2020.128437>
- Philibert, M., Luo, S., Moussanas, L., Yuan, Q., Filloux, E., Zraick, F., & Murphy, K. R. (2022). Drinking water aromaticity and treatability is predicted by dissolved organic matter fluorescence. *Water Research*, 220. <https://doi.org/10.1016/j.watres.2022.118592>
- Pifer, A. D., & Fairey, J. L. (2014). Suitability of organic matter surrogates to predict trihalomethane formation in drinking water sources. *Environmental Engineering Science*, 31(3), 117–126. <https://doi.org/10.1089/ees.2013.0247>
- Planas, C., Palacios, Ó., Ventura, F., Boleda, M. ^aR, Martín, J., & Caixach, J. (2019). Simultaneous analysis of 11 haloacetic acids by direct injection-liquid chromatography-electrospray ionization-triple quadrupole tandem mass spectrometry and high resolution mass spectrometry: occurrence and evolution in chlorine-treated water. *Analytical and Bioanalytical Chemistry*, 411(17), 3905–3917. <https://doi.org/10.1007/s00216-019-01864-5>
- Postigo, C., & Zonja, B. (2019). Iodinated disinfection byproducts: Formation and concerns. In *Current Opinion in Environmental Science and Health* (Vol. 7, pp. 19–25). Elsevier B.V. <https://doi.org/10.1016/j.coesh.2018.08.006>
- Raeke, J., Lechtenfeld, O. J., Tittel, J., Oosterwoud, M. R., Bornmann, K., & Reemtsma, T. (2017). Linking the mobilization of dissolved organic matter in catchments and its removal in drinking water treatment to its molecular characteristics. *Water Research*, 113, 149–159. <https://doi.org/10.1016/j.watres.2017.01.066>
- Richardson, S. D., & Plewa, M. J. (2020). To regulate or not to regulate? What to do with more toxic disinfection by-products? *Journal of Environmental Chemical Engineering*, 8(4). <https://doi.org/10.1016/j.jece.2020.103939>
- Richardson, S. D., Plewa, M. J., Wagner, E. D., Schoeny, R., & DeMarini, D. M. (2007). Occurrence, genotoxicity, and carcinogenicity of regulated and emerging disinfection by-products in drinking water: A review and roadmap for research. In *Mutation Research - Reviews in Mutation Research* (Vol. 636, Issues 1–3, pp. 178–242). <https://doi.org/10.1016/j.mrrev.2007.09.001>
- Roccaro, P., Chang, H. S., Vagliasindi, F. G. A., & Korshin, G. V. (2008). Differential absorbance study of effects of temperature on chlorine consumption and formation of disinfection by-products in chlorinated water. *Water Research*, 42(8–9), 1879–1888. <https://doi.org/10.1016/j.watres.2007.11.013>
- Roccaro, P., & Vagliasindi, F. G. A. (2009). Differential vs. absolute UV absorbance approaches in studying NOM reactivity in DBPs formation: Comparison and applicability. *Water Research*, 43(3), 744–750. <https://doi.org/10.1016/j.watres.2008.11.007>

- Roccaro, P., Vagliasindi, F. G. A., & Korshin, G. V. (2009). Changes in NOM Fluorescence Caused by Chlorination and their Associations with Disinfection by-Products Formation. *Environmental Science & Technology*, 43(3), 724–729. <https://doi.org/10.1021/es801939f>
- Rougé, V., von Gunten, U., & Allard, S. (2020). Efficiency of pre-oxidation of natural organic matter for the mitigation of disinfection byproducts: Electron donating capacity and UV absorbance as surrogate parameters. *Water Research*, 187. <https://doi.org/10.1016/j.watres.2020.116418>
- Sanchís, J., Jaén-Gil, A., Gago-Ferrero, P., Munthali, E., & Farré, M. J. (2020). Characterization of organic matter by HRMS in surface waters: Effects of chlorination on molecular fingerprints and correlation with DBP formation potential. *Water Research*, 176. <https://doi.org/10.1016/j.watres.2020.115743>
- Sanchís, J., Petrović, M., & Farré, M. J. (2021). Emission of (chlorinated) reclaimed water into a Mediterranean River and its related effects to the dissolved organic matter fingerprint. *Science of the Total Environment*, 760. <https://doi.org/10.1016/j.scitotenv.2020.143881>
- Sérodes, J. B., Rodriguez, M. J., Li, H., & Bouchard, C. (2003). Occurrence of THMs and HAAs in experimental chlorinated waters of the Quebec City area (Canada). *Chemosphere*, 51(4), 253–263. [https://doi.org/10.1016/S0045-6535\(02\)00840-8](https://doi.org/10.1016/S0045-6535(02)00840-8)
- Sgroi, M., Gagliano, E., Vagliasindi, F. G. A., & Roccaro, P. (2020). Inner filter effect, suspended solids and nitrite/nitrate interferences in fluorescence measurements of wastewater organic matter. *Science of the Total Environment*, 711. <https://doi.org/10.1016/j.scitotenv.2019.134663>
- Sgroi, M., Roccaro, P., Korshin, G. V., Greco, V., Sciuto, S., Anumol, T., Snyder, S. A., & Vagliasindi, F. G. A. (2017). Use of fluorescence EEM to monitor the removal of emerging contaminants in full scale wastewater treatment plants. *Journal of Hazardous Materials*, 323, 367–376. <https://doi.org/10.1016/j.jhazmat.2016.05.035>
- Shi, W., Zhuang, W. E., Hur, J., & Yang, L. (2021). Monitoring dissolved organic matter in wastewater and drinking water treatments using spectroscopic analysis and ultra-high resolution mass spectrometry. In *Water Research* (Vol. 188). Elsevier Ltd. <https://doi.org/10.1016/j.watres.2020.116406>
- Sillanpää, M. (2014). *Natural Organic Matter in Water: characterization and treatment methods*. IWA publishing.
- Sillanpää, M., Ncibi, M. C., Matilainen, A., & Vepsäläinen, M. (2018). Removal of natural organic matter in drinking water treatment by coagulation: A comprehensive review. *Chemosphere*, 190, 54–71. <https://doi.org/10.1016/j.chemosphere.2017.09.113>
- Singer, P. C. (1992). Control of Disinfection By-Products in Drinking Water. *Environmental Engineering*, 727–744.
- Singer, P. C., & Bilyk, K. (2002). Enhanced coagulation using a magnetic ion exchange resin. In *Water Research* (Vol. 36).
- Sorlini, S., Gialdini, F., Biasibetti, M., & Collivignarelli, C. (2014). Influence of drinking water treatments on chlorine dioxide consumption and chlorite/chlorate formation. *Water Research*, 54, 44–52. <https://doi.org/10.1016/j.watres.2014.01.038>

- Tan, Y., & Kilduff, J. E. (2007). Factors affecting selectivity during dissolved organic matter removal by anion-exchange resins. *Water Research*, 41(18), 4211–4221. <https://doi.org/10.1016/j.watres.2007.05.050>
- Tan, Y., Kilduff, J. E., Kitis, M., & Karanfil, T. (2005). Dissolved organic matter removal and disinfection byproduct formation control using ion exchange. *Desalination*, 176(1-3 SPEC. ISS.), 189–200. <https://doi.org/10.1016/j.desal.2004.10.019>
- Toroz, I., & Uyak, V. (2005). Seasonal variations of trihalomethanes (THMs) in water distribution networks of Istanbul City. *Desalination*, 176(1-3 SPEC. ISS.), 127–141. <https://doi.org/10.1016/j.desal.2004.11.008>
- US EPA. (1979). *National Interim Primary Drinking Water Regulations; Control of Trihalomethanes in Drinking Water; Final Rule - Part III*.
- US EPA. (1999). *25 Years of the Safe Drinking Water Act: History and Trends*.
- US EPA. (2001). *Stage 1 Disinfectants and Disinfection Byproducts Rule*.
- US EPA. (2005). *Stage 2 Disinfectants and Disinfection Byproducts Rule*.
- Valenti-Quiroga, M., Daunis-i-Estadella, P., Emiliano, P., Valero, F., & Martin, M. J. (2022). NOM fractionation by HPSEC-DAD-OCD for predicting trihalomethane disinfection by-product formation potential in full-scale drinking water treatment plants. *Water Research*, 227. <https://doi.org/10.1016/j.watres.2022.119314>
- Valero, F., & Arbós, R. (2010). Desalination of brackish river water using Electrodialysis Reversal (EDR). Control of the THMs formation in the Barcelona (NE Spain) area. *Desalination*, 253(1–3), 170–174. <https://doi.org/10.1016/j.desal.2009.11.011>
- Vikesland Y, Kenan Ozekin, P. J., & Valentine, R. L. (2001). MONOCHLORAMINE DECAY IN MODEL AND DISTRIBUTION SYSTEM WATERS. In *Wat. Res* (Vol. 35, Issue 7).
- Von Gunten, U. (2003). Ozonation of drinking water: Part II. Disinfection and by-product formation in presence of bromide, iodide or chlorine. In *Water Research* (Vol. 37, Issue 7, pp. 1469–1487). Elsevier Ltd. [https://doi.org/10.1016/S0043-1354\(02\)00458-X](https://doi.org/10.1016/S0043-1354(02)00458-X)
- Wagner, E. D., & Plewa, M. J. (2017). CHO cell cytotoxicity and genotoxicity analyses of disinfection by-products: An updated review. In *Journal of Environmental Sciences (China)* (Vol. 58, pp. 64–76). Chinese Academy of Sciences. <https://doi.org/10.1016/j.jes.2017.04.021>
- Wang, G.-S., & Hsieh, S.-T. (2001). Monitoring natural organic matter in water with scanning spectrophotometer. *Environment International*, 26, 205–212. www.elsevier.com/locate/envint
- Wang, P., Ding, S., Xiao, R., An, G., Fang, C., & Chu, W. (2021). Enhanced coagulation for mitigation of disinfection by-product precursors: A review. *Advances in Colloid and Interface Science*, 296. <https://doi.org/10.1016/j.cis.2021.102518>
- Wassink, J. K., Andrews, R. C., Peiris, R. H., & Legge, R. L. (2011). Evaluation of fluorescence excitation-emission and LC-OCD as methods of detecting removal of NOM and DBP precursors by

- enhanced coagulation. *Water Science & Technology*, 11.5, 621–630. <https://doi.org/10.2166/ws.2011.101>
- Watson, K., Farré, M. J., & Knight, N. (2012). Strategies for the removal of halides from drinking water sources, and their applicability in disinfection by-product minimisation: A critical review. In *Journal of Environmental Management* (Vol. 110, pp. 276–298). <https://doi.org/10.1016/j.jenvman.2012.05.023>
- Wenk, J., Aeschbacher, M., Salhi, E., Canonica, S., von Gunten, U., & Sander, M. (2013). Chemical Oxidation of Dissolved Organic Matter by Chlorine Dioxide, Chlorine, And Ozone: Effects on Its Optical and Antioxidant Properties. *Environmental Science & Technology*, 47(19), 11147–11156. <https://doi.org/10.1021/es402516b>
- Westerhoff, P., Chao, P., & Mash, H. (2004). Reactivity of natural organic matter with aqueous chlorine and bromine. *Water Research*, 38(6), 1502–1513. <https://doi.org/10.1016/j.watres.2003.12.014>
- Wu, Z., Zhang, Y., Jiang, J., Pu, J., Takizawa, S., Hou, L. an, & Yang, Y. (2022). Insights into graphene oxide/ferrihydrite adsorption as pretreatment during ultrafiltration: Membrane fouling mitigation and disinfection by-product control. *Journal of Hazardous Materials*, 436. <https://doi.org/10.1016/j.jhazmat.2022.129098>
- Xie, Y. F. (2004a). *Disinfection byproducts in drinking water: formation, analysis, and control*. Lewis Publishers.
- Xie, Y. F. (2004b). *Disinfection Byproducts in Drinking Water: Formation, Analysis, and Control: Vol. Chapter I*. Lewis Publishers.
- Yan, M., Korshin, G., Wang, D., & Cai, Z. (2012). Characterization of dissolved organic matter using high-performance liquid chromatography (HPLC)-size exclusion chromatography (SEC) with a multiple wavelength absorbance detector. *Chemosphere*, 87(8), 879–885. <https://doi.org/10.1016/j.chemosphere.2012.01.029>
- Yan, M., Korshin, G. V., & Chang, H. S. (2014). Examination of disinfection by-product (DBP) formation in source waters: A study using log-transformed differential spectra. *Water Research*, 50, 179–188. <https://doi.org/10.1016/j.watres.2013.11.028>
- Yang, X., Gan, W., Zhang, X., Huang, H., & Sharma, V. K. (2015). Effect of pH on the formation of disinfection byproducts in ferrate(VI) pre-oxidation and subsequent chlorination. *Separation and Purification Technology*, 156, 980–986. <https://doi.org/10.1016/j.seppur.2015.09.057>
- Yang, Y., Komaki, Y., Kimura, S. Y., Hu, H. Y., Wagner, E. D., Mariñas, B. J., & Plewa, M. J. (2014). Toxic impact of bromide and iodide on drinking water disinfected with chlorine or chloramines. *Environmental Science and Technology*, 48(20), 12362–12369. <https://doi.org/10.1021/es503621e>
- Yin, T., Wu, Y., Shi, P., Li, A., Xu, B., Chu, W., & Pan, Y. (2020). Anion-exchange resin adsorption followed by electrolysis: A new disinfection approach to control halogenated disinfection byproducts in drinking water. *Water Research*, 168. <https://doi.org/10.1016/j.watres.2019.115144>
- Zhang, C., Maness, J. C., Cuthbertson, A. A., Kimura, S. Y., Liberatore, H. K., Richardson, S. D., Stanford, B. D., Sun, M., & Knappe, D. R. U. (2020). Treating water containing elevated bromide and iodide

levels with granular activated carbon and free chlorine: Impacts on disinfection byproduct formation and calculated toxicity. *Environmental Science: Water Research and Technology*, 6(12), 3460–3475. <https://doi.org/10.1039/d0ew00523a>

Zhang, H., Zhang, Y., Shi, Q., Hu, J., Chu, M., Yu, J., & Yang, M. (2012). Study on transformation of natural organic matter in source water during chlorination and its chlorinated products using ultrahigh resolution mass spectrometry. *Environmental Science and Technology*, 46(8), 4396–4402. <https://doi.org/10.1021/es203587q>

Zhang, H., Zhang, Y., Shi, Q., Ren, S., Yu, J., Ji, F., Luo, W., & Yang, M. (2012). Characterization of low molecular weight dissolved natural organic matter along the treatment trait of a waterworks using Fourier transform ion cyclotron resonance mass spectrometry. *Water Research*, 46(16), 5197–5204. <https://doi.org/10.1016/j.watres.2012.07.004>

Zhang, W., Li, L., Wang, D., Wang, R., Yu, S., & Gao, N. (2022). Characterizing dissolved organic matter in aquatic environments by size exclusion chromatography coupled with multiple detectors. *Analytica Chimica Acta*, 1191. <https://doi.org/10.1016/j.aca.2021.339358>

APPENDIX

APPENDIX A. INTRODUCTION

Table A 1: Methodological parameters of most relevant SEC methods for NOM characterization.

LC -INSTRUMENT	INJ. VOL.	COLUMN (L x ID x particle size)	OVEN	RESIN TYPE	ELUENT (+IONIC TRENGTH)	FLOW	UV-VIS DETECTION	OCD	REF.
HPLC pump Solvent Delivery Module 112 (Beckman Instruments, USA) with sample injection pump P- 500 (Pharmacia Biotech, Sweden)	1.5 mL	TSK HW-40 (900 mm x 16 cm x 30 µm), 50 Å pore size (Merk)		Hydroxylated methacrylate	Phosphate buffer (1.5 g/L Na ₂ HPO ₄ ·2H ₂ O +2.5g/L KH ₂ PO ₄), pH 6.37	1 mL/min	254 nm, UV-vis detector Model 200 Linear Instruments (USA)	OCD Grätzel thin-film reactor	Huber & Frimmel 1991
Waters 510 solvent pump (Waters Corporation, USA)	20 µL	Waters Protein-Pak 125 (300 mm x 19 mm x 10 µm), 125 Å pore size (Waters Corp., USA)		Glycol functionalised silica gel column	Phosphate buffer, pH 6.8 (+0.1 M NaCl)		224 nm, Waters 486 variable wavelength detector (Waters Corp., USA)		Chin 1994
Waters 501 high- pressure pump (Waters Corporation, USA)	100 µL or 200 µL	Waters Protein-Pak 125 (300 mm x 19 mm x 10 µm), 125 Å pore size (Waters Corp., USA)	30 °C	Glycol functionalised silica gel column	0.02M phosphate buffer, pH 6.8 (+0.1 M NaCl)	0.7 mL/min to 1 mL/min (dependin g on column)	260 nm, Waters 484 UV/vis detector, (Waters Corp., USA)		Pelekani 1999
LC-OCD system Grätzel thin-film reactor	2 mL	Toyopearl HW-50S (250 mm x 20 mm x 30 µm), 125 Å pore size (Tosoh Corp., Japan)		Hydroxylated methacrylate	Phosphate buffer (1.25 g/L K ₂ HPO ₄ ·2H ₂ O + 2.5 g/L NaH ₂ PO ₄ ·2H ₂ O), pH 6.8	1 mL/min	254 nm, LCD 500 (Gamma Analysentechnik, Germany)	OCD Grätzel thin-film reactor	Specht 2000
LC-600 (Shimadzu Corporation, Japan)	150 µL 500 µL	Waters Protein-Pak 125 (Waters Corp., USA) Polyacrylamide Bio- Gel P-6 (Bio-Rad, USA) Toyopearl HW-50S (Tosoh Corp., Japan)		Glycol functionalised silica gel column Polyacrylamid e Hydroxylated methacrylate	Phosphate buffer with NaCl Na ₂ SO ₄ (+0 to 0.15 M NaCl)		254nm, SPD-6A (Shimadzu Corp., Japan)	Modified Sievers Turbo Total Organic Carbon (TOC) analyser (Veolia, France)	Her 2002
Dionex DX-500 Chromatography System	100 µL	TSKgel SW Guard Column & TSKgel G3000SW _{XL} (300 mm x 7.8 mm x 5 µm), 250 Å pore size (Tosoh Corp., Japan)	30 °C	Diol functionalised silica gel column	0.01 M phosphate buffer, pH 6.8	1 mL/min	254nm & 220nm, Dionex AD 25 detector (USA)		Swietlik 2004
HP 1090 Series II (Hewlett Packard, USA)	100 µL 500 µL 2000 µL	Toyopearl HW-50S (250 mm x 22 mm x 30 µm), 125 Å pore size semipreparative: Toyopearl HW-50S (250 mm x 10 mm x 30 µm), 125 Å pore size (Tosoh Corp., Japan)		Hydroxylated methacrylate	10mM phosphate buffer (1.36 g/L KH ₂ PO ₄ + 3.58 g/L Na ₂ HPO ₄), pH 6.8	1 mL/min	254 nm, Photometric Detector (FPD)	OCD Sievers (Veolia, France)	Allpike 2007

Waters 1535 Binary HPLC Pump (Waters Corporation, USA)		Waters Protein-Pak 125 (300 mm x 19 mm x 10 µm), 125 Å pore size (Waters Corp., USA)		Glycol functionalised silica gel column	0.02M phosphate buffer, pH 6.8 (+0.1 M NaCl)	0.7 mL/min	260 nm, Waters 2487 dual, (Waters Corp., USA)		Siva 2007
Waters 600s HPLC (Waters Corporation, USA)	0.5 µL	TSKgel G2500PWXL (300 mm x 7.8 mm x 7 µm), 125 Å pore size (Tosoh Corp., Japan)		Hydroxylated methacrylate	Phosphate buffer, pH 6.8 (+0.1 M NaCl)	0.5 mL/min	250 nm, Waters 996 photodiode array detector (PDA), (Waters Corp., USA)		Wu 2007
Waters 600s HPLC (Waters Corporation, USA)	100 µL	YMC-60 (5 µm), 60 Å pore size (Waters Corp., USA)		Diol functionalised silica gel column	0.004M phosphate buffer, pH 6.8 (+0.1 M NaCl)	0.5 mL/min			Wu 2007b
		Toyopearl HW-505 (250 mm x 20 mm x 30 µm), 125 Å pore size (Tosoh Corp., Japan)		Hydroxylated methacrylate	10mM phosphate buffer (1.36 g/L KH ₂ PO ₄ + 3.58 g/L Na ₂ HPO ₄), pH 6.8	1 mL/min	254 nm	OCD Sievers (Veolia, France)	Chong 2008
Waters Alliance 2690 (Waters Corporation, USA)		Protein KW-802.5 (300 mm x 8.0 mm x 5 µm), 400 Å pore size (Shodex, USA)		Diol functionalised silica gel column	0.02M phosphate buffer, pH 6.8 (+0.1 M NaCl)		260 nm, Waters 996 PDA, (Waters Corp., USA)		Fabris 2008
LC-600 (Shimadzu Corporation, Japan)	2 mL	Toyopearl HW-505 (250 mm x 20 mm x 30 µm), 125 Å pore size (Tosoh Corp., Japan)		Hydroxylated methacrylate	4 mM phosphate buffer, pH 6.8 (100 mM Na ₂ SO ₄)		254nm, SPD-6A (Shimadzu Corp., Japan)	Modified Sievers Turbo Total Organic Carbon (TOC) analyser (Veolia, France)	Her 2008
Waters Alliance 2690 (Waters Corporation, USA)		Protein KW-802.5 (300 mm x 8.0 mm x 5 µm), 400 Å pore size (Shodex, USA)	30 °C	Diol functionalised silica gel column			254 nm, Waters 966 PDA, (Waters Corp., USA)		Liu 2008
Waters 1525 Binary Pump (Waters Corporation, USA)	200 µL	Ultrahydrogel (300 mm x 7.8 mm x 6 µm), 250 Å pore size (Waters Corp., USA)		Polymer-based	0.01M phosphate buffer, pH 7	0.4 mL/min	254 nm, Waters 2487 UV detector, (Waters Corporation, USA)		Zhang 2008
Waters 501 pump (Waters Corporation, USA)		Protein KW-802.5 (300 mm x 8.0 mm x 5 µm), 400 Å pore size (Shodex, USA)	30 °C	Diol functionalised silica gel column	0.02M phosphate buffer, pH 6.8 (+0.1 M NaCl)	1 mL/min	260 nm, Water 484 tunable UV detector, (Waters Corp., USA)		Chow 2009
Waters Alliance 2690 (Waters Corporation, USA)		Protein KW-802.5 (300 mm x 8.0 mm x 5 µm), 400 Å pore size (Shodex, USA)		Silica-based	0.02M phosphate buffer, pH 6.8 (+0.1 M NaCl)	1 mL/min	205-285 nm, Waters 996 PDA, (Waters Corp., USA)		Korshin 2009
LC-OCD system Gräntzel thin-film reactor		Novogrom column (250 mm x 20 mm) (Alltech Grom, Germany) packed		Polymer-based	Phosphate buffer (1.5g/L Na ₂ HPO ₄ ·2H ₂ O)		254 nm, LC-OCD Gräntzel thin-film reactor	OCD Gräntzel thin-film reactor	Lankes 2009

LC-OCD system Grüntzel thin-film reactor	1 mL	with Toyopearl HW-50S resin (30 µm) 125 Å pore size, (Tosoh Corp., Japan) Novogrom column (250 mm x 20 mm) (Alltech Grom, Germany) packed with Toyopearl HW-50S resin (30 µm) 125 Å pore size, (Tosoh Corp., Japan) Guard Column (30 mm x 7.8 mm x 5 µm) + BioSep SEC-s2000 (300 mm x 7.8mm x 5 µm) 145 Å pore size (Phenomenex, USA)		Polymer-based	Phosphate buffer (1.5g/L Na ₂ HPO ₄ ·2H ₂ O + 2.5 g/L KH ₂ PO ₄), pH 6.8	1 mL/min	254 nm, LC-OCD Grüntzel thin-film reactor	OCD Grüntzel thin-film reactor	Tercero 2009
	20 µL	Protein KW-802.5 (300 mm x 7.8 mm x 5 µm) + BioSep SEC-s2000 (300 mm x 7.8mm x 5 µm) 145 Å pore size (Phenomenex, USA)	25 °C	Silica-based	2mM phosphate buffer, pH 6.8 (+0.1 M NaCl)	1.5 mL/min	254 nm		Zhao 2009
Waters Alliance 2690 (Waters Corp., USA)	100 µL	Protein KW-802.5 (300 mm x 8.0 mm x 5 µm), 400 Å pore size (Shodex, USA)	30 °C	Diol functionalised silica gel column	0.02M phosphate buffer, pH 6.8 (+0.1 M NaCl)	1 mL/min	260 nm, Waters 966 PDA, (Waters Corp., USA)		Liu 2010
Waters Alliance 2690 (Waters Corp., USA)	1 mL	Protein KW-802.5 (300 mm x 8.0 mm x 5 µm), 400 Å pore size (Shodex, USA)	30 °C	Diol functionalised silica gel column	Phosphate buffer (1.5 g/L Na ₂ HPO ₄ ·2H ₂ O +2.5g/L KH ₂ PO ₄), pH 6.8	1.1 mL/min	MW: 205 nm to 285 nm (1.2 nm resolution), Waters 966 PDA, (Waters Corp., USA)	OCD Grüntzel thin-film reactor	Liu 2010
S-100 HPLC pump (Knauer, Germany)	1 mL	Toyopearl HW-50S (250 mm x 20 mm x 30 µm), 125 Å pore size (Tosoh Corporation, Japan)		Hydroxylated methacrylate	Phosphate buffer (1.5 g/L Na ₂ HPO ₄ ·2H ₂ O +2.5g/L KH ₂ PO ₄), pH 6.8	1.1 mL/min	254 nm, UVD S-200 (Knauer, Germany)	OCD Grüntzel thin-film reactor	Huber 2011
Hewlett Packard 1100-series	80 µL	TSKgel G3000SW (300 mm x 7.5 mm x 10 µm), 250 Å pore size (Tosoh Corp., Japan)		Diol functionalised silica gel column	0.01M sodium acetate (+0.1 M NaCl)	1 mL/min	254 nm, DAD		Matilainen 2016
LC-30AD (Shimadzu Corp., Japan)	50 µL	Yarra SEC-3000 (300 mm x 7.6 mm x 3 µm), 290 Å pore size, (Phenomenex, USA)	25 °C	Silica-based	5 mM phosphate buffer (0.45 g/L Na ₂ HPO ₄ ·2H ₂ O + 0.39 g/L NaH ₂ PO ₄ ·2H ₂ O), pH 6.8 (+0.1 mM)	1 mL/min	MW: 200 nm to 400 nm (1.2 nm resolution, 4.17 Hz), SPD-M20A PDA, (Shimadzu Corp., Japan)	TOC-L (Shimadzu Corp., Japan)	Ignatev 2019
ACQ-QSM pump (Waters Corp., USA)	1 mL	Toyopearl HW-50S (250 mm x 25 mm x 30 µm), 125 Å pore size (Tosoh Corp., Japan)		Hydroxylated methacrylate	Phosphate buffer (1.6 mM Na ₂ HPO ₄ +2.4 mM NaH ₂ PO ₄), pH 6.8 (+ 0.1M Na ₂ SO ₄)	0.8 mL/min	254 nm, TUV Waters (Waters Corp., USA)	OCD Grüntzel thin-film reactor	Zhang 2021
EXTERNAL ANALYSIS BASED ON LC-OCD (Huber et al. 2011 method)									
Andersson 2020									
Carra 2021									

APPENDIX B. MATERIALS & METHODS

Table A 2: Summary of compounds used for SEC cutoff calibration.

COMPOUND	MOLECULAR WEIGHT (Da)	RETENTION TIME (min)	SUPPLIER
Acetone	58.08	36.36	Sigma-Aldrich
Methanol	32.04	28.57	Sigma-Aldrich
NH ₄ Cl	53.49	21.53	Sigma-Aldrich
NaNO ₃	84.99	23.22	Sigma-Aldrich
KBr	119.00	23.20	Sigma-Aldrich
p-aminobenzoic acid	137.14	36.46	Sigma-Aldrich
Na ₂ SO ₄	142.04	22.78	Sigma-Aldrich
l-glutamine	146.14	24.48	Sigma-Aldrich
Phenylalanine	165.19	30.35	Sigma-Aldrich
Potassium hydrogen phthalate	204.00	21.87	Sigma-Aldrich
Tryptophan	204.23	51.02	Sigma-Aldrich
PSS 210	208	52.18	Sigma Aldrich
PSS 1K	1100	20.8	PSS Polymer Standards Service GmbH
Tannic acid	1701.20	27.17	Sigma-Aldrich
Suwannee river Humic Acid standard	~1000	20.54	International Humic Substances Society (IHSS)
Suwannee river Fulvic acid standard	~1000	20.78	International Humic Substances Society (IHSS)
PSS 10K	9680	18.84	Sigma Aldrich
BSA	66463	17.68	Sigma-Aldrich
PSS 77K	80100	16.60	Sigma Aldrich

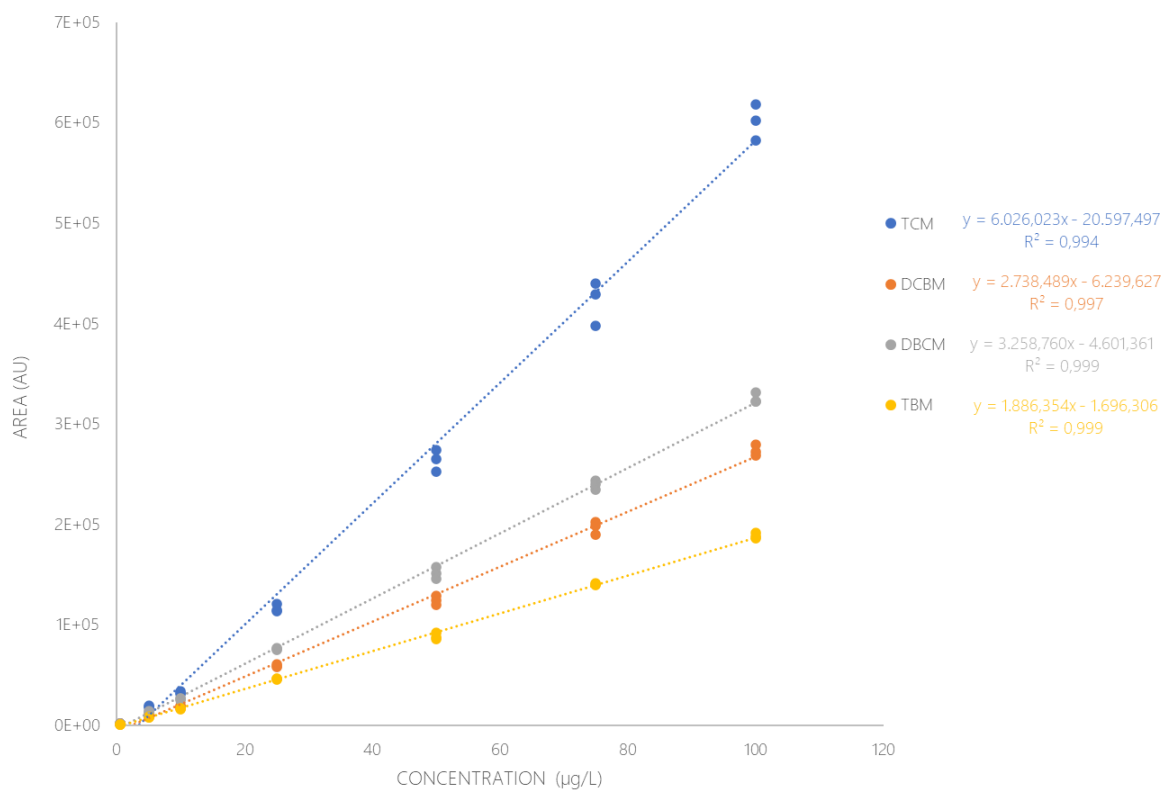


Figure A 1: Calibration curves of THMs standards analyzed by HS-GC-MS.

Table A 3: Retention times and limits of detection (LODs) of THMs analyzed by HS-GC-MS.

THM	Retention Time (min)	LOD (µg/L)	LOQ (µg/L)
TCM	2.44	0.02	0.05
DCBM	3.22	0.03	0.10
DBCМ	4.51	0.05	0.15
TBM	6.26	0.04	0.14

Table A 4: Retention times (min) and ion list (m/z) of DBP standards for GC-HRMs analysis.

Name	Retention Time (min)	LOD ($\mu\text{g/L}$)	LOQ ($\mu\text{g/L}$)	SIM (m/z)
IS: TCM ^P	4.32			84. 86
TCM	4.34	0.025	0.83	83. 85
TCAN	5.2	0.08	0.27	108. 110
BDCM	7.23	0.03	0.10	83. 85
1,1-DCP	8.32	0.20	0.68	43. 83
TCNM	8.34	0.19	0.62	117. 119
DCAN	9.52	0.10	0.32	74. 82
DBCM	9.54	0.02	0.08	127. 129
1,1,1-TCP	10.38	0.06	0.19	43. 125
IS: 1,2-Dibromopropane ^D	10.39			127. 129
TBM	11.64	0.01	0.02	171. 173
BCAN	11.8	0.03	0.10	74. 155
DBAN	13.45	0.03	0.09	118. 120

Table A 5: Parameters for the general characterization of sampling campaigns 1 and 2.

Sampling Campaign	DWTP	Sample	TOC (mg C / L)	A ₂₅₄ (UA)	SUVA (L/mg-C UA)	Conductivity (µS/cm)	Turbidity (NTU)	pH	F ⁻ (mg/L)	ClO ₂ ⁻ (mg/L)	Cl ⁻ (mg/L)	NO ₂ ⁻ (mg/L)	Br ⁻ (mg/L)	ClO ₃ ⁻ (mg/L)	NO ₃ ⁻ (mg/L)	PO ₄ ²⁻ (mg/L)	SO ₄ ²⁻ (mg/L)
1	PTLL	Catchment	3.17	5.98	1.89	1186	23.00	8.07	0.14	0.00	189.26	0.03	0.55	<LOQ	4.10	0.18	123.78
1	PTLL	Flocculated	2.57	4.65	1.81	1204	0.33	7.72	0.13	0.00	197.46	0.08	0.56	<LOQ	3.71	0.06	123.59
1	PTLL	Flocculated + ClO ₂	2.45	4.63	1.89	1200	0.44	7.66	0.11	0.81	195.46	<LOQ	0.55	0.23	3.67	0.08	123.31
1	PTLL	GAC filters	1.74	2.73	1.57	1212	0.48	7.64	0.12	<LOQ	199.37	<LOQ	0.56	0.27	4.68	0.08	123.58
1	PTLL	EDR	1.22	1.37	1.12	345	0.28	6.91	0.07	<LOQ	38.26	<LOQ	0.10	0.04	0.98	0.01	27.30
1	PTLL	Pilot Scale EDR I	1.66	1.90	1.14	538	0.24	7.08	0.07	<LOQ	66.47	<LOQ	0.17	0.08	1.57	0.01	51.58
1	PTLL	Pilot Scale EDR II	1.33	1.79	1.35	342	0.23	7.16	0.09	<LOQ	33.46	<LOQ	0.08	0.03	0.81	0.01	27.47
1	PTLL	Treated water	1.49	2.43	1.64	647	0.28	7.91	0.08	<LOQ	89.69	<LOQ	0.18	0.16	2.17	0.02	49.48
1	PTLL	Catchment + IEX	1.83	1.52	0.83	1295	14.10	8.04	0.09	<LOQ	349.04	0.02	0.09	<LOQ	0.85	0.04	3.65
1	PTLL	Catchment+IEX +JT	1.99	2.91	1.46	1293	2.30	7.68	0.08	<LOQ	658.47	0.02	0.00	<LOQ	0.92	9.35	20.06
1	PTLL	Flocculated + IEX	1.64	1.15	0.70	1298	0.37	7.71	0.09	<LOQ	350.27	0.03	0.09	<LOQ	0.76	0.00	3.93
1	PTT	Catchment	2.92	6.61	2.26	392	0.85	8.08	0.04	<LOQ	4.76	<LOQ	<LOQ	<LOQ	1.91	0.01	10.87
1	PTT	Flocculated	2.51	4.21	1.68	382	0.27	7.72	0.06	0.24	15.76	<LOQ	0.15	<LOQ	5.30	<LOQ	29.03
1	PTT	AC Filtration	2.00	2.74	1.37	376	0.35	7.77	0.05	<LOQ	12.09	<LOQ	0.12	<LOQ	4.03	<LOQ	21.89
1	PTT	Treated water	1.86	2.82	1.51	396	0.21	7.84	0.05	0.01	12.83	<LOQ	<LOQ	0.16	3.92	<LOQ	18.88
1	PTT	Catchment + IEX	1.32	1.04	0.79	460	0.70	8.02	0.04	<LOQ	122.42	<LOQ	<LOQ	<LOQ	0.60	<LOQ	1.64
1	PTT	Catchment+IEX +JT	2.53	1.39	0.55	458	0.64	7.69	0.02	<LOQ	478.01	<LOQ	0.02	<LOQ	0.67	8.21	20.16
1	PTT	Flocculated + IEX	1.02	0.79	0.77	461	0.37	7.75	0.03	0.09	105.02	<LOQ	<LOQ	0.01	0.47	<LOQ	1.67
1	PTC	Catchment	1.38	2.51	1.82	568	0.60	8.09	0.09	<LOQ	33.93	<LOQ	0.01	<LOQ	0.98	0.06	79.99
1	PTC	Flocculated	1.30	2.42	1.86	568	0.33	8.11	0.09	<LOQ	34.42	<LOQ	0.01	<LOQ	0.99	0.05	80.52
1	PTC	Treated water	1.27	1.49	1.17	572	0.15	8.11	0.06	<LOQ	30.83	<LOQ	<LOQ	0.02	0.82	0.00	62.26
2	PTLL	Storage tanks	1.55	2.42	1.57	1120	0.39	7.63	0.13	<LOQ	179.4	<LOQ	0.39	0.11	7.41	0.05	148.03
2	PTC	Treated water	0.85	1.46	1.72	617	0.13	8.09	0.11	<LOQ	48.32	<LOQ	<LOQ	0.03	0.88	<LOQ	100.36

Table A 6: Parameters for the general characterization of sampling campaign 3.

Sampling Campaign	DWTP	Sample	DOC (mg/L)	pH	Turbidity (NTU)	Conductivity (μ S/cm)	F ⁻ (mg/L)	Cl ⁻ (mg/L)	NO ₂ ⁻ (mg/L)	Br ⁻ (mg/L)	NO ₃ ⁻ (mg/L)	SO ₄ ²⁻ (mg/L)	NH ₄ ⁺ (mg/L)	Na ⁺ (mg/L)	K ⁺ (mg/L)	Mg ²⁺ (mg/L)	Ca ²⁺ (mg/L)
3	PTM	Catchment	2.72	6.39	0.94	417	0.07	29.12	0.86	<LOQ	0.98	14.71	<LOQ	22.75	3.80	9.55	52.14
3	PTM	Flocculated	2.48	6.26	0.606	443	0.03	33.52	1.12	<LOQ	1.02	15.14	<LOQ	23.47	3.89	9.45	52.28
3	PTM	Sand Filters	3.17	6.32	0.424	445	0.07	33.46	1.19	<LOQ	1.11	15.23	<LOQ	23.49	3.80	9.63	52.35
3	PTM	AC Filter (newest)	2.09	6.38	0.431	433	0.06	34.49	1.14	<LOQ	1.11	15.97	<LOQ	23.71	3.78	9.61	52.25
3	PTM	AC Filter (mid)	2.27	6.53	0.425	441	0.07	33.94	1.19	<LOQ	1.10	15.64	<LOQ	23.50	3.79	9.62	52.26
3	PTM	AC Filter (oldest)	2.23	6.62	0.433	418	0.04	33.64	1.10	<LOQ	1.11	15.13	<LOQ	23.94	3.86	9.62	52.33
3	PTM	Treated (pre chlorination)	2.25	6.5	0.321	445	0.06	32.46	1.10	<LOQ	1.10	14.64	<LOQ	23.62	3.82	9.62	52.41
3	PTT	Catchment	2.24	7.9	1.17	470	0.07	29.10	1.22	<LOQ	1.07	14.67	<LOQ	24.18	3.96	9.81	53.55
3	PTT	Flocculated	1.94	7.86	0.47	454	0.07	35.94	1.54	<LOQ	0.93	15.15	<LOQ	26.29	3.93	9.77	54.40
3	PTT	AC Filter (oldest)	1.71	6.47	1.31	457	0.07	38.61	1.55	<LOQ	0.92	14.89	<LOQ	26.06	7.66	9.76	54.62
3	PTT	AC Filter (newest)	1.13	6.92	0.682	439	0.07	42.10	1.67	<LOQ	0.96	15.43	<LOQ	26.03	10.15	9.74	54.91
3	PTT	Treated (pre chlorination)	1.58	7.867	0.223	449	0.07	36.14	1.23	<LOQ	0.95	15.17	<LOQ	26.43	3.97	9.80	54.49
3	PTL	Catchment	3.23	8.22	19.133	1485	0.09	278.48	7.64	0.56	1.62	46.24	0.20	145.38	34.53	29.97	103.33
3	PTL	Flocculated	2.58	7.383	1.143	1493	0.10	287.51	8.64	0.72	1.70	45.68	0.13	149.97	33.60	30.73	106.46
3	PTL	GAC Filters	2.08	6.84	0.203	1539	0.09	290.68	9.06	0.69	1.82	46.10	0.02	152.21	34.25	30.78	105.77
3	PTL	EDR	1.60	7.43	0.44	651	0.07	101.06	4.05	0.16	0.70	13.54	<LOQ	82.11	12.51	9.19	33.55
3	PTL	Treated (50%, pre chlorination)	1.61	6.69	0.278	1103	0.08	200.27	7.35	0.39	1.21	29.73	0.01	117.50	28.30	19.93	69.73

Table A 7: THM formation potential (µg/L) at 24h, 48h, and 72 h for samples of campaigns 1 and 2.

Sampling Campaign	DWTP	Sample	24h	48h	72h	24h	48h	72h	24h	48h	72h	24h	48h	72h	24h	48h	72h
			tTHM	tTHM	tTHM	TCM	TCM	TCM	BDCM	BDCM	BDCM	DBCM	DBCM	DBCM	TBM	TBM	TBM
1	PTL	Catchment	230.94	331.53	351.94	25.47	42.47	38.81	60.48	101.72	108.55	88.06	122.49	134.54	56.93	64.85	70.05
1	PTL	Flocculated	153.18	179.16	199.58	10.8	13.54	14.31	32.63	40.64	35.35	58.12	60.13	81.99	51.63	64.84	67.92
1	PTL	Flocculated + ClO ₂	123.4	150.08	174.51	7.4	9.41	10.8	24.41	30.14	35.35	47.23	57.32	67.22	44.37	53.22	61.13
1	PTL	GAC filters	87	122.93	134.58	2.52	4.72	4.14	12.19	18.85	19.62	31.95	44.11	48.61	40.33	55.26	62.2
1	PTL	EDR	32.53	45.25	52.49	4.36	7.35	8.76	10.35	14.98	17.74	12.9	16.88	19.32	4.92	6.05	6.67
1	PTL	Pilot Scale EDR I	51.29	71.81	83.64	4.69	6.56	10.77	13.72	19.21	24.24	21.52	30.13	32.44	11.37	15.91	16.2
1	PTL	Pilot Scale EDR II	38.75	56.33	69.92	6.92	11.63	18.59	13.03	19.33	23.84	14.25	19.56	21.68	4.55	5.81	5.82
1	PTL	Treated water	64.32	83.97	96.68	4.17	7.16	9.13	12.97	19.2	22.83	24.52	31.55	35.87	22.66	26.06	28.85
1	PTL	Catchment + IEX	60.86	79.83	91.81	17.04	23.56	28.86	20.93	27.36	31.08	17.79	22.67	25.01	5.1	6.24	6.87
1	PTL	Catchment+ IEX +JT	38.96	52.72	67.56	14.82	21.36	28.87	15.77	20.71	25.65	8.37	10.65	13.04	<LOQ	<LOQ	<LOQ
1	PTL	Flocculated + IEX	49.12	69.78	82.3	13.37	18.05	21.3	17.15	21.17	24.98	14.63	25.77	30.4	3.97	4.8	5.66
1	PTT	Catchment	110.48	133.15	138.37	87.61	102.64	112.23	20.11	26.79	23.09	2.76	3.72	3.06	<LOQ	<LOQ	<LOQ
1	PTT	Flocculated	80.68	98.06	98.76	59.43	74.27	75.92	17.44	19.61	18.89	3.82	4.18	3.95	<LOQ	<LOQ	<LOQ
1	PTT	AC Filtration	66.2	82.77	81.75	46.47	59.28	59.95	15.68	18.83	17.56	4.05	4.66	4.24	<LOQ	<LOQ	<LOQ
1	PTT	Treated water	65.21	84.34	84.3	44.7	60.08	61.42	16.11	19	18.13	4.4	5.26	4.75	<LOQ	<LOQ	<LOQ
1	PTT	Catchment + IEX	30.94	45.46	51.02	25	36.87	41.53	5.13	7.42	8.22	0.82	1.17	1.27	<LOQ	<LOQ	<LOQ
1	PTT	Catchment+ IEX +JT	21.05	32.31	37.54	13.52	21.91	25.89	5.94	8.52	9.66	1.59	1.88	2	<LOQ	<LOQ	<LOQ
1	PTT	Flocculated + IEX	45.6	57.83	60.54	31.61	40.77	42.91	11.29	13.77	14.23	2.7	3.28	3.4	<LOQ	<LOQ	<LOQ
1	PTC	Catchment	49.11	60.8	65.52	27.45	36.12	38.45	15.29	17.62	19.22	6.37	7.06	7.85	<LOQ	<LOQ	<LOQ
1	PTC	Flocculated	41.61	50.05	51.93	22.43	26.63	25.96	13.15	15.47	16.73	6.04	7.95	9.25	<LOQ	<LOQ	<LOQ
1	PTC	Treated water	41.07	44.6	47.92	20.51	24.42	26.59	13.26	13.87	14.67	7.3	6.31	6.66	<LOQ	<LOQ	<LOQ
2	PTLL	Storage tanks	98	128.9	143.7	<LOQ	<LOQ	<LOQ	9.3	10.8	11.8	35.8	43.6	47	52.8	72.2	85
2	PTC	Treated water	39.2	50.2	52.7	16	23.7	23.8	13.9	15.9	17.4	9.4	10.6	11.5	<LOQ	<LOQ	<LOQ

Table A 8: Concentration of regulated DBPs-FP (µg/L) at 48 h for samples of campaign 3.

Sampling Campaign	DWTP	Sample	TCM	DCBM	DBCM	TBM	Σ4THMs	MCAA**	MBAA**	DCAA**	BCAA	MIAA	DBAA**	DIAA	TCAA**	BDCAA	DBCAA	TBAA	Σ5HAAs**	Σ11HAAs
3	PTM	Catchment	57.9	13.3	3.7		74.9	2.1	0.4	20	1.7	<LOQ	0.6	<LOQ	30	8.5	1	0.2	53	65
3	PTM	Flocculated	38.2	13.2	5.2		56.6	1.4	0.5	12	3.9	<LOQ	0.8	<LOQ	13	5.5	1.1	0.2	28	38
3	PTM	Sand Filters	33.0	12.6	5.2		50.8	1.7	0.5	15	3.1	<LOQ	0.8	<LOQ	21	6.3	1.3	0.2	39	50
3	PTM	AC Filter (newest)	32.0	10.8	4.5		47.2	1.2	0.4	6.5	2.6	<LOQ	0.7	<LOQ	7.8	4	1	0.2	17	24
3	PTM	AC Filter (mid)	34.6	11.7	4.7		50.9	1.4	0.4	9	1.8	<LOQ	0.9	<LOQ	12	5	1	0.2	24	32
3	PTM	AC Filter (oldest)	37.6	11.5	4.4		53.5	1.0	0.5	6.5	1.3	<LOQ	0.9	<LOQ	9.2	4.2	1	0.2	20	25
3	PTM	Treated (pre chlorination)	41.0	11.9	4.4		57.4	1.3	0.5	8.5	3.3	<LOQ	1	<LOQ	9.7	4.7	0.9	0.1	21	30
3	PTT	Catchment	61.0	15.3	3.8		80.0	0.7	0.4	10	3.8	<LOQ	<LOQ	<LOQ	41	11	1.2	0.2	52	68
3	PTT	Flocculated	52.3	16.3	5.3		74.0	1.4	0.9	13	6.2	<LOQ	1.6	<LOQ	28	10	1.4	0.2	45	63
3	PTT	AC Filter (oldest)	33.5	12.3	4.6		50.5	<LOQ	0.4	3.1	<LOQ	<LOQ	0.7	<LOQ	15	5.8	1.4	0.2	19	27
3	PTT	AC Filter (newest)	15.4	7.6	3.6		26.6	<LOQ	0.3	2.8	<LOQ	<LOQ	0.7	<LOQ	12	6.2	1.2	0.2	16	23
3	PTT	Treated (pre chlorination)	31.3	12.1	4.3		47.7	<LOQ	0.3	1.6	<LOQ	<LOQ	1.5	<LOQ	5.3	4.2	1.3	0.2	8.7	14
3	PTL	Catchment	8.2	15.3	31.4	43.7	98.6	1.1	2.3	1.7	7.7	<LOQ	27	<LOQ	3.9	12	19	18	36	93
3	PTL	Flocculated	5.0	4.4	5.9	40.2	55.6	<LOQ	1	<LOQ	2	<LOQ	5	<LOQ	1	2.5	5	3.1	7	20
3	PTL	GAC Filters	5.3	6.4	18.1	39.1	68.9	<LOQ	3	<LOQ	3.3	<LOQ	23	<LOQ	1.1	1.3	4.6	14	27	50
3	PTL	EDR	6.4	8.6	13.5	9.4	38.0	<LOQ	2.3	<LOQ	2.4	<LOQ	17	<LOQ	1.1	1.8	8.7	16	20	49
3	PTL	Treated (50%, pre chlorination)	6.2	8.8	18.6	20.2	53.9	<LOQ	2	<LOQ	<LOQ	<LOQ	13	<LOQ	1.3	3.1	8.9	8	16	36

Table A 9: Concentration of unregulated DBPs-FP (µg/L) at 48 h for samples of campaign 3.

Sampling Campaign	DWTP	Sample	DCAN	TCAN	BCAN	DBAN	1,1-DCP	1,1,1-TCP	TCNM	DCAN	TCAN
3	PTM	Catchment	3.1	<LOQ	0.9	<LOQ	<LOQ	<LOQ	<LOQ	3.1	<LOQ
3	PTM	Flocculated	2.4	<LOQ	1.2	<LOQ	<LOQ	<LOQ	<LOQ	2.4	<LOQ
3	PTM	Sand Filters	2.6	<LOQ	1.2	<LOQ	<LOQ	<LOQ	<LOQ	2.6	<LOQ
3	PTM	AC Filter (newest)	1.0	<LOQ	0.6	<LOQ	<LOQ	<LOQ	<LOQ	1.0	<LOQ
3	PTM	AC Filter (mid)	1.3	<LOQ	0.7	<LOQ	<LOQ	<LOQ	<LOQ	1.3	<LOQ
3	PTM	AC Filter (oldest)	1.6	<LOQ	0.8	<LOQ	<LOQ	<LOQ	<LOQ	1.6	<LOQ
3	PTM	Treated (pre chlorination)	1.5	<LOQ	0.7	<LOQ	<LOQ	<LOQ	<LOQ	1.5	<LOQ
3	PTT	Catchment	3.51	<LOQ	0.83	0.12	<LOQ	1.72	<LOQ	3.51	<LOQ
3	PTT	Flocculated	2.96	<LOQ	0.93	0.24	<LOQ	1.83	<LOQ	2.96	<LOQ
3	PTT	AC Filter (oldest)	1.89	<LOQ	0.70	0.20	<LOQ	1.18	<LOQ	1.89	<LOQ
3	PTT	AC Filter (newest)	0.63	<LOQ	0.37	0.18	<LOQ	0.32	<LOQ	0.63	<LOQ
3	PTT	Treated (pre chlorination)	1.51	<LOQ	0.55	0.17	<LOQ	0.87	<LOQ	1.51	<LOQ
3	PTL	Catchment	0.58	<LOQ	2.37	7.98	<LOQ	<LOQ	<LOQ	0.58	<LOQ
3	PTL	Flocculated	<LOQ	<LOQ	0.67	6.74	<LOQ	<LOQ	<LOQ	<LOQ	<LOQ
3	PTL	GAC Filters	<LOQ	<LOQ	1.23	5.47	<LOQ	<LOQ	<LOQ	<LOQ	<LOQ
3	PTL	EDR	0.33	<LOQ	0.84	1.99	<LOQ	<LOQ	<LOQ	0.33	<LOQ
3	PTL	Treated (50%, pre chlorination)	0.41	<LOQ	1.22	3.43	<LOQ	<LOQ	<LOQ	0.41	<LOQ

APPENDIX C. CHAPTER IV: RESULTS I

Table A 10: Quantification of DOC fractions for LC-OCD and HPSEC-DAD-DOC (% of CDOC).

Sampling Campaign	DWTP	Sample	LC-OCD (%)					HPSEC-DAD-DOC (%)								
			Biopolymers (BioP)	Humics	Building Blocks (BB)	LMW neutrals	LMW acids	BioP	Total Humics	Humics I	Humics II	Total BB	BB I	BB II	LMW acids	LMW neutrals
1	PTL	Catchment	8.7	51.9	17.6	0.0	14.4	3.9	38.5	9.8	28.7	36.9	35.6	1.3	3.2	11.6
1	PTL	Flocculated	5.5	47.3	22.7	0.0	16.7	2.8	32.5	5.3	27.2	41.5	38.1	3.4	4.0	12.8
1	PTL	Flocculated + ClO ₂	6.0	46.6	25.5	0.0	19.0	3.2	40.0	2.7	37.3	39.4	39.4	0.0	3.5	12.8
1	PTL	GAC filters	4.3	56.9	25.3	0.0	15.2	1.6	31.9	5.4	26.5	51.6	45.5	6.1	4.2	12.9
1	PTL	EDR	7.2	50.7	22.4	0.0	15.2	2.8	35.4	7.1	28.3	54.2	54.1	0.1	3.9	17.2
1	PTL	Pilot Scale EDR I	5.1	56.7	24.9	0.0	15.6	2.9	49.6	8.4	41.2	41.6	41.5	0.1	2.7	15.5
1	PTL	Pilot Scale EDR II	5.2	58.6	21.4	0.0	13.3	3.5	46.1	2.7	43.5	39.2	38.4	0.8	3.8	12.8
1	PTL	Treated water	7.6	52.2	25.4	0.0	20.6	3.0	39.8	2.6	37.2	47.2	45.9	1.4	3.8	11.6
1	PTL	Catchment + IEX	17.4	25.2	18.7	0.0	24.3	7.0	22.1	0.0	22.1	46.3	46.3	0.0	4.9	19.7
1	PTL	Catchment+IEX +JT	5.4	n.n.	24.8	6.5	47.3	3.4	32.8	0.0	32.8	26.6	26.6	0.0	11.6	25.6
1	PTL	Flocculated + IEX	18.4	n.n.	23.6	9.7	27.3	5.5	21.7	0.0	21.7	43.7	43.7	0.0	6.0	23.1
1	PTT	Catchment	2.3	67.0	18.1	0.0	12.6	2.0	51.1	11.5	39.5	35.2	33.5	1.7	3.4	12.7
1	PTT	Flocculated	2.9	61.0	21.7	0.0	14.4	1.5	47.4	1.6	45.8	35.7	31.3	4.4	3.3	11.7
1	PTT	AC Filtration	3.8	63.9	20.3	0.0	12.0	1.7	43.4	3.9	39.5	44.0	43.5	0.5	2.8	12.5
1	PTT	Treated water	3.2	58.5	23.2	0.0	15.0	2.2	43.9	2.4	41.5	36.4	36.0	0.5	3.6	13.9
1	PTT	Catchment + IEX	6.5	40.5	20.2	0.0	32.8	3.1	31.0	0.0	31.0	32.0	23.0	9.0	9.5	24.6
1	PTT	Catchment+IEX +JT	0.8	47.0	18.7	-0.2	33.8	2.2	33.9	0.0	33.9	16.9	6.8	10.1	10.4	29.0
1	PTT	Flocculated + IEX	6.2	32.1	21.6	0.3	39.9	3.9	29.9	0.0	29.9	30.6	22.6	7.9	10.8	27.1
1	PTC	Catchment	n.d	n.d	n.d	n.d	n.d	2.6	34.2	0.6	33.7	52.1	51.6	0.5	4.8	18.5
1	PTC	Flocculated	n.d	n.d	n.d	n.d	n.d	2.6	34.2	0.2	34.0	55.9	55.3	0.6	4.9	17.7
1	PTC	Treated water	n.d	n.d	n.d	n.d	n.d	1.9	33.8	0.8	33.0	52.0	51.3	0.6	3.6	13.8
2	PTLL	Storage tanks	n.d	n.d	n.d	n.d	n.d	3.1	39.1	6.1	33.0	34.7	34.7	0.1	3.5	19.3
2	PTC	Treated water	n.d	n.d	n.d	n.d	n.d	3.2	35.9	2.4	33.5	31.6	31.3	0.3	3.0	24.4

Table A 11: Quantification of spectroscopical fractions (AU).

Sampling Campaign	DWTP	Sample	F1	F2	F3	F4	F5	F1	F2	F3	F4	F5	F1	F2	F3	F4	F5	F6
			A ₂₅₄	S ₃₅₀₋₃₈₀	S ₂₀₆₋₂₄₀	S ₂₀₆₋₂₄₀	S ₂₀₆₋₂₄₀	S ₂₀₆₋₂₄₀										
1	PTL	Catchment	9.06	4.01	0.72	0.63	2.53	0.18	0.07	0.01	0.01	0.06	0.31	0.13	-0.03	3.28	3.66	0.07
1	PTL	Flocculated	4.87	3.30	0.58	0.54	1.58	0.10	0.06	0.01	0.01	0.04	0.21	0.16	-0.02	2.99	3.61	0.10
1	PTL	Flocculated + ClO ₂	4.84	2.05	0.48	1.94	0.45	0.10	0.04	0.01	0.04	0.01	0.01	0.62	-0.07	3.48	3.39	0.09
1	PTL	GAC filters	3.92	1.76	0.35	0.37	0.80	0.08	0.03	0.01	0.01	0.01	0.18	0.12	-0.07	3.57	4.46	0.11
1	PTL	EDR	1.67	1.78	0.21	<LOQ	5.54	0.03	0.03	<LOQ	<LOQ	<LOQ	0.14	0.38	-0.93	1.29	0.86	0.10
1	PTL	Pilot Scale EDR I	2.37	3.09	0.27	<LOQ	0.17	0.05	0.06	0.01	<LOQ	<LOQ	0.14	0.14	-0.10	1.47	1.55	0.10
1	PTL	Pilot Scale EDR II	1.69	2.87	0.32	<LOQ	3.58	0.01	0.05	0.03	<LOQ	0.01	0.09	0.24	-0.42	0.92	0.60	0.11
1	PTL	Treated water	1.75	0.97	0.25	0.63	<LOQ	0.03	0.02	<LOQ	0.01	<LOQ	0.16	0.30	-0.48	6.59	5.63	0.11
1	PTL	Catchment + IEX	0.20	0.64	0.20	0.22	1.15	<LOQ	<LOQ	0.01	0.01	0.05	0.12	-0.04	-0.07	0.63	0.96	0.09
1	PTL	Catchment+IEX +JT	0.00	0.15	0.29	0.07	1.34	<LOQ	<LOQ	<LOQ	<LOQ	0.01	0.09	-0.06	0.12	0.42	1.17	0.09
1	PTL	Flocculated + IEX	0.10	0.64	0.21	0.22	0.98	<LOQ	0.01	<LOQ	<LOQ	0.03	0.12	-0.04	-0.06	0.60	0.94	0.09
1	PTT	Catchment	10.03	8.60	1.43	0.46	1.80	0.19	0.16	0.03	0.01	0.04	0.42	0.11	-0.17	6.59	5.41	0.12
1	PTT	Flocculated	8.01	4.50	1.25	<LOQ	0.16	0.16	0.04	0.04	<LOQ	<LOQ	0.34	0.18	-0.14	6.67	5.32	0.10
1	PTT	AC Filtration	4.31	4.30	0.66	0.21	0.39	0.08	0.07	0.01	<LOQ	0.02	0.09	1.29	-2.14	7.32	5.03	0.10
1	PTT	Treated water	3.92	3.55	0.88	<LOQ	0.83	0.09	0.02	0.03	<LOQ	0.02	0.15	1.26	-2.27	8.13	4.46	0.09
1	PTT	Catchment + IEX	0.41	0.06	0.97	0.45	0.17	<LOQ	0.01	0.01	<LOQ	0.01	0.10	-0.01	-0.33	0.71	0.46	0.10
1	PTT	Catchment+IEX +JT	0.00	0.58	0.78	0.01	0.68	0.01	0.02	0.01	<LOQ	0.02	0.06	-0.06	-0.06	0.58	0.69	0.09
1	PTT	Flocculated + IEX	0.08	0.39	0.12	0.50	0.51	0.01	0.01	0.01	<LOQ	0.01	0.10	-0.01	-0.29	0.62	0.52	0.08
1	PTC	Catchment	2.53	3.52	0.60	<LOQ	0.87	0.05	0.07	0.01	<LOQ	0.01	0.05	0.33	-0.49	1.20	0.91	0.10
1	PTC	Flocculated	1.85	3.02	0.62	<LOQ	0.42	0.04	0.06	0.01	<LOQ	<LOQ	0.17	0.23	-1.10	1.70	0.95	0.10
1	PTC	Treated water	1.40	2.61	0.50	<LOQ	0.27	0.02	0.04	0.01	<LOQ	<LOQ	0.17	0.25	-1.11	1.65	0.92	0.09
1	PTLL	Storage tanks	3.15	0.66	1.30	0.17	0.24	n.d.	n.d.	n.d.	n.d.	n.d.	0.16	0.11	<LOQ	1.08	0.72	0.08
2	PTC	Treated water	3.91	1.59	0.50	0.97	0.28	n.d.	n.d.	n.d.	n.d.	n.d.	0.06	0.08	<LOQ	6.22	6.39	0.11

Table A 12: Summary of previous reported THMFP and DOC/spectroscopical correlations.

Correlations	R ²	Source Water	Reference
TTHMFP (sum CHCl ₃ , CHBrCl ₂ , CHBr ₂ Cl, CHBr ₃ , others) vs bulk DOC	0.75	Surface and ground water from several DWTPs. DOC concentrations ranging 1 to 4.1 mg/l	Pifer & Fairey, 2014
TTHMFP (sum CHCl ₃ , CHBrCl ₂ , CHBr ₂ Cl, CHBr ₃) vs bulk DOC	0.79	Surface water. DOC concentration of 7.34 mg/l	Golea et al., 2017
THM (CHCl ₃ and tTHM _{Br}) vs bulk DOC	0.74	River and reservoir. DOC concentrations of 6 mg/l and 5.6 mg/l respectively.	Carra et al., 2021
THM (CHCl ₃ and tTHM _{Br}) vs LC-OCD	0.93	River and reservoir. DOC concentrations of 6 mg/l and 5.6 mg/l respectively.	Carra et al., 2021
Carbonaceous-DBPs vs SUVA	0.68	Reservoir DOC 3 mg/l, low SUVA (<2 mg/L·m)	Hua et al., 2020
TTHMFP (sum DCM, DCBM, DBCM, TBM, others) vs bulk A ₂₅₄	0.89	Surface and ground water from several DWTPs. UV ₂₅₄ 0.05 – 0.15 cm ⁻¹	Pifer & Fairey, 2014
TTHMFP (sum DCM, DCBM, DBCM, TBM) vs bulk A ₂₅₄	0.82	Surface water. UV ₂₅₄ 0.37 cm ⁻¹	Golea et al., 2017
TTHM vs bulk A ₂₅₄	0.79	Riverine samples UV ₂₅₄ 0.05 – 0.16 cm ⁻¹	Li et al., 2016

APPENDIX D. CHAPTER V: RESULTS II

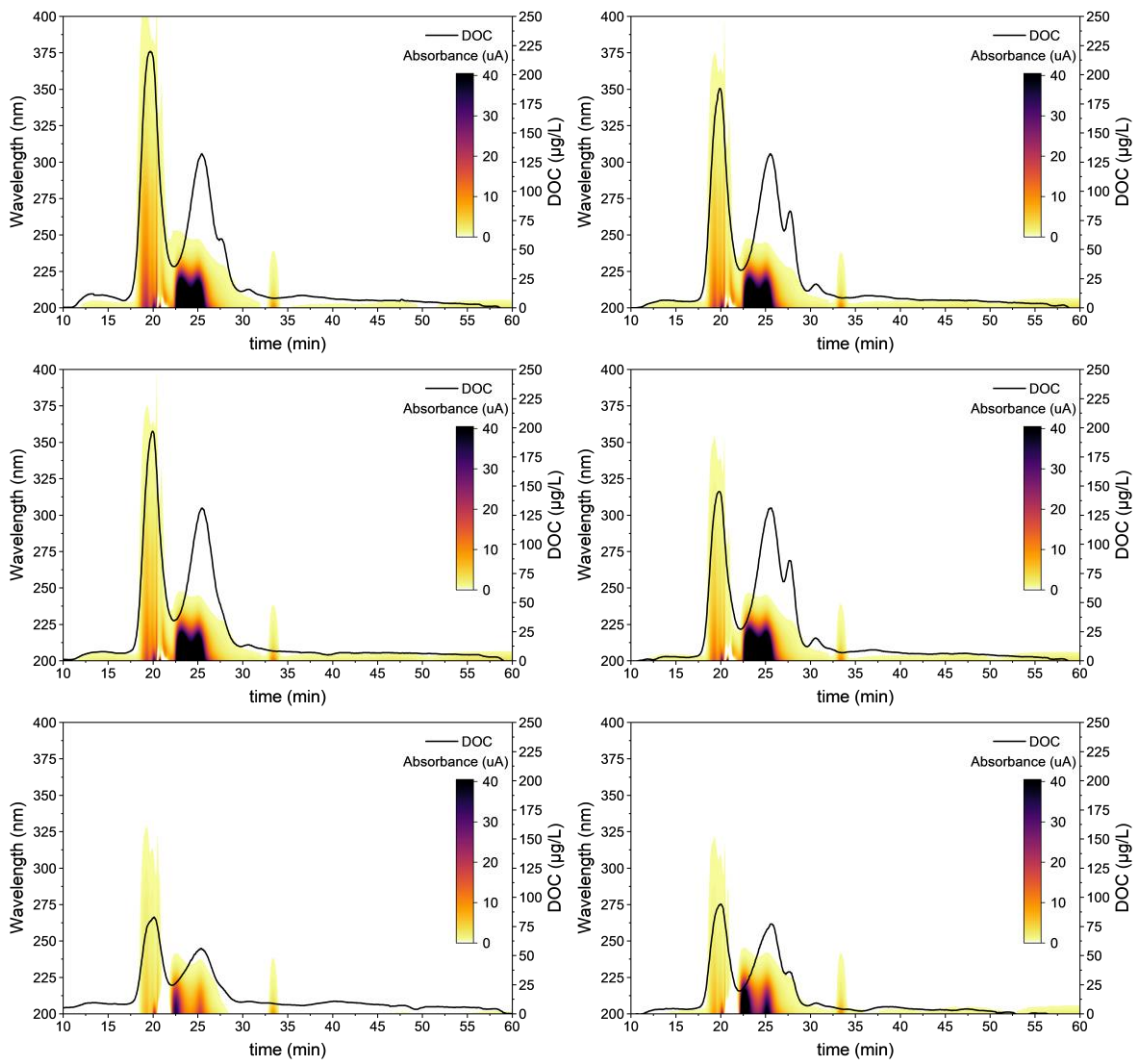


Figure A 2: Overlapped DOC and UV-multiwavelength profiles from HPSEC chromatograms of full treatment train in Abrera DWTP.

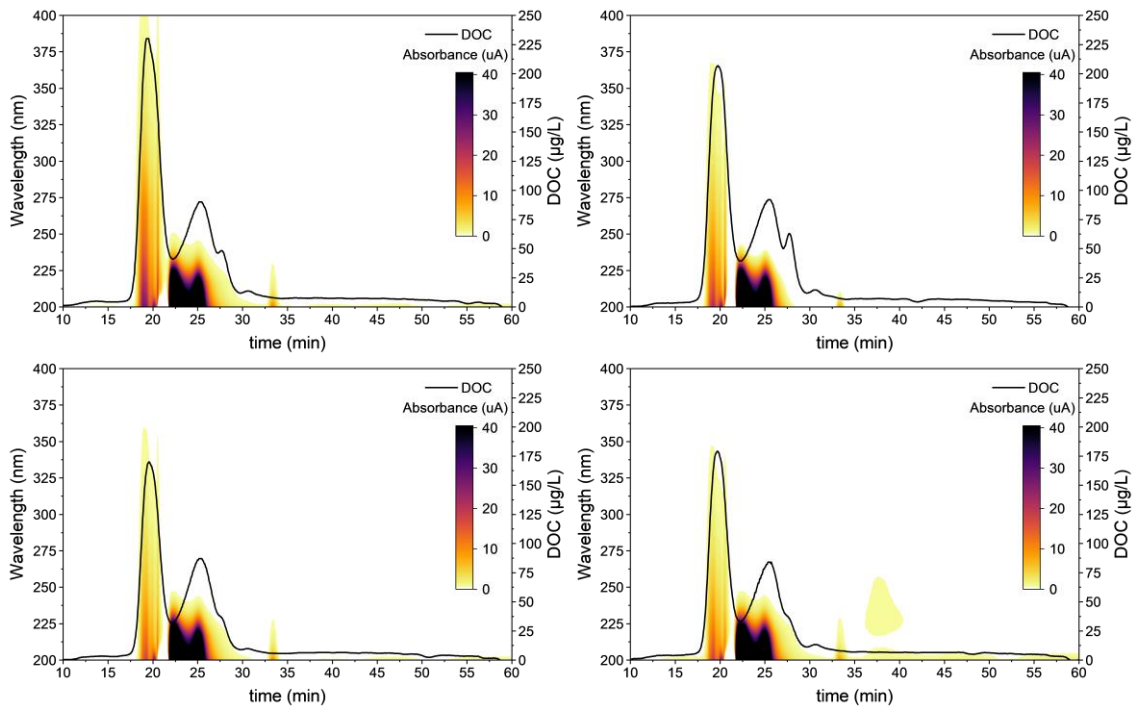


Figure A 3: Overlapped DOC and UV-multiwavelength profiles from HPSEC chromatograms of full treatment train in Cardedeu DWTP.

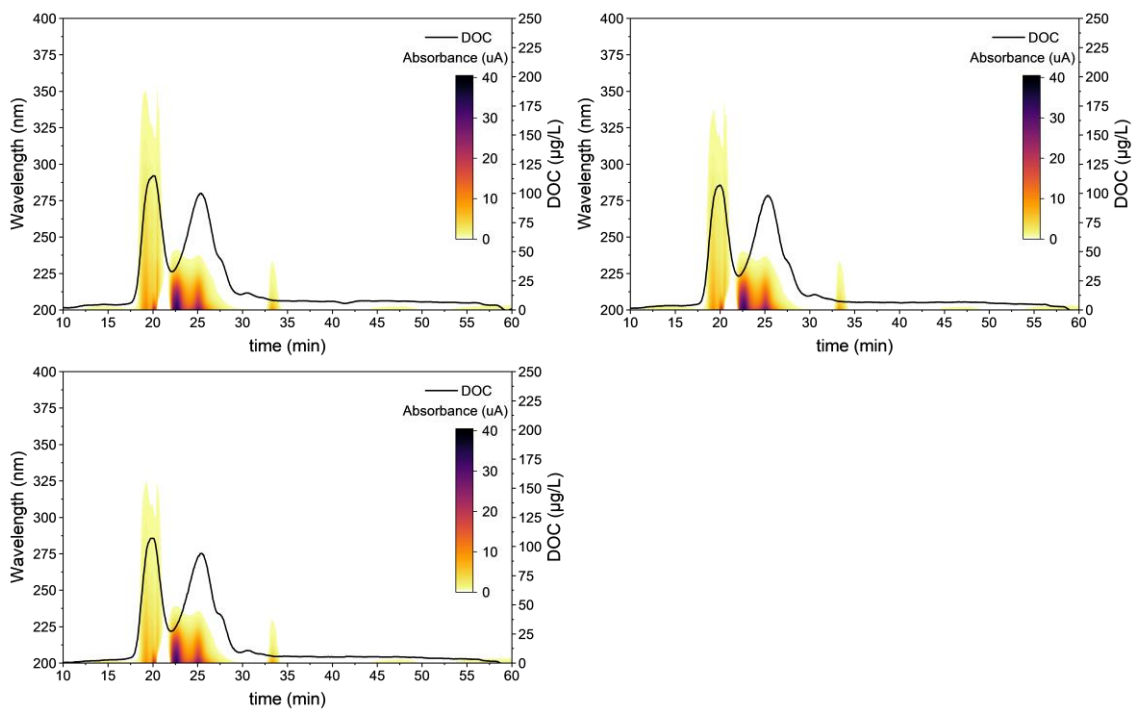


Figure A 4: Overlapped DOC and UV-multiwavelength profiles from HPSEC chromatograms of full treatment train in Cardener DWTP.

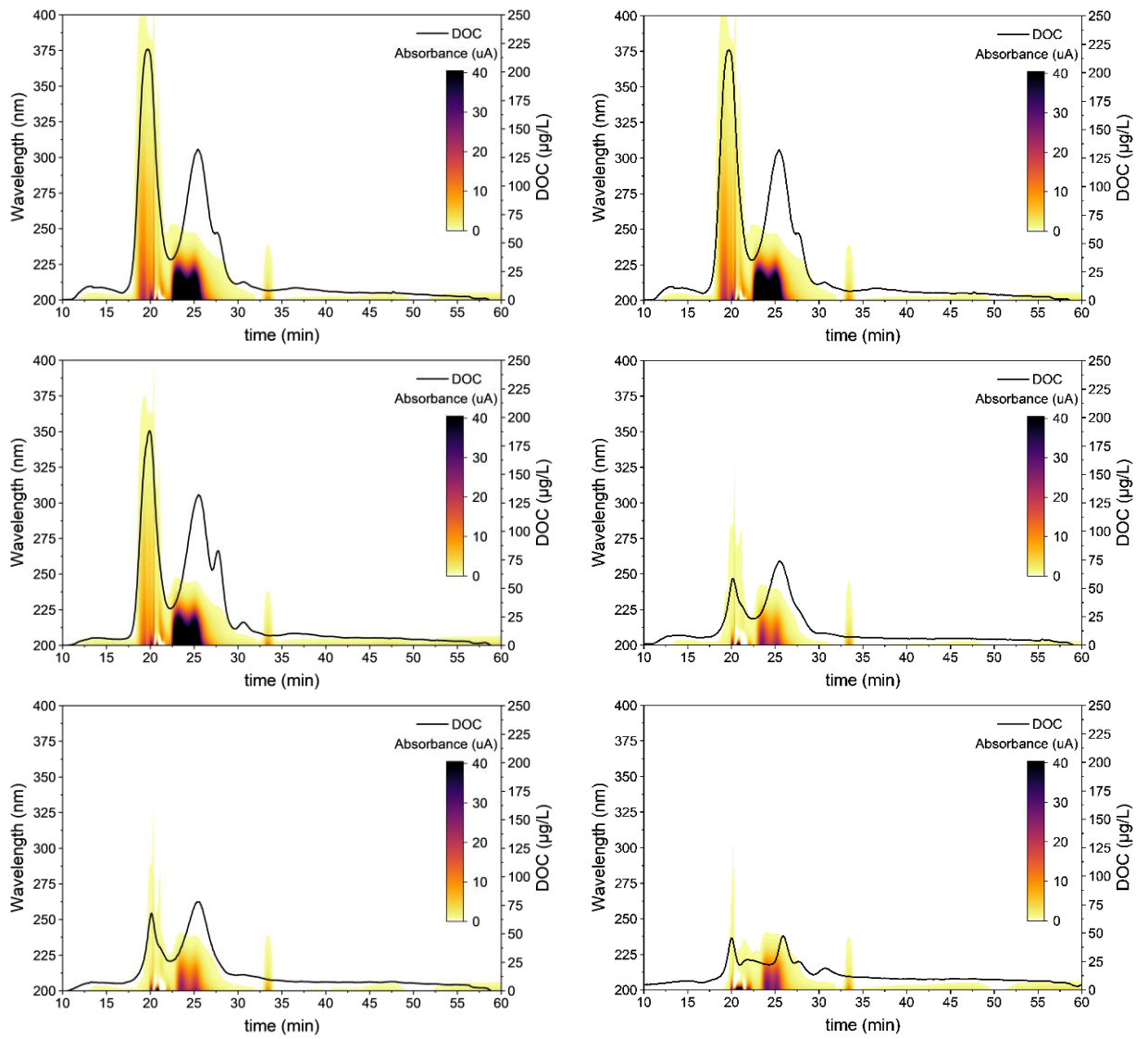


Figure A 5: Overlapped DOC and UV-multiwavelength profiles from HPSEC chromatograms of BS-1 and BS2 in PTL DWPT.

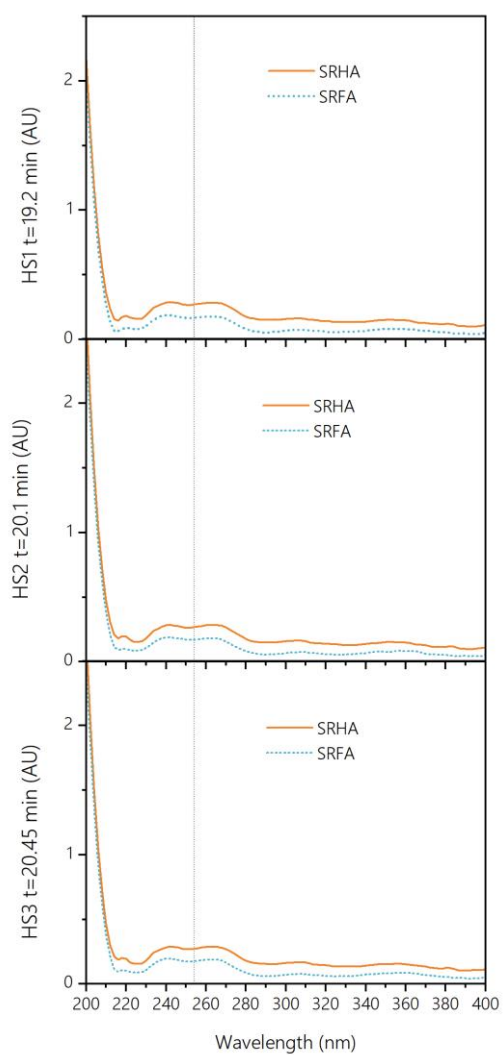


Figure A 6: Overlap of absorbance spectra from Humic Substances peaks (HS1, HS2, HS3) of SRHA (3S101H) and SRFA (3S101F) standards from IHSS. Vertical lines mark 254 nm.

APPENDIX E. CHAPTER VI: RESULTS III

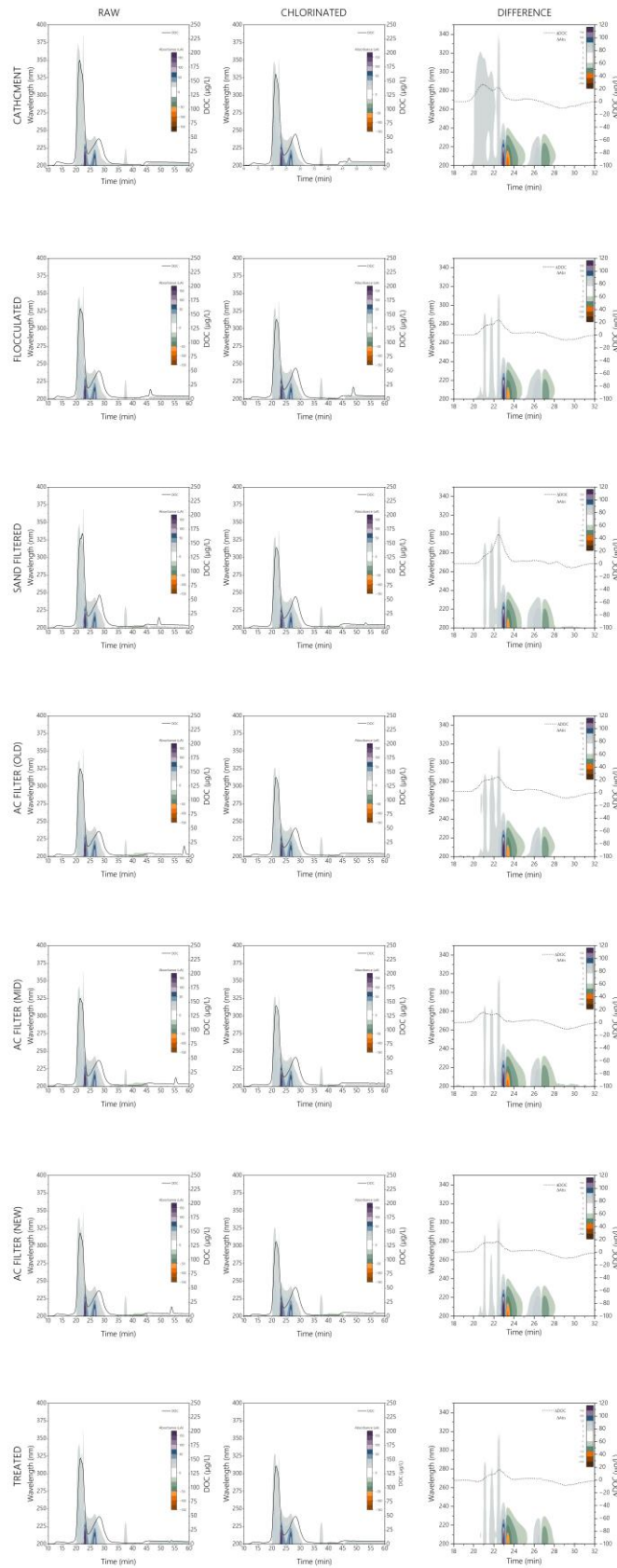


Figure A 7: Overlapped DOC and absorbance chromatograms of raw, chlorinated, and the difference of samples from Montfullà DWTP.

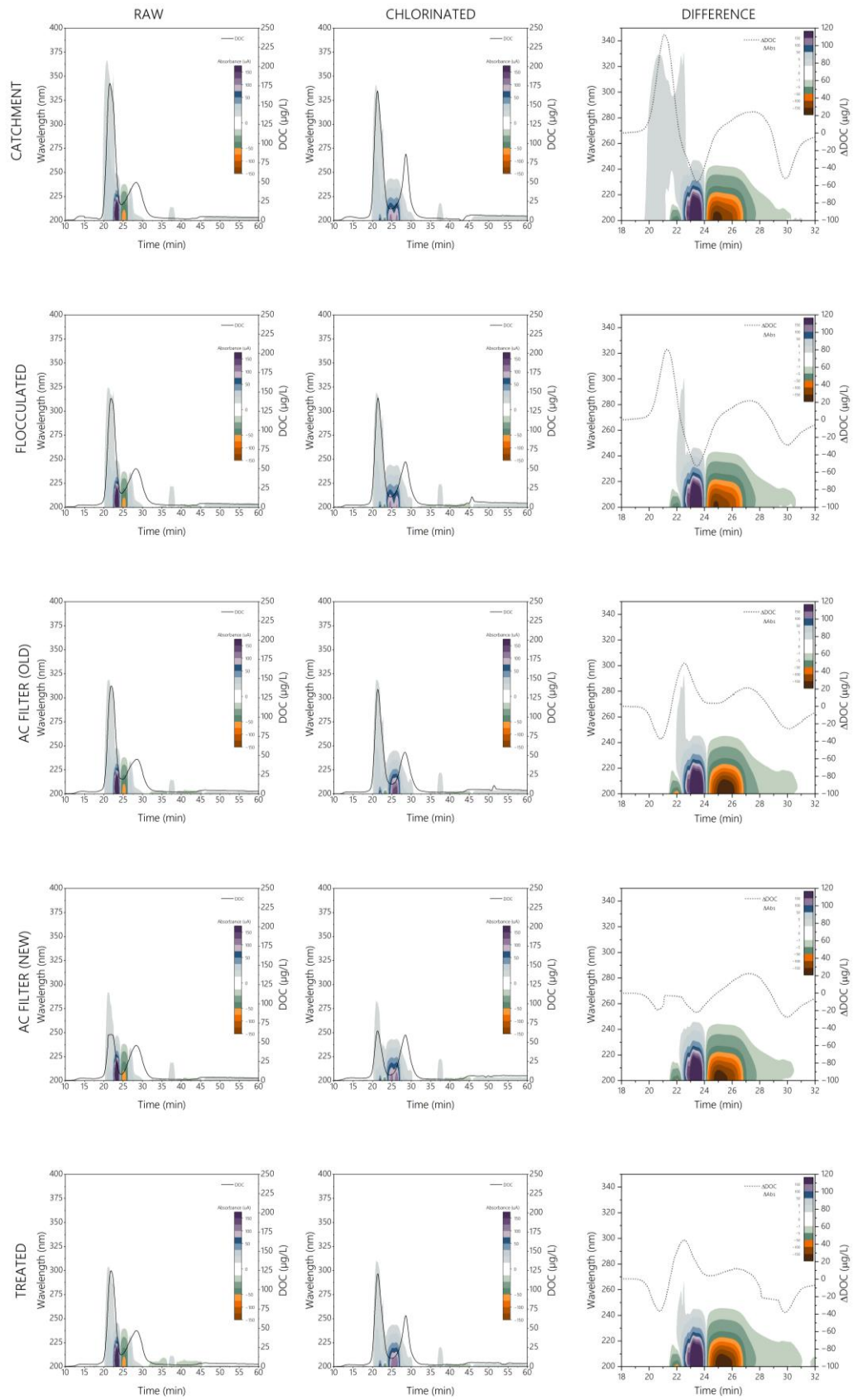


Figure A 8: Overlapped DOC and absorbance chromatograms of raw, chlorinated, and the difference of samples from Cardedeu DWTP.

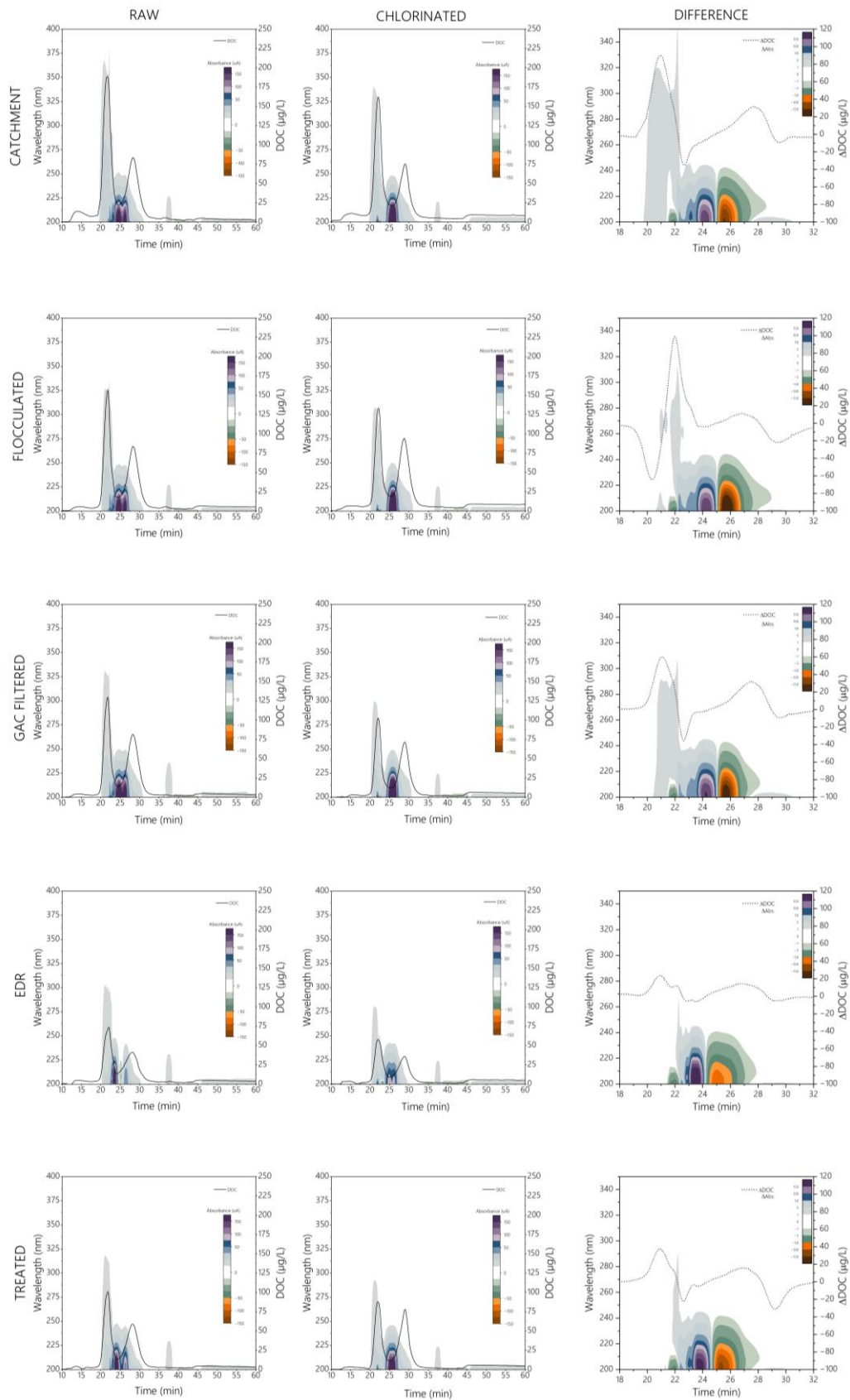


Figure A 9: Overlapped DOC and absorbance chromatograms of raw, chlorinated, and the difference of samples from Abreera DWTP.

Table A 13: Summary table of bibliographic findings about correlations between spectroscopic NOM properties and DBPs.

Reference	Models	Water type	Parameters	DBP	R ²	Variables (Wavelength, nm)
				tTHM	0.89	A270, DA270
(Beauchamp et al., 2019)	Multilinear Regression Models combining initial absorbance (A) and differential absorbance (DA)	Low brominated surface waters	Combination of initial absorbance (A) and differential absorbance (DA)	DCAA	0.93	A255, DA255
				TCAA	0.88	A250, DA250
					0.90	A320, DA320
				HAA6	0.91	A250, DA250
				tTHM	0.90	DA260, DA425, A310, A490, DA272
				DCAA	0.94	DA255, DA425, A220, A490, DA272
				TCAA	0.88	DA250, DA450, A225, DA272
(Korshin et al., 2002)	Linear Regression Models	Low brominated surface water	Differential absorbance	TCM	0.99	DA272
				BDCM	0.95	DA272
				TCAA	0.94	DA272
				DCAA	0.98	DA272
				MCAA	0.89	DA272
(Roccaro et al., 2008)	Non-linear regression (Exponential)	Low brominated surface water	Differential absorbance	TCM	0.95	DA272
				BDCM	0.95	DA272
				THAA	0.95	DA272
(Roccaro & Vagliasindi, 2009)	Linear Regression Models	Low brominated surface water	Differential absorbance	tTHM	0.93	DA272

Table A 14: Values of Calinski-Harabasz Index (CHI) for each fold (k).

DWTP	Sample	CHI k=2	CHI k=3	CHI k=4	CHI k=5	CHI k=6	k of higher CHI
PTM	Catchment	692	2117	2595	1965	1684	4
PTM	Flocculated	1615	894	810	658	1574	2
PTM	Sand Filters	801	425	1266	1050	1461	6
PTM	AC Filter (newest)	1611	816	676	1706	1492	5
PTM	AC Filter (mid)	1701	874	793	1723	1589	5
PTM	AC Filter (oldest)	1095	557	1453	1185	1106	4
PTM	Treated (pre chlorination)	1077	2059	1467	1176	1165	3
PTT	Catchment	2136	1374	2289	2338	1872	5
PTT	Flocculated	640	767	626	513	454	3
PTT	Activated Carbon (oldest)	814	854	634	548	833	3
PTT	Activated Carbon (newest)	167	328	245	442	400	5
PTT	Treated (pre chlorination)	435	341	496	481	515	6
PTL	Catchment	791	1987	3659	2764	2280	4
PTL	Flocculated	1687	1000	1409	1181	1109	2
PTL	GAC Filters	1623	830	677	1045	1050	2
PTL	EDR	478	311	441	347	544	6
PTL	Treated (50%, pre chlorination)	1623	830	677	1045	1050	2
						MEAN k	4

Table A 15: MLR parameters for models based on HS DAS at 272 nm.

Water	Approach	N	DBP	R ² _{adj}	272 coefficient	p-value	p-value Shapiro-Wilk	p-value Breusch-Pagan	Normality	Homoscedasticity
River & Reservoir	DAS 272 HS	17	TCM	0.635	7.8	5E-05	3E-01	8E-01	OK	OK
River & Reservoir	DAS 272 HS	17	BDCM	0.7598	2.9	2E-06	2E-01	4E-01	OK	OK
River & Reservoir	DAS 272 HS	17	DBCM	0.5185	2.3	5E-04	1E-01	2E-03	OK	FAIL
River & Reservoir	DAS 272 HS	17	TBM	0.9052	8.5	2E-03	8E-01	6E-01	OK	OK
River & Reservoir	DAS 272 HS	17	TTHM	0.8694	15.8	1E-08	1E-01	8E-01	OK	OK
River & Reservoir	DAS 272 HS	17	MCAA	0.6217	0.2	6E-05	3E-01	3E-01	OK	OK
River & Reservoir	DAS 272 HS	17	MBAA	0.4266	0.2	2E-03	1E-01	4E-01	OK	OK
River & Reservoir	DAS 272 HS	17	DCAA	0.5312	1.8	4E-04	8E-01	3E-01	OK	OK
River & Reservoir	DAS 272 HS	17	DBAA	0.2792	1.6	1E-02	9E-03	4E-02	FAIL	FAIL
River & Reservoir	DAS 272 HS	17	TCAA	0.6203	3.8	6E-05	1E+00	3E-01	OK	OK
River & Reservoir	DAS 272 HS	17	5HAA	0.8462	7.7	4E-08	2E-01	3E-01	OK	OK
River	DAS 272 HS	5	TCM	0.8269	1.6	8E-03	9E-01	3E-01	OK	OK
River	DAS 272 HS	5	BDCM	0.8635	2.4	5E-03	5E-01	2E-01	OK	OK
River	DAS 272 HS	5	DBCM	0.8971	4.9	3E-03	5E-01	3E-01	OK	OK
River	DAS 272 HS	5	TBM	0.9052	8.5	2E-03	8E-01	6E-01	OK	OK
River	DAS 272 HS	5	TTHM	0.9705	17.4	2E-04	3E-01	9E-01	OK	OK
River	DAS 272 HS	5	MCAA	0.8175	0.1	8E-03	6E-01	3E-01	OK	OK
River	DAS 272 HS	5	MBAA	0.7172	0.5	2E-02	7E-01	7E-01	OK	OK
River	DAS 272 HS	5	DCAA	0.5354	0.2	6E-02	7E-02	3E-01	OK	OK
River	DAS 272 HS	5	DBAA	0.8306	4.6	7E-03	1E+00	3E-01	OK	OK
River	DAS 272 HS	5	TCAA	0.9126	0.5	2E-03	7E-01	6E-01	OK	OK
River	DAS 272 HS	5	5HAA	0.8686	5.9	4E-03	1E+00	3E-01	OK	OK
Reservoir	DAS 272 HS	11	TCM	0.8455	10.8	5E-06	7E-01	7E-01	OK	OK
Reservoir	DAS 272 HS	11	BDCM	0.7385	3.1	1E-04	1E-01	1E+00	OK	OK
Reservoir	DAS 272 HS	11	DBCM	0.6243	1.0	8E-04	3E-03	6E-01	FAIL	OK
Reservoir	DAS 272 HS	11	TTHM	0.8138	15.0	2E-05	5E-01	9E-01	OK	OK
Reservoir	DAS 272 HS	11	MCAA	0.6716	0.3	4E-04	4E-02	4E-02	FAIL	FAIL
Reservoir	DAS 272 HS	11	MBAA	0.5647	0.1	2E-03	8E-02	9E-01	OK	OK
Reservoir	DAS 272 HS	11	DCAA	0.7629	2.6	6E-05	8E-01	1E-01	OK	OK
Reservoir	DAS 272 HS	11	DBAA	0.3137	0.2	3E-02	1E-01	8E-01	OK	OK
Reservoir	DAS 272 HS	11	TCAA	0.8606	5.3	3E-06	5E-02	1E-01	FAIL	OK
Reservoir	DAS 272 HS	11	5HAA	0.8623	8.5	3E-06	1E-01	4E-01	OK	OK

Table A 16: MLR parameters for models based on multiwavelength (MWL) HS DAS at 220, 252, 290 and 362 nm.

Water	Approach	N	DBP	R2adj	220 coefficient	252 coefficient	290 coefficient	362 coefficient	p-value	p-value Shapiro- Wilk	p-value Breusch- Pagan	Normality	Homoscedasticity
River & Reservoir	RAW MWL HS	17	TCM	0.6118	1.34E-01	11.1	-6.4	-5.8	2E-03	3E-01	2E-01	OK	OK
River & Reservoir	RAW MWL HS	17	BDCM	0.8499	6.84E-02	1.3	1.2	-2.6	5E-06	2E-01	5E-01	OK	OK
River & Reservoir	RAW MWL HS	17	DBCM	0.5326	2.23E-02	-4.2	7.3	3.2	6E-03	1E-01	2E-01	OK	OK
River & Reservoir	RAW MWL HS	17	TBM	0.9999	-3.07E-01	-43.0	72.8	8.8	8E-03	5E-01	4E-01	OK	OK
River & Reservoir	RAW MWL HS	17	TTHM	0.9446	2.21E-01	-7.8	25.7	2.7	9E-09	5E-01	5E-01	OK	OK
River & Reservoir	RAW MWL HS	17	MCAA	0.5561	2.56E-04	0.1	0.3	-0.5	5E-03	7E-01	5E-01	OK	OK
River & Reservoir	RAW MWL HS	17	MBAA	0.597	1.61E-03	-0.9	1.1	1.3	3E-03	1E-01	5E-01	OK	OK
River & Reservoir	RAW MWL HS	17	DCAA	0.4113	5.65E-03	1.8	0.9	-3.4	3E-02	6E-01	3E-01	OK	OK
River & Reservoir	RAW MWL HS	17	DBAA	0.2872	-1.70E-03	-6.2	8.3	7.5	8E-02	2E-02	3E-01	FAIL	OK
River & Reservoir	RAW MWL HS	17	TCAA	0.5889	7.06E-02	8.9	-6.6	-7.6	3E-03	7E-01	2E-01	OK	OK
River & Reservoir	RAW MWL HS	17	5HAA	0.8319	7.66E-02	3.8	4.3	-3.5	1E-05	9E-01	1E+00	OK	OK
River	RAW MWL HS	5	TCM	0.9999	8.51E-02	3.8	-4.9	-1.0	8E-03	5E-01	4E-01	OK	OK
River	RAW MWL HS	5	BDCM	0.9997	1.56E-01	14.2	-18.6	-3.8	1E-02	5E-01	4E-01	OK	OK
River	RAW MWL HS	5	DBCM	0.9984	2.34E-01	30.9	-41.9	2.4	3E-02	5E-01	4E-01	OK	OK
River	RAW MWL HS	5	TBM	0.9999	-3.07E-01	-43.0	72.8	8.8	8E-03	5E-01	4E-01	OK	OK
River	RAW MWL HS	5	TTHM	0.9999	1.68E-01	5.9	7.3	6.4	5E-03	5E-01	4E-01	OK	OK
River	RAW MWL HS	5	MCAA	0.9803	3.89E-03	0.7	-0.7	-0.5	9E-02	5E-01	4E-01	OK	OK
River	RAW MWL HS	5	MBAA	0.8964	2.41E-02	1.9	-3.0	1.7	2E-01	5E-01	4E-01	OK	OK
River	RAW MWL HS	5	DCAA	0.9628	4.20E-03	1.3	-1.3	-1.0	1E-01	5E-01	4E-01	OK	OK
River	RAW MWL HS	5	DBAA	0.7973	2.01E-01	24.6	-34.9	7.6	3E-01	5E-01	4E-01	OK	OK

River	RAW MWL HS	5	TCAA	0.9984	1.91E-02	2.5	-2.6	-1.4	3E-02	5E-01	4E-01	OK	OK
River	RAW MWL HS	5	5HAA	0.8362	2.42E-01	30.6	-41.8	6.1	3E-01	5E-01	4E-01	OK	OK
Reservoir	RAW MWL HS	11	TCM	0.9249	1.48E-01	-10.8	25.3	4.3	3E-05	7E-01	6E-01	OK	OK
Reservoir	RAW MWL HS	11	BDCM	0.8714	6.75E-02	-3.1	6.7	1.0	3E-04	1E-01	2E-01	OK	OK
Reservoir	RAW MWL HS	11	DBCM	0.7538	2.93E-02	-1.2	2.7	-0.6	3E-03	2E-01	1E-01	OK	OK
Reservoir	RAW MWL HS	11	TTHM	0.9096	2.45E-01	-15.0	34.7	4.7	6.273-5	4E-01	4E-01	OK	OK
Reservoir	RAW MWL HS	11	MCAA	0.6239	4.42E-04	-0.4	1.1	-0.2	2E-02	8E-02	4E-01	OK	OK
Reservoir	RAW MWL HS	11	MBAA	0.6999	3.28E-03	-0.2	0.4	-0.1	7E-03	9E-01	6E-01	OK	OK
Reservoir	RAW MWL HS	11	DCAA	0.7304	1.31E-02	-3.8	9.6	-2.4	4E-03	7E-01	7E-01	OK	OK
Reservoir	RAW MWL HS	11	DBAA	0.5697	5.63E-03	-0.5	0.5	0.9	3E-02	7E-02	2E-01	OK	OK
Reservoir	RAW MWL HS	11	TCAA	0.8826	8.95E-02	-0.7	8.8	-8.0	2E-04	1E-01	5E-01	OK	OK
Reservoir	RAW MWL HS	11	5HAA	0.8728	1.14E-01	-5.9	21.1	-11.0	2E-04	6E-02	7E-01	OK	OK

Table A 17: MLR parameters for models based on multiwavelength (MWL) HS raw absorbance at 220, 252, 290 and 362 nm.

Water	Approach	N	DBP	R ² _{adj}	220 coefficient	252 coefficient	290 coefficient	362 coefficient	p-value	p-value Shapiro- Wilk	p-value Breusch- Pagan	Normality	Homoscedasticity
River & Reservoir	RAW MWL HS	17	TCM	0.8306	-2.6E-02	13.2	-20.5	5.6	1E-05	9E-01	1E-02	OK	FAIL
River & Reservoir	RAW MWL HS	17	BDCM	0.9644	4.4E-02	1.8	-3.1	3.3	5E-10	7E-01	2E-01	OK	OK
River & Reservoir	RAW MWL HS	17	DBCM	0.6116	9.7E-02	-5.5	8.9	3.0	2E-03	8E-01	2E-03	OK	FAIL
River & Reservoir	RAW MWL HS	17	TBM	0.9385	-1.2E-01	19.0	-23.1	-15.4	2E-01	9E-01	2E-01	OK	OK
River & Reservoir	RAW MWL HS	17	TTHM	0.9725	2.4E-01	-2.3	8.0	1.5	9E-11	2E-01	3E-01	OK	OK
River & Reservoir	RAW MWL HS	17	MCAA	0.8481	-6.0E-03	0.4	-0.4	-0.2	6E-06	1E+00	1E+00	OK	OK
River & Reservoir	RAW MWL HS	17	MBAA	0.6679	1.1E-02	-0.7	1.4	-0.9	8E-04	4E-01	2E-02	OK	FAIL
River & Reservoir	RAW MWL HS	17	DCAA	0.7021	-4.9E-02	3.0	-3.3	-1.5	4E-04	3E-01	4E-01	OK	OK
River & Reservoir	RAW MWL HS	17	DBAA	0.4447	9.3E-02	-7.1	12.3	-0.7	2E-02	6E-01	1E-02	OK	FAIL
River & Reservoir	RAW MWL HS	17	TCAA	0.6443	7.4E-03	4.1	-7.5	9.0	1E-03	6E-01	1E-02	OK	FAIL
River & Reservoir	RAW MWL HS	17	5HAA	0.8806	5.0E-02	0.1	1.8	5.7	1E-06	6E-01	7E-01	OK	OK
River	RAW MWL HS	5	TCM	0.9816	5.6E-02	-2.9	4.5	1.5	9E-02	9E-01	2E-01	OK	OK
River	RAW MWL HS	5	BDCM	0.9974	8.8E-02	-6.1	9.1	6.2	3E-02	9E-01	2E-01	OK	OK
River	RAW MWL HS	5	DBCM	0.9026	1.4E-01	-15.2	24.6	9.7	2E-01	9E-01	2E-01	OK	OK
River	RAW MWL HS	5	TBM	0.9385	-1.2E-01	19.0	-23.1	-15.4	2E-01	9E-01	2E-01	OK	OK
River	RAW MWL HS	5	TTHM	0.9617	1.7E-01	-5.1	15.1	2.1	1E-01	9E-01	2E-01	OK	OK
River	RAW MWL HS	5	MCAA	0.9998	-1.9E-04	-0.1	0.2	0.4	9E-03	9E-01	2E-01	OK	OK
River	RAW MWL HS	5	MBAA	0.9226	4.9E-03	-3.5	6.6	-1.4	2E-01	9E-01	2E-01	OK	OK
River	RAW MWL HS	5	DCAA	0.9991	-2.8E-03	-0.1	0.2	0.8	2E-02	9E-01	2E-01	OK	OK
River	RAW MWL HS	5	DBAA	0.9058	-3.0E-02	-32.6	61.6	-9.2	2E-01	9E-01	2E-01	OK	OK

River	RAW MWL HS	5	TCAA	0.9999	7.7E-03	-0.4	0.5	1.5	6E-03	9E-01	2E-01	OK	OK
River	RAW MWL HS	5	5HAA	0.9223	-2.8E-02	-36.3	68.4	-7.9	2E-01	9E-01	2E-01	OK	OK
Reservoir	RAW MWL HS	11	TCM	0.9643	1.1E-01	1.1	1.2	1.6	2E-05	3E-01	4E-01	OK	OK
Reservoir	RAW MWL HS	11	BDCM	0.9887	5.0E-02	0.6	0.7	-5.5	2E-08	9E-01	3E-01	OK	OK
Reservoir	RAW MWL HS	11	DBCM	0.9913	1.8E-02	0.3	0.7	-4.8	6E-09	8E-01	2E-01	OK	OK
Reservoir	RAW MWL HS	11	TTHM	0.9772	1.8E-01	2.0	2.6	-8.7	3E-07	3E-01	4E-01	OK	OK
Reservoir	RAW MWL HS	11	MCAA	0.9272	-2.9E-03	-0.01	0.6	-2.0	3E-05	2E-01	9E-01	OK	OK
Reservoir	RAW MWL HS	11	MBAA	0.9267	1.7E-03	0.03	0.1	-0.6	3E-05	4E-03	5E-01	FAIL	OK
Reservoir	RAW MWL HS	11	DCAA	0.9026	3.0E-03	-1.8	7.2	-12.0	8E-05	6E-02	8E-01	OK	OK
Reservoir	RAW MWL HS	11	DBAA	0.8919	6.0E-03	-9.21E-04	0.4	-1.9	1E-04	2E-01	3E-01	OK	OK
Reservoir	RAW MWL HS	11	TCAA	0.8446	8.3E-02	-1.6	0.1	20.1	5E-04	6E-02	6E-01	OK	OK
Reservoir	RAW MWL HS	11	5HAA	0.8909	8.5E-02	-3.1	8.1	2.9	1E-04	4E-02	5E-01	FAIL	OK

Table A 18: MLR parameters for models based on multiwavelength (MWL) bulk measurements of raw absorbance at 220, 252, 290 and 362 nm.

Water	Approach	N	DBP	k folds	R ² _{adj}	220	252	290	362	p-value	p-value	p-value	Normality	Homoscedasticity
						coefficient	coefficient	coefficient	coefficient		Shapiro-Wilk	Breusch-Pagan		
River & Reservoir	RAW BULK	26	TCM	10	0.76	0.03	9.62	-16.32	16.72	2.64E-07	0.19	0.06	OK	OK
River & Reservoir	RAW BULK	26	BDCM	10	0.49	0.01	-0.74	-0.68	21.54	7.49E-04	0.00	0.02	FAIL	FAIL
River & Reservoir	RAW BULK	26	DBCM	10	0.26	-3.0E-03	-4.96	6.32	25.26	2.75E-02	0.01	0.01	FAIL	FAIL
River & Reservoir	RAW BULK	26	TTHM	10	0.60	0.06	-1.43	1.52	57.19	5.83E-05	0.04	0.01	FAIL	FAIL
River	RAW BULK	10	TCM	5	0.63	-0.19	1.00	5.21	-9.80	2.9E-02	0.64	0.20	OK	OK
River	RAW BULK	10	BDCM	5	0.58	-0.61	4.40	11.28	-23.63	4.08E-02	0.97	0.16	OK	OK
River	RAW BULK	10	DBCM	5	0.67	-0.78	8.90	10.19	-30.36	2.19E-02	0.07	0.17	OK	OK
River	RAW BULK	10	TBM	5	0.81	-0.44	11.12	1.47	-34.44	4.02E-03	0.40	0.86	OK	OK
River	RAW BULK	10	TTHM	5	0.75	-2.03	25.43	28.15	-98.24	9.70E-03	0.18	0.12	OK	OK
Reservoir	RAW BULK	16	TCM	5	0.89	0.07	10.48	-25.00	53.19	1.8E-06	0.22	0.14	OK	OK
Reservoir	RAW BULK	16	BDCM	5	0.94	0.05	2.23	-3.91	4.00	7.4E-08	0.20	0.47	OK	OK
Reservoir	RAW BULK	16	DBCM	5	0.99	0.02	0.16	0.89	-4.73	1.4E-12	0.21	0.25	OK	OK
Reservoir	RAW BULK	16	TTHM	5	0.93	0.15	11.73	-17.36	6.76	1.5E-07	0.19	0.47	OK	OK

